

# MANITOBA



INVEST. BUILD. GROW.

## REPORT OF ACTIVITIES 2019

Manitoba Geological Survey





# **REPORT OF ACTIVITIES 2019**

**Manitoba Agriculture and Resource Development  
Manitoba Geological Survey**



Every possible effort is made to ensure the accuracy of the information contained in this report, but Manitoba Agriculture and Resource Development does not assume any liability for errors that may occur. Source references are included in the report and users should verify critical information.

Any third party digital data and software accompanying this publication are supplied on the understanding that they are for the sole use of the licensee, and will not be redistributed in any form, in whole or in part. Any references to proprietary software in the documentation and/or any use of proprietary data formats in this release do not constitute endorsement by Manitoba Agriculture and Resource Development of any manufacturer's product.

When using information from this publication in other publications or presentations, due acknowledgment should be given to the Manitoba Geological Survey. The following reference format is recommended:

Manitoba Agriculture and Resource Development 2019: Report of Activities 2019; Manitoba Agriculture and Resource Development, Manitoba Geological Survey, 101 p.

**Published by:**

Manitoba Agriculture and Resource Development  
Manitoba Geological Survey  
360–1395 Ellice Avenue  
Winnipeg, Manitoba  
R3G 3P2 Canada  
Telephone: 1-800-223-5215 (General Enquiry)  
              204-945-6569 (Publication Sales)  
Fax:        204-945-8427  
E-mail:     [minesinfo@gov.mb.ca](mailto:minesinfo@gov.mb.ca)  
Website:   [manitoba.ca/minerals](http://manitoba.ca/minerals)

**ISBN No.:** 978-0-7711-1599-8

This publication is available to download free of charge at [manitoba.ca/minerals](http://manitoba.ca/minerals)

**Cover photo:**

Aerial image captured by drone during bedrock geological mapping of mafic volcanic rocks at the south end of Wekusko Lake (GS2019-4, this volume).

# REPORT OF ACTIVITIES 2019



## Minister's Message

As Minister of Manitoba Agriculture and Resource Development, I am pleased to introduce the Manitoba Geological Survey's *Report of Activities 2019*, featuring the latest geoscientific research on key investigations into our province's rich and diverse mineral resources sector.

Built on a scientific commitment to excellence, the geoscientific research in this publication underscores the significance to which mining, exploration, and development contributes to our province's economic prosperity. This year's volume features ten comprehensive professional geoscience reports, which both reaffirms and expands upon our solid knowledge base.

Manitoba is home to large areas of high mineral potential in remote and relatively under-explored regions of the province. Exploring this potential is vital as the industry depends upon the discovery of new deposits to succeed, and contributes towards sustainable economic growth and quality of life to many remote communities.

We also recognize the importance of upholding commitments to stewardship, development, and industry growth. By collaborating and focusing on building strong relationships between all levels of government, First Nations, northern communities, industry representatives and other

interest groups, I am confident we are on the path to resetting the climate for investment in the province, promising a future of both sustainability and renewal.

In addition to the geoscientific research found in this volume, I encourage you to explore the Survey's website at [Manitoba.ca/minerals](http://Manitoba.ca/minerals). With a wide range of materials ranging from databases to maps to reports, there are hundreds of files available to assist you in your research and strategic planning.

I believe that there is more to explore within Manitoba's distinctive mining sector, and our Government remains committed to creating an environment where businesses can invest, build, and grow.

Sincerely,

A handwritten signature in black ink that reads "Blaine Pedersen". The signature is fluid and cursive.

Honourable Blaine Pedersen  
Manitoba Agriculture and Resource Development



# Rapport d'activités 2019



## Message du ministre

En tant que ministre de l'Agriculture et du Développement des ressources du Manitoba, j'ai le plaisir de déposer le *Rapport d'activités 2019* de la Direction des services géologiques du Manitoba, qui présente les plus récentes recherches géoscientifiques sur les principales études dans le secteur riche et diversifié des ressources minières de notre province.

Fondée sur un engagement scientifique à l'excellence, la recherche géoscientifique présentée dans cette publication souligne l'importance de la contribution de l'exploitation minière, de l'exploration et du développement à la prospérité économique de notre province. Le volume de cette année présente dix rapports géoscientifiques professionnels exhaustifs, qui confirment et élargissent notre solide base de connaissances.

Le Manitoba abrite de vastes zones à fort potentiel minier dans des régions éloignées et relativement sous-explorées de la province. L'exploration de ce potentiel est vitale, car l'industrie dépend de la découverte de nouveaux gisements pour réussir et contribue à la croissance économique durable et à la qualité de vie de nombreuses collectivités éloignées.

Nous reconnaissons également l'importance de respecter nos engagements en matière de gestion, de développement et de croissance de l'industrie. En collaborant et en mettant l'accent sur l'établissement de relations solides

entre tous les paliers de gouvernement, les Premières Nations, les collectivités du Nord, les représentants de l'industrie et d'autres groupes d'intérêt, je suis convaincu que nous sommes en voie de rétablir un climat propice aux investissements dans la province, promettant un avenir à la fois de durabilité et de renouveau.

En plus de la recherche géoscientifique présentée dans ce volume, je vous encourage à explorer le site Web de la Direction à l'adresse <https://www.gov.mb.ca/iem/index.fr.html>. Grâce à une vaste gamme de documents allant des bases de données aux cartes en passant par les rapports, des centaines de dossiers sont consultables pour vous aider dans vos recherches et votre planification stratégique.

Je crois qu'il y a encore beaucoup à explorer dans le secteur minier particulier du Manitoba, et notre gouvernement demeure résolu à créer un environnement où les entreprises peuvent investir, bâtir et croître.

Je vous prie d'agréer mes salutations les meilleures.

A handwritten signature in black ink that reads "Blaine Pedersen".

Blaine Pedersen  
Agriculture et Développement des ressources

## In Memoriam: Gerry Bengler

by M.P.B. Nicolas and C. Epp

Gerald Leonard Bengler passed away in Winnipeg on July 1, 2019 at the age of 60. He was born in Winnipeg on May 24, 1959 where he grew up in St. James and raised his family. Gerry was married to the love of his life Debbie for 36 years. Together they had two sons they adored, Matthew (Caitlynn) and Andrew. Gerry loved sports and was a competitive swimmer from the age of 4. He enjoyed playing water polo, hockey and spending time on the lake with his Laser sailboat. He also was a coach for his sons' hockey and soccer teams. During his retirement, he and Debbie had extensive vacation stays in Mexico, and loved to spend their summers at the family cottage in Laclu, Ontario.

Gerry attended the University of Winnipeg receiving his B.Sc. in Physical Geography. Following his graduation he worked as a summer student for Hugh McCabe before permanently joining the Manitoba Geological Survey (MGS). Through his 35-year career, Gerry worked as a drill rig operator, laboratory technician, conference organizer and lab manager, making lifelong friends along the way. Most of his career in the field working on the stratigraphic drillcore program involved drilling, boxing and labelling long lengths of precious Phanerozoic core. His great sense of humour and fun personality made the weeks on the drill much more bearable, setting apart the usual mood of "an adventure for the first two days and then you are just cold and wet on a drill for 14 hours straight" (Rick Unruh). Gerry was detail-orientated and took great care in this work, making sure all core was accurate and available for the geologists who were waiting patiently for it, as well as for the archival record it was generating. Back in the core lab, he prepared samples that came back from the geologists in the field, and laid out core for viewing by staff and clients. Each fall, Gerry helped organize the annual Manitoba Mining and Minerals Convention where he was responsible for organizing floor plans, setting up the convention area and being the go-to person if any problems arose. Gerry was well known by all on the



convention floor. Later in his career, he became the Core Lab Manager. In this role he had the opportunity to closely mentor and inspire many students.

Gerry was an honourable person and a trusted friend, who was always willing to help and lend a hand when needed. He knew how to get people working together and made sure you had what you needed to do your work efficiently and effectively. He was always kind and considerate, had a great work ethic and was well respected by his peers. His positive attitude and laugh was infectious and his smile was always genuine and welcoming.

Gerry retired in May 2016 where he looked forward to spending his retirement with Debbie and his family at the cottage and travelling.



## In Memoriam: Paul Lenton

by G.R. Keller and E.C. Syme

Paul Gerald Lenton passed away in Winnipeg on September 4, 2019 at the age of 70. He was born in Winnipeg on April 26, 1949 where he remained for his entire life. Paul attended the University of Manitoba, completing a B.Sc. in Geology (1972) followed by an M.Sc. in 1979. Paul and Bonnie, his wife of 46 years, had two children; a daughter Regan (granddaughter Madeleine) and a son Mitchell. Paul was a man of many talents and interests; he immersed himself in geology, but he also loved classical music, poetry and astronomy. He enjoyed science fiction, both novels and movies, often speaking about his time watching countless hours of DVDs with his son Mitch. In his own words, Paul was a self-professed computer ‘geek’, spending hours learning about software and hardware as well as immersing himself in computer gaming. Most importantly, Paul was a family man; he was very close to his siblings and friends, always making sure that everyone stayed in touch.

Paul was also a respected and talented geologist, giving the Manitoba Geological Survey (MGS) 43 years of service. He began his career with the Manitoba government in the early 1970s as a summer student on projects in the Southern Indian Lake and Churchill areas. Upon graduation, Paul found employment with the Mineral Resources Division and first worked primarily in the lab as an “engineering aid” to staff geologists. His first solo mapping projects were on the north flank of the Kiseeynew Domain, southwest of Lynn Lake (the McKnight–McCallum Lakes area in 1975–76 and the McNeill Lake–Pistol Lake area in 1978). Paul completed his Masters degree in 1979 on the mineralogy and petrology of the Buck claim lithium pegmatite at Bernic Lake. Soon after, Paul and his colleague Tim Corkery began the Lower Churchill project. This helicopter-assisted program continued through to the 1981 field season and focused on a large tract of Paleoproterozoic supracrustal and granitoid rocks east of Southern Indian Lake and north of the Nelson River. From 1982 to 1985, Paul was involved in a project to inventory and characterize rare-element enriched granite pegmatites in the Lynn Lake, Cross Lake, and Knee Lake areas of the province. While working on this project, Paul and Tim Corkery teamed up once again (1983 to 1986) for a mapping program at Cross Lake in the Archean Superior Province, with Paul’s portion of the program focusing on granitoid rocks and pegmatites. In 1987, Paul and colleague Herman Zwanzig conducted a mapping project in the Limestone Point Lake–Star Lake area of the Kiseeynew Domain in order to identify the types of high-grade gneisses; the aim was to assign them to existing stratigraphic divisions and to interpret their origin.

In the late 1980s, Paul transitioned from field mapping to providing services in the newly emerging field of



computer-based data collection and mapping. By the early 1990s, Paul was responsible for managing Branch computer systems, developing data management systems, and implementing new digital technologies such as Computer Assisted Drawing (CAD) and Geographic Information Systems (GIS). He was instrumental in bringing this, at the time new, digital mapping technology (GIS) to the MGS. In the spring of 1994, Paul was promoted to Section Head of the newly formed Geoscience Information Services Section (GIS Section). At this time, he was given the additional responsibilities of directly supervising two geologists and managing all computer resources and information management systems for the Geological Services Branch. This was further expanded in late 1995 when he was given seven additional staff to supervise and assumed responsibility for managing all geological compilation, Internet resources, drafting, graphic and report production for the Branch. Paul’s passion for computers, GIS and the digitization of geological data saw him grow and thrive in the position, quickly becoming a respected expert in all three. His extraordinary vision, commitment and skill were instrumental in his pioneering digital data collection at the MGS. Paul designed a geological field database system that he called GEODATA. In this system, geologists wrote their field notes, longhand, on specially designed note sheets based on a template. The longhand notes were then transcribed into the GEODATA database resulting in complete digital capture of every observation

made by the geologist in the field. Without the incredibly important GEODATA database, some reports could not have been written.

Between 1991 and 1996 Paul was the Manitoba leader on an innovative and groundbreaking federal-provincial collaborative program. The National Geoscience Mapping Program (NATMAP) aimed to foster a multi-disciplinary team approach to bedrock and surficial mapping and related research. During NATMAP, Paul helped drive Manitoba's considerable commitment to the project and was responsible for collaboration with federal and provincial colleagues on the digital collection and dissemination of magnetic, gravity and geology maps.

From the early 2000s onward, Paul was responsible for all computer-based geological compilation programs, the production of maps and graphics for hard copy reports, the production of e-documents, providing input into website content and the development of geological information management systems for managing office data and field observations. He was also responsible for managing all aspects of the function of the cartographic support unit, guiding and managing the development of systems including geospatial databases, directing all aspects of geological information management and computer operations in the Branch, and acting as an authoritative resource for the Division on computer technology, CAD, GIS systems and database design and implementation. Throughout his career, Paul was instrumental in providing GIS and database support to a number of projects. These include the Manitoba Geochronology Database (1993), industrial minerals information systems (1993), 1:250,000 compilation map program (1990s), Operation Superior multimedia sampling program (1999–2002), kimberlite potential in Manitoba (2004), till geochemistry in northeast Manitoba (2005) and a study of the alkaline rocks in the Knee Lake area (2008). Despite the considerable workload, Paul's attitude was always characterized by a calm, can-do attitude.

In 2010, Paul was diagnosed with an aggressive type of Non-Hodgkin Lymphoma; a cancer that, at the time, was

usually fatal. He faced his illness head-on, taking a hiatus from work to undergo extensive and invasive treatment. Paul fought, and eventually beat cancer with dignity and a sense of unstoppable positivity. He returned to work with a renewed sense of purpose, once again pouring himself into every project with which he was involved. On top of his already extensive list of responsibilities, over the next nine years Paul was involved in a myriad of projects from the initial relaunch and redesign of the GIS Map Gallery, the Survey's online data distribution platform, to beginning a compilation of the bedrock geology of the Lynn Lake area. In his final years at the Survey, Paul spent much of his time mentoring, educating and doing everything he could to pass on his vast institutional knowledge; not an easy task, as he was a brilliant scientist with an analytical mind that never ceased to amaze. He always had an answer and provided solutions to complex problems whether they were in relation to databases, CAD, GIS or any topic at hand (including computer gaming and whether or not iOS was as good as Android). There wasn't a single complex problem he wouldn't tackle; he kept a large red button on his desk that when pressed stated "that was easy!", even when the problem seemed insurmountable. His encyclopedic knowledge of geology, science and technology was legendary in the Branch, as was his recall of Branch history and milestones.

After a long and incredible career, Paul retired in early 2018. He was hoping to spend a lot more time with his family, especially his granddaughter Madeleine (Maddie) of whom he spoke of incessantly. Unfortunately, the earlier cancer treatments that helped to extend his life would ultimately be the reason for his struggles. Although Paul fought and beat cancer, over the years his body wasn't able to combat the damage that the chemotherapy did to his heart. Paul was a dedicated father, grandfather, husband, friend and mentor. He is missed by all those who knew him; family, friends and colleagues. Paul is survived by his wife Bonnie, his daughter Regan (granddaughter Madeleine, son-in-law Robert), son Mitchell, sisters Pat and Judy and brother Tom.



## Foreword

On behalf of the Manitoba Geological Survey (MGS), it is my privilege to present the *Report of Activities 2019*—the annual peer-reviewed volume of the geoscience project results by the MGS and its partners.

The Resource Development Division (RDD), of which the MGS is part of, underwent restructuring this year, with some significant changes to its branches. The RDD is now divided into three branches: (1) Regulatory Services, (2) Land-use and Resource Tenure, and (3) the Manitoba Geological Survey. The MGS represents a consolidation of all geological-related services that RDD provides. The MGS consists of four sections: (1) Precambrian and (2) Sedimentary Geoscience sections (Christian Böhm, Chief Geologist for both), (3) Regulatory Geoscience Support Services (Pamela Fulton-Regula, Acting Chief Geologist), and (4) Geoscience Data Management (Greg Keller, Acting Manager).

The MGS conducts a wide range of investigations, which include the examination of exposed bedrock, subsurface materials, and surficial sediments including sand, gravel and organic deposits throughout Manitoba. It also provides geoscience support for the regulatory framework and tenure systems managed by RDD, which includes assessment files review, oil field-pool code designations, land use, and community consultations. By developing an understanding of Manitoba's geology and geological processes, the MGS provides fundamental data and unbiased technical support to inform government policy and decision making, mineral exploration, and wise land use management.

The MGS started this year's field season with eight new exciting projects. This volume and accompanying preliminary maps present findings of both new and advanced projects, and includes important contributions to Manitoba's vast mineral wealth and geological endowment. This volume emphasises new information on gold (GS2019-1, GS2019-2, GS2019-4), graphite and vanadium (GS2019-3, GS2019-6), base-metal (GS2019-4), and lithium (GS2019-5) occurrences. Also included are continued contributions on regional diamond potential (GS2019-9, GS2019-10), silica sand and Mississippi-Valley Type (MVT) deposit investigations (GS2019-8), glacial history and paleo ice flow reconstructions (GS2019-9, GS2019-10), and Phanerozoic stratigraphic mapping (GS2019-7, GS2019-8).

The importance of remapping geological terranes and re-evaluating geological interpretations throughout the years is critical to staying relevant in a global market, staying current to an ever-evolving science, and maintaining and improving our economic advantage. Global demands for commodities fluctuate over time, and previously ignored, seemingly unimportant, or simply overlooked details and

site observations made decades ago suddenly become critically important and highly sought after. An example of this is the bedrock remapping in the Russell–McCallum lakes area in northwestern Manitoba (GS2019-3), where graphite was mentioned briefly 40 years ago. Natural graphite is a very important commodity for our everyday lives and technology but currently is a well-sought commodity due to its anticipated demand associated with the production of Li-ion batteries. This is a reflection of our ever-changing world and technology advances where electrification and moving toward a carbon neutral economy are currently our biggest drivers.

The MGS, while fully engaged with field projects, is also hard at work on internal initiatives to improve service delivery, project tracking, standardizing our geochemistry data releases, map creation and compilation, including a new 250k scale common map legend. The Geoscience Data Management Section are key players in the integration of Petrinex (provides services that facilitate management and exchange of essential information in the petroleum sector), ongoing maintenance of iMaQs and Map Gallery, development of maps for land tenure, and staff GIS training and support. The MGS is an active player on the Manitoba Liaison Committee on Mining and Exploration which, since its formation in June 2019, has made significant progress. The MGS is also an active participant on the Block Planning Committee, ensuring the mineral resource lens is not forgotten during land-use planning. In addition, the MGS participates and engages regularly in many collaborative geoscience projects and initiatives with industry and academia.

Over the last year, the MGS saw some staff changes. We continue to strategically build capacity with the hiring of three new staff: Ashley Santucci (GIS Technician), Paul Belanger (Laboratory Technician), and Shaun Gallagher (Assessment and Consultation Geologist). The addition of these talented individuals to our team will allow us to progress on our path of continuous improvement for better service delivery. Precambrian project geologist Simon Gagné and GIS geologist Sharon Lee have left the MGS to pursue new adventures and opportunities in Ottawa. The recent, too-early passing of fellow MGS retirees Paul Lenton (Precambrian and GIS geologist and manager) and Gerry Bengert (core lab manager) leave us with heavy hearts. They both touched everyone deeply in their lives and will never be forgotten for their friendships, talents, positive attitude and contagious smiles.

The dedicated and diligent work of MGS geologists, lab technicians, expeditors, students and GIS technicians went into the production of the *Report of Activities 2019*. Bob Davie and his team from RnD Technical carefully performed technical editing and Craig Steffano managed report production and publication layout. I would like

to thank everyone on the MGS team for their valuable contributions, dedication, passion and energy to the projects and initiatives tackled over the last year which have yielded great success.

Michelle P.B. Nicolas, P. Geo., FGC  
Acting Director, Manitoba Geological Survey

## Avant-propos

J'ai l'honneur de présenter au nom de la Direction des services géologique du Manitoba (la Direction) le *Rapport d'activités 2019*, un recueil annuel examiné par les pairs compilant les résultats de projets géoscientifiques exécutés par la Direction et ses partenaires.

La Division du développement des ressources (la Division), dont fait partie la Direction, a cette année fait l'objet d'une réorganisation se traduisant par des changements importants à ses directions. La Division est désormais formée de trois directions : (1) la Direction des services de réglementation, (2) la Direction de l'aménagement du territoire et de l'exploitation des ressources et (3) la Direction des services géologiques. La Direction représente un regroupement de tous les services géologiques que la Division fournit. La Direction se compose de quatre sections : (1) la Section du Précambrien et (2) la Section de la géologie sédimentaire (Christian Böhm, géologue en chef des deux sections), (3) la Section des services de soutien géoscientifique lié à la réglementation (Pamela Fulton-Regula, géologue en chef par intérim) et (4) la Section de la gestion des données géoscientifiques (Greg Keller, gestionnaire par intérim).

La Direction mène un vaste éventail d'études, qui incluent l'examen du substrat rocheux exposé, des matériaux en subsurface et des sédiments superficiels, comme le sable, le gravier et les dépôts organiques, dans tout le Manitoba. La Direction fournit également un soutien géoscientifique concernant le cadre de réglementation et les régimes fonciers gérés par la Division, ce qui inclut l'examen de dossiers d'évaluation, l'attribution de codes aux champs et gisements de pétrole, l'aménagement du territoire et les consultations communautaires. En approfondissant la compréhension de la géologie et des processus géologiques du Manitoba, la Direction fournit des données fondamentales et un soutien technique impartial à l'appui des politiques et de la prise de décision gouvernementales, de l'exploration minière et d'un aménagement judicieux du territoire.

Cette année, la Direction a amorcé sa saison sur le terrain par huit nouveaux projets passionnants. Ce recueil et les cartes préliminaires qui l'accompagnent présentent les conclusions des projets (ceux qui viennent ainsi d'être lancés et d'autres, plus avancés) et comprennent des contributions importantes au vaste éventail de riches gisements miniers et géologiques du Manitoba. Le recueil est centré sur les nouvelles données concernant les occurrences d'or (GS2019-1, GS2019-2, GS2019-4), de graphite et de vanadium (GS2019-3, GS2019-6), de métaux communs (GS2019-4) et de lithium (GS2019-5). On y trouve également la suite de contributions sur le potentiel diamantifère régional (GS2019-9, GS2019-10), des études sur les dépôts de sable siliceux et de type Mississippi Valley (GS2019-8), des reconstructions de l'histoire glaciaire

et des paléoécoulements glaciaires (GS2019-9, GS2019-10) et une cartographie stratigraphique Phanérozoïque (GS2019-7, GS2019-8).

Une nouvelle cartographie des terranes géologiques et de nouvelles évaluations des interprétations géologiques au fil des ans sont essentielles si l'on veut conserver notre poids dans le marché mondial, demeurer informés des avancées scientifiques continues et maintenir et renforcer notre avantage concurrentiel. Compte tenu des variations de la demande mondiale en produits de base au fil du temps, des détails et des observations relevés sur le terrain il y a plusieurs décennies et qui étaient jusqu'ici sous-estimés ou ignorés ont soudain acquis une importance primordiale et sont devenus très recherchés. Mentionnons à titre d'exemple la nouvelle cartographie des substrats rocheux dans la région des lacs Russell et McCallum du nord-ouest du Manitoba (GS2019-3), où le graphite était brièvement mentionné il y a 40 ans. Le graphite naturel est un produit de base très important dans notre quotidien et la technologie actuelle, mais est aussi très recherché en raison de la demande prévue liée à la production de batteries au Li-ion. C'est là le reflet de l'évolution soutenue de notre société et de progrès technologiques où l'électrification et la recherche d'une économie à bilan carbone neutre sont actuellement nos principaux moteurs.

La Direction, tout en étant pleinement engagée dans des projets sur le terrain, travaille également d'arrache-pied à des initiatives internes visant à améliorer la prestation de services, le suivi des projets, l'uniformisation des publications de données géochimiques ainsi que la création et la compilation de cartes, avec notamment une nouvelle légende de carte commune à l'échelle 1:250 000°. La Section de la gestion des données géoscientifiques est un acteur clé dans l'intégration de Petrinex (qui fournit des services facilitant la gestion et l'échange d'information essentielle dans le secteur pétrolier), la maintenance continue d'iMaQs et de Map Gallery, l'élaboration de cartes pour le régime foncier de même que la formation et le soutien du personnel en SIG. La Direction est un membre actif du Comité de liaison sur l'exploration et l'exploitation minières du Manitoba qui, depuis sa formation en juin 2019, a fait des avancées importantes. Elle participe aussi activement au comité d'établissement de plans de masse, veillant à ce que la dimension de l'exploitation des ressources minières soit prise en compte dans l'aménagement du territoire. De plus, la Direction participe régulièrement à un grand nombre d'initiatives et de projets géoscientifiques collaboratifs avec l'industrie et le milieu universitaire et interagit avec ces intervenants.

Au cours de l'année écoulée, la Direction a connu des changements de personnel. Nous continuons de renforcer stratégiquement nos compétences par le recrutement de



trois nouveaux employés : Ashley Santucci (technicien de SIG), Paul Belanger (technicien de laboratoire) et Shaun Gallagher (géologue chargé des évaluations et des consultations). L'intégration de ces personnes talentueuses à notre équipe nous permettra d'avancer sur la voie de l'amélioration continue en vue d'une meilleure prestation de services. Simon Gagné, géologue de projets axés sur le Précambrien, et Sharon Lee, géologue SIG, ont quitté la Direction pour relever de nouveaux défis à Ottawa. Récemment, les décès prématurés de deux de nos collègues retraités de la Direction, Paul Lenton (géologue et gestionnaire, Précambrien et SIG) et Gerry Benger (gestionnaire d'activités de laboratoire de base) nous ont profondément émus. Ces deux collègues ont profondément marqué leur entourage et laisseront un souvenir impérissable du fait de leur attitude amicale et constructive, de leur talent et de leur sourire contagieux.

Le *Rapport d'activités 2019* est le fruit du travail dévoué et méticuleux de géologues, de techniciens de laboratoire, d'agents d'ordonnancement, d'étudiants stagiaires et de techniciens SIG de la Direction. Bob Davie et son équipe à RnD Technical ont pris soin de la révision technique et Craig Steffano a géré la production du rapport et la mise en pages de la publication. Je tiens à remercier tous les membres de la Direction de leurs précieuses contributions ainsi que du dévouement, de l'ardeur et du dynamisme dont ils font preuve dans le cadre des projets et des initiatives de l'année écoulée, qui ont donné de formidables résultats.

La directrice par intérim des Services géologiques,  
Michelle P. B. Nicolas, P. Geo., FGC

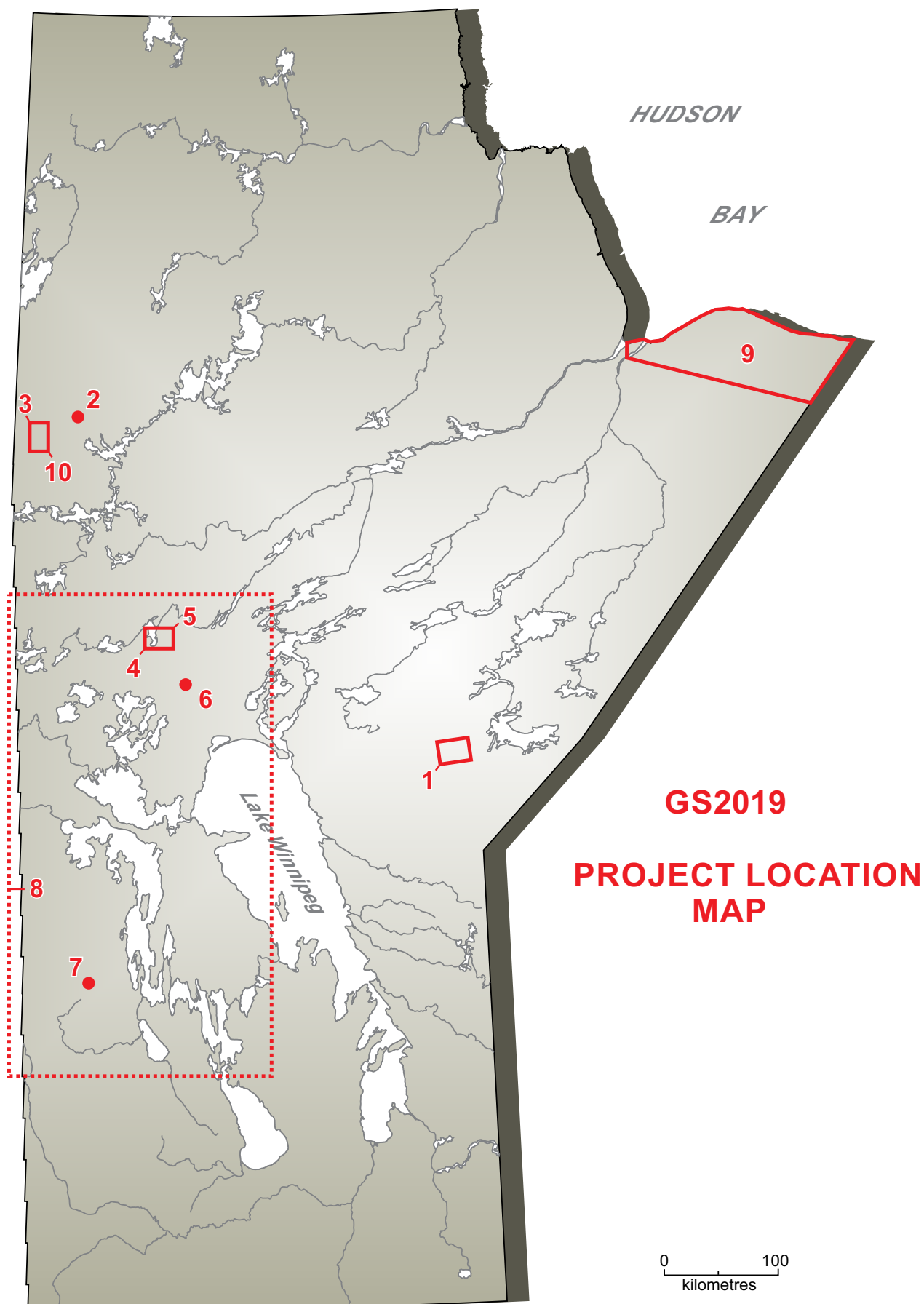


## Table of Contents

Minister's Message.....	iii
Message du ministre .....	iv
In Memoriam: Gerry Bengert .....	v
In Memoriam: Paul Lenton.....	vi
Foreword by M.P.B. Nicolas .....	viii
Avant-propos par M.P.B. Nicolas.....	x
GS2019 Project Location Map .....	xii

### PRECAMBRIAN

GS2019-1 Results of bedrock mapping at Knight Lake, east-central Manitoba (parts of NTS 53E11, 12, 13, 14) by M.L. Rinne.....	1
GS2019-2 Preliminary results of bedrock mapping in the Gemmell Lake area, Lynn Lake greenstone belt, northwestern Manitoba (parts of NTS 64C11, 14) by X.M. Yang .....	10
GS2019-3 Geological investigations in the Russell–McCallum lakes area, northwestern Manitoba (parts of NTS 64C3–6) by T. Martins and C.G. Couëslan .....	30
GS2019-4 Bedrock geological mapping of the Puella Bay area (Wekusko Lake), north-central Manitoba (part of NTS 63J12) by K.D. Reid .....	42
GS2019-5 Interpretation of U-Pb isotopic dates of columbite-group minerals in pegmatites, Wekusko Lake pegmatite field, central Manitoba (part of NTS 63J13) by D. Benn, T. Martins and R.L. Linnen .....	52
GS2019-6 Evaluation of graphite- and vanadium-bearing drillcore from the Huzyk Creek property, sub-Phanerozoic Kiseynew domain, central Manitoba (NTS 63J6) by C.G. Couëslan.....	60

### PHANEROZOIC

GS2019-7 First discovery of a Cretaceous fossil leaf in Manitoba (NTS 62N15) by K. Lapenskie .....	72
--	----



GS2019-8	
Summary of Phanerozoic core logging activities in Manitoba in 2019 (parts of NTS 63C3, 14, 63J5, 6, 11, 12, 14)	
by K. Lapenskie .....	77

## QUATERNARY

GS2019-9	
Quaternary stratigraphy and till sampling in the Machichi–Kettle rivers area, far northeastern Manitoba (parts of NTS 54A–C)	
by T.J. Hodder and M.S. Gauthier .....	83

GS2019-10	
Till sampling and ice-flow mapping in the Russell–McCallum lakes area, northwestern Manitoba (parts of NTS 64C3–6)	
by T.J. Hodder .....	90

## PUBLICATIONS

Manitoba Geological Survey Publications Released December 2018 to November 2019 .....	98
External Publications .....	101

### In Brief:

- Regional silicification and calcite alteration spatially associated with a number of known gold occurrences
- Gold mineralization hosted in a conjugate array of late brittle-ductile shears
- Widespread unit previously mapped as andesite confirmed to be silicified basalt

### Citation:

Rinne, M.L. 2019: Results of bedrock mapping at Knight Lake, east-central Manitoba (parts of NTS 53E11, 12, 13, 14); in Report of Activities 2019, Manitoba Agriculture and Resource Development, Manitoba Geological Survey, p. 1–9.

### Summary

The Manitoba Geological Survey resumed 1:20 000 scale bedrock mapping of the Bigstone Lake greenstone belt in the Knight Lake area. Field observations and geochemical analyses confirm that widespread units previously described as andesite are regionally silicified basalt. The extensive silicification and calcite alteration mapped through the eastern part of the belt is spatially associated with several known gold occurrences. Building on results from the 2017 field season, gold mineralization in the area is hosted primarily in a conjugate array of late brittle–ductile shears evident at both regional and outcrop scales. The completion of the 2019 field season marks the end of the planned mapping campaign, with results indicating strong potential for widespread and locally high-grade gold mineralization in the Bigstone Lake greenstone belt.

---

### Introduction

The Manitoba Geological Survey (MGS) resumed 1:20 000 scale mapping of the bedrock geology of the Bigstone Lake greenstone belt (BLGB). The primary aims of this mapping program were to

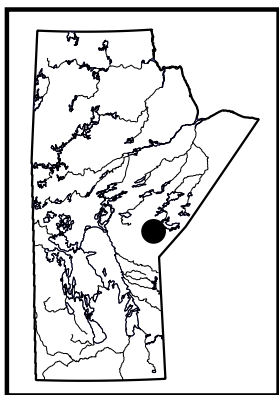
- document the supracrustal rocks of the BLGB through systematic mapping of unvisited areas along with remapping of some areas last visited in the 1980s; and
- provide a modern assessment of mineral potential in the area, including investigations of volcanogenic massive sulphide, magmatic Ni-Cu-PGE and lode-gold mineralization.

A related objective of the 2019 mapping program was to examine structural controls and alteration in the vicinity of known gold occurrences at Knight Lake, particularly in areas burned by a wildfire in 2017. Investigations in 2019 revealed that the recent wildfire exposed very little new outcrop (except for some granodiorite ridges); most of the inland burn areas were found to contain partially scorched but mostly standing forest with an intact ground layer of soil and superficially charred moss. The 2019 field season marks the completion of planned MGS field work on the BLGB. An open file release of geochemical data from the project is planned following receipt of results from the analysis of the 2019 field samples.

### Regional geology

The BLGB forms part of the Island Lake domain of the northwestern Superior Province. The western half of the BLGB, around Bigstone Lake, was mapped by the MGS during the 2016 and 2017 field seasons (Rinne et al., 2016; Rinne, 2017). The eastern half of the BLGB, around Knight, Wass and Clam lakes, is contiguous with the western part but offset by a thin corridor of regional southeast-trending dextral shears (Figure GS2019-1-1). Results of shoreline and inland mapping completed in the Knight Lake area during the 2019 field season are summarized in this report.

The oldest and stratigraphically lowermost units around Knight Lake occupy the northern and southern flanks of the BLGB (Figure GS2019-1-1). This mirrors the belt-scale syncline pattern in the western part of the belt around Bigstone Lake (Rinne et al., 2016), allowing for straightforward stratigraphic correlations between rock units in the Knight Lake and Bigstone Lake areas. Rocks of the BLGB have been metamorphosed to upper-greenschist to lower-amphibolite facies; the ‘meta’ prefix is omitted from this report for brevity.



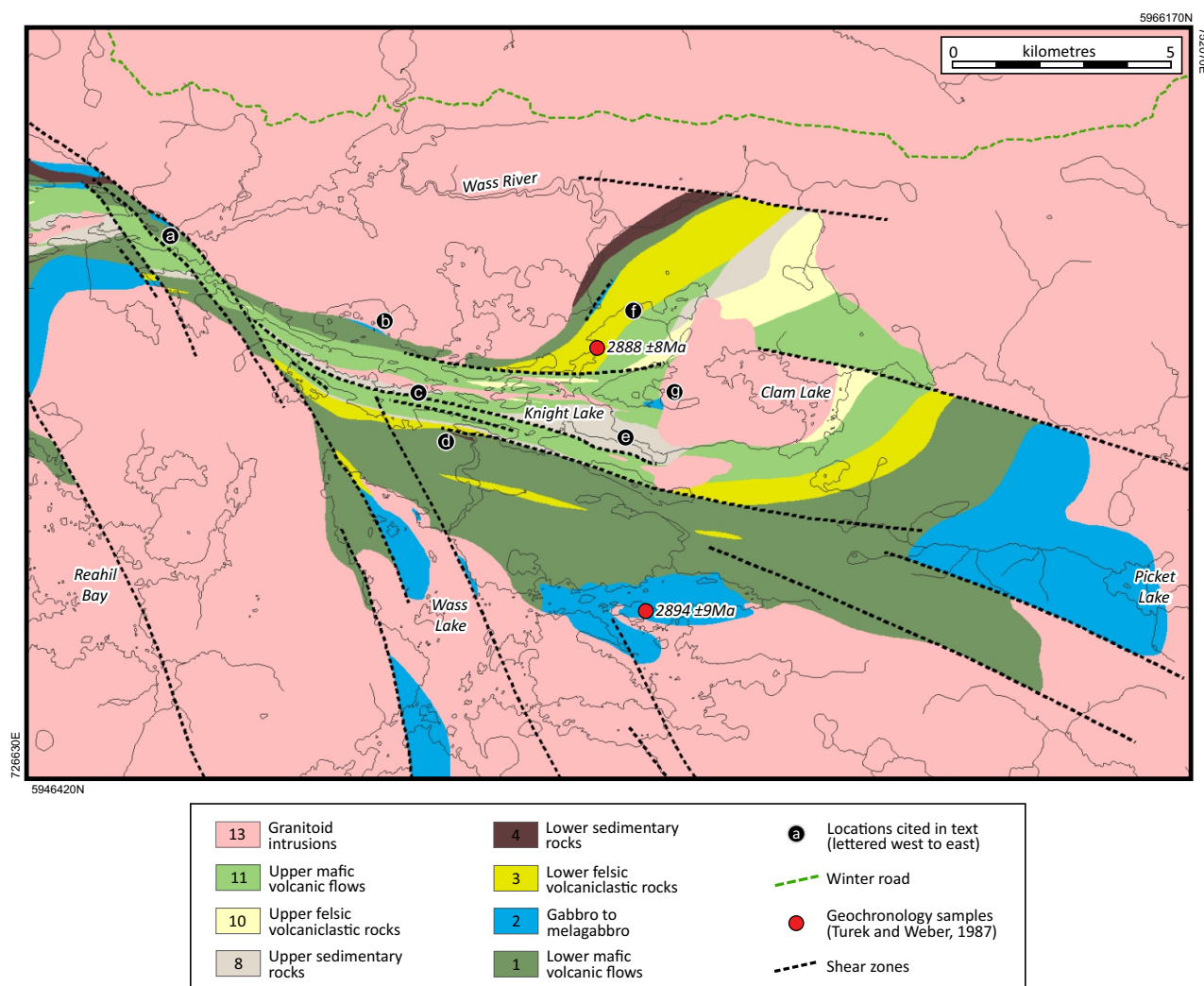


**Figure GS2019-1-1:** Bedrock geology of the Knight Lake area, simplified from Preliminary Map PMAP2019-1 (Rinne, 2019)<sup>1</sup>. Some features, such as fold axial traces, have been omitted for clarity and are indicated in Rinne (2019). Missing numbers in the unit legend correspond to units either not encountered in the Knight Lake area (peridotite, pyroxenite, komatiite and mafic-ultramafic lapilli tuff) or too small to display at the map scale (late tonalite and diorite intrusions). Units shown in the vicinity of Clam Lake, Picket Lake and Wass Lake are based mostly on a compilation of mapping by McIntosh (1941), Ermanovics (1975) and Neale (1985), along with bed-rock intercepts in drillcore (Assessment Files 91147, 92263, 92302, Manitoba Agriculture and Resource Development, Winnipeg). The regional shear zones (black dashed lines) correspond to distinct topographic lineaments, visible in satellite or airphoto imagery (with shears typically marked by darker, conspicuously linear valleys). Corner UTM coordinates are in NAD83, zone 14.

The unit numbers used in this report correspond to unit numbering in Rinne (2019). The numbering is discontinuous because of units not encountered in the Knight Lake area, namely peridotite, pyroxenite, komatiite, and mafic-ultramafic lapilli tuff, and of units too small to depict, specifically tonalite and diorite intrusions.

### Lower stratigraphic sequence

Rocks of the lower stratigraphic sequence are assigned to the Hayes River Group; published U-Pb ages from the

lower sequence indicate emplacement at ca. 2.9 Ga (Figure GS2019-1-1; Turek and Weber, 1987).

#### Lower mafic volcanic flows (unit 1)

Lower mafic volcanic flows are the most abundant unit in the eastern half of the BLGB, exposed along the northern and southern shores of Knight Lake as well as the northern part of Wass Lake (Figure GS2019-1-1). The rocks are grey-green on most weathered and fresh surfaces. Aphyric and variolitic pillows are predominant, with rare

<sup>1</sup> The units discussed in this report correspond to those shown on Preliminary Map PMAP2019-1 (Rinne, 2019), and Figure GS2019-1-1 represents a simplified version of this map.



quartz- and calcite-filled pillow shelves indicating way-up toward the centre of Knight Lake. Massive, plagioclase-phyric basalt is less common, along with rare interflow hyaloclastite breccia and garnetiferous mudstone in beds <40 cm thick. Interflow chert-magnetite iron formation was also noted by Noranda Exploration Company Limited at an unspecified location in the southwestern part of Knight Lake (Assessment File 94022).

#### **Gabbro to melagabbro (unit 2)**

Relatively thin (<200 m) gabbro intrusions were encountered near the northern margin of the BLGB near Wapatinasing Narrows (Figure GS2019-1-1, location a), in small islands in the northern part of Knight Lake (location b) and in a highly strained corridor in the northeastern part of Knight Lake (west of location f). Larger intrusions (~1–3 km thick) were documented by previous workers along the southern flank of the BLGB, including at Wass Lake and Picket Lake (Figure GS2019-1-1). The large gabbro unit at Picket Lake corresponds to a large magnetic-high feature and was noted in outcrop by Herd et al. (1987). A small body of gabbro west of Clam Lake (location g) was mapped inland by Ermanovics (1975) and was not visited in 2019. With the limited information available, this gabbro occurrence is provisionally assigned to the lower gabbro–melagabbro unit, but its stratigraphic position suggests it may instead represent either a late mafic dike or a massive portion of the upper mafic flow unit.

At Knight Lake, gabbro is equigranular and homogeneous at the outcrop scale, apart from strain partitioning. Fresh and weathered surfaces are grey-green to dark green and show approximately equal parts pyroxene (chlorite- and actinolite-replaced) and plagioclase <2 mm across. Contacts with adjacent units were not observed in 2019, although intrusive contacts with the lower mafic flow unit were noted at Bigstone Lake (Rinne, 2017). Turek and Weber (1987) also described inclusions of the lower mafic flow unit within a large gabbro intrusion in the northeastern part of Wass Lake. A sample of the same gabbro intrusion returned a U-Pb age of  $2894 \pm 9$  Ma (Figure GS2019-1-1; Turek and Weber, 1987).

#### **Lower felsic volcanoclastic and volcanic rocks (unit 3)**

Felsic rocks are intercalated with the lower mafic flow unit at several locations and consist mostly of tuff to lapilli tuff, with less abundant monomictic volcanic breccia. The felsic volcanoclastic rocks are exposed along much of the southern shore of Knight Lake, parts of the northeastern shore (near location f in Figure GS2019-1-1) and in inland areas south of Knight Lake and Clam Lake. The rocks have pale cream to light grey weathered surfaces and grey or

light grey fresh surfaces, commonly with conchoidal fractures. Ash to lapilli tuffs along the southwestern shores of Knight Lake contain black, glassy lenses or wisps up to 4 mm long that are interpreted as fiamme (Figure GS2019-1-2a); such outcrops were therefore identified as welded tuff.

Plagioclase-phyric dacite forms a minor component of the lower felsic unit in the northeastern corner of Knight Lake. The dacite contains an aphanitic and massive groundmass, unlike most tuff outcrops that show weak stratification. Although interpreted as a dome or flow within a thicker felsic tuff-dominated package, contacts were not observed and it is possible that the dacite represents a later dike (e.g., a porphyritic member of unit 12 described below).

Turek and Weber (1987) reported a U-Pb zircon age of  $2888.2 \pm 8$  Ma from a sample of plagioclase-phyric tuff from the northern shore of Knight Lake, in a location corresponding with the lower stratigraphic sequence (Figure GS2019-1-1). The same data were reportedly recalculated by Parks et al. (2014) to an age of 2852 Ma, although supporting data and errors were not provided with this revised age determination.

#### **Lower sedimentary rocks (unit 4)**

Mappable packages of the lower sedimentary unit were found only in the highly strained northeast-trending segment in the northeastern part of Knight Lake (northwest of location f in Figure GS2019-1-1) and near a series of rapids in the southern part of Knight Lake (location d). The grey rocks consist of planar-bedded quartzofeldspathic greywacke to mudstone in highly strained beds <10 cm thick, with ambiguous way-up indicators. An intrusive contact with granodiorite was noted in the northeastern part of Knight Lake, but contacts with adjacent supracrustal units were not observed.

#### **Upper stratigraphic sequence**

Rocks of the upper stratigraphic sequence occur in the centre of the BLGB and are provisionally assigned to the Island Lake Group (Rinne et al., 2016). Insufficient zircon yields from samples of upper felsic supracrustal rocks (with corresponding Zr contents of 6–19 ppm) have so far impeded age constraints on the emplacement of the upper sequence.

#### **Upper sedimentary rocks (unit 8)**

Sedimentary rocks are widely distributed throughout the upper stratigraphic sequence (Figure GS2019-1-1), and consist of greywacke-mudstone turbidites, ungraded

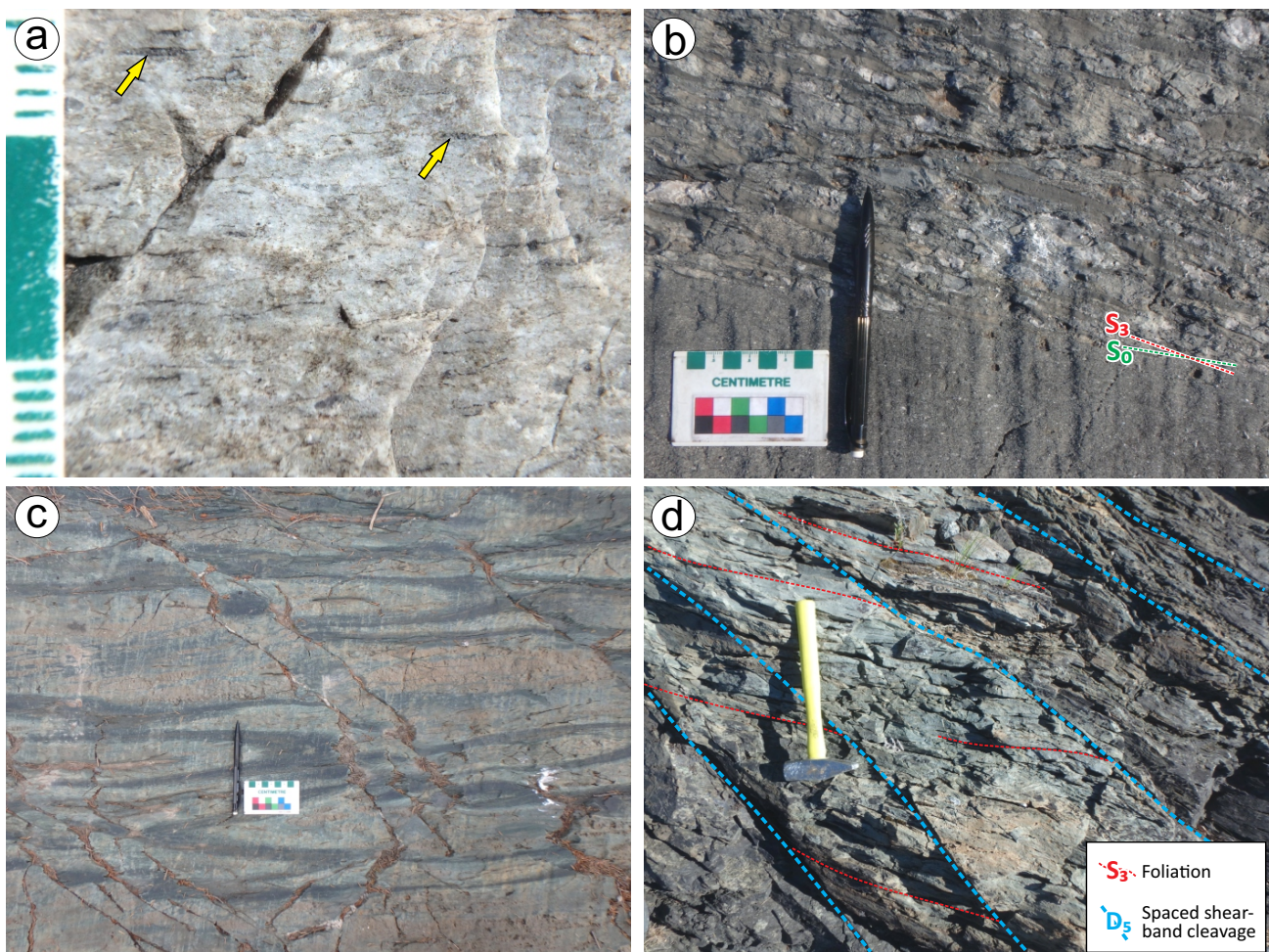


**Figure GS2019-1-2:** Outcrop photographs of Bigstone Lake greenstone belt units mapped in 2019, showing **a)** welded felsic ash tuff containing features interpreted as fiamme (thin black features; two examples are marked with arrows); **b)** ungraded coarse sandstone (bottom) and polymictic conglomerate (top), showing a nearly transposed angular relationship between bedding ( $S_0$ ; parallel to sandstone–conglomerate contact) and  $S_3$  foliation with clast flattening; **c)** silicified and calcite-altered pillow basalt with darker grey selvages and minor dextral offsets; **d)** silicified and intensely foliated basalt proximal to a late shear zone, showing  $S_3$  foliation dragged and offset by  $D_5$  shear-band cleavage planes. North is to the top in panels b–d.

coarse sandstone and polymictic conglomerate. Planar-bedded and normally graded greywacke-mudstone turbidites 5–40 cm thick are the most common. In the least-altered outcrops, the rocks are light grey to grey-green on weathered surfaces and grey (sandstone) to dark grey (mudstone) on fresh surfaces. Most clasts are <0.5 mm across, but thin pebbly bases are common, with sparse quartz clasts up to 5 mm across.

A few beds of ungraded, coarse quartz sandstone 5–80 cm thick were documented in spatial association with polymictic conglomerate. The rocks are similar in colour to the greywacke and contain abundant sub-rounded to subangular clasts 0.5–1.5 mm across, supported in a fine-grained, semipelitic sandstone matrix that locally contains dark grey muddy lenses. Clasts consist of approximately 70% quartz, 20% plagioclase or pale grey potassium feldspar and 10% pale cream-coloured

aphanitic fragments possibly derived from a felsic volcanic source. The ungraded coarse sandstone is most common in the central and eastern parts of the BLGB (Rinne, 2017).

Polymictic conglomerate was observed mostly at the eastern end of Knight Lake (Figure GS2019-1-1; location e), along with two isolated occurrences within turbidite-dominated packages along the southern shore of Knight Lake (south of location c) and in the high-strain corridor between Bigstone and Knight lakes (south of location a). The conglomerate occurs in beds ranging from 3 cm to greater than 2 m in thickness (in the case of single beds occupying whole outcrop exposures), with well-rounded clasts dominantly <2 cm but reaching up to 40 cm in length in some outcrops. The clasts are elongated parallel to  $S_3$  foliation (Figure GS2019-1-2b) and consist of white crystalline quartz (20–50% of clasts); pale cream-coloured

to light grey aphanitic felsic clasts (20–60%); dark grey mudstone (5–10%, locally cut by quartz veins truncated at clast margins); and rare greywacke, basalt and medium-grained granitic clasts. The clasts make up between 5 and 40% of the rock and are supported in a coarse matrix identical to the ungraded, coarse quartz sandstone described above. Bedding contacts with ungraded coarse sandstone were observed at several locations and are commonly nearly parallel to  $S_3$  foliation and clast flattening (Figure GS2019-1-2b).

#### **Upper felsic volcanoclastic rocks (unit 10)**

Mappable packages of upper felsic volcanoclastic rocks are limited mostly to the central and northeastern parts of Knight Lake and Clam Lake (Figure GS2019-1-1). The rocks are pale grey-beige, massive to crudely stratified tuff to lapilli tuff and locally grade into rare layers of monomictic felsic volcanic breccia with fine-grained plagioclase-phyric fragments up to 10 cm long. Contacts with adjacent supracrustal units were not observed at Knight Lake, but conformable contacts with the upper sedimentary unit were noted at Bigstone Lake (Rinne et al., 2016).

#### **Upper mafic volcanic flows (unit 11)**

The upper mafic volcanic flow unit dominates the upper stratigraphic sequence (Figure GS2019-1-1). Least-altered outcrops are grey-green to dark grey-green on weathered and fresh surfaces, and are compositionally identical to the lower flow unit. Strongly elongated varioles and vesicles are only locally preserved due to the intense strain in much of the Knight Lake area. At Bigstone Lake, vesicles were found to be more common in the upper mafic flows than in the lower mafic flows (Rinne et al., 2016). However, at Knight Lake the higher strain hinders textural distinctions between lower and upper mafic flows in outcrop. In most of the area shown in Figure GS2019-1-1, the location of the regional contact between the lower and upper mafic flow units is estimated to preserve stratigraphic continuity with the western half of the BLGB. This contact occurs at or above the lowermost occurrence of pebbly turbiditic sandstone and conglomerate, and stratigraphically below the first appearance of abundant vesicles (which are only locally preserved). Along both northern and southern shores of Knight Lake, the estimated lower contact of the upper volcanic flow unit also broadly corresponds with the locations of regional shear structures.

At Knight Lake, most outcrops of the upper mafic flows are silicified and calcite altered ( $\pm$ epidote and fuchsite). In cases of ‘moderate’ alteration (as identified in the field on the basis of overall colour, hardness and reaction to hydro-

chloric acid), the rocks have a light grey-beige colour on weathered surfaces and a grey or grey-green colour on fresh surfaces (Figure GS2019-1-2c). The regional extent of alteration is indicated in Figure GS2019-1-3a and appears to be spatially associated with an east-southeast-trending zone of higher strain through the centre of Knight Lake.

In areas previously mapped by the MGS (Neale, 1985), the altered basalt was identified as andesite. However, mapping in 2019 revealed several examples of gradational variations from relatively unaltered basalt to light grey, altered basalt, in some cases within uninterrupted outcrop exposures. Geochemical analyses of the silicified basalt, including one sample collected in 2017 from the northern shore of Knight Lake, yielded Zr/Ti ratios of 0.007 to 0.011 and Co contents of 30–52 ppm. In conjunction with the gradational changes from basalt to altered basalt described above, these results point to a silicified basalt as opposed to a primary andesite composition.

### ***Intrusive rocks***

#### **Tonalite to dacite dikes (unit 12)**

At Knight Lake, several aphyric dikes were identified in the field as dacite. These light grey dikes are interpreted as aphanitic equivalents to the fine-grained tonalite dikes documented at Bigstone Lake (Rinne et al., 2016; Rinne, 2017) and range from 5 cm to 3 m in thickness. As in all other dikes documented in the BLGB, they predate the  $D_3$  deformation event (they are commonly tightly folded about  $F_3$  fold axes and are overprinted by axial-planar  $S_3$  foliation) as well as regional calcite alteration.

#### **Granitoid intrusions (unit 13)**

Granodiorite to granite batholiths surround the BLGB, along with smaller intrusions that mostly crosscut upper stratigraphic units at Knight Lake and Clam Lake (Figure GS2019-1-1). The rocks are typically medium-grained and equigranular to weakly porphyritic, and vary in colour from white or light grey to light pink. Fine-grained mafic xenoliths, in places partially assimilated with amoeboid shapes and diffuse margins, are more common near the margins of the intrusions. They range from a few centimetres to 5 m across and are interpreted to have been sourced from the adjacent mafic flow units. Granodiorite dikes are also common throughout the BLGB and are most abundant near batholith margins.

#### **Diorite dikes (unit 14)**

Porphyritic diorite dikes crosscut several units in the Knight Lake area but are not mappable at 1:20 000 scale. They are light grey or light grey-green on fresh and



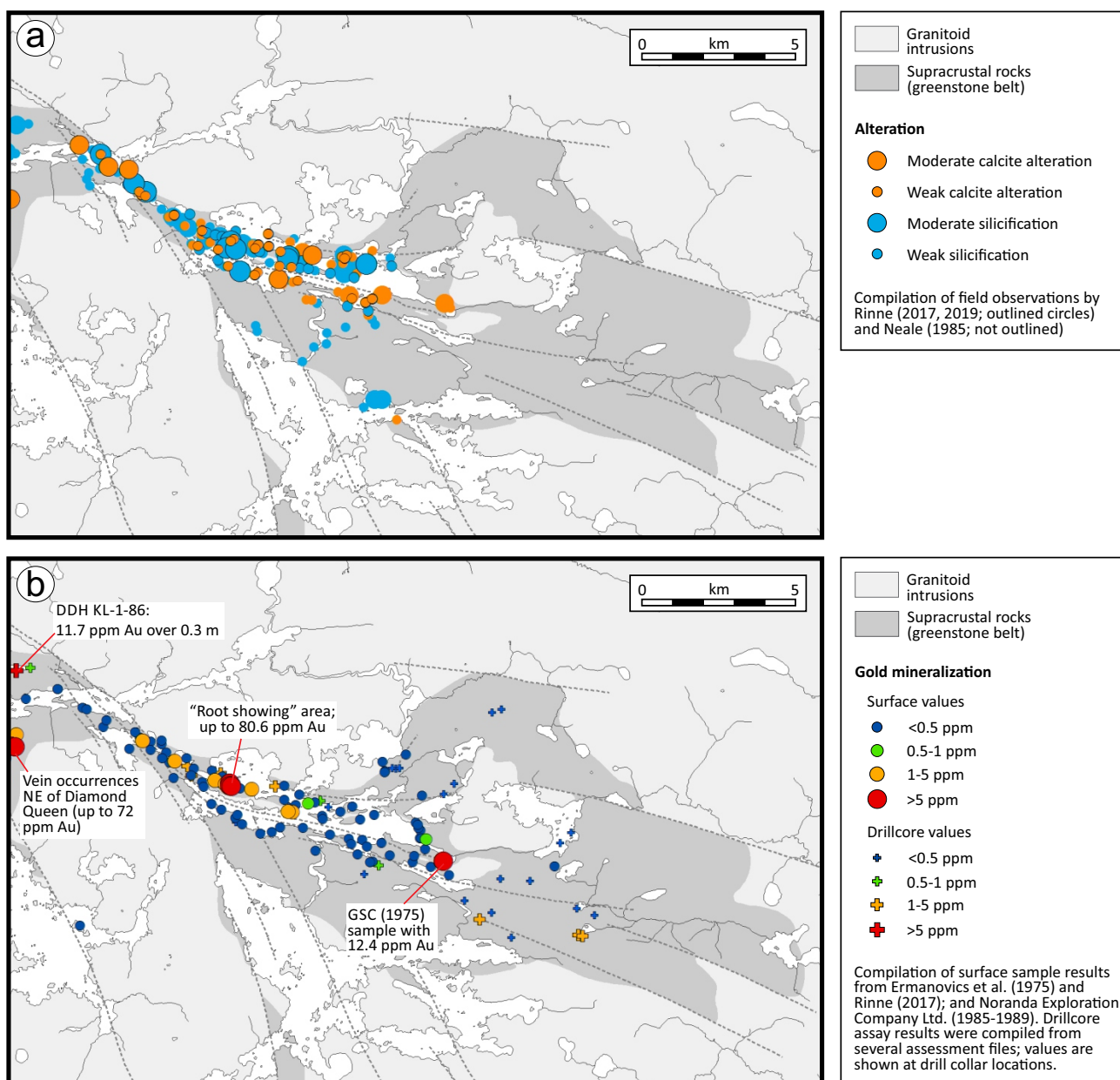


**Figure GS2019-1-3:** Maps of the eastern part of the Bigstone Lake greenstone belt (same area as in Figure GS2019-1-1), showing **a)** locations of calcite alteration and silicification documented by qualitative field assessments carried out by Neale (1985) and Rinne (during the 2017 and 2019 field seasons); **b)** locations of known gold mineralization at surface and in drillcore, with selected high-grade occurrences labeled.

weathered surfaces, and typically contain approximately 30% subhedral hornblende and approximately 10% plagioclase phenocrysts 0.5–10 mm across in a light grey, very fine-grained groundmass. In 2019, a plagioclase- and hornblende-phyric diorite dike was found to have crosscut a large granodiorite intrusion. The relative timing of the diorite and granitoid units was adjusted accordingly. In the Bigstone Lake area, the plagioclase- and hornblende-phyric diorite dikes were also found to have crosscut tonalite dikes and were crosscut by rare mafic dikes (the

latter representing the latest intrusive phase documented in the BLGB; Rinne, 2017).

### Structural geology

The BLGB records a complex structural history, as summarized in Rinne et al. (2016). Evidence for the  $D_1$ ,  $D_2$  and  $D_4$  events (pre-existing fabric developed in breccia clasts, early isoclinal folding expressed in structural facing reversals and late open folds, respectively) was not recognized during the 2019 field season, except for



possible early foliation in conglomerate clasts. Most of the map-scale patterns at Knight Lake and most of the structures measured in outcrop relate to the  $D_3$  and  $D_5$  events described below.

### ***D<sub>3</sub> deformation***

A well-developed, penetrative, near-vertical  $S_3$  foliation is readily identified in almost all supracrustal outcrops, with an overall eastward but variable strike that broadly parallels the supracrustal unit contacts in Figure GS2019-1-1. Limited way-up indicators in the Knight Lake area also point to a belt-scale  $F_3$ -syncline axial trace that trends east through the upper stratigraphic units, flanked by a series of at least two regional  $F_3$  anticlines and synclines (Rinne, 2019). Although parasitic isoclinal  $F_3$  folds with near-vertical plunges were noted in several outcrops throughout the BLGB, the regional  $F_3$ -fold architecture is not well constrained outside of areas containing turbiditic sandstone and pillow shelves.

### ***D<sub>5</sub> deformation***

The  $D_5$  deformation event is characterized by late brittle–ductile shears that range from outcrop (Figure GS2019-1-2d) to regional (Figure GS2019-1-1) scale. In the Knight Lake area,  $D_5$  dextral shears dominantly strike southeast, whereas the sinistral shears dominantly strike northeast. The shears are classified as brittle–ductile structures because they include both a discrete offset plane (brittle faulting) and a wider zone of deflection or drag of pre-existing fabric across the shear (ductile deformation).

Both dextral and sinistral shear sets were measured throughout the BLGB, but southeast-striking dextral shears are most prevalent in outcrop, particularly near the western end of Knight Lake. Outcrops within the higher strain corridor that separates the eastern and western halves of the BLGB (i.e., the thin zone of dextral offset panels around location a in Figure GS2019-1-1) commonly show either a southeast-striking and steeply dipping dextral crenulation cleavage or a spaced dextral shear-band cleavage (Figure GS2019-1-2d).

Although sinistral shears were found in the Bigstone Lake area to have offset the dextral shears, at Knight Lake they were found to both pre- and postdate the dextral shears. The simplest explanation for this relationship is that the late brittle–ductile shears form a mutually cross-cutting conjugate array that formed in response to the same stress field. Sinistral shears previously assigned to a tentative  $D_6$  event (Rinne et al., 2016; Rinne, 2017) are therefore re-assigned to the earlier  $D_5$  deformation event. This interpretation, which involves a single (though possibly prolonged) episode of late brittle–ductile deformation,

is also the simplest scenario that would account for the occurrence of the same gold-bearing vein assemblages in both the dextral and sinistral shear sets.

## **Gold mineralization**

Known gold occurrences in the Knight Lake area were mostly discovered during mapping and trenching by Noranda Exploration Company Limited in the late 1980s, with the highest grade of 80.6 ppm Au recovered near the ‘Root showing’ labeled in Figure GS2019-1-3b (Assessment File 94511). Noranda workers noted shear-hosted pyrite, arsenopyrite, sphalerite and galena in the Root showing area, along with chlorite and calcite alteration (Assessment File 94022). Much of the Root showing area has revegetated (and more recently burned) since the Noranda trenching. Traverses of the area in 2019 did not reveal significant vein or sulphide occurrences other than a gossanous float sample.

In 2017, several previously undocumented gold-bearing veins were sampled approximately 1.5 km northeast of historical gold occurrences known as the Diamond Queen veins (near the area labeled at the western side of Figure GS2019-1-3b). The veins contain quartz±calcite, pyrite, chalcopyrite, galena, arsenopyrite, chlorite, fuchsite, epidote, and (in one vein) visible gold. They range from <1 cm to 2 m thick and were found in both the sinistral and dextral shear sets (Rinne, 2017).

In 2019, inland investigations of historical gold occurrences and potentially related topographic lineaments in the Knight Lake area did not reveal occurrences of visible gold. However, the area was found to contain several examples of  $D_5$  shear-hosted veins containing similar assemblages (quartz±calcite, pyrite, chlorite, fuchsite, epidote and likely tourmaline). In outcrops of granodiorite, the veins are also commonly rimmed by diffuse and recessively weathered chlorite-calcite halos a few centimetres wide. The veins range from 1 to 40 cm in width and were found in both sinistral and dextral shears. Although assay results from the 2019 field season are pending, the distribution of gold occurrences found to date indicates widespread and locally high-grade gold mineralization in the BLGB (Figure GS2019-1-3b).

## **Alteration**

Mapped alteration patterns in the Knight Lake area show an overall east-southeast-trending zone of calcite alteration and silicification, extending from the eastern part of Bigstone Lake through the centre of Knight Lake (Figure GS2019-1-3a). Unlike the multiple (and in places spatially distinct) alteration assemblages identified at Bigstone Lake, the alteration at Knight Lake shows little

separation between zones of silicification ( $\pm$ epidote, chlorite) and calcite ( $\pm$ fuchsite, minor sericite) alteration. Instead, most outcrops in the centre of Knight Lake show additions of both silica and calcite.

The regional calcite alteration and silicification is both pervasive (diffuse, very fine grained) and texturally selective (e.g., quartz and calcite after pillow selvages). The alteration is also commonly accompanied by isolated patches of bright green fuchsite, along with submillimetre calcite veinlets and the shear-hosted quartz-calcite-pyrite veins described above. The presence of an orange carbonate mineral was noted in a few outcrops near the centre of Knight Lake (near location c in Figure GS2019-1-1) and it was tentatively identified as ankerite. More detailed mapping of the alteration zones may provide vectors to lode-gold mineralization in the area, especially with respect to potentially ore-proximal occurrences of Fe-carbonates or abundant sericite (e.g., Groves et al., 1998).

### **Exploration implications**

Results of the 2017 mapping program confirmed that topographic lineaments in the BLGB (shallow, mostly vegetated linear valleys, ranging from metres to tens of metres in width) correspond to late brittle–ductile shears that host gold-bearing veins (Rinne, 2017). Although the 2019 investigations of topographic lineaments at Knight Lake were largely unsuccessful in terms of sample recovery, workers of Noranda Exploration Company Limited did note that most of the gold-bearing zones in the Knight Lake area were found “along topographic lows ... beneath shallow overburden” (Assessment File 94011). These findings present an opportunity given that: 1) zones of shallowly buried shear-hosted mineralization would have been easily overlooked by previous workers in the BLGB; and 2) the geometry and density of topographic lineaments can be applied toward a targeted-drilling or shallow-trenching campaign, particularly in the context of other information such as alteration zonation.

### **Economic considerations**

The bedrock geology of the BLGB demonstrates broad potential for both ultramafic-hosted Ni-Cu ( $\pm$ Co, Cr, PGE) mineralization and volcanogenic massive sulphide mineralization (Rinne et al., 2016). The mafic–ultramafic lapilli tuff identified in the southern part of Bigstone Lake (Rinne et al., 2016) could also be further investigated with respect to its similarities with the diamond-bearing alkaline volcanoclastic rocks discovered at Knee Lake (Anderson, 2017). Felsic intrusions surrounding the BLGB may even be prospective for Archean porphyry-style Cu-Mo mineralization as in the Island Lake greenstone belt (Bella Lake pluton).

However, the most obvious potential for economic mineralization in the BLGB, based on the results of renewed mapping and compilation work, is in orogenic lode-gold mineralization.

Detailed exploration work in the BLGB was last undertaken between 1986 and 1993 (e.g., Assessment Files 94359, 94022, 94035). Recent mapping results in the BLGB, along with information compiled from past work in the area (such as shown in Figure GS2019-1-3b), would readily support surface and subsurface exploration for gold mineralization near the known occurrences, including new structural targets and related exploration suggestions outlined in Rinne (2017).

### **Acknowledgments**

The author thanks K. Roberts for his capable and cheerful assistance during an unusually smoke-filled field season, E. Anderson and M. Schreckenbach for their expediting assistance; C. Epp for his assistance with sample preparation; C. Couëslan and C. Böhm for their reviews; A. Santucci for her assistance with mapping software; and staff and pilots of Wings Over Kissing for crew transport and resupply flights.

### **References**

- Anderson, S.D. 2017: Detailed stratigraphic and structural mapping of the Oxford Lake–Knee Lake greenstone belt at southern and central Knee Lake, Manitoba (parts of NTS 53L15, 53M2); *in* Report of Activities 2017, Manitoba Growth, Enterprise and Trade, Manitoba Geological Survey, p. 1–11.
- Ermanovics, I.F. 1975: Preliminary map of Bigstone and Knight lakes, Island Lake area, Manitoba; Geological Survey of Canada, Open File 282, scale 1:63 360.
- Ermanovics, I.F., Park, G., Hill, J. and Goetz, P.A. 1975: Geology of Island Lake map area (53E), Manitoba and Ontario; *in* Report of Activities, Part A, Geological Survey of Canada, Paper 75-1A, p. 311–316.
- Groves, D.I., Goldfarb, R.J., Gebre-Mariam, M., Hagemann, S.G. and Robert, F. 1998: Orogenic gold deposits: a proposed classification in the context of their crustal distribution and relationship to other gold deposit types; *Ore Geology Reviews*, v. 13, p. 7–27.
- Herd, R.K., Currie, K.L. and Ermanovics, I.F. 1987: Island Lake area, Manitoba and Ontario; Geological Survey of Canada, Map 1646A, scale 1:250 000, with descriptive notes.
- McIntosh, R.T. 1941: Bigstone Lake area; Manitoba Mines and Natural Resources, Mines Branch, Publication 38-1, 12 p., map at scale 1:63 360.
- Neale, K.L. 1985: Geological investigations in the Knight Lake–Bigstone Lake area; *in* Report of Field Activities 1985, Manitoba Energy and Mines; Geological Services/Mines Branch, p. 200–202.

- Parks, J., Lin, S., Davis, D.W., Yang, X.-M., Creaser, R.A. and Corkery, M.T. 2014: Meso- and Neoarchean evolution of the Island Lake greenstone belt and the northwestern Superior Province: evidence from lithogeochemistry, Nd isotope data, and U–Pb zircon geochronology; *Precambrian Research*, v. 246, p. 160–179.
- Rinne, M.L., Anderson, S.D. and Reid, K.D. 2016: Preliminary results of bedrock mapping at Bigstone Lake, northwestern Superior province, Manitoba (parts of NTS 53E12, 13); *in* Report of Activities 2016, Manitoba Growth, Enterprise and Trade, Manitoba Geological Survey, p. 51–62.
- Rinne, M.L. 2017: Preliminary results of bedrock mapping at Bigstone Lake and Knight Lake, northwestern Superior province, Manitoba (parts of NTS 53E11, 12, 13, 14); *in* Report of Activities 2017, Manitoba Growth, Enterprise and Trade, Manitoba Geological Survey, p. 19–29.
- Rinne, M.L. 2019: Bedrock geology of the Knight Lake area, Manitoba (parts of NTS 53E11, 12, 13, 14); Manitoba Agriculture and Resource Development, Manitoba Geological Survey, Preliminary Map PMAP2019-1, scale 1:20 000.
- Turek, A. and Weber, W. 1987: U-Pb zircon geochronology of Bigstone Lake–Knight Lake area; *in* Report of Field Activities 1987, Manitoba Energy and Mines, Minerals Division, p. 148–150.

## Preliminary results of bedrock mapping in the Gemmell Lake area, Lynn Lake greenstone belt, northwestern Manitoba (parts of NTS 64C11, 14)

by X.M. Yang

### In Brief:

- Detailed bedrock mapping provides an updated geological framework for gold mineralization
- Gold mineralization is hosted in mylonite and silicified-sericitized felsic volcanic to volcanoclastic rocks and in quartz diorite intrusions
- Quartz diorite intrusions of the Post-Sickle intrusive suite may provide an important guide to gold mineralization

### Citation:

Yang, X.M. 2019: Preliminary results of bedrock mapping in the Gemmell Lake area, Lynn Lake greenstone belt, northwestern Manitoba (parts of NTS 64C11, 14); in Report of Activities 2019, Manitoba Agriculture and Resource Development, Manitoba Geological Survey, p. 10–29.

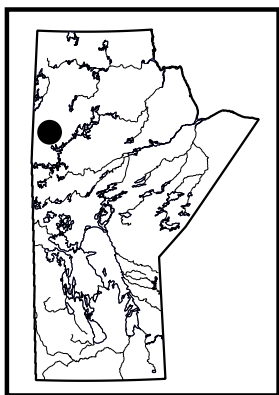
### Summary

In 2019, the Manitoba Geological Survey continued a multiyear bedrock mapping project in the Paleoproterozoic Lynn Lake greenstone belt. Detailed mapping at 1:20 000 scale was focused on the southern supracrustal belt in the Gemmell Lake area to resolve some of the key questions about the relationship of Au mineralization to structures, hostrocks, granitoid intrusions and tectonic evolution, and to support ongoing exploration activity in the belt. Preliminary mapping indicates that the area is underlain dominantly by the Wasekwan group supracrustal rocks, comprising massive to pillowed basalt, basaltic andesite, dacite to rhyolite and related volcanoclastic rocks, and subordinate sedimentary rocks. The volcanic sequence is spatially and temporally associated with reworked volcanoclastic and epiclastic rocks, suggestive of deposition in a setting comparable to modern volcanic arcs or back-arc basins. Unconformably overlying the Wasekwan group are the Sickle group sandstone and polymictic conglomerate, which are interpreted to have formed in localized synorogenic basin(s). A set of intrusions divided into pre-Sickle, post-Sickle and late intrusive suites cuts the supracrustal rocks, which were subjected to multiple phases ( $D_1$  to  $D_6$ ) of deformation and metamorphism.

Two styles of Au mineralization are evident in the map area: 1) Au-bearing mylonite and silicified-sericitized ( $\pm$ disseminated arsenopyrite, pyrite) felsic volcanic to volcanoclastic rocks controlled by the Johnson shear zone, which is related to  $D_2$  deformation and intersected by  $D_3$  faults and associated structures; and 2) intrusion-hosted Au-bearing quartz ( $\pm$ carbonate, sulphide) vein systems controlled by intersections of  $D_4$  faults and the  $D_2$  Johnson shear zone. Although the source of auriferous fluids is enigmatic, the field relationships suggest that timing of the Au mineralization was syn- to post- $D_2$  deformation. The  $D_2$  event postdated the pre-Sickle intrusions, postdated or was contemporaneous with the post-Sickle intrusive suites, and predated the late intrusive suite. The post-Sickle adakite-like quartz diorite intrusions (subunit 7a) were likely emplaced in a post-subduction extensional setting resulting from the upwelling of asthenosphere mantle due to the rollback of the subducting slab (or collapse of the orogen and/or relaxation due to delamination from the base of thickened lithosphere after terminal terrane collision). This was accompanied by anomalous heating that may have triggered the upward migration of auriferous fluids from the lower crust or upper lithosphere mantle along deep fault(s) connecting to the Johnson shear zone and associated structures in the middle to upper crust, consequently concentrating Au mineralization in favourable sites (e.g., chemical-structural traps). Simultaneously, these processes led to the formation of restricted synorogenic basin(s) that were filled by the Sickle group sediments, eroded from the uplifted greenstone belt.

### Introduction

Detailed mapping at 1:20 000 scale in the summer of 2019 was concentrated on the Gemmell Lake area in the southern belt of the Lynn Lake greenstone belt (LLGB; Figure GS2019-2-1), where Au mineralization displays features distinct from those at the MacLellan, Gordon (formerly Farley Lake) and Burnt Timber Au deposits elsewhere in the LLGB. Gold mineralization in the mapping area occurs either as 1) Au-bearing silicified-sericitized mylonite and sheared felsic volcanic to volcanoclastic rocks ( $\pm$ very fine grained arsenopyrite, pyrite disseminations) confined by the Johnson shear zone (JSZ), which is intersected by north-northwest-trending fault structures (e.g., the Gemmell Lake Au





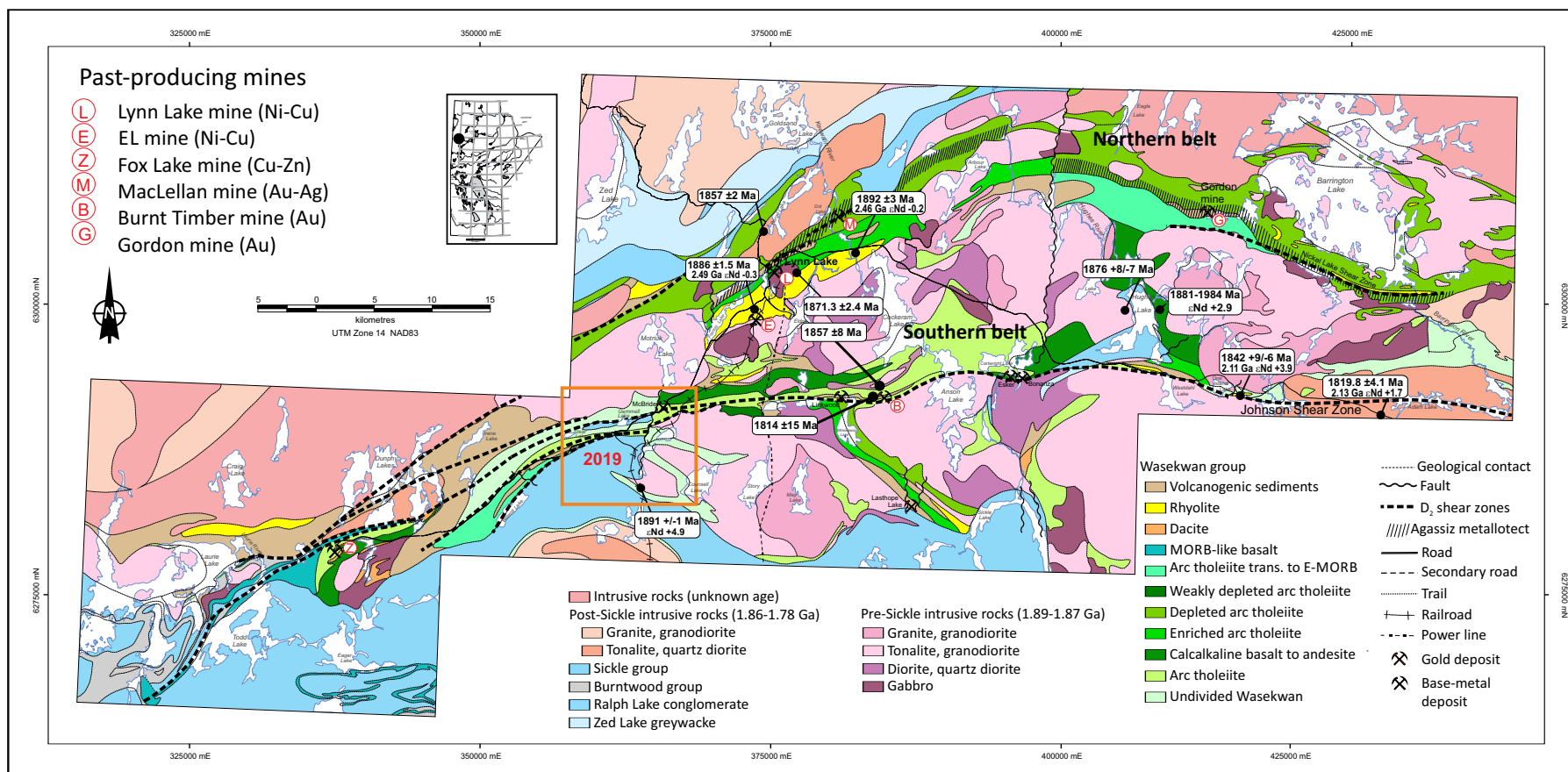


**Figure GS2019-2-1:** Regional geology with U-Pb zircon ages and Nd isotopic compositions of the Lynn Lake greenstone belt (modified and compiled from Gilbert et al., 1980; Manitoba Energy and Mines, 1986; Gilbert, 1993; Zwanzig et al., 1999; Turek et al., 2000; Beaumont-Smith and Böhm, 2002, 2003, 2004; Jones, 2005; Beaumont-Smith et al., 2006; Jones et al., 2006; Beaumont-Smith, 2008; Yang and Beaumont-Smith, 2015b, 2016, 2017). The 2019 mapping area is indicated by the orange box. Abbreviation: E-MORB, enriched mid-ocean-ridge basalt.

occurrence; Beaumont-Smith and Edwards, 2000; this study), or 2) Au-bearing quartz ( $\pm$ carbonate, sulphide, Te-bearing minerals) vein systems cutting quartz diorite intrusions (e.g., McBride and Finlay McKinlay Au occurrences; Baldwin, 1987; Sherman et al., 1988, 1989; Sherman, 1992; Ferreira, 1993). In the southern belt, the Burnt Timber deposit is controlled mainly by chemical-structural traps (Yang and Beaumont-Smith, 2017) within the JSZ (Fedikow et al., 1991; Peck et al., 1998; Jones, 2005; Jones et al., 2006). The MacLellan and Gordon deposits in the northern belt of the LLGB are hosted in the regionally extensive Agassiz metatolite (Fedikow and Gale, 1982; Fedikow, 1986, 1992; Ma et al., 2000; Ma and Beaumont-Smith, 2001; Park et al., 2002; Yang and Beaumont-Smith, 2015a, 2015b, 2016). Detailed bedrock mapping is critical to understanding these differences in order to provide crucial constraints for the Au metallogeny of the LLGB and assistance for Au exploration in the belt.

This report presents new data on the geology, structure and metamorphism of the Gemmell Lake area; provides an updated geological and regional structural framework for the mapping area; and discusses implications for Au mineralization by the post-Sickle intrusive suite. The accompanying preliminary map (PMAP2019-2; Yang, 2019a) was created from 228 field stations, including 251 structural measurements collected in 2019 as well as compiled historical data (167 stations from Gilbert et al., 1980; 3 stations from Zwanzig et al., 1999; 131 stations from Beaumont-Smith, 2008; and a handful of historical drill data), and detailed airborne magnetic data kindly provided by Alamos Gold Inc.

## Regional geology

The LLGB (Bateman, 1945) is endowed with various minerals, such as orogenic Au, magmatic Ni-Cu-Co and volcanogenic massive sulphide (VMS) Zn-Cu. It is a major tectonic element of the internal Reindeer zone of the Trans-Hudson orogen (Stauffer, 1984; Lewry and Collerson, 1990), which is the largest Paleoproterozoic orogenic belt of Laurentia (Hoffman, 1988; Corrigan et al., 2007, 2009; Corrigan, 2012). The belt is bounded to the north by the Southern Indian domain, composed of variably migmatitic metasedimentary rocks, various granitoids and minor metavolcanic and volcanoclastic rocks (Kremer et al., 2009; Martins et al., 2019). Synorogenic basins, including the Kiseynew metasedimentary domain, represent the southern limit of the LLGB (Gilbert et al., 1980; Fedikow and Gale, 1982; Syme, 1985; Zwanzig et al., 1999; Beaumont-Smith and Böhm, 2003, 2004; Zwanzig and Bailes, 2010). Paleoproterozoic greenstone belts with ages and lithological assemblages similar to the LLGB occur to the

east (Rusty Lake belt), to the west (La Ronge belt) and to the far south (Flin Flon belt; e.g., Ansdell et al., 1999; Park et al., 2002; Ansdell, 2005; Corrigan et al., 2007, 2009, 2012; Glendenning et al., 2015; Hastie et al., 2018; Lawley et al., 2019).

The LLGB consists of two east-trending, steeply dipping belts that contain various supracrustal rocks, known locally as the Wasekwan group (Bateman, 1945; Gilbert et al., 1980), along with younger, molasse-type sedimentary rocks that constitute the Sickle group (Norman, 1933). The southern and northern belts are separated by granitoid plutons of the 1.89–1.87 Ga Pool Lake intrusive suite (Gilbert et al., 1980; Baldwin et al., 1987; Beaumont-Smith et al., 2006), which are further divided into pre- and post-Sickle intrusions based on their temporal relationships to the Sickle group. In the central and southern parts of the LLGB, the Sickle group overlies the Wasekwan group and felsic–mafic plutonic rocks of the Pool Lake intrusive suite along an angular unconformity (Gilbert et al., 1980). The Sickle group correlates well with the 1850–1840 Ma MacLennan group in the La Ronge greenstone belt of Saskatchewan in terms of lithological composition, stratigraphic position and contact relationships (Ansdell et al., 1999; Ansdell, 2005; Corrigan et al., 2009). Volcanic and plutonic rocks in the LLGB underwent peak metamorphism at 1.81–1.80 Ga. Cutting the entire LLGB are the much younger Mackenzie dikes (ca. 1267 Ma; Baragar et al., 1996), as indicated by regional aeromagnetic data.

Significant differences in the geology and geochemistry of the northern and southern belts in the LLGB may reflect regional differences in tectonic settings that were obscured by structural transposition and imbrication during multiple stages of deformation (Gilbert et al., 1980; Syme, 1985; Zwanzig et al., 1999). This complexity leads to the suggestion that the term ‘Wasekwan group’ should be abandoned because it contains disparate volcanic assemblages that were later structurally juxtaposed during the evolution of the LLGB (Zwanzig et al., 1999), and thus may represent a tectonic collage similar to that described in the Flin Flon belt (e.g., Stern et al., 1995). However, this report retains the term ‘Wasekwan group’ to maintain consistency with previous LLGB-related literature.

## Geology of the Gemmell Lake area

The Gemmell Lake area, outlined in orange in Figure GS2019-2-1, is located in the southern belt of the LLGB and consists dominantly of the Wasekwan group supracrustal rocks intruded by plutons of the Pool Lake intrusive suite, which were unconformably overlain by the Sickle group epiclastic rocks (Figure GS2019-2-2; Yang, 2019a). Following the convention of previous workers (e.g., Beaumont-

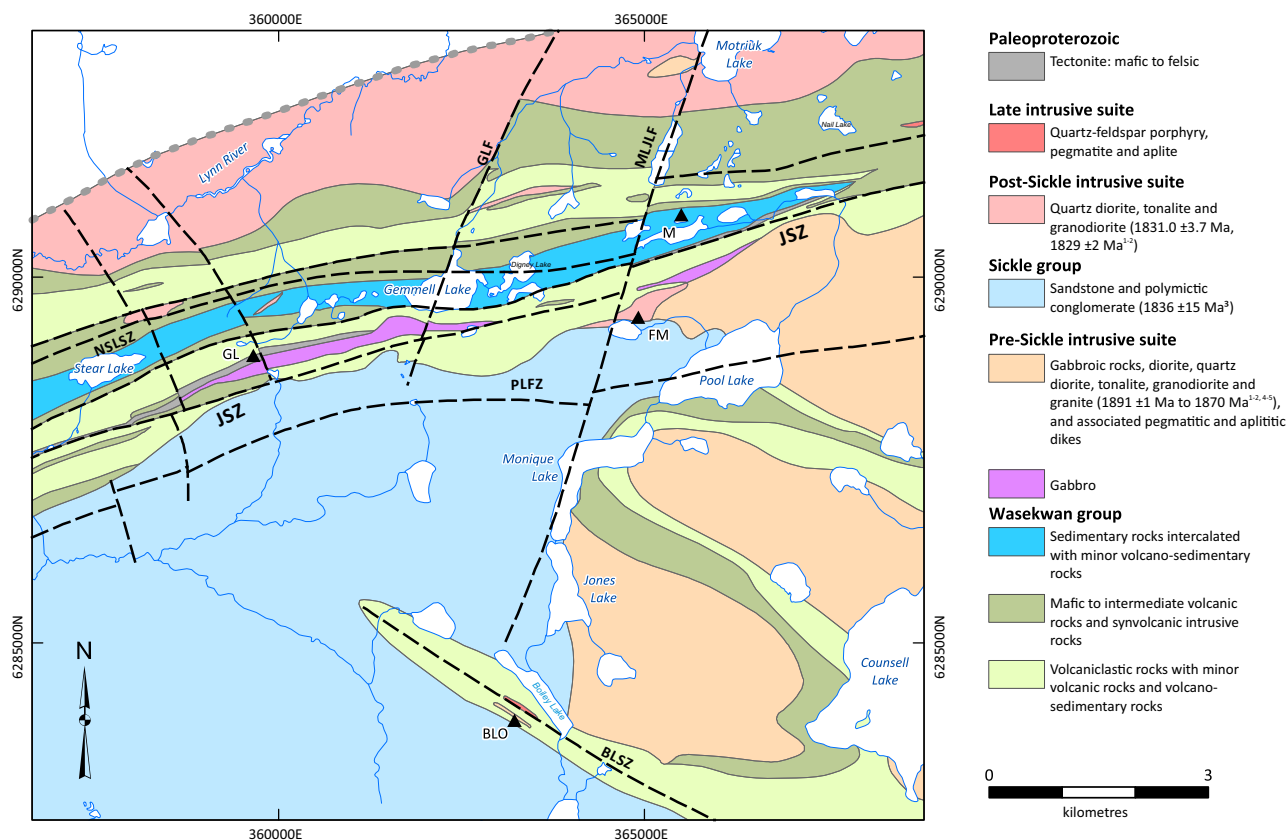


**Figure GS2019-2-2:** Simplified geology of the Gemmell Lake area, Lynn Lake greenstone belt, northwestern Manitoba (modified from Yang, 2019a). Black triangles indicate mineral occurrences: BLO, Boiley Lake Cu-(Au-Zn) occurrence; FM, Finlay McKinlay Au occurrence; GL, Gemmell Lake Au occurrence; M, McBride Au occurrence. Coarse dashed line indicates shear zone or fault: BLSZ, Boiley Lake shear zone; GLF, Gemmell Lake fault; JSZ, Johnson shear zone; MLJLF, Motriuk Lake–Jones Lake fault; NSLSZ, North Stear Lake shear zone; PLFZ, Pool Lake fault zone. Superscript numbers following U-Pb zircon ages in legend correspond to references in footnote of Table GS2019-2-1.

Smith and Böhm, 2004), intrusions cutting the Wasekwan group (i.e., the Pool Lake intrusive suite of Gilbert et al., 1980) and those cutting the Sickle group are called, respectively, the pre-Sickle and post-Sickle (e.g., Milligan, 1960) suites; both are cut by a late intrusive suite, comparable to those identified in the areas of the MacLellan, Gordon and Burnt Timber Au mines (Yang and Beaumont-Smith, 2015a, b, 2017). Note that the structural terms used in this report follow those in Beaumont-Smith and Böhm (2003, 2004).

Nine map units comprising 18 subunits were defined during the course of bedrock mapping, which led to grouping into six affiliations: Wasekwan group, pre-Sickle intrusive suite, Sickle group, post-Sickle intrusive suite, late intrusive suite and tectonite (Table GS2019-2-1). These map units are described in the following sections and shown in Figure GS2019-2-2. The supracrustal rocks in the LLGB were mostly deformed and metamorphosed to greenschist and amphibolite facies (Gilbert et al., 1980; Beaumont-Smith and Böhm, 2004; Yang and Beaumont-

Smith, 2015b, 2016, 2017); however, for brevity, this report omits the prefix ‘meta’.

### Wasekwan group (units 1 to 3)

Supracrustal rocks of the Wasekwan group exposed in the Gemmell Lake area are divided into the three units described below (see also Table GS2019-2-1).

#### Volcaniclastic rocks with minor volcanic rocks (unit 1)

Rocks of unit 1 are widespread in the central (e.g., north of Gemmell Lake), east-central (e.g., south of Pool Lake), southeastern (e.g., south of Boiley Lake) and western parts of the map area (Figure GS2019-2-2; Yang, 2019a). Covering a spectrum of rock types, unit 1 consists of mafic volcaniclastic rocks and intermediate–felsic volcanic and volcaniclastic rocks that, in places, appear to have been reworked by sedimentary processes. The volcaniclastic rocks of unit 1 include mafic breccia, tuff breccia, lapillistone, lapilli tuff and tuff; minor mafic mudstone and

**Table GS2019-2-1:** Lithostratigraphic units of the Gemmell Lake area, Lynn Lake greenstone belt, northwestern Manitoba

Unit <sup>1</sup>	Rock type	Affiliation
9	Tectonite: mafic to felsic	Tectonite
<i>Structural contact</i>		
8	Quartz-feldspar porphyry, pegmatite and aplite	Late intrusive suite
<i>Intrusive contact</i>		
7	Quartz diorite, tonalite and granodiorite (1831.0 ±3.7 Ma, 1829 ±2 Ma <sup>2,3</sup> )	Post-Sickle intrusive suite
7a	Quartz diorite, tonalite	
7b	Granodiorite	
<i>Intrusive contact</i>		
6	Sandstone and polymictic conglomerate (1836 ±15 Ma <sup>4</sup> )	Sickle group
6a	Arkosic sandstone and quartz pebbly sandstone	
6b	Polymictic conglomerate with minor pebbly sandstone	
<i>Unconformity</i>		
5	Gabbroic rocks, diorite, quartz diorite, tonalite, granodiorite, and granite (1891 ±1 Ma to ~1870 Ma <sup>2,3,5,6</sup> ) and associated pegmatitic and aplitic dikes	Pre-Sickle intrusive suite
5a	Tonalite, granodiorite and granite, and associated pegmatitic and aplitic dikes	
5b	Diorite, quartz diorite and minor gabbroic rocks	
5c	Muscovite-bearing granite	
4	Gabbro	
<i>Intrusive contact</i>		
3	Sedimentary rocks intercalated with minor volcanic sedimentary rocks	
3a	Argillite, siltstone and greywacke	
3b	Banded iron formation	
3c	Volcanic mudstone, siltstone, sandstone and minor volcanic breccia	
<i>Structural contact</i>		
2	Mafic–intermediate volcanic rocks and synvolcanic intrusive rocks	Wasekwan group
2a	Diabase and gabbro	
2b	Porphyritic basaltic andesite	
2c	Plagioclase-phyric basalt and aphyric basalt	
2d	Pillow basalt	
<i>Structural contact</i>		
1	Volcaniclastic rocks with minor volcanic rocks	
1a	Felsic–intermediate volcanic and volcaniclastic rocks	
1b	Intermediate lapilli tuff and tuff	
1c	Mafic lapillistone, mafic lapilli tuff, tuff, minor mafic mudstone and derivative garnet-biotite schist	
1d	Mafic tuff breccia and breccia	
?		

<sup>1</sup>Yang (2019a)<sup>2</sup>Beaumont-Smith and Böhm (2003)<sup>3</sup>Turek et al. (2000)<sup>4</sup>Lawley et al. (unpublished data, 2019)<sup>5</sup>Baldwin et al. (1987)<sup>6</sup>Yang and Lawley (2018)

intermediate to felsic lapilli tuff and tuff; and derivative garnet-biotite schist (e.g., south of Boiley Lake).

Outcrops of massive to foliated dacite and rhyolite (subunit 1a) with minor andesitic rocks and related volcaniclastic rocks are present in various places in the

mapping area, and more abundant than similar rocks in the northern belt. Subunit 1a is exposed mainly in the central and west-central portions of the map area (Figure GS2019-2-2). These felsic–intermediate rocks are very fine grained, pale grey to white on weathered surfaces

and light to medium greyish red or grey on fresh surfaces. Primary features (i.e., flow banding, porphyritic texture) are preserved despite these rocks being foliated and recrystallized (Figure GS2019-2-3a). Porphyritic dacite and rhyolite contain equant or subrounded quartz (1–2 mm) and locally subhedral to euhedral feldspar (0.5–1.5 mm) phenocrysts embedded in a very fine grained to aphanitic groundmass. Locally, very fine grained dark grey bands (up to 1 cm) alternate with pale to light reddish felsic bands, forming flowbanding. In ductile-brittle shear zones, these rocks are commonly mylonitized, and silicified and sericitized, locally containing scattered pyrite (and arsenopyrite,  $\pm$ chalcopyrite) disseminations. Some of them are likely Au bearing, forming Au occurrences such as at Gemmell Lake. Boudinaged vein quartz occurs in some outcrops along the main  $S_2$  foliation planes, some of it containing fine-grained pyrite.

Intermediate lapilli tuff and tuff (subunit 1b) typically display millimetre- to centimetre- scale layers, interpreted to represent beds even though they are foliated and locally folded. Lapilli tuff contains elongated lithic fragments (up to 6 cm in length) of variable composition (e.g., rhyolite, porphyritic andesite, aphanitic basalt) that are embedded in a fine-grained matrix consisting of amphibole, biotite, chlorite, epidote, plagioclase and aphanitic material. Alternating  $\sim$ 0.5–1 cm thick, dark grey and pale yellow-grey layers are common and interpreted to represent mafic and intermediate–felsic intercalations. Lapilli tuff appears to grade laterally to fine-grained tuff that contains interbedded mafic and felsic laminae ( $\sim$ 0.5–2 mm), and in which larger lapilli-sized lithic fragments are rare or absent. Some tuff and lapilli tuff are moderately to strongly magnetic due to the presence of scattered, euhedral to subhedral magnetite porphyroblasts (up to 1%; 0.5–2 mm). Noteworthy are plagioclase crystal tuff and lapilli tuff, with thin felsic layers up to 1 cm thick (Figure GS2019-2-3b) that contain up to 10% plagioclase fragments of varied shape (e.g., angular, irregular), ranging in size from 0.1 to 20 mm and unevenly distributed at the outcrop scale. This feature distinguishes the plagioclase crystal tuff and lapilli tuff from plagioclase-phyric basalt and basaltic andesite (see subunit 2b and 2c described below). Subunit 2a diabase and/or gabbroic dikes cut laminated andesitic tuff and lapilli tuff (Figure GS2019-2-3c).

Mafic volcanoclastic rocks are grouped into two subunits: subunit 1c consists of lapillistone, lapilli tuff, tuff, minor mafic mudstone and derivative garnet-biotite schist, whereas subunit 1d consists mainly of mafic tuff breccia and breccia (Table GS2019-2-1). Mafic lapillistone, lapilli tuff and tuff (subunit 1c) are characterized by the presence of mafic lithic fragments in a chloritic matrix. Minor greenish grey, very fine grained, thinly bedded mafic mudstone

is also included in subunit 1c, which usually weathers light greenish brown to light grey and contains disseminated pyrrhotite and pyrite. Dark green, acicular amphibole (actinolite?) porphyroblasts (up to 5–10 mm), concentrated in foliation or fracture planes in mafic tuff and lapilli tuff, are interpreted to have formed by retrograde metamorphism to greenschist facies. The mafic lapilli tuff and tuff (subunit 1c) are generally moderately to strongly foliated and range from texturally variable to relatively homogeneous. These rocks consist of varied amounts of aphyric lithic fragments, plagioclase (up to 40%; 0.1–5 mm) and chloritic amphibole pseudomorphs after pyroxene (up to 15%; 0.2–12 mm) in a fine-grained mafic-tuff matrix. Magnetite and amphibole porphyroblasts are evident in places. Mafic lapilli-sized fragments make up <25% of subunit 1c but can locally account for up to 80% of the rocks, which are then termed mafic lapillistone.

Garnet-biotite schist of subunit 1c occurs mainly close to the contact zone of a muscovite-bearing granite dike (subunit 5c; see below) with mafic mudstone and tuff to lapilli tuff, south of Boiley Lake, where the northwest-trending Boiley Lake shear zone cuts through these rock units. The garnet-biotite schist is composed of biotite, plagioclase, garnet, chlorite, quartz and minor magnetite. Relicts of lithic fragments and rotated garnet porphyroblasts (up to 2.2 cm) are locally evident along  $S_2$  foliation planes (Figure GS2019-2-3d). More complex metamorphic-mineral assemblages present in the schist were reported previously, including garnet-chlorite $\pm$ magnetite, garnet-anthophyllite-chlorite-magnetite and kyanite-muscovite-biotite-chlorite (Anderson and Beaumont-Smith, 2001; Assessment File 92793, Manitoba Agriculture and Resource Development, Winnipeg). This schist constitutes the Boiley Lake alteration zone (Gale, 1983; Ferreira, 1993), which likely resulted from contact and/or regional metamorphism of hydrothermally altered volcanoclastic to volcanic sedimentary rocks (Anderson and Beaumont-Smith, 2001). Similar garnet-biotite schist containing minor magnetite porphyroblasts is also present east of Digney Lake, where it occurs close to the contact of a gabbro (unit 4) intrusion emplaced into the unit 1 volcanoclastic rocks.

Subunit 1d consists of moderately to strongly deformed and foliated heterolithic mafic tuff breccia and breccia. Lithic fragments, ranging from 8 to 25 cm in length, include plagioclase-phyric basalt, plagioclase-amphibole-phyric basalt, aphyric basalt, lapilli tuff, very fine grained andesite and minor rhyolite clasts embedded in a lapilli tuff and tuff matrix (Figure GS2019-2-3e). The basaltic fragments are subrounded to subangular, varying in shape from irregular to rarely ellipsoidal, and have been stretched along the generally east- to southeast-trending foliation ( $S_2$ ). In high-strain zones, lithic fragments are



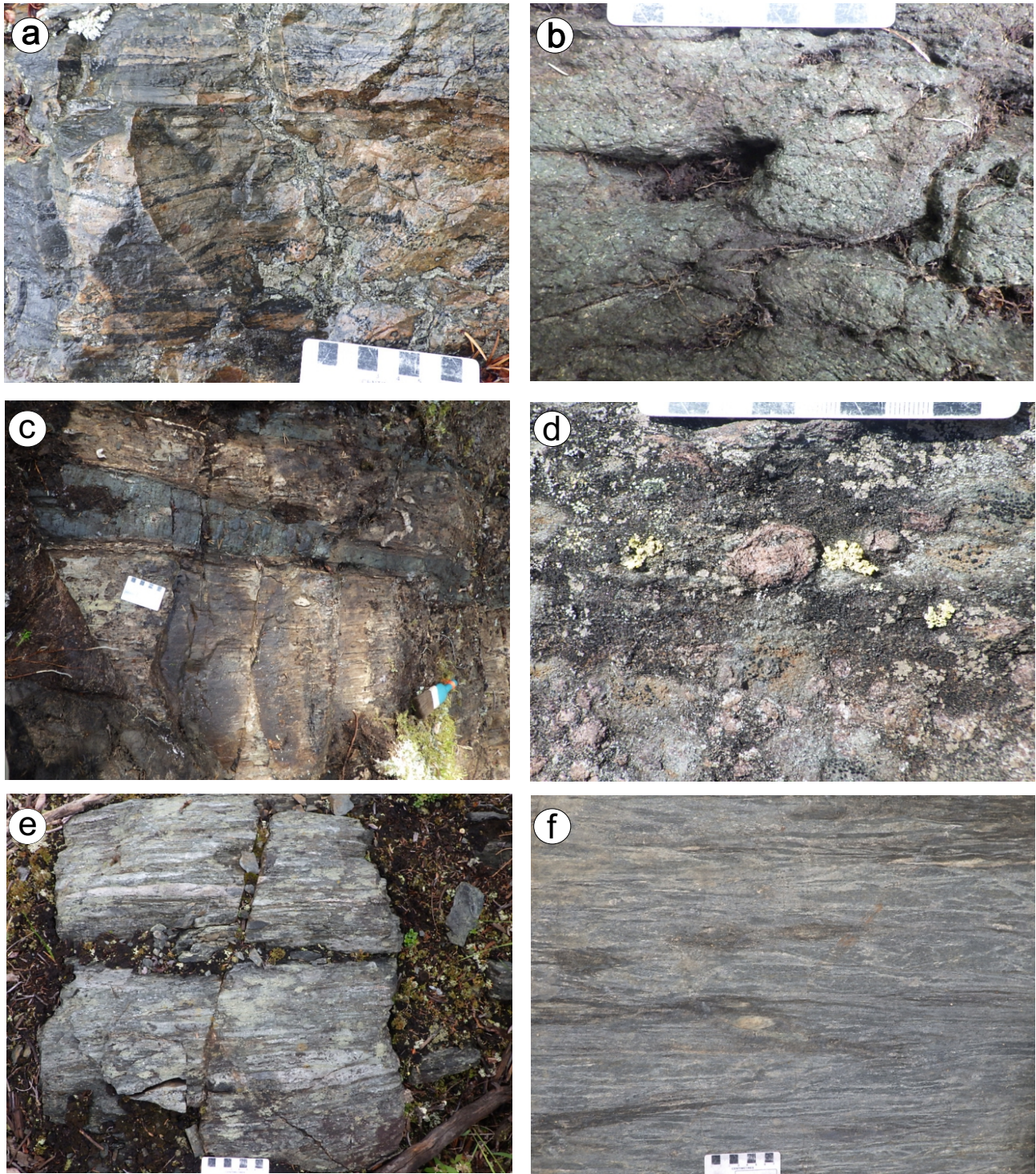


**Figure GS2019-2-3:** Field photographs of unit 1 volcaniclastic rocks with minor volcanics of the Wasekwan group in the Gemmell Lake area: **a)** very fine grained quartz- and feldspar-phyric rhyolite with flow bands, and locally felsic fragments (subunit 1a; UTM Zone 14N, 361000E, 6288737, NAD 83); **b)** intermediate tuff to lapilli tuff (with up to 10% 0.2–1.5 mm plagioclase fragments) with rare lithic fragments (subunit 1b; UTM 357536E, 6288334N); **c)** laminated andesitic tuff to lapilli tuff (subunit 1b) cut by a diabase dike (subunit 2a; UTM 363174E, 6291169N); **d)** garnet-biotite schist with reddish garnet porphyroblasts, up to 2 cm (centre of photo), that are rotated clockwise due to dextral shear along  $S_2$  foliation (subunit 1c; UTM 363432E, 6284030N); **e)** foliated mafic tuff breccia and breccia with basaltic to andesitic fragments transposed along  $S_2$  foliation (subunit 1d; UTM 364998E, 6288128N); **f)** very strongly foliated basaltic tuff breccia in high-strain zone (subunit 1d; UTM 357722E, 6287441N).



sheared and flattened, although the margins of some of the fragments are still discernible (Figure GS2019-2-3f). Some of the aphanitic basalt fragments display epidote alteration and others show reaction rims with very fine grained assemblages of chlorite, epidote, sericite and albite. Some porphyritic basalt blocks contain well-preserved plagioclase and amphibole (after pyroxene) phenocrysts.

#### **Mafic to intermediate volcanic rocks and synvolcanic intrusive rocks (unit 2)**

Unit 2 mafic to intermediate volcanic rocks occur mainly in the northeastern (e.g., Nail Lake), northern, east-central (e.g., south of Poll Lake) and southeastern (e.g., south of Monique Lake) parts of the map area (Figure GS2019-2-2). The volcanic succession of unit 2 in the Gemmell Lake area is dominated by plagioclase-phyric and aphyric basalts and pillow basalts, with subordinate porphyritic basaltic andesite and synvolcanic diabase and gabbro dikes (Table GS2019-2-1).

Synvolcanic diabase and gabbroic rocks (subunit 2a) usually occur as dikes and small plugs intruded into unit 2 volcanic rocks (Figure GS2019-2-4a) and, in some cases, into unit 1 volcanoclastic rocks (Figure GS2019-2-3c). The diabase dikes weather greenish grey to grey and are greenish to dark green on fresh surfaces; they are very fine to medium grained, porphyritic and moderately to strongly foliated (Figure GS2019-2-4b). Equant to subhedral plagioclase phenocrysts (up to 10 mm) occur in a fine-grained groundmass of plagioclase, amphibole, chlorite and Fe oxides. Generally, the diabase and gabbroic rocks consist of 50–60% amphibole and 40–50% plagioclase, reflecting an amphibolite-facies metamorphic-mineral assemblage. Grain boundaries between the phenocrysts and groundmass are diffuse due to sericite and chlorite alteration, regardless of the extent of deformation. Trace disseminated sulphides (e.g., pyrrhotite; ~0.5–1 mm) are locally evident.

Porphyritic basaltic andesite (subunit 2b) contains amphibole ( $\pm$ biotite) and lesser amounts of plagioclase phenocrysts in a fine-grained groundmass (Figure GS2019-2-4c), although, in some cases, it lacks plagioclase phenocrysts. Biotite and sericite alteration is a common feature of the rock. When plagioclase and amphibole phenocrysts coexist in basaltic andesite (subunit 2b), it is difficult to distinguish it from plagioclase-phyric basalt (subunit 2c), although the latter commonly lacks amphibole ( $\pm$ biotite) phenocrysts (Figure GS2019-2-4d, e).

Massive aphyric basalt (subunit 2c) is also common in the map area. Vesicles and quartz $\pm$ calcite amygdules are present in some outcrops. The basalt is greyish green

on weathered surfaces and dark greyish green on fresh surfaces. In most cases, it is aphanitic. Chlorite and epidote alteration is common in the aphyric basalt, as shown by epidote domains ranging from a few centimetres to a metre across. These epidote domains are generally irregular to ovoid, displaying sharp to gradational contacts with the host aphyric basalt, although some epidote is fracture controlled as veins or veinlets, similar to those described by Gilbert et al. (1980), Gilbert (1993) and Yang and Beaumont-Smith (2016, 2017).

Pillow basalt (subunit 2d) is exposed and well preserved in a relatively low-strain area along the southern shore of Pool Lake (Figure GS2019-2-2). Pillow size ranges from 20 to 40 cm (Figure GS2019-2-4f) and locally reaches up to 150 cm, with well-preserved hyaloclastite selvages up to 3 cm thick. Locally, subrounded to rounded quartz $\pm$ carbonate amygdules up to 1.0 cm in diameter are concentrated along the inner margin of pillow selvages. In high-strain areas, pillows are strongly deformed and contain a penetrative foliation, with width to length ratios of the flattened pillows being up to 1:10. Some pillow selvages are still recognizable and contain stretched vesicles and quartz amygdules transposed along  $S_2$  foliation. Epidote alteration as veinlets, patches or nodules was commonly observed in the basalt with few plagioclase phenocrysts. Late quartz veins occur either along or cutting  $S_2$  foliation planes; some are boudinaged or folded.

#### **Sedimentary rocks intercalated with minor volcanic sedimentary rocks (unit 3)**

Unit 3 sedimentary rocks of the Wasekwan group are subordinate to volcanic and volcanoclastic rocks in the map area. The sedimentary rocks are exposed mainly in the central and southwestern portions of the map area (Figure GS2019-2-2). This unit consists of argillite, siltstone and greywacke (subunit 3a), and banded iron formation (BIF; subunit 3b), intercalated with minor volcanic mudstone, siltstone, sandstone and breccia (subunit 3c) (Table GS2019-2-1).

Thin- to medium-bedded quartzofeldspathic greywacke and siltstone (subunit 3a) dominate the sedimentary succession. Greywacke contains more than 15% clay minerals in its matrix. Primary bedding ( $S_0$ ) in the sedimentary rocks was transposed by the regional  $S_2$  foliation. The medium- to coarse-grained greywacke is medium tan to yellowish grey on weathered surfaces, and light grey on fresh surfaces. Quartz, feldspar, amphibole and lithic clasts (1.3–2 mm) are angular to subrounded, and well aligned on foliation planes defined by biotite flakes and manifested by felsic- and mafic-rich layering that is likely to reflect transposed bedding (Figure GS2019-2-5a).



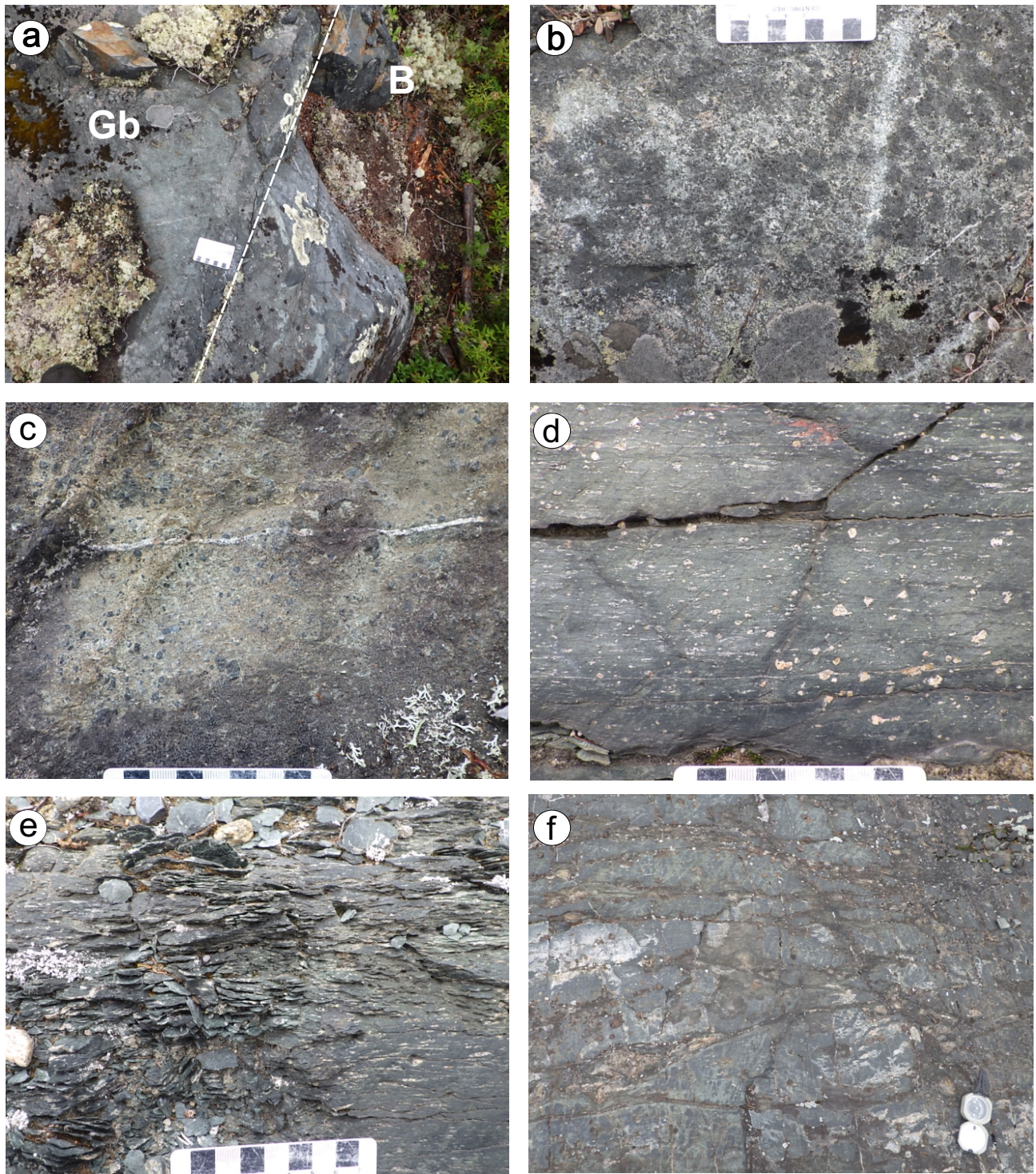


**Figure GS2019-2-4:** Field photographs of mafic to intermediate volcanic rocks and synvolcanic intrusive rocks (unit 2) of the Wasekwan group in the Gemmell Lake area: **a)** synvolcanic, massive gabbro (subunit 2a) cuts very fine grained aphyric basalt (subunit 2c; UTM Zone 14N, 366090E, 6288191N, NAD 83); **b)** massive gabbro with subhedral to euhedral plagioclase laths in very fine grained mafic groundmass (subunit 2a; same location as photo a); **c)** amphibole-phyric basaltic andesite (subunit 2b; UTM 368905E, 6292155N); **d)** foliated plagioclase-phyric basalt (subunit 2c; UTM 357621E, 6287253N); **e)** strongly foliated plagioclase-phyric basalt (subunit 2c; UTM 357621E, 6287253N); **f)** foliated pillow basalt with well-preserved hyaloclastite selvage up to 3 cm thick; the stretched pillows are aligned along east-trending  $S_2$  foliation planes (subunit 2d; UTM 365139E, 6288262N). Abbreviations: B, basalt; Gb, gabbro.



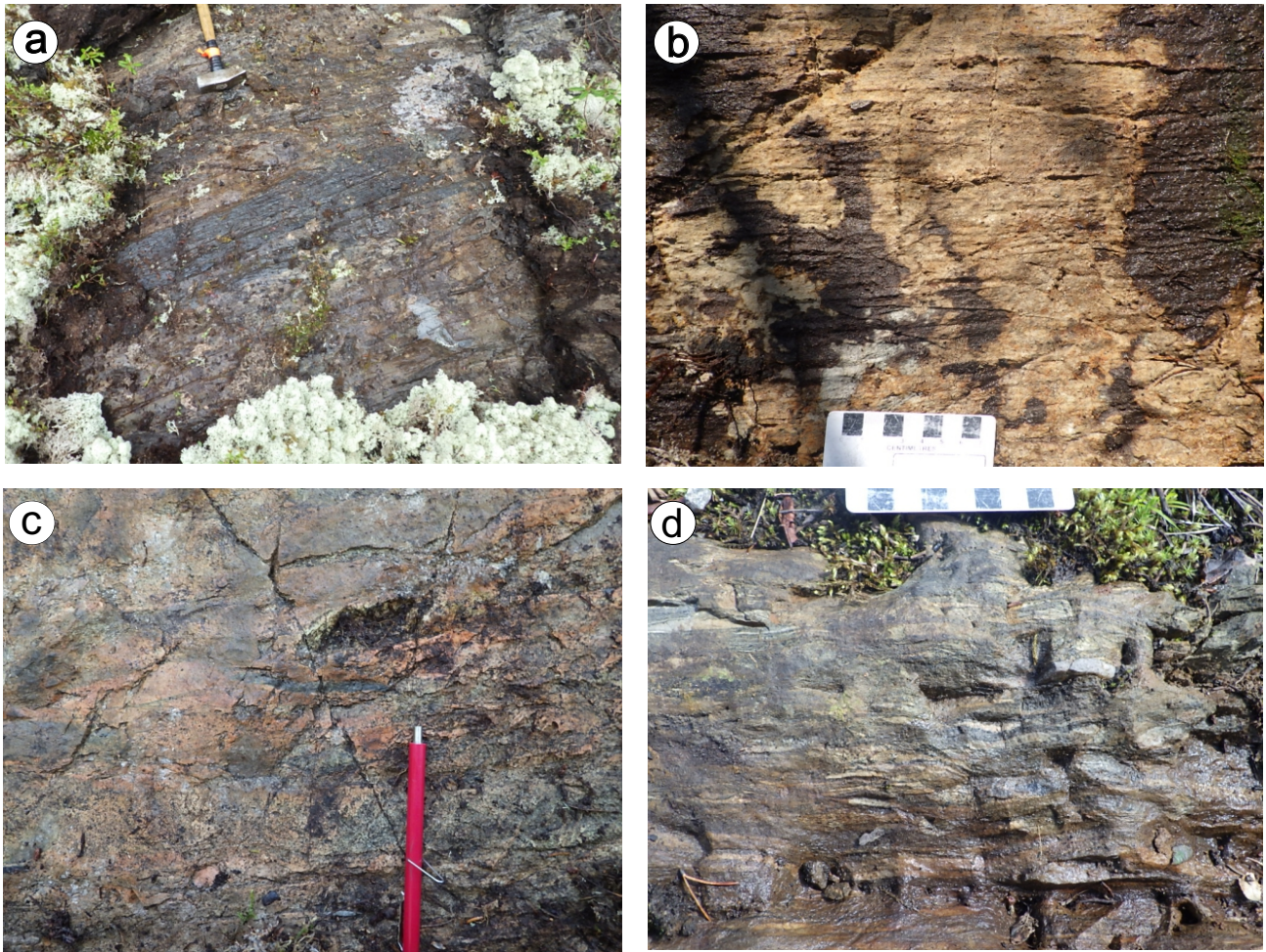


**Figure GS2019-2-5:** Field photographs of sedimentary rocks intercalated with minor volcano-sedimentary rocks (unit 3) of the Wasekwan group in the Gemmell Lake area: **a)** fine- to medium-grained, foliated quartzofeldspathic greywacke with alternating felsic and mafic bands or layering (subunit 3a; UTM Zone 14N, 359742E, 6289520N, NAD 83); **b)** laminated volcanic (andesitic) sandstone with biotite flakes and plagioclase clasts (0.5–2 mm) that have diffuse margins (subunit 3c; UTM 364058E, 6290114N); **c)** volcanic sandstone containing disseminated magnetite, as well as magnetite aggregates up to 10 cm in length (subunit 3c; UTM 363996E, 6289919N); **d)** volcanic breccia with felsic and mafic volcanic fragments in a felsic to intermediate sandy matrix; bedding transposed by  $S_2$  foliation (subunit 3c; UTM, 364850E, 6290199N).

Scattered sulphide minerals dominated by pyrite are evident in the greywacke; in many cases, they are associated with quartz veins and veinlets. Low-strain domains show millimetre- to centimetre-thick beds indicated by dark green mafic to light tan felsic layers.

Although no BIF (subunit 3b) was found at exposed outcrops during the course of mapping, it was intersected by a number of historical drill holes in the central, north-eastern and southwestern parts of the map area. The BIF is well correlated with highly magnetic, east-northeast-trending domains indicated by detailed airborne magnetic surveys, and consistently overlies unit 2 mafic–intermediate volcanic rocks.

Thin to thick beds of minor volcanic sedimentary rocks (subunit 3c), present in the upper section of unit 3, consist of volcanic mudstone, siltstone and sandstone,

and minor volcanic breccia (Table GS2019-2-1). Volcanic sandstone is dominated by laminated, fine- to medium-grained andesitic sandstone consisting mainly of irregular plagioclase, biotite flakes and lithic fragments (0.5–2 mm) in a fine sandy matrix; locally, a few large lithic fragments occur along bedding transposed by regional  $S_2$  foliation (Figure GS2019-2-5b). Recrystallized acicular amphibole crystals (actinolite; up to 1.5 cm in length) are randomly oriented along  $S_2$  planes in the andesitic sandstone, indicating that it experienced greenschist-facies retrograde metamorphism (Yang and Beaumont-Smith, 2017). Locally, subunit 3c volcanic sandstone contains ~1% cubic magnetite grains (0.2–0.3 mm), as well as magnetite fragments (~0.5 cm wide) up to 10 cm in length (Figure GS2019-2-5c). Similar volcanic sedimentary rocks occur west of Wasekwan Lake (Yang and Beaumont-Smith, 2017).

Thick-bedded volcanic breccia (a minor component of subunit 3c) at the base of unit 3 consists dominantly of felsic and intermediate–mafic volcanic clasts in a coarse-grained sandy matrix (Figure GS2019-2-5d). These clasts are stretched or flattened and well aligned along  $S_2$  planes that transposed primary bedding. Although strongly deformed, the breccia appears to grade upward to volcanic sandstone, suggesting that the beds young to the north.

### ***Pre-Sickle intrusive suite (units 4 and 5)***

Rocks of the pre-Sickle intrusive suite crosscut the supracrustal rocks of the Wasekwan group (Gilbert et al., 1980; Baldwin et al., 1987; Beaumont-Smith and Bohm, 2004). Unit 4 gabbro and unit 5 granitoid rocks, diorite, quartz diorite and minor gabbroic rocks were attributed to this suite (Table GS2019-2-1).

#### **Gabbro (unit 4)**

Gabbro of unit 4 occurs mainly in the central to southwestern part of the Gemmell Lake area (Figure GS2019-2-2). It occurs as a sill-like intrusion cutting the Wasekwan group supracrustal rocks, and is cut by unit 5 granitoids. The gabbro weathers greenish grey and is dark greenish grey to dark grey on fresh surfaces. It is medium to coarse grained, equigranular, massive, and moderately to locally strongly foliated. It consists of 30–40% plagioclase laths (1–3 mm), 55–60% amphibole (pseudomorphs after pyroxene), minor Fe-oxide minerals and trace pyrrhotite (Figure GS2019-2-6a). The edges of both plagioclase and amphibole crystals are diffuse due to chlorite and sericite alteration. Locally, epidote veins and veinlets up to 4 cm wide are evident along  $S_2$  planes.

#### **Granitoid rocks (subunit 5a)**

Granitoid plutons of the pre-Sickle intrusive suite (unit 5), exposed in the southeastern and southern parts of the map area (Figure GS2019-2-2), comprise diorite, quartz diorite, tonalite, granodiorite, granite and associated pegmatitic and aplitic dikes, as well as minor gabbroic rock. These intrusive rocks are divided into three subunits based on field relations and lithology: 1) tonalite, granodiorite and granite, and associated pegmatitic and aplitic rocks (subunit 5a); 2) diorite, quartz diorite and minor gabbroic rocks (subunit 5b); and 3) muscovite-bearing granite (subunit 5c; Table GS2019-2-1).

Subunit 5a granodiorite is commonly medium to coarse grained, massive, equigranular to locally porphyritic and weakly to moderately foliated. It weathers greyish pink to light beige and consists of 20–30% anhedral quartz, 25–35% subhedral plagioclase, 20–25% K-feldspar,

5–10% hornblende±biotite, and accessory Fe-oxide minerals. Some of the porphyritic variety contains 5% quartz phenocrysts up to 1.2 cm across (Figure GS2019-2-6b), suggesting relatively shallow emplacement into the Wasekwan group supracrustal package. Less commonly, granite of subunit 5a contains slightly higher K-feldspar and quartz contents than the granodiorite, whereas tonalite of subunit 5a is relatively enriched in plagioclase and hornblende, and lacks (or has <10%) K-feldspar. Pegmatite and/or aplite of unit 5a are more commonly associated with granite and granodiorite than with tonalite. They occur as dikes that are a few centimetres to a few metres wide and consist of quartz, feldspar and minor biotite (±muscovite).

#### **Diorite, quartz diorite and minor gabbroic rocks (subunit 5b)**

Diorite and quartz diorite (subunit 5b) occur mostly as marginal phases of the Counsell Lake pluton in the southern part of the map area (Figure GS2019-2-2). Quartz diorite is fine to medium grained, massive, equigranular and moderately to strongly foliated. It consists of 5–10% anhedral quartz, 50–60% plagioclase with diffuse grain boundaries, 20–30% hornblende, and minor biotite. Where the rock lacks quartz or contains <5% quartz, it is termed diorite.

An outcrop (~15 m across) southwest of Motriuk Lake displays a cumulate-layering texture with variations in mineral-grain size and percentage from base to top. This sequence consists of megacrystic pyroxenite to melagabbro grading to very coarse grained pyroxenite to melagabbro, coarse- to medium-grained gabbro and fine- to medium-grained quartz diorite, all of which are cut by pinkish pegmatite dikes. The megacrystic phase is dark grey, massive and equigranular, and composed of 85–90% euhedral cumulus pyroxene (up to 2 cm) and 10–15% anhedral to subhedral plagioclase interstitial to the former (Figure GS2019-2-6c). Very coarse grained pyroxenite to melagabbro comprises similar minerals, also exhibiting cumulate texture (Figure GS2019-2-6d), and grades into gabbro containing about 60–80% pyroxene and 20–40% plagioclase. The contact between the mafic rocks and quartz diorite (Figure GS2019-2-6e) is gradational at the outcrop scale, suggesting that they formed by fractional crystallization from the same magmatic system.

#### **Muscovite-bearing granite (subunit 5c)**

Muscovite-bearing granite of subunit 5c is only exposed immediately southwest of Boiley Lake (Figure GS2019-2-2), where it occurs as a dike-like intrusion up to 20 m wide cutting unit 1 volcanic to volcanoclastic rocks. Its southwestern margin is strongly sheared and



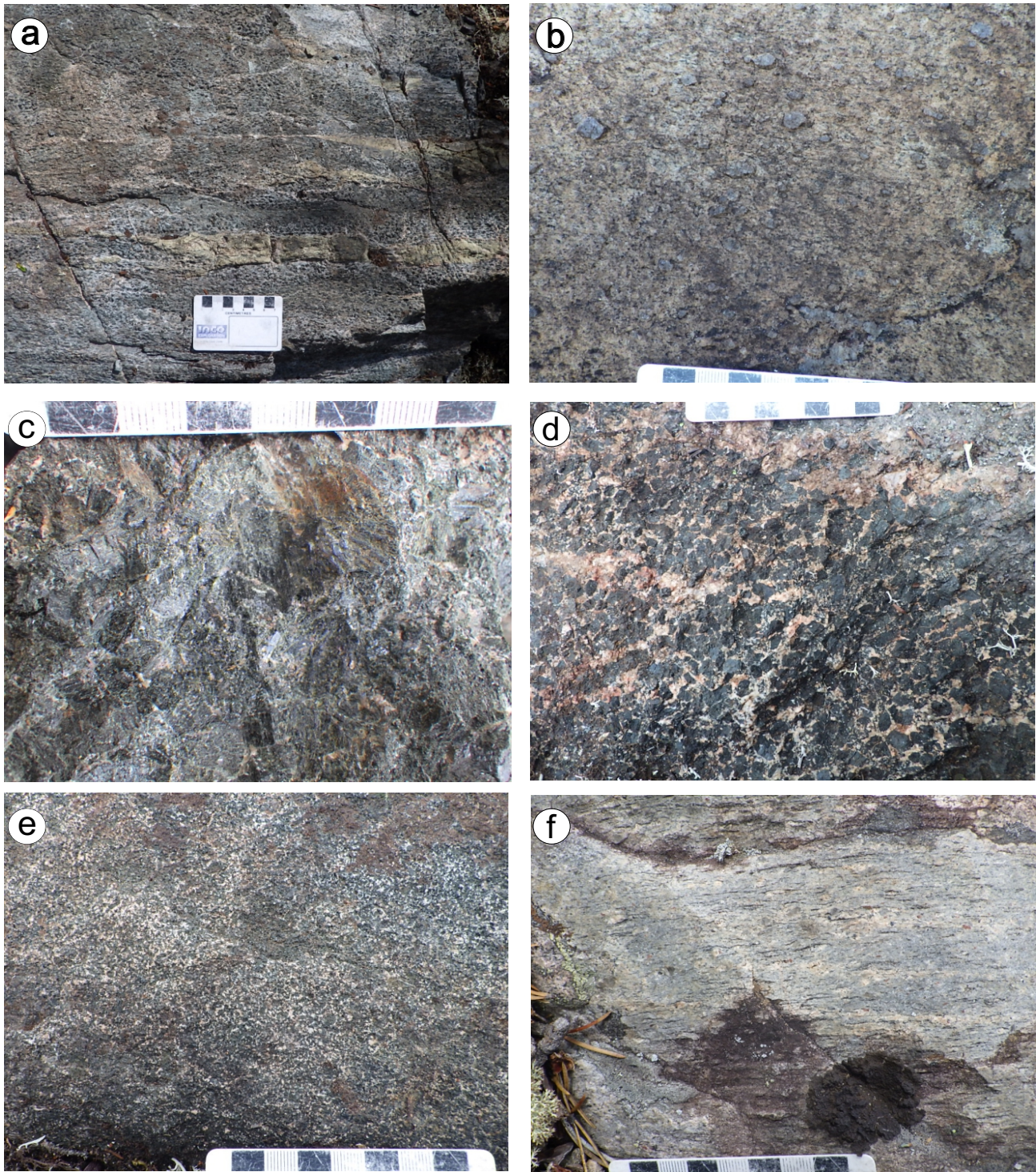


**Figure GS2019-2-6:** Outcrop photographs of units 4 and 5 in the Gemmell Lake area: **a)** foliated, massive, medium- to coarse-grained equigranular gabbro with epidote veinlets and veins up to 4 cm wide present along  $S_2$  planes (unit 4; UTM Zone 14N, 361527E, 6289275N, NAD 83); **b)** foliated, medium- to coarse-grained porphyritic granodiorite with quartz phenocrysts (2–5 mm; subunit 5a; UTM 365201E, 6283371N); **c)** megacrystic pyroxenite to melagabbro and **d)** massive, very coarse grained pyroxenite to melagabbro with cumulate texture, cut by pegmatitic veins (and dike; not shown; subunit 5b; UTM 365566E, 6293020N); **e)** massive, fine- to medium-grained quartz diorite (subunit 5b; UTM 365566E, 6293020N); **f)** foliated, porphyritic muscovite-bearing granite (subunit 5c) with K-feldspar and quartz phenocrysts in felsic groundmass consisting of quartz, feldspar, biotite and muscovite, intruding unit 1 volcaniclastic and volcanic sedimentary rocks (UTM 363298E, 6283932N); note that magnetite-garnet-biotite schist occurs in the contact zone between two-mica granite and unit 1 volcaniclastic rock and volcanic mudstone.



becomes protomylonitic to mylonitic in contact with the subunit 1c garnet-biotite schist. This light grey granite is fine to medium grained and massive to locally porphyritic but strongly foliated, as indicated by biotite aligned along  $S_2$  foliation (Figure GS2019-2-6f). Potassium feldspar phenocrysts with diffuse grain boundaries are also aligned along the foliation. Typically, the granite contains ~0.5% muscovite flakes (0.2–0.5 mm across) evenly distributed with 25–35% quartz, 55–60% feldspars and 5–6% biotite. This two-mica granite is likely an S-type granite in terms of its mineral assemblage and formed in relatively reducing conditions.

### ***Sickle group (unit 6)***

Sickle group sandstone (subunit 6a) and polymictic conglomerate (subunit 6b), which outcrop in the central and southwest-central parts of the map area (Figure GS2019-2-2), unconformably overlie the Wasekwan group supracrustal rocks as well as the pre-Sickle intrusive rocks. Stratigraphically, sandstone overlies conglomerate (Norman, 1933; Gilbert et al., 1980). A maximum depositional age of  $1836 \pm 15$  Ma for the Sickle group was recently obtained from the youngest, reproducible detrital zircon grain retrieved from a quartz pebbly sandstone sample collected west of Pool Lake (Lawley et al., unpublished data, 2019).

#### **Arkosic sandstone and quartz pebbly sandstone (subunit 6a)**

Medium- to thick-bedded arkosic sandstone and quartz pebbly sandstone display varied colours on fresh surface, including pale grey, dark grey and tan to light red-dish. The sandstones are fine to coarse grained and are composed of feldspar, quartz, mica, lithic fragments and finer material. Up to 10% quartz pebbles (3–5 mm) are common in the quartz pebbly sandstone (Figure GS2019-2-7a), together with sand- to pebble-sized feldspar clasts. Locally, variation in grain size may indicate the top of sandy beds, although this subunit was deformed and foliated by the extensive  $D_2$  deformation that resulted in the transposition of primary bedding ( $S_0$ ) along the  $S_2$  foliation. In places, arkosic sandstone contains more pebbly lithic clasts (up to 15 mm) in a finer matrix of feldspar, quartz, mica, chlorite, magnetite and clays. Arkose to arenite lacking quartz or lithic pebbles is exposed west of Jones Lake.

#### **Polymictic conglomerate with minor pebbly sandstone (subunit 6b)**

In domains of low- to moderate-strain, the polymictic conglomerate (subunit 6b) is poorly sorted and matrix to clast supported, and contains varied sizes (2–30 cm)

of rounded and subrounded to irregular clasts ranging from pebble to boulder size. Generally, cobble-size clasts are more common. Clast types include mafic–felsic volcanic rocks, granitoids, vein quartz, epidotized fragments, magnetic BIF and chert in a sandy to wacke matrix (Figure GS2019-2-7b, c). Some of the matrix contains sand-sized K-feldspar, biotite, muscovite, chlorite and magnetite grains. In high-strain domains, conglomerate displays strong clast flattening and stretching along the  $S_2$  foliation (Figure GS2019-2-7d) that entirely transposed bedding ( $S_0$ ). Locally, medium- to thin-bedded pebbly sandstone to coarse-grained arkosic sandstone is interbedded with polymictic conglomerate.

### ***Post-Sickle intrusive suite (unit 7)***

Post-Sickle intrusive rocks of unit 7, represented by the Motriuk Lake pluton, occur dominantly in the northern part of the map area, and a few dikes and stock-like intrusions cut the Wasekwan group rocks southwest of Gemmell Lake (Figure GS2019-2-2). This unit comprises two subunits: quartz diorite and tonalite (subunit 7a) and granodiorite (subunit 7b) (Table GS2019-2-1). Quartz diorite is medium to coarse grained, massive, weakly to moderately deformed and equigranular, although porphyritic texture is locally evident. It is composed of 5–10% quartz, 60–70% plagioclase and 15–20% amphibole (Figure GS2019-2-8a). Quartz diorite and tonalite of the Motriuk Lake pluton (Yang and Beaumont-Smith, 2015a) in the current map area coincide with magnetic lows on detailed airborne magnetic imagery. The rocks have high Sr/Y and La/Yb ratios (Yang, unpublished data, 2015), similar to those of post-Sickle quartz diorite at Farley Lake that exhibits geochemical characteristics of adakite-like rocks (see Yang and Lawley, 2018).

Granodiorite of subunit 7b is pinkish on fresh surfaces and weathers beige to tan, and is medium to coarse grained, foliated and equigranular to locally porphyritic. It consists of 5–8% hornblende (partly altered to biotite), 3–5% discrete biotite flakes, 25–30% quartz, 30–40% plagioclase and 25–30% K-feldspar.

### ***Late intrusive suite (unit 8)***

Unit 8 quartz-feldspar porphyry, pegmatite and/or aplite occur mostly as dikes in the southwestern and north-eastern portions of the map area (Figure GS2019-2-2). These dikes tend to be isolated, relatively less deformed and apparently not associated with any of the larger intrusions mapped at surface. Unit 8 intrusives have an unclear relationship to the pre- and post-Sickle intrusive suites (unit 5 and unit 6, respectively) and are therefore ascribed to the late intrusive suite. A quartz-feldspar porphyry dike

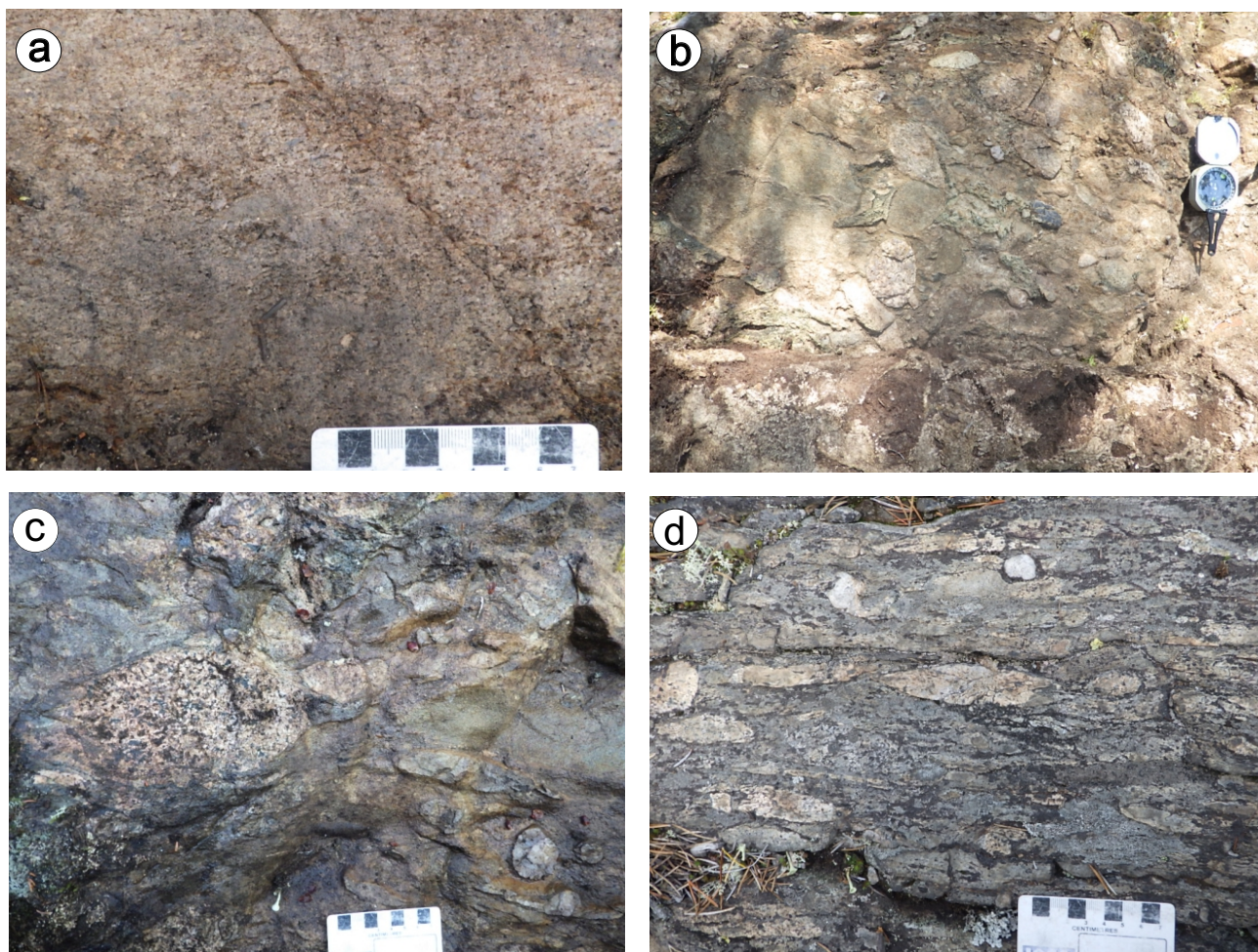


**Figure GS2019-2-7:** Outcrop photographs of unit 6 Sickie group sandstone and polymictic conglomerate in the Gemmell Lake area: **a)** quartz pebbly arkosic sandstone (subunit 6a; UTM Zone 14N, 3639917E, 6287707N, NAD 83); **b)** poorly sorted, polymictic cobble conglomerate with wacke matrix and variously shaped clasts consisting of granitoid, vein quartz, banded iron formation, chert and felsic and mafic volcanic rocks, together with a few irregular felsic boulder-sized clasts (subunit 6b; UTM 364101E; 6286914N); **c)** weakly foliated, matrix- to clast-supported, poorly sorted, polymictic pebble to cobble conglomerate with sandy matrix (subunit 6b; UTM 365031E; 6289411N); **d)** strongly foliated polymictic conglomerate with stretched granitoid, rhyolite, chert and banded iron formation clasts and subrounded quartz clasts, aligned along  $S_2$  foliation planes that transposed  $S_0$  bedding (subunit 6b; UTM 363910E; 6287957N).

(up to 10 m wide) south of Boiley Lake contains ~2% magnetite phenocrysts that are cubic to subhedral (1–3 mm), together with quartz and K-feldspar embedded evenly in a felsic groundmass (Figure GS2019-2-8b). The presence of magnetite phenocrysts indicates that the dike may have formed in relatively oxidized conditions. Hydrothermal fluids associated with such oxidized intrusion(s) can effectively scavenge and transport gold (e.g., Boyle, 1979), and thus may have played a role in Au mineralization.

Unit 8 pegmatite and aplite commonly have muscovite ( $\pm$ tourmaline) in addition to biotite, suggesting that they are likely not related to the pre-Sickie (subunit 5) and post-Sickie (subunit 7) intrusive suites (Yang and Beaumont-Smith, 2017).

### **Tectonite (unit 9)**

Tectonite of unit 9 comprises mafic to felsic mylonite to protomylonite within the JSZ (Figure GS2019-2-2), characterized by the development of intense  $S_2$  tectonic fabrics. The protoliths of such high-strain rocks are difficult to determine in the field, although some feldspar and quartz relicts may be partly preserved in felsic tectonite that shows brittle-ductile deformation (Figure GS2019-2-8c, d). Mafic tectonites derived from mafic volcanic flows and/or volcanoclastic rocks are indistinguishable, particularly those that were altered to very fine grained chlorite and sericite. Quartz veins or veinlets in tectonite are concentrated primarily along the  $S_2$  foliation. Asymmetric quartz boudins are a reliable shear-sense indicator (e.g., dextral shear, as shown in Figure GS2019-2-8e).



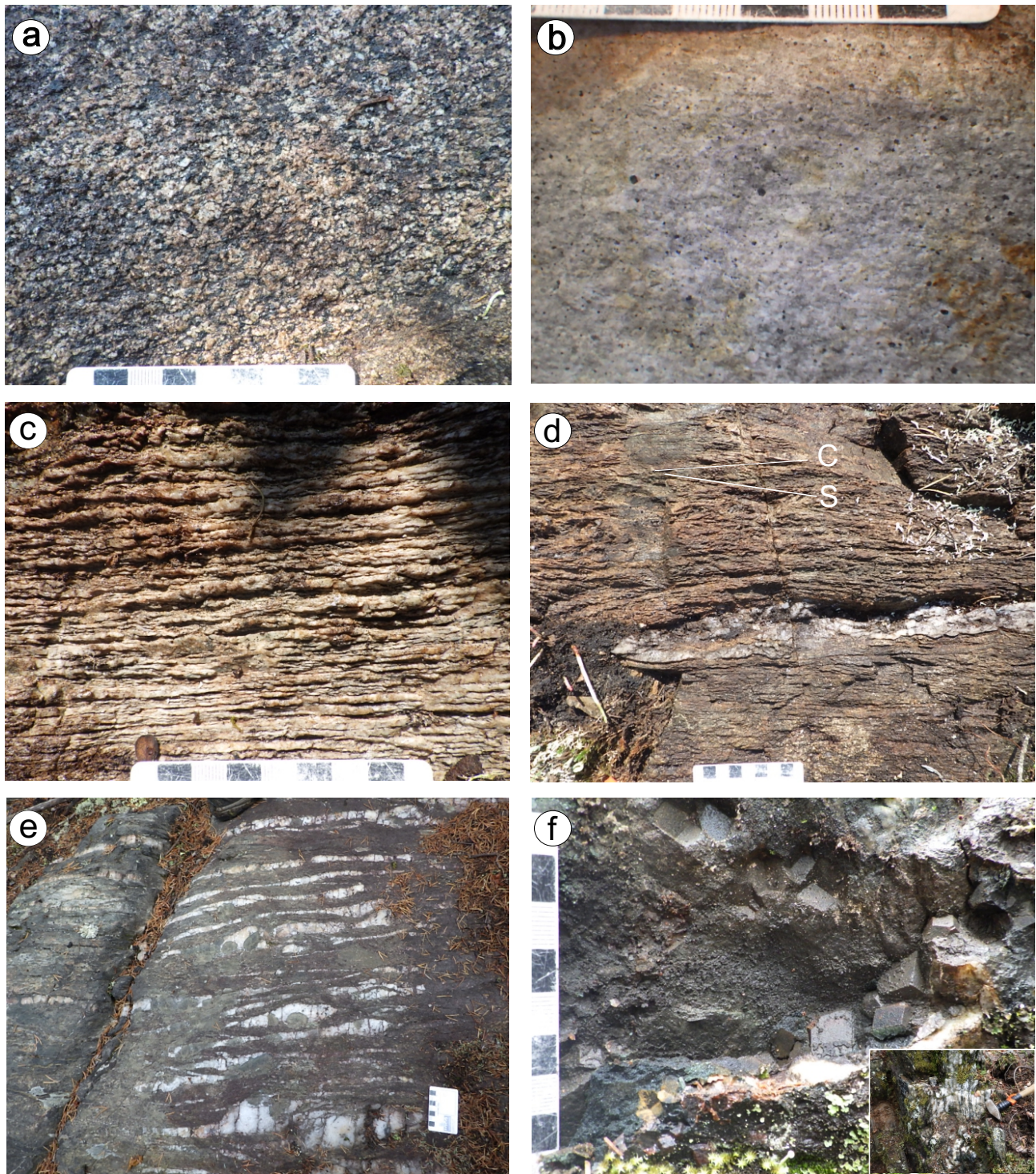


**Figure GS2019-2-8:** Outcrop photographs of units 7, 8 and 9 in the Gemmell Lake area: **a)** weakly foliated, massive, coarse-grained quartz diorite (subunit 7a; UTM Zone 14N, 365243E, 6292252N, NAD 83); **b)** massive quartz-feldspar porphyry with up to 2% euhedral to subhedral magnetite (up to 3 mm) phenocrysts (unit 8; UTM 363619E; 6283902N); **c)** dacitic to rhyolitic mylonite showing brittle-ductile fabrics ( $S_2$ ) and shear bands (unit 9; UTM 367059E, 6290899N); **d)** S-C fabric indicative of sinistral shear in felsic protomylonite with boudinaged quartz in dominant  $S_2$  plane that cuts shallowly dipping  $S_1$  fabrics (unit 9; UTM 367020E, 6290960N); **e)** silicified mafic mylonite cut by numerous quartz veins along a subvertical shear zone; dextral shear sense indicated by the asymmetric sigmoid quartz at the bottom of the photo (unit 9; UTM 359555E, 6288809N); **f)** quartz vein (~30 cm in width as shown by inset photo in lower right corner) containing megacrystic euhedral garnet crystals, which was emplaced along the contact between sheared unit 1 dacitic to rhyolitic rock and unit 2 basalt (UTM 362308E, 6289245N).



Within the JSZ, an approximately 30 cm wide quartz vein occurs along the contact between strongly sheared felsic and mafic rocks south of Gemmell Lake. This quartz vein contains maroon, megacrystic, euhedral garnet crystals (up to 1.5 cm; Figure GS2019-2-8f) together with acicular amphibole and chlorite concentrated toward the mafic side, whereas smaller (3–5 mm) garnet crystals cluster in the central part of the vein.

## Structural geology

Six regional deformation events ( $D_1$  to  $D_6$ ) were defined in the LLGB (Beaumont-Smith and Böhm, 2002, 2004). Structures related to  $D_1$  deformation are represented by penetrative, shallow-dipping  $S_1$  foliation (e.g., Figure GS2019-2-8c) overprinted by vertical  $S_2$  fabrics associated with  $D_2$  deformation. Although locally preserved in the Wasekwan group supracrustal rocks,  $D_1$  fabrics are not evident in the Sickie group, Pool lake suite (Gilbert et al., 1980; Anderson and Beaumont-Smith, 2001) or pre-Sickie intrusive suite rocks (this study). Therefore,  $D_1$  deformation likely reflects the assembly of volcanic terranes that constitute the LLGB (e.g., Beaumont-Smith and Böhm, 2002, 2004).

In the Gemmell Lake area,  $D_2$  structures are the most penetrative and manifest as a steeply north-dipping  $S_2$  foliation and tight to isoclinal folds ( $F_2$ ) that have shallowly plunging hinges and associated minor chevron folds. Foliations of this deformation ( $S_2$ ) were observed in all map units except the late intrusive suite. Typically,  $S_2$  foliations dip steeply to the north and contain a down-dip to steeply plunging mineral and stretching lineation (e.g., Sherman, 1992; Anderson and Beaumont-Smith, 2000; Beaumont-Smith et al., 2001). These  $L_2$  lineations are well defined by a preferred orientation of minerals (e.g., amphibole, biotite, feldspar), stretched pillows and flattened pebbles and cobbles (e.g., Figure GS2019-2-7d).

Ductile shear zones that generally define map-unit contacts are commonly related to  $D_2$  deformation, as the intensity of  $S_2$  fabrics and tightness of  $F_2$  folds increase toward contacts. The  $D_2$  shear zones are characterized by dextral shear-sense indicators (e.g., Figure GS2019-2-7e) on horizontal surfaces and steeply plunging, generally down-dip to slightly oblique (easterly pitch) stretching lineations.

The Johnson shear zone (JSZ), a regional east-trending shear zone, transects the southern part of the map area (Figure GS2019-2-1) and can be traced more than 100 km along strike. The JSZ is a dominantly dextral transpressional fault zone (Beaumont-Smith and Rogge, 1999; Jones, 2005; Jones et al., 2006). Numerous dextral shear-sense indicators (e.g., shear bands, S-C fabrics, asymmetric

quartz boundins, rotated garnet porphyroblasts) were observed on the horizontal surface within the JSZ. The development of narrow zones of shallowly plunging stretching lineations in the core of the shear zone reflects kinematics consistent with shear-zone development in response to dextral transpression. Similar shear zones (e.g., the North Stear Lake shear zone and Pool Lake fault zone; Beaumont-Smith, 2001; this study) are parallel to subparallel to the JSZ and could also be associated with  $D_2$  deformation (Figure GS2019-2-2).

The  $D_3$  deformation is represented in the map area by close to tight, S-asymmetric  $F_3$  folds and northwest-trending, axial-planar  $S_3$  crenulation cleavage. A set of northwest- to west-northwest-trending faults (e.g., the Boiley Lake shear zone; Figure GS2019-2-2) is thought to be related to the  $D_3$  event.  $F_4$  folds are also pervasive throughout the map area. These folds plunge steeply to the northeast and are associated with steeply dipping, northeast-striking, axial-planar  $S_4$  crenulation cleavage. The Gemmell Lake fault and Motriuk Lake–Jones Lake fault strike north-northeast and display sinistral movement, which is likely associated with  $D_4$  deformation. Mesoscopic structures associated with  $D_5$  deformation include open  $F_5$  conjugate folds, kink bands and crenulations, and a brittle  $D_5$  fault.

The  $D_6$  deformation was brittle to ductile and represented by sinistral reactivation of  $D_2$  shear zones (Figure GS2019-2-8d; Beaumont-Smith and Böhm, 2004). In places, retrograde actinolite crystals (up to 1.5 cm in length) are randomly oriented on the planes of associated planar structures (cleavages, fractures). The garnet-bearing quartz veins shown in Figure GS2019-2-8f may have formed at this stage.

## Economic considerations

New mapping of the LLGB in the Gemmell Lake area suggests that rheological differences between volcanoclastic rocks (unit 1), Fe-rich mafic volcanic rocks (unit 2) and sedimentary rocks (unit 3) acted as foci for ductile strain during multiple phases of deformation along the JSZ and associated subsidiary  $D_2$  structures, focusing Au-bearing fluids into structural and chemical traps. Potential structural traps include areas where  $D_2$  shear zones and  $D_3$  and  $D_4$  structures intersect, as these may form dilatant zones.

To the east of the Motriuk Lake–Jones Lake fault, the McBride Au occurrence (Figure GS2019-2-2) consists of north-northeast-trending Au-bearing quartz-vein systems cutting an unexposed quartz diorite intrusion emplaced within the JSZ (Ferreira, 1993). Historical drill data indicate that significant intersections returned 373.5 g/t Au over



0.4 m and 7.9 g/t over 2.5 m (Assessment File 72937). The McBride quartz diorite could be part of the Motriuk Lake pluton (subunit 7a; Yang and Beaumont-Smith, 2015c) about 1.2 km to the north. The latter body displays a geochemical signature similar to that of the quartz diorite intrusion at the southern margin of the Gordon Au deposit in the Farley Lake area of the northern belt (Yang and Beaumont-Smith, 2016). Notably, the Farley Lake quartz diorite has an adakite-like signature and has been attributed to the post-Sickle intrusive suite (Yang and Lawley, 2018).

Recent studies suggest that rollback of a subducting slab may have resulted in upwelling of asthenosphere and partial melting of previously metasomatized lithospheric mantle. The resulting adakitic melts could transfer Au and other metals from the mantle (Holwell et al, 2019) or lower crust (Hou and Wang, 2019) to the middle to upper crust along deep fault systems (e.g., the JSZ), forming Au deposits aided by favourable chemical-structural traps. Therefore, occurrences of adakite-like intrusions as part of the post-Sickle intrusive suite in the LLGB are worthy of further study in terms of mineral targeting.

The Finlay McKinlay Au occurrence (Ferreira, 1993) also comprises Au-bearing quartz veins in an approximately 10 m wide north-northeast-trending shear zone that can be traced about 100 m along strike and cuts a quartz diorite intrusion (subunit 7a). Bulk-rock sampling from the quartz veins yielded 17 g/t Au (Sherman et al., 1989), not only confirming the presence of visible Au (Baldwin, 1987) but also highlighting the importance of granitoid-hosted Au-bearing quartz-vein systems. More importantly, the association of Te minerals (e.g., hessite [Ag<sub>2</sub>Te], tellurobismuthite [Bi<sub>2</sub>Te<sub>3</sub>]; see Sherman, 1992) within the Au-bearing quartz-vein systems suggests that auriferous fluids may have been sourced from granitoid magmas derived from the mantle (e.g., Holwell et al., 2019) to the lower crust (Hou and Wang, 2019). The quartz diorite intrusion displaying a relative magnetic low is in structural contact with Sickle group polymictic conglomerate (subunit 6b) that appears to have been thrust over the intrusion.

The Gemmell Lake Au occurrence is hosted in mylonite and silicified-sericitized rhyolitic to dacitic volcanic to volcanoclastic rocks (subunit 1a and unit 9) within the JSZ and related structures in the west Gemmell Lake area (Beaumont-Smith and Edwards, 2000). Unlike most Au deposits of the LLGB, the Gemmell Lake occurrence lacks a relatively reducing chemical trap (e.g., Fe-rich mafic volcanic to volcanoclastic rocks at MacLellan and Burnt Timber, BIFs at Gordon). However, the intersection of silicification and sulphidization (disseminated arsenopyrite,

pyrite) of mylonitized felsic volcanic to volcanoclastic rocks controlled by D<sub>2</sub> deformation with D<sub>3</sub> faults may have created favourable structural site(s) for Au precipitation.

South of Boiley Lake, VMS Cu-(Au-Zn) mineralization is hosted in subunit 1c garnet-biotite schist that constitutes the major portion of the Boiley Lake alteration zone (Gale, 1983; Ferreira, 1993; Anderson and Beaumont-Smith, 2001). Drillhole intersections returned 2.02% Cu and 1.2 g/t Au over 0.8 m (Assessment File 92793). The area contains both muscovite-bearing granite (pre-Sickle intrusive suite; subunit 5c) and magnetite-phyric quartz-feldspar porphyry (late intrusive suite; unit 8). The sources of auriferous fluids are the subject of ongoing collaborative research between the Manitoba Geological Survey and the Geological Survey of Canada (GSC). It is worth noting that the fluid sources may be tracked by investigation of the partitioning behaviour of rare-earth elements in magmatic-hydrothermal systems (e.g., Yang, 2019b).

## Acknowledgments

The author thanks M. Kohli for providing enthusiastic field assistance; E. Anderson for thorough logistical support; L. Chackowsky for technical support; and C. Epp for cataloguing, processing and preparing the samples. C.J.M. Lawley of the GSC is thanked for communication of detrital U-Pb zircon age data. Thanks go to Alamos Gold Inc. for generously providing detailed airborne geophysical data. The manuscript benefited greatly from constructive reviews by M. Rinne, K.D. Reid and C.O. Böhm, and from technical editing by R.F. Davie.

## References

- Anderson, S.D. and Beaumont-Smith, C.J. 2001: Structural analysis of the Pool Lake–Boiley Lake area, Lynn Lake greenstone belt (NTS 64C/11); *in* Report of Activities 2001, Manitoba Industry, Trade and Mines, Manitoba Geological Survey, p. 76–85.
- Ansdell, K.M. 2005: Tectonic evolution of the Manitoba-Saskatchewan segment of the Paleoproterozoic Trans-Hudson Orogen, Canada; *Canadian Journal of Earth Sciences*, v. 42, p. 741–759.
- Ansdell, K.M., Corrigan, D., Stern, R. and Maxeiner, R. 1999: SHRIMP U-Pb geochronology of complex zircons from Reindeer Lake, Saskatchewan: implications for timing of sedimentation and metamorphism in the northwestern Trans-Hudson Orogen; Geological Association of Canada–Mineralogical Association of Canada, Joint Annual Meeting, Program with Abstracts, v. 24, p. 3.
- Baldwin, D.A. 1987: Gold mineralization associated with the Johnson Shear Zone; *in* Report of Field Activities 1987, Manitoba Energy and Mines, Minerals Division, p. 7–11.

- Baldwin, D.A., Syme, E.C., Zwanzig, H.V., Gordon, T.M., Hunt, P.A. and Stevens, R.P. 1987: U-Pb zircon ages from the Lynn Lake and Rusty Lake metavolcanic belts, Manitoba: two ages of Proterozoic magmatism; *Canadian Journal of Earth Sciences*, v. 24, p. 1053–1063.
- Baragar, W.R.A., Ernst, R.E., Hulbert, L. and Peterson, T. 1996: Longitudinal petrochemical variation in the Mackenzie dyke swarm, northwestern Canadian Shield; *Journal of Petrology*, v. 37, p. 317–359.
- Bateman, J.D. 1945: McVeigh Lake area, Manitoba; *Geological Survey of Canada, Paper 45-14*, 34 p.
- Beaumont-Smith, C.J. 2008: Geochemistry data for the Lynn Lake greenstone belt, Manitoba (NTS 64C11-16); Manitoba Science, Technology, Energy and Mines, Manitoba Geological Survey, Open File OF2007-1, 5 p.
- Beaumont-Smith, C.J. and Böhm, C.O. 2002: Structural analysis and geochronological studies in the Lynn Lake greenstone belt and its gold-bearing shear zones (NTS 64C10, 11, 12, 14, 15 and 16), Manitoba; *in Report of Activities 2002*, Manitoba Industry, Trade and Mines, Manitoba Geological Survey, p. 159–170.
- Beaumont-Smith, C.J. and Böhm, C.O. 2003: Tectonic evolution and gold metallogeny of the Lynn Lake greenstone belt, Manitoba (NTS 64C10, 11, 12, 14, 15 and 16), Manitoba; *in Report of Activities 2003*, Manitoba Industry, Economic Development and Mines, Manitoba Geological Survey, p. 39–49.
- Beaumont-Smith, C.J. and Böhm, C.O. 2004: Structural analysis of the Lynn Lake greenstone belt, Manitoba (NTS 64C10, 11, 12, 14, 15 and 16); *in Report of Activities 2004*, Manitoba Industry, Economic Development and Mines, Manitoba Geological Survey, p. 55–68.
- Beaumont-Smith, C.J. and Edwards, C.D. 2000: Detailed structural analysis of the Johnson Shear Zone in the west Gemmell Lake area (NTS 64C/11); *in Report of Activities 2000*, Manitoba Industry, Trade and Mines, Manitoba Geological Survey, p. 64–68.
- Beaumont-Smith, C.J. and Rogge, D.M. 1999: Preliminary structural analysis and gold metallogeny of the Johnson Shear Zone, Lynn Lake greenstone belt (parts of NTS 64C/10, 11, 15); *in Report of Activities 1999*, Manitoba Industry, Trade and Mines, Geological Services, p. 61–66.
- Beaumont-Smith, C.J., Anderson, S.D. and Böhm, C.O. 2001: Structural analysis and investigations of shear-hosted gold mineralization in the southern Lynn Lake greenstone belt (parts of NTS 64C/11, /12, /15, /16); *in Report of Activities 2001*, Manitoba Industry, Trade and Mines, Manitoba Geological Survey, p. 67–75.
- Beaumont-Smith, C.J., Machado, N. and Peck, D.C. 2006: New uranium-lead geochronology results from the Lynn Lake greenstone belt, Manitoba (NTS 64C11-16); Manitoba Science, Technology, Energy and Mines, Manitoba Geological Survey, Geoscientific Paper GP2006-1, 11 p.
- Boyle, R.W. 1979: The geochemistry of gold and its deposits (together with a chapter on geochemical prospecting for the element); *Geological Survey of Canada, Bulletin 280*, 584 p.
- Corrigan, D. 2012: Paleoproterozoic crustal evolution and tectonic processes: insights from the Lithoprobe program in the Trans-Hudson orogen, Canada; Chapter 4 *in Tectonic Styles in Canada: The LITHOPROBE Perspective*, J.A. Percival, F.A. Cook and R.M. Clowes (ed.), Geological Association of Canada, Special Paper 49, p. 237–284.
- Corrigan, D., Galley, A.G. and Pehrsson, S. 2007: Tectonic evolution and metallogeny of the southwestern Trans-Hudson Orogen; *in Mineral Deposits of Canada: A Synthesis of Major Deposit-Types, District Metallogeny, the Evolution of Geological Provinces, and Exploration Methods*, W.D. Goodfellow (ed.), Geological Association of Canada, Mineral Deposits Division, Special Publication 5, p. 881–902.
- Corrigan, D., Pehrsson, S., Wodicka, N. and de Kemp, E. 2009: The Palaeoproterozoic Trans-Hudson Orogen: a prototype of modern accretionary processes; *in Ancient Orogens and Modern Analogues*, J.B. Murphy, J.D. Keppie, and A.J. Hynes (ed.), Geological Society of London, Special Publications, v. 327, p. 457–479.
- Fedikow, M.A.F. 1986: Geology of the Agassiz stratabound Au-Ag deposit, Lynn Lake, Manitoba; Manitoba Energy and Mines, Geological Services, Open File Report OF85-5, 80 p.
- Fedikow, M.A.F. 1992: Rock geochemical alteration studies at the MacLellan Au-Ag deposit, Lynn Lake, Manitoba; Manitoba Energy and Mines, Geological Services, Economic Geology Report ER92-1, 237 p.
- Fedikow, M.A.F. and Gale, G.H. 1982: Mineral deposit studies in the Lynn Lake area; *in Report of Field Activities 1982*, Manitoba Department of Energy and Mines, Mineral Resources Division, p. 44–54.
- Fedikow, M.A.F., Ferreira, K.J. and Baldwin, D.A. 1991: The Johnson shear zone – a regional metallogenic feature in the Lynn Lake area; Manitoba Energy and Mines, Geological Services, Minerals Division, Mineral Deposit Thematic Map MDT91-1, scale 1:50 000.
- Ferreira, K.J. 1993: Mineral deposits and occurrences in the McGavock Lake area, NTS 64C/11; Manitoba Energy and Mines, Geological Services, Mineral Deposit Series Report No. 26, 49 p.
- Gale, G.H. 1983: Mineral deposit investigations in the Lynn Lake area; *in Report of Field Activities 1983*, Manitoba Department of Energy and Mines, Mineral Resources Division, p. 84–87.
- Gilbert, H.P. 1993: Geology of the Barrington Lake–Melvin Lake–Fraser Lake area; Manitoba Energy and Mines, Geological Services, Geological Report GR87-3, 97 p.
- Gilbert, H.P., Syme, E.C. and Zwanzig, H.V. 1980: Geology of the metavolcanic and volcanoclastic metasedimentary rocks in the Lynn Lake area; Manitoba Energy and Mines, Mineral Resources Division, Geological Paper GP80-1, 118 p.
- Glendenning, M.W.P., Gagnon, J.E. and Polat, A. 2015: Geochemistry of the metavolcanic rocks in the vicinity of the MacLellan Au-Ag deposit and an evaluation of the tectonic setting of the Lynn Lake greenstone belt, Canada: evidence for a Paleoproterozoic-aged rifted continental margin; *Lithos*, v. 233, p. 46–68.

- Hastie, E.C.G., Gagnon, J.E. and Samson, I.M. 2018: The Paleoproterozoic MacLellan deposit and related Au-Ag occurrences, Lynn Lake greenstone belt, Manitoba: an emerging, structurally controlled gold camp; *Ore Geology Reviews*, v. 94, p. 24–45.
- Hoffman, P.H. 1988: United plates of America, the birth of a craton: Early Proterozoic assembly and growth of Laurentia; *Annual Reviews of Earth and Planetary Sciences*, v. 16, p. 543–603.
- Holwell, D.A., Fiorentini, M., McDonald, I., Lu, Y., Giuliani, A., Smith, D.J., Keith, M. and Locmelis, M. 2019: A metasomatized lithospheric mantle control on the metallogenic signature of post-subduction magmatism; *Nature Communication*, v. 10, p. 3511, URL <<https://doi.org/10.1038/s41467-019-11065-4>> [October 2019].
- Hou, Z. and Wang, R. 2019: Fingerprinting metal transfer from mantle; *Nature Communication*, v. 10, p. 3510, URL <<https://doi.org/10.1038/s41467-019-11445-w>> [October 2019].
- Jones, L.R. 2005: Geology of the shear-hosted Burnt Timber deposit, Lynn, northern Manitoba; M.Sc. thesis, Laurentian University, Sudbury, Ontario, 63 p.
- Jones, L.R., Lafrance, B. and Beaumont-Smith, C.J. 2006: Structural controls on gold mineralization at the Burnt Timber Mine, Lynn Lake Greenstone Belt, Trans-Hudson Orogen, Manitoba; *Exploration and Mining Geology*, v. 15, p. 89–100.
- Kremer, P.D., Rayner, N. and Corkery, M.T. 2009: New results from geological mapping in the west-central and northeastern portions of Southern Indian Lake, Manitoba (parts of NTS 64G1, 2, 8, 64H4, 5); *in* Report of Activities 2009, Manitoba Science, Innovation, Energy and Mines, Manitoba Geological Survey, p. 94–107.
- Lawley, C.J.M., Davis, W.J., Jackson, S.E., Petts, D.C., Yang, E., Zhang, S. Selby, D., O'Connor, A.R. and Schneider, D.A. 2019: Paleoproterozoic gold and its tectonic triggers and traps; *in* Targeted Geoscience Initiative: 2018 report of activities, N. Rogers (ed.), Geological Survey of Canada, Open File 8549, p. 71–75.
- Lewry, J.F. and Collerson, K.D. 1990: The Trans-Hudson Orogen: extent, subdivisions and problems; *in* The Early Proterozoic Trans-Hudson Orogen of North America, J.F. Lewry and M.R. Stauffer (ed.), Geological Association of Canada, Special Paper 37, p. 1–14.
- Ma, G. and Beaumont-Smith, C.J. 2001: Stratigraphic and structural mapping of the Agassiz Metallotect near Lynn Lake, Lynn Lake greenstone belt (parts of NTS 64C/14, /15); *in* Report of Activities 2001, Manitoba Industry, Trade and Mines, Manitoba Geological Survey, p. 86–93.
- Ma, G., Beaumont-Smith, C.J. and Lentz, D.R. 2000: Preliminary structural analysis of the Agassiz Metaltect near the MacLellan and Dot lake gold deposits, Lynn Lake greenstone belt (parts of NTS 64C/14, /15); *in* Report of Activities 2000, Manitoba Industry, Trade and Mines, Manitoba Geological Survey, p. 51–56.
- Manitoba Energy and Mines 1986: Granville Lake, NTS 64C; Manitoba Energy and Mines, Minerals Division, Bedrock Geology Compilation Map Series, Map 64C, scale 1:250 000.
- Martins, T., Kremer, P.D., Corrigan, D. and Rayner, N. 2019: Geology of the Southern Indian Lake area, north-central Manitoba (parts of NTS 64G1, 2, 7–10, 64H3–6); Manitoba Growth, Enterprise and Trade, Manitoba Geological Survey, Geoscientific Report GR2019-1, 51 p. and 4 colour maps at 1:50 000 scale.
- Milligan, G.C. 1960: Geology of the Lynn Lake district; Manitoba Department of Mines and Natural Resources, Mines Branch, Publication 57-1, 317 p.
- Norman, G.W.H. 1933: Granville Lake district, northern Manitoba; Geological Survey of Canada, Summary Report, Part C, p. 23–41.
- Park, A.F., Beaumont-Smith, C.J. and Lentz, D.R. 2002: Structure and stratigraphy in the Agassiz Metaltect, Lynn Lake greenstone belt (NTS 64C/14 and /15), Manitoba; *in* Report of Activities 2002, Manitoba Industry, Trade and Mines, Manitoba Geological Survey, p. 171–186.
- Peck, D.C., Lin, S., Atkin, K. and Eastwood, A.M. 1998: Reconnaissance structural studies of Au metaltectes in the Lynn Lake greenstone belt (parts of NTS 63C/10, C/11, C/15); *in* Report of Activities 1998, Manitoba Energy and Mines, Geological Services, p. 69–74.
- Sherman, G.R. 1992: Geology, hydrothermal activity and gold mineralization in the Gemmell Lake area of the early Proterozoic Lynn Lake greenstone belt, Manitoba; M.Sc. thesis, University of Windsor, Windsor, Ontario, 148 p.
- Sherman, G.R., Samson, I.M. and Holm, P.E. 1988: Preliminary observations of a detailed geological investigation of the Gemmell Lake area, Lynn Lake; *in* Report of Field Activities 1988, Manitoba Energy and Mines, Minerals Division, p. 16–19.
- Sherman, G.R. Samson, I.M. and Holm, P.E. 1989: Deformation, veining and gold mineralization along part of the Johnson shear zone, Lynn Lake greenstone belt, Manitoba; *in* Report of Field Activities 1989; Manitoba Energy and Mines; Minerals Division, p. 16–18.
- Stauffer, M.R. 1984: Manikewan: an Early Proterozoic ocean in central Canada, its igneous history and orogenic closure; *Precambrian Research*, v. 25, p. 257–281.
- Stern, R.A., Syme, E.C. and Lucas, S.B. 1995: Geochemistry of 1.9 Ga MORB- and OIB-like basalts from the Amisk collage, Flin Flon Belt, Canada: evidence for an intra-oceanic origin; *Geochimica et Cosmochimica Acta*, v. 59, p. 3131–3154.
- Syme, E.C. 1985: Geochemistry of metavolcanic rocks in the Lynn Lake Belt; Manitoba Energy and Mines, Geological Services/ Mines Branch, Geological Report GR84-1, 84 p.
- Turek, A., Woodhead, J. and Zwanzig H.V. 2000: U-Pb age of the gabbro and other plutons at Lynn Lake (part of NTS 64C); *in* Report of Activities 2000, Manitoba Industry, Trade and Mines, Manitoba Geological Survey, p. 97–104.
- Yang, X.M. 2019a: Bedrock geology of the Gemmell Lake area, Lynn Lake greenstone belt, northwestern Manitoba (parts of NTS 64C11, 14); Manitoba Agriculture and Resource Development, Manitoba Geological Survey, Preliminary Map PMAP2019-2, scale 1:20 000.

- Yang, X.M. 2019b: Using rare earth elements (REE) to decipher the origin of ore fluids associated with granite intrusions; *Minerals*, v. 9, p. 426, URL <<https://doi.org/10.3390/min9070426>> [October 2019].
- Yang, X.M. and Beaumont-Smith, C.J. 2015a: Bedrock geology of the Keewatin River area, Lynn Lake greenstone belt, northwestern Manitoba (parts of NTS 64C14, 5); *Manitoba Mineral Resources*, Manitoba Geological Survey, Preliminary Map PMAP2015-3, scale 1:20 000.
- Yang, X.M. and Beaumont-Smith, C.J. 2015b: Geological investigations of the Keewatin River area, Lynn Lake greenstone belt, northwestern Manitoba (parts of NTS 64C14, 15); *in* Report of Activities 2015, Manitoba Mineral Resources, Manitoba Geological Survey, p. 52–67.
- Yang, X.M. and Beaumont-Smith, C.J. 2015c: Granitoid rocks in the Lynn Lake region, northwestern Manitoba: preliminary results of reconnaissance mapping and sampling; *in* Report of Activities 2015, Manitoba Mineral Resources, Manitoba Geological Survey, p. 68–78.
- Yang, X.M. and Beaumont-Smith, C.J. 2016: Geological investigations in the Farley Lake area, Lynn Lake greenstone belt, northwestern Manitoba (part of NTS 64C16); *in* Report of Activities 2016, Manitoba Growth, Enterprise and Trade, Manitoba Geological Survey, p. 99–114.
- Yang, X.M. and Beaumont-Smith, C.J. 2017: Bedrock geology of the Wasekwan Lake area, Lynn Lake greenstone belt, northwestern Manitoba (parts of NTS 64C10, 15); *Manitoba Growth, Enterprise and Trade*, Manitoba Geological Survey, Preliminary Map PMAP2017-3, scale 1:20 000.
- Yang, X.M. and Lawley, C.J.M. 2018: Tectonic setting of the Gordon gold deposit, Lynn Lake greenstone belt, northwestern Manitoba (parts of NTS 64C16): evidence from litho-geochemistry, Nd isotopes and U-Pb geochronology; *in* Report of Activities 2018, Manitoba Growth, Enterprise and Trade, Manitoba Geological Survey, p. 89–109.
- Zwanzig, H.V. and Bailes, A.H. 2010: Geology and geochemical evolution of the northern Flin Flon and southern Kisseynew domains, Kississing–File lakes area, Manitoba (parts of NTS 63K, N); *Manitoba Innovation, Energy and Mines*, Manitoba Geological Survey, Geoscientific Report GR2010-1, 135 p.
- Zwanzig, H.V., Syme, E.C. and Gilbert, H.P. 1999: Updated trace element geochemistry of ca. 1.9 Ga metavolcanic rocks in the Paleoproterozoic Lynn Lake belt; *Manitoba Industry, Trade and Mines*, Geological Services, Open File Report OF99-13, 46 p.

## Geological investigations in the Russell–McCallum lakes area, northwestern Manitoba (parts of NTS 64C3–6)

by T. Martins and C.G. Couëslan

### In Brief:

- Updated bedrock geology and regional framework and interpretation of this part of the Kiseynew basin of the Trans-Hudson orogeny
- Bedrock outcrops are dominated by the coeval sedimentary rocks of the Burntwood and Sickle groups
- Graphite contents of Burntwood sedimentary rocks suggest widespread economic potential for this commodity in the Kiseynew domain

### Citation:

Martins, T. and Couëslan, C.G. 2019: Geological investigations in the Russell–McCallum lakes area, northwestern Manitoba (parts of NTS 64C3–6); in Report of Activities 2019, Manitoba Agriculture and Resource Development, Manitoba Geological Survey, p. 30–41.

### Summary

Bedrock mapping at a scale of 1:20 000 was undertaken by the Manitoba Geological Survey in the Russell–McCallum lakes area in the summer of 2019. The information gathered resulted in an updated regional framework and interpretation of this part of the Kiseynew basin. Outcrops in the Russell–McCallum lakes area are dominated by the coeval sedimentary rocks of the Burntwood and Sickle groups, granodiorite, and minor intrusive bodies and volcanic rocks. These rock units were sampled for lithogeochemical, petrographic, metamorphic, isotopic and geochronological studies. Details provided in this report are restricted to field descriptions and observations. Graphite contents of Burntwood sedimentary rocks suggest widespread economic potential for this commodity in the study area and possibly the Kiseynew domain in general.

### Introduction

Multidisciplinary geological fieldwork, investigating bedrock and surficial geology, was undertaken by the Manitoba Geological Survey (MGS) in the Russell–McCallum lakes area during July and August of 2019. Bedrock mapping was focused on the central and southern areas of Russell Lake, as well as the east–west channel that links Russell Lake to McCallum Lake. A few outcrops of Burntwood group rocks and iron formation were also examined and sampled at McCallum Lake. Results from bedrock mapping are presented here and on the accompanying map PMAP2019-3 (Martins and Couëslan, 2019), while surficial geology results are reported in Hodder (2019).

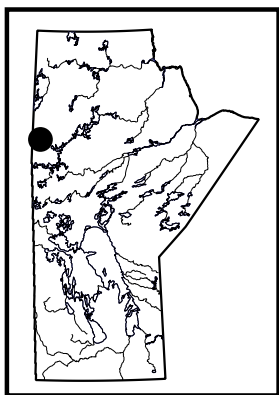
The main objectives of bedrock mapping in the Russell–McCallum lakes area were to

- 1) update the bedrock geology of the area and carry out lithogeochemistry, isotope and geochronology studies;
- 2) update the regional framework and tectonic interpretation of the area by taking into account recent work in the Trans-Hudson orogen (THO), particularly in the Granville Lake area (e.g., Zwanzig, 2019) on the north flank of the Kiseynew domain (KD);
- 3) provide an updated interpretation of the metamorphic conditions of the study area; and
- 4) update the knowledge of the economic potential of the KD, especially graphite occurrences reported by previous authors (e.g., Lenton, 1981) in light of the current market trends and growing interest in this commodity.

Rock descriptions and mineral estimates given in this report are based on outcrop observation. Further studies are needed to carry out metamorphic, tectonic and stratigraphic interpretations of the Russell–McCallum lakes area. All rocks in the study area were metamorphosed at upper-amphibolite-facies conditions (Lenton, 1981); however, for the sake of brevity, the term ‘meta’ has been omitted from rock names. Where possible, protolith interpretation was used in the naming of rock units.

### Previous work

The Russell–McCallum lakes area was previously mapped by Downie (1936) of the Geological Survey of Canada (GSC) at a scale of one inch to four miles. Later, geological mapping by Hunter (1953) extended the regional coverage into McKnight Lake at a scale of one inch to two miles. The area last saw geological mapping by the MGS in the 1970s. McRitchie (1975a, b) mapped Russell Lake at a scale of one inch to one-half mile. The adjoining areas were mapped by Baldwin (1976) and Zwanzig and Wielezyski (1975) at a scale of one inch





to one-half mile, and Pollock (1966) at a scale of one inch to one mile. The area to the west of Russell–McCallum lakes was mapped by Gilboy (1976) at a scale of 1:100 000. Lenton (1981) mapped from the Russell–McCallum lakes area to McKnight Lake. The Russell Lake area was also the target of economic studies focused on base-metal mineralization along the contact zone between two major stratigraphic units (Baldwin, 1976, 1980).

There are records of base-metal exploration work in the Russell–McCallum lakes area from 1954 until 1983 (e.g., Assessment Files 91616, 93803, Manitoba Agriculture and Resource Development, Winnipeg). As a result of this work, airborne electromagnetic surveys located a number of areas with good conductors. The airborne anomalies were commonly followed up by diamond-drilling. Base- and precious-metal assay results (e.g., Ni, Au, Ag, Cu) were not promising and led to abandonment of the claims. However, significant graphite mineralization was reported in the majority of drillholes (e.g., Assess-

ment Files 92387, 93001, 93804). For example, graphite was described in Assessment File 90985 on work completed by Hudson Bay Exploration and Development Company Limited. The company drilled six holes in 1962 and reported up to 2.23 m (7.3 feet) of near-solid to solid graphite, pyrite and pyrrhotite; 1.9 m (6.2 feet) of well-mineralized graphite; and 1.2 m (4.1 feet) of mineralized graphite.

## Regional geology

The Russell–McCallum lakes area is located along the north flank of the KD, a subdivision introduced by Zwanzig and Bailes (2010; Figure GS2019-3-1). The Kiseynew north flank is dominated by Paleoproterozoic metasedimentary rocks of the Burntwood and Sickie groups and granitoid rocks, which are bounded to the north by the Lynn Lake belt, to the east by the Thompson nickel belt and to the south by the central KD.

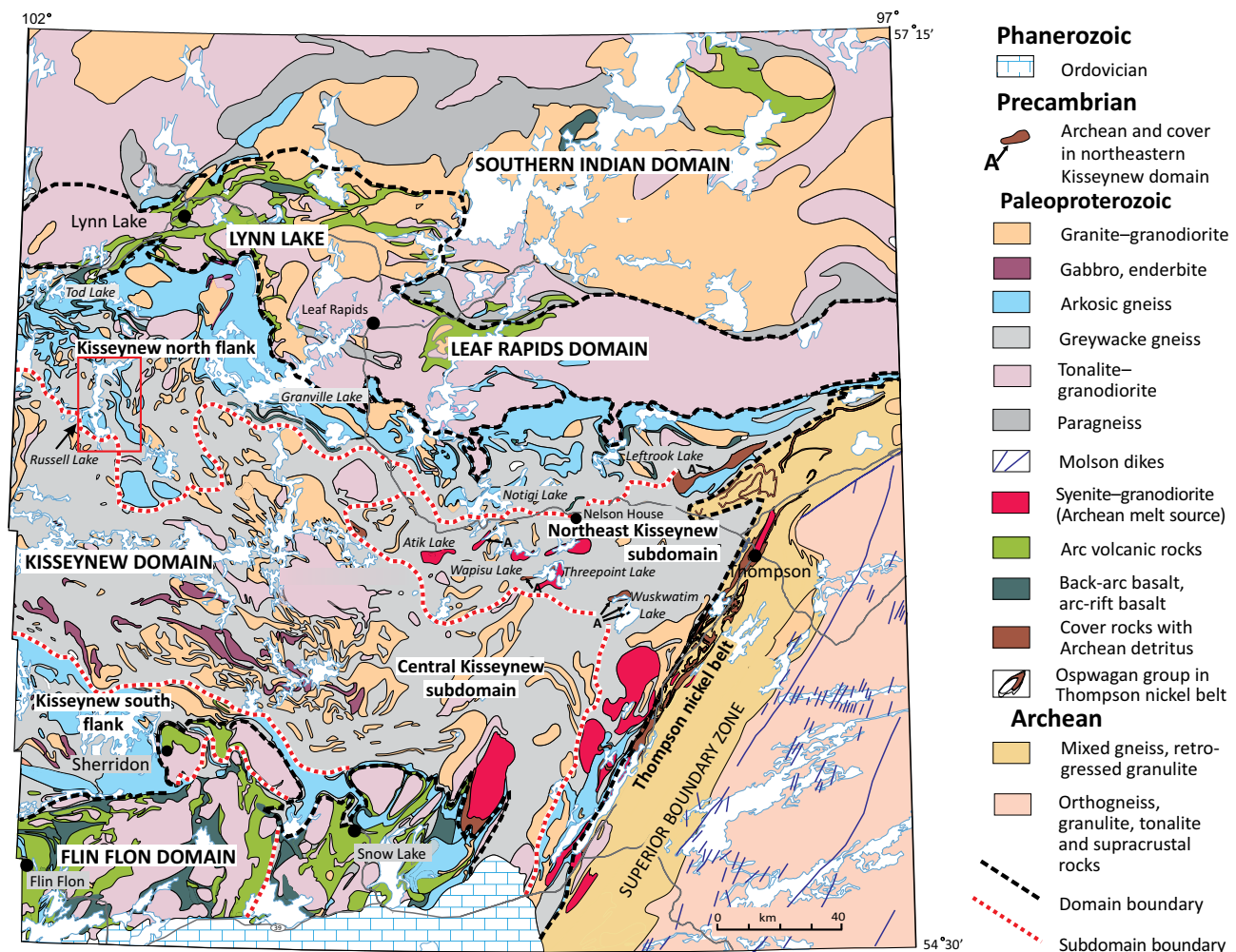


**Figure GS2019-3-1:** Regional geology of the Trans-Hudson orogen (THO) in Manitoba, indicating the subdivision of the KD proposed by Zwanzig and Bailes (2010). Red rectangle outlines the study area.

The KD forms the large central part of the predominantly juvenile Paleoproterozoic internides, which make up the Reindeer zone of the THO in Manitoba (Stauffer, 1984; Lewry and Collerson, 1990). It is dominated by metamorphosed greywacke and mudstone of the Burntwood group. The provenance of the Burntwood group is interpreted to be the adjacent magmatic-arc terranes. Detritus from the arcs was deposited in coalescing turbidite fans (Bailes, 1980; Zwanzig, 1999). The turbidites were deformed and metamorphosed to amphibolite and transitional granulite facies, resulting in migmatization. Rocks from the Sickle group are typically metamorphosed arkosic units interpreted to have been deposited unconformably on the Lynn Lake arc massif (Zwanzig, 2008), and prograded over the Burntwood group during the onset of terminal continental collision. Intrusive bodies in rocks of both the Burntwood and Sickle groups include foliated granitoid bodies ranging from granite to tonalite and later pegmatite (e.g., Lenton, 1981; Zwanzig and Bailes, 2010; Zwanzig, 2019).

The geological setting of the KD is a matter of debate. Some authors (Ansdell, 2005; Corrigan et al., 2005, 2009) favour the interpretation of the KD as a back-arc basin to the Flin Flon volcanic arc that was filled during its opening. However, other authors (e.g., Zwanzig, 1999; Zwanzig and Bailes, 2010) favour an interpretation of a longer lived and dynamic evolution in which the present geographic distribution of rocks resulted from crustal-scale overturning and oroclinal bending during continental collision.

## Description of rock units

The majority of outcrops in the Russell–McCallum lakes area are dominated by sedimentary rocks of the Burntwood and Sickle groups, granodiorite and minor intrusive bodies, and volcanic rocks (Figure GS2019-3-2). The Burntwood and Sickle groups are interpreted to be coeval (e.g., Zwanzig and Bailes, 2010); therefore, the succession of units presented below is not to be interpreted as a true chronostratigraphic sequence. Figure GS2019-3-3 represents an idealized stratigraphic column for the area.

### ***Mafic to ultramafic rocks (unit 1a–d)***

Massive basalt (subunit 1a) is dark green-grey, medium to coarse grained and foliated, with massive layering <2 m thick. The composition is variable but typically consists of 60–70% amphibole, 20–30% plagioclase and 5–10% biotite, with trace amounts of pyrite and chalcopyrite, and rare magnetite. Local layers contain up to 10% garnet, which can be partially or completely pseudomorphously replaced by plagioclase (Figure GS2019-3-4a). Gossanous zones, typically <40 cm wide, are often associ-

ated with the mafic volcanic flows near the contact with the sedimentary rocks. In selected outcrops, discontinuously and heterogeneously banded (<10 cm) basalt may represent flow breccia. Local, patchy, green-coloured layers could either be a product of calcsilicate alteration or represent strongly attenuated pillowed basalt.

Pillowed basalt (subunit 1b) was identified in a few outcrops in the central and south parts of Russell Lake, as well as in the channel to Moyer Lake (Figure GS2019-3-1). The best preserved outcrops are located in the central area of Russell Lake. Pillowed flows, up to 5 m thick, range in colour from very dark green to black (Figure GS2019-3-4b). Pillows vary in size from 15 cm to 2 m and are typically densely packed or bun shaped with a 1:10 ratio of flattening. Pillow selvages are composed mostly of coarse-grained hornblende and plagioclase, or locally of only plagioclase, and exhibit positive relief. Selvages are typically 2–3 cm wide but can locally reach 12 cm. Rare top indicators are present west of Marshall Island, where pillow cusps indicate younging to the northeast. In the channel to Moyer Lake, pillow tops appear to young toward the south. Patchy to irregular, pale green calcsilicate alteration, present in some pillowed basalts, consists of varying amounts of epidote and carbonate. Where strain is high, this alteration was transposed parallel to the dominant deformation fabric, imparting a structural and metamorphic layering on the rock. The pillowed basalt is locally associated with gossanous zones that can be up to 20 cm in width. Assay results from these zones are pending.

Sparse intrusions (subunit 1c) of coarse-grained gabbro are associated with the basalt along the channel to Moyer Lake. The gabbro is dark green-grey, foliated and relatively homogeneous, with 50–60% hornblende in a groundmass of plagioclase. Discrete, relatively equant hornblende, <1 cm across, may be pseudomorphous after pyroxene phenocrysts. The contact between the basalt and gabbro appears disconformable. At one location, melagabbro with 10–20% plagioclase appears to grade over ~5 m into peridotite.

Ultramafic rocks (subunit 1d) range in composition from pyroxenite to peridotite. The pyroxenitic rocks are very dark green-brown to black, coarse grained, foliated and moderately to locally magnetic. Composition is variable, with 30–40% black clinoamphibole, 20–30% orthoamphibole, 20–30% green clinoamphibole, 3–5% serpentine and trace amounts of magnetite. Outcrops locally contain abundant biotite and magnetite, which are likely the result of hydrothermal alteration.

Peridotite is dark brown on weathered surfaces and very dark grey when fresh. It is weakly foliated to foliated and weakly to strongly magnetic. Outcrops are character-

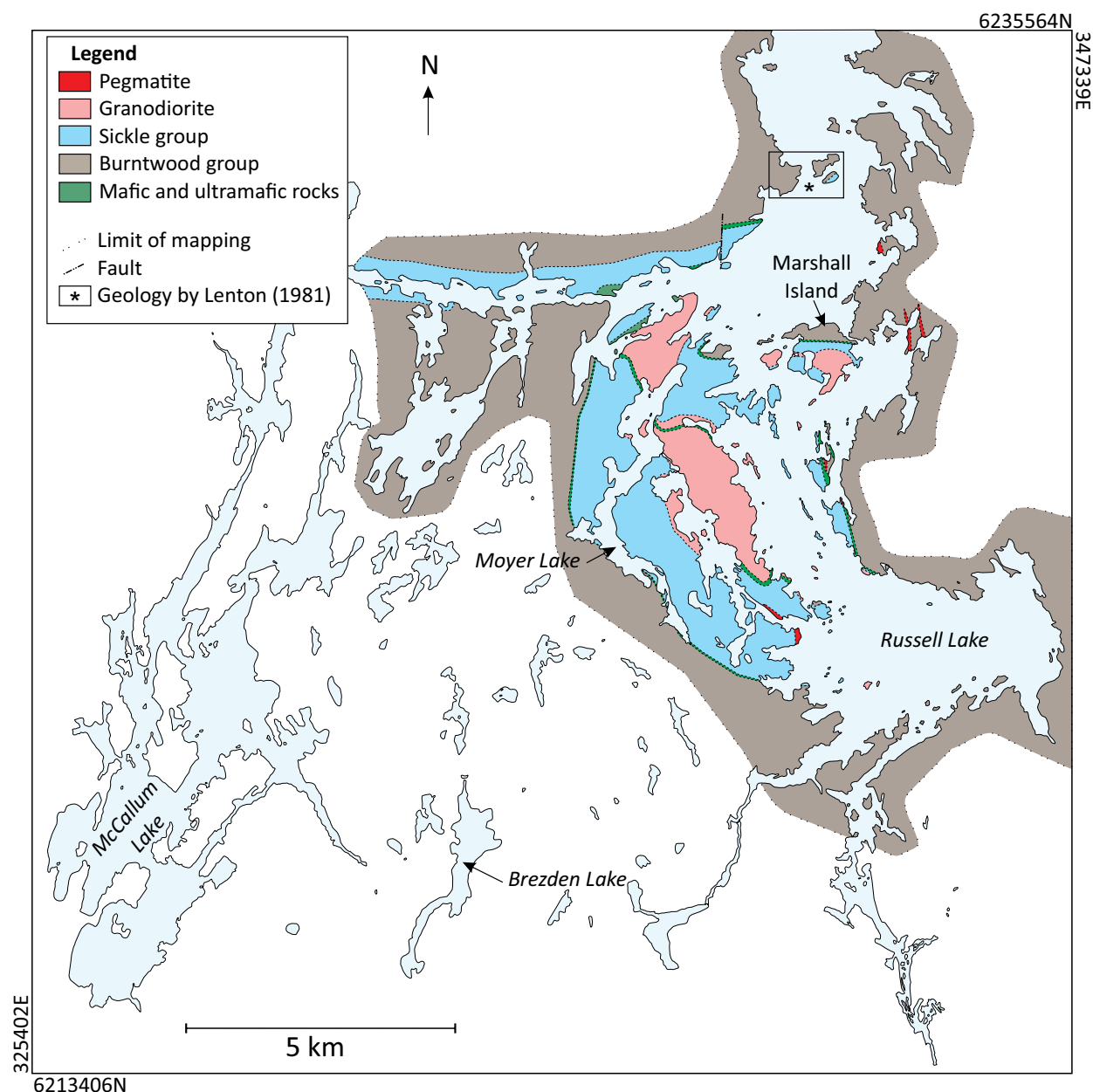


**Figure GS2019-3-2:** Simplified geology of Russell Lake (after Martins and Couëslan, 2019; Lenton, 1981).

ized by a fine- to medium-grained, amphibole-rich groundmass, commonly with patchy zones of knobby-textured surfaces dominated by coarse-grained orthoamphibole and/or orthopyroxene, alternating with zones dominated by a fine- to medium-grained, brown granular mineral, possibly olivine, with negative relief (Figure GS2019-3-4c). The composition of the groundmass is variable but typically consists of green clinoamphibole (10–20%), brown orthoamphibole (10–20%) and black clinoamphibole (hornblende, 20–30%). Local plagioclase (<5% as segregations <3 cm in width) and biotite (<15%) were identified at a few outcrops. Outcrops are locally transected by arrays of dextral shear bands separating relatively undeformed

lenses of peridotite <1 m across. Local vuggy textures may be the result of differential weathering of carbonate or olivine, and local gossanous patches are present. The majority of peridotite outcrops occur as isolated reefs and islands, commonly surrounded by exposures of granodiorite (unit 11). These are interpreted as large-scale (tens of metres) xenoliths within the granodiorite. At one outcrop in the channel to Moyer Lake, a succession of massive and pillowed basalt, melagabbro and peridotite was observed, suggesting that the ultramafic rock is a subunit of the mafic volcanic rock suite. Samples were submitted for lithogeochemistry and results are pending.

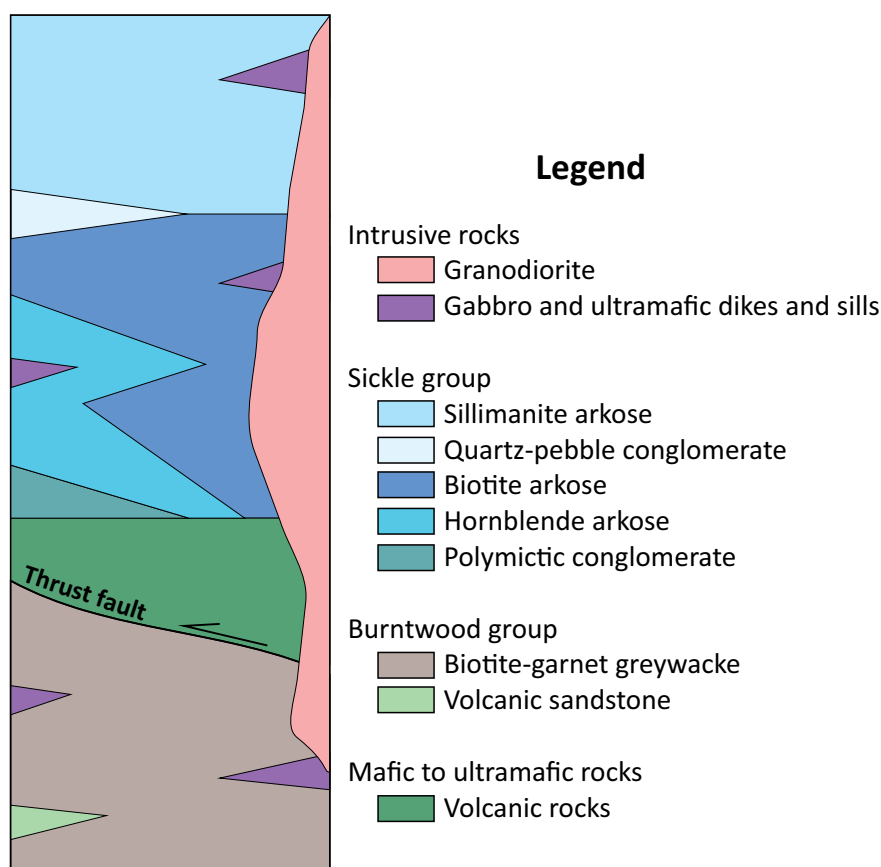


**Figure GS2019-3-3:** Idealized, schematic stratigraphic column of the Burntwood and Sickle group rocks and volcanic rocks found in the Russell–McCallum lakes area.

### **Burntwood group rocks (unit 2)**

Typical outcrops of Burntwood group rocks consist of monotonous and rhythmically interbedded psammitic and pelitic layers with local pods of calcsilicate and sparse iron formation. The lack of unique marker horizons, combined with ubiquitous isoclinal folding, does not allow for the subdivision of Burntwood group rocks into smaller stratigraphic packages, nor for the tracing of stratigraphy between outcrops. A package of volcanoclastic rocks was identified within the Burntwood group in southern Russell Lake.

#### **Garnet-biotite greywacke (subunit 2a)**

The Burntwood group is dominated by garnet-biotite greywacke. It is typically light grey on weathered surfaces and medium grey where fresh, and nonmagnetic. Bedding typically varies from 30 cm to 1 m thick and alternates between psammitic and pelitic compositions. Psammitic layers are typically composed of quartz (30–40%), feldspar (20–30%), biotite (up to 15%), garnet (up to 10%) and graphite (trace amounts to 6%). The pelitic layers are composed of quartz (10–20%), feldspar (20–30%), biotite

(20–30%), garnet (10–12%) and graphite (trace to 7%), with local sillimanite (<10%) and cordierite (<5%). Graphite is ubiquitous with apparently no preferential association with either the psammitic or the pelitic beds. Garnet can be absent in local exposures, with rare beds containing 3–5% orthoamphibole and/or orthopyroxene in place of garnet.

Younging-direction information is scarce. Graded bedding (Figure GS2019-3-4d) is visible at some outcrops, but opposite younging directions can be observed in the same outcrop, a characteristic also observed by Lenton (1981). The garnet-biotite greywacke is commonly isoclinally folded. Folding becomes complex with proximity to large-scale fold noses, making primary structural observations and measurements difficult. Local centimetre-scale calcsilicate nodules and minor layers consist of varying amounts of epidote, carbonate, amphibole, plagioclase and quartz. A combination of both in-source leucosome and pegmatite injections is present in the majority of outcrops. Pods of leucosome <20 cm thick commonly contain peritectic garnet±cordierite. Typically, more than a single generation of injections is present.



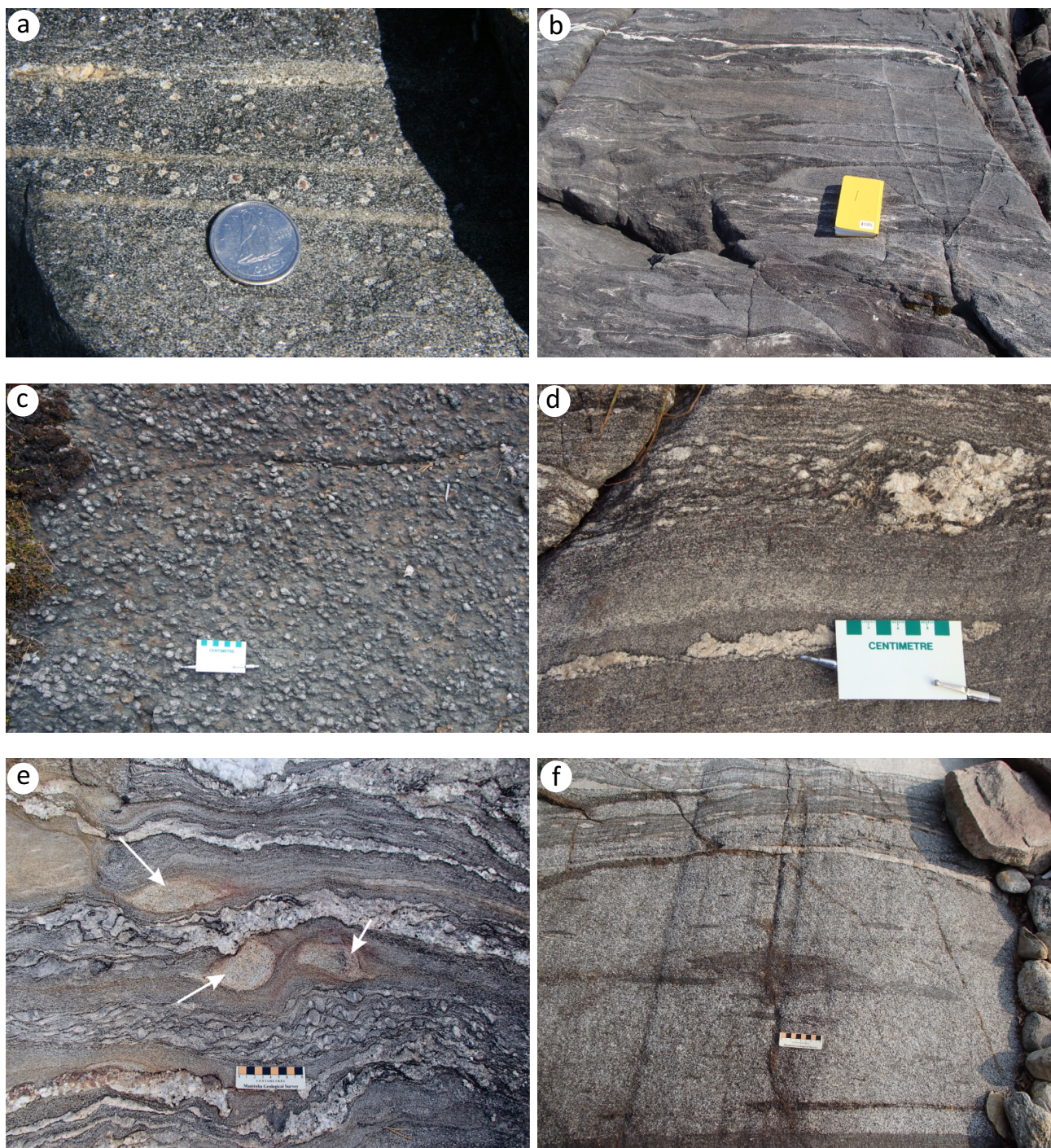


**Figure GS2019-3-4:** Outcrop photographs from the Russell Lake area: **a)** basalt (subunit 1a) with garnet partially replaced by plagioclase; **b)** pillowed basalt (subunit 1b), characterized by pillow selvages with positive relief; **c)** peridotite (subunit 1d), exhibiting knobby-textured surfaces dominated by coarse-grained orthoamphibole and/or orthopyroxene in a fine- to medium-grained, brown granular groundmass of possibly olivine, with negative relief; **d)** garnet-biotite greywacke of the Burntwood group (subunit 2a), showing a rare example of preserved graded bedding (younging toward the top of the photo); **e)** rounded felsic clasts (arrows) in garnet-biotite greywacke of the Burntwood group (subunit 2a); **f)** fragmental volcaniclastic rock of the Burntwood group (subunit 2b).

In the south basin of Russell Lake, an outcrop of Burntwood group contains a pebbly layer (Figure GS2019-3-4e) that possibly marks the base of a turbidite sequence, or the pebbles could represent a low-stand or deposits in

close proximity to a submarine channel. Clasts and cobbles within the pebbly layer are rounded and mostly felsic in composition; alternatively, the clasts and cobbles could represent intensely boudinaged felsic dikes.



On the east shoreline of central Russell Lake and in minor bays south of the channel to McCallum Lake, rose quartz was found in boudinaged segregation pieces up to 30 cm wide in quartz veins within the garnet-biotite greywacke. Rusty layers in the garnet-biotite greywacke were observed in the south part of the mapping area, and a graphitic, sulphide-facies iron formation, >5 m thick, occurs along the west shore of McCallum Lake. Assay results for these rusty layers are pending.

#### **Volcaniclastic rocks (subunit 2b)**

Volcaniclastic rocks were found associated with the garnet-biotite greywacke of the Burntwood group along the southwest shore of Russell Lake. This subunit is variable in composition (felsic to mafic) and texture (massive to fragmental; Figure GS2019-3-4f). The more felsic variety is coarse grained, homogeneous, foliated and non-magnetic. It weathers medium grey and is dark grey on fresh surfaces. It contains plagioclase (60–70%), quartz (10–15%) and biotite (12–15%). The mafic variety is locally coarse grained and magnetic, and contains hornblende and biotite (55–65%), plagioclase (20–30%), quartz (5–8%) and trace amounts of magnetite. The matrix of the fragmental rock is felsic to mafic in composition, with hornblende and biotite. Fragments (<15 cm) are subrounded to angular and typically intermediate to mafic but rarely felsic. Rare calcsilicate nodules were also observed within the fragmental rock unit. Locally, the intermediate fragmental rock grades into the garnet-biotite greywacke with sparse layers of mafic tuff. All the outcrops are cut by 15–20 cm wide tonalitic injections.

The more felsic and massive variety of the volcaniclastic rock subunit could be interpreted as tonalite, recrystallized felsic volcanic sandstone or a dacitic flow. The more mafic rock could be interpreted as a gabbro intrusion or recrystallized mafic volcaniclastic rock. The fragmental variety could be interpreted as a volcanic sandstone or conglomerate, or the fragments could be considered cognate xenoliths of an intermediate to mafic intrusion. Pending further analyses, the authors favour a volcaniclastic origin. Volcanic deposits within the Burntwood group were described by Zwanzig and Bailes (2010) near Puffy Lake on the south flank of the KD.

#### **Gabbro and pyroxenite (unit 3)**

Gabbro and pyroxenite were identified at two locations in the south basin of Russell Lake. A crosscutting intrusive contact between pyroxenite and Burntwood group rocks was observed at both locations.

Gabbro is dark grey weathering to salt and pepper, medium to coarse grained and nonmagnetic. It con-

tains hornblende (50–60%), plagioclase (40–50%) and quartz (<5%). Pyroxenite is dark grey, coarse grained, foliated and weakly magnetic. At the contact with the Burntwood group garnet-biotite greywacke, partially digested calcsilicate nodules are observed, likely originating from the sedimentary rocks. An intrusive breccia consisting of pyroxenite fragments in a tonalitic matrix is locally associated with the pyroxenite (Figure GS2019-3-5a).

#### **Sickle group rocks (units 4–8)**

Five different arkosic rocks were distinguished within the Sickle group (listed by inferred stratigraphic order): polymictic conglomerate, hornblende arkose, biotite arkose, quartz-pebble conglomerate and sillimanite arkose.

##### **Polymictic conglomerate (unit 4)**

Polymictic conglomerate is poorly exposed in the map area. Outcrops of this unit were found on a peninsula on the east–west channel that connects Russell and McCallum lakes, and in the channel to Moyer Lake. Typically, outcrops are highly deformed and the conglomerate assumes a strongly banded, gneissic texture. A less deformed portion of an outcrop in the channel to Moyer Lake shows conglomerate in direct contact with gabbro (subunit 1c; Figure GS2019-3-5b). Conglomerate is clast supported, with clasts varying in size (up to 30 cm but typically <15 cm across). Composition of the clasts varies from felsic (20–30%) to mafic (20–30%), and the matrix is intermediate. Clasts of intermediate composition may also be present but would be indistinguishable from the matrix due to recrystallization.

##### **Hornblende arkose (unit 5)**

This unit typically occurs at the contact with the mafic to ultramafic rocks (unit 1). It is crudely layered but can be well bedded in close proximity to basalt; however, this could be the result of strain partitioning toward the contact. Compositional layering was observed in some outcrops where 20–40 cm thick light grey layers alternate with 5–15 cm thick dark grey layers, reflecting variations in the mafic mineral content. Hornblende arkose is green-pink and weathers to green-grey. It is foliated, weakly magnetic and typically medium to coarse grained. Composition is variable but typically consists of feldspar (40–50%), quartz (25–30%, locally up to 50%), hornblende (10–15%, locally up to 30%), biotite (5–7%), epidote (2–3%) and magnetite (trace to 1%). Hornblende arkose locally grades into mafic sandstone at the basalt contact. The mafic sandstone is quartzofeldspathic (plagioclase>>K-feldspar), with

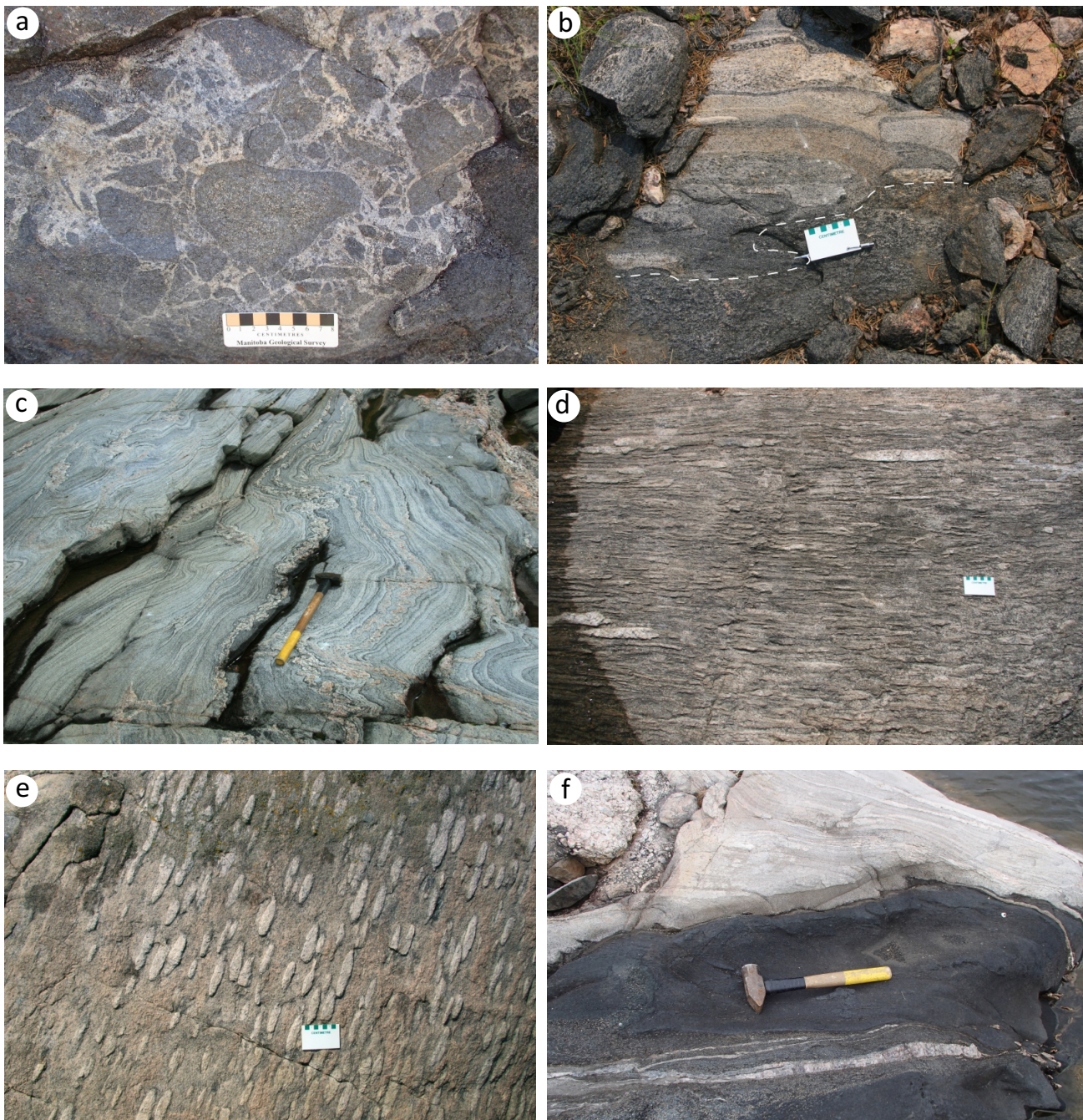


**Figure GS2019-3-5:** Outcrop photographs of mafic and ultramafic rocks and Sickie group rocks from the Russell Lake area: **a)** intrusive breccia (unit 3) with tonalitic matrix; **b)** polymictic conglomerate of the Sickie group (unit 4) in contact (dashed line) with gabbro, along the channel to Moyer Lake; **c)** example of well-bedded biotite arkose of the Sickie group (unit 6); **d)** attenuated clasts of the quartz-pebble conglomerate of the Sickie group (unit 7); **e)** sillimanite knots in sillimanite arkose (unit 8); **f)** ultramafic dike cutting biotite arkose of the Sickie group.

30–50% hornblende. Granitic injections are common. Hornblende arkose contains calcsilicate boudins up to 75 cm wide.

A local variation of hornblende arkose is a coarsely recrystallized gneiss with a slightly different composition. It appears bleached and is strongly foliated and strongly magnetic, with nodules of carbonate, epidote and scap-

olite. The rock contains feldspar (40–50%), quartz (20–30%), green pyroxene (10–15%), titanite (3–5%), epidote (3–5%), magnetite (1–2%) and scapolite (1–2%). Lithogeochemical results may aid in determining the petrogenesis of this unit. Contacts between hornblende arkose and overlying biotite arkose are generally gradational; however, relatively sharp contacts were also observed.



### **Biotite arkose (unit 6)**

Biotite arkose is light pink-grey and weathers to light grey (Figure GS2019-3-5c). It is medium to coarse grained, layered to locally laminated, magnetic, foliated and folded with minor isoclinal folds. Biotite arkose typically consists of quartz (30–40%, locally up to 50%), feldspar (20–30%), biotite (7–10%, locally up to 20% in more aluminous layers) and magnetite (trace to locally 2%). Layering typically consists of thin biotite-enriched laminations (2–3 mm) alternating with thicker quartzofeldspathic layers (<10 cm). Sparse crossbedding was identified. Local calcsilicate layers and nodules are composed mostly of epidote, quartz and plagioclase, with local carbonate. Biotite arkose locally contains well-rounded pebbles, especially along the channel to Moyer Lake. Both concordant and discordant granitic injections are present in most outcrops, which suggests more than one generation. Local pods of leucosome were also identified (commonly <7 cm wide). A local variety of biotite arkose in the channel to McCallum Lake contains garnet (up to 5%) and sillimanite (up to 7%). There, biotite arkose appears to grade into the overlying sillimanite arkose.

### **Quartz-pebble conglomerate (unit 7)**

Quartz-pebble conglomerate was only recognized in and near the channel to Moyer Lake, where it grades into the underlying biotite arkose and overlying sillimanite arkose as discrete conglomerate and pebbly beds <50 cm thick. It is dark grey weathering to light grey on fresh surfaces and locally magnetic. The conglomerate ranges from clast to matrix supported and is massively bedded at a scale of <2 m. Gravel clasts are well rounded, <10 cm and consist dominantly of quartz. Local felsic and sparse granite, calcsilicate, mafic and intermediate clasts are also present. The clasts are typically stretched and attenuated (Figure GS2019-3-5d). The matrix of the conglomerate varies from compositions similar to the biotite and sillimanite arkoses with minor garnet to a plagioclase-rich matrix with 2–3% garnet, 10–20% biotite and 10–20% quartz. Local plagioclase-rich clasts of similar composition can occur within these same beds. The conglomerate contains calcsilicate concretions and discontinuous calcareous layers, <1 m thick, that are epidote and quartz rich.

### **Sillimanite arkose (unit 8)**

Sillimanite arkose is dark grey weathering to light pinkish grey on fresh surfaces. It is medium grained, foliated, massively bedded and weakly magnetic (local <15 cm thick beds are strongly magnetic), with local calcsilicate layers. Sillimanite arkose contains quartz (30–40%, locally up to 50%), plagioclase and K-feldspar (30–50%), biotite

(3–5%), sillimanite (up to 30% in the more aluminous layers), magnetite (trace to 1%) and trace amounts of ilmenite. The amount of sillimanite in this unit can be variable, with less aluminous horizons containing 3–5% and more aluminous sections 15–30%. Sillimanite commonly occurs along foliation planes; in more aluminous layers, it occurs as abundant sillimanite knots, typically <2 cm but locally up to 20 cm (Figure GS2019-3-5e). Magnetite is commonly present in the core of the sillimanite knots.

### ***Mafic to ultramafic dikes and sills (unit 9)***

Mafic to ultramafic dikes and sills intrude both the Sickie and Burntwood group rocks. Although generally similar, the intrusions in the Sickie group are typically ultramafic (Figure GS2019-3-5f), whereas intrusions in the Burntwood group are usually mafic and locally layered. The intrusions are typically <40 cm but reach up to 2 m in width; are black, medium to coarse grained, foliated and locally boudinaged; and range from nonmagnetic to magnetic. Conformable and layered examples could represent flows rather than sills; however, local discordancy suggests an intrusive origin for at least some of this unit. The composition is variable but is typically hornblende (90–95%), plagioclase (5–7%) and phlogopite (2–5%) for the ultramafic sills intruding the Sickie group; and hornblende (70–80%), plagioclase (10–15%, locally up to 30%), biotite (1–2%) and trace amounts of magnetite for mafic intrusions in Burntwood group greywacke. Mafic sills were described from the Missi group on the south flank of the KD (Zwanzig and Bailes, 2010) and could be similar to the ones observed at Russell Lake. Lithogeochemical data may help clarify the petrogenesis and potential relationships between these intrusions.

### ***Hornblende-biotite diorite (unit 10)***

Hornblende-biotite diorite was recognized in two locations along the channel into Moyer Lake, where it occurs enclosed in granodiorite. The diorite weathers dark grey to light grey and is medium grained and foliated. Mafic minerals consist of 5–10% biotite and 10–15% hornblende. It is relatively homogeneous and has local granitic pegmatite injections. An exposed contact suggests that granodiorite is intrusive into diorite. The close spatial association and textural similarity, however, may suggest that diorite is an early magmatic phase related to granodiorite.

### ***Granodiorite (unit 11)***

Granodiorite forms the most abundant type of granitoid rock in the Russell Lake area. These intrusions are interpreted as domes within the cores of major fold structures (Zwanzig and Bailes, 2010). Granodiorite is pale pink

and weathers white to beige. It is medium grained, foliated and nonmagnetic. It typically contains 40–50% plagioclase, 20–30% quartz, 10–15% K-feldspar and 5–7% biotite. Granodiorite is relatively homogeneous, with local pods of leucosome and pegmatite injections. Local exposures display a discontinuous gneissosity. Minor isoclinal folds were observed in gneissic sections. A porphyritic texture of relatively coarse-grained quartz (<0.5 cm) was observed at selected outcrops. Local, partially digested xenoliths of Burntwood or Sickie group, as well as mafic rocks (unit 1), can be present in the granodiorite.

### **Granitic pegmatite (unit 12)**

Pegmatite bodies are common in the Russell–McCallum lakes area and cut all map units; however, multiple generations of intrusions are present. They are typically albite dominant, but K-feldspar–dominant pegmatite bodies are also present. Other major constituents are quartz and biotite. Common accessory minerals are magnetite, muscovite, garnet and, locally, cordierite and sillimanite. Pegmatite bodies are typically steeply dipping and occur either discordant to the main foliation and gneissosity or concordant and locally folded (most likely by  $F_3$ ). Most pegmatite dikes are <2 m wide (some can be up to 30 m) and unzoned or very crudely zoned, with characteristic granitic pegmatite textures such as graphic and local comb textures. Dikes locally display both pegmatitic and aplitic zones.

### **Metamorphism**

The metamorphic history of the Russell–McKnight lakes area, which includes the present study area, was described in detail by Lenton (1981) based on textures identified in both outcrop and thin section. Four metamorphic events ( $M_1$  to  $M_4$ ) were identified: two prograde events culminated in upper-amphibolite–facies metamorphic conditions and two events were retrograde. The  $M_1$  event is best preserved in psammitic rocks, whereas the  $M_2$  event is best preserved in pelitic rocks. It is possible that this discrepancy is simply the result of different metamorphic reactions that occurred in different bulk compositions during a single prograde event. Maximum temperature and pressure during peak metamorphism were estimated at 600–700°C and 2–3 kbar, respectively. A zone of lower metamorphic grade was interpreted to occur at the south end of McCallum Lake. Metamorphic conditions there were estimated to be subsolidus (middle amphibolite facies) and attained 600–630°C and 2.5 kbar; however, examples of in-situ and in-source leucosome were observed, calling this interpretation into question.

Additional work is planned to re-examine the metamorphic geology of the Russell Lake area.

### **Structural geology**

The central area of Russell Lake presents a complex structural history. The structural interpretation from McRitchie (1975a, b) and Lenton (1981) was adopted for this project. Various discussions with H. Zwanzig (MGS, retired) also contributed to the understanding and interpretation of the structural geology of the central Russell Lake area. Lenton (1981) divided the deformation history of the Russell–McCallum lakes area into five components: three generations of folding and two generations of brittle fractures with different orientations. All deformation is interpreted to postdate the deposition of the Burntwood and Sickie groups. The  $D_1$  event resulted in large-scale recumbent isoclinal  $F_1$  folds with major inversions and repetitions. Subsequent deformation largely obscures  $D_1$  structures. The  $D_2$  phase resulted in northwest-trending, shallowly plunging, inclined isoclinal  $F_2$  folds. The  $F_2$  folds are characterized by large amplitude to wavelength ratios. As a result, fold noses were rarely observed and the presence of  $F_2$  folds was recognized by repetitions of the stratigraphic section. The  $D_3$  event resulted in northeast-trending, irregularly shaped and disharmonic open folds, and associated strong linear and planar fabrics in the direction of the  $F_3$  fold axes. Most linear fabrics observed in the map area parallel regional  $F_3$  fold axes. The  $D_4$  and  $D_5$  events are manifested by brittle faults and cataclastic zones, which are northwest trending and north trending, respectively. The brittle structures postdate all phases of folding.

### **Economic considerations**

Infrastructure and accessibility are important aspects in any mineral-development project. The Russell–McCallum lakes area is easily accessible by float plane out of Lynn Lake and rail from The Pas, and a power line and two power-generating stations (Laurie River I and II) are present nearby.

Sediment-hosted stratiform base-metal mineralization and volcanogenic massive-sulphide exploration took place in the Russell–McCallum lakes area until the early 1980s. However, the area was abandoned when no significant occurrences of Ni, Cu, Zn, Au or Ag were found. Assessment files from the area reveal that drill testing of geophysical conductors typically resulted in the intersection of graphite mineralization, and graphite is noted in the majority of drill logs. Because graphite was not a widely sought commodity at that time, no significance was given to those findings.

Natural graphite has several uses, including anode material for Li-ion batteries, brake linings, lubricants, powdered metals, refractory applications and steelmaking (U.S. Geological Survey, 2019). Currently, natural graphite is a highly-sought commodity due to its anticipated demand associated with the production of Li-ion batteries. Graphite is listed by the U.S. Department of the Interior as one of 35 critical minerals for the United States (U.S. Department of the Interior, 2018) and by the European Commission as part of its list of critical raw materials for the European Union (European Commission, 2017).

The Russell–McCallum lakes area shows clear evidence of and economic potential for graphite mineralization. Lenton (1981) reported up to 0.16 wt. % total carbon in pelitic rocks from the Burntwood group. During this study, however, it was not possible to establish a clear relationship between the graphite content and the composition of the Burntwood group rocks (psammitic versus pelitic bulk compositions). It is possible that the graphite is widespread throughout the Burntwood group sequence. Field observations identified up to 7% graphite in Burntwood group garnet-biotite greywacke. Assay results from graphite mineralization associated with sulphide-facies iron formation at McCallum Lake, as well as from garnet-biotite greywacke at Russell Lake, are pending.

A syenite complex with potential to host rare-earth-element mineralization occurs at Brezden Lake (Martins et al., 2012; Martins, 2016), between Russell and McCallum lakes (Figure GS2019-3-2). Similar intrusions were not observed during the course of the 2019 fieldwork, even though the KD in general is considered to have potential for these types of intrusions (e.g., Martins et al., 2011).

Archean cratons can be important regional vectors for diamond exploration. In east-central Saskatchewan, two diamond occurrences (the Fort à la Corne kimberlite field and the Pikoo kimberlite) are located in areas thought to be underlain at depth by the mostly buried Archean Sask craton. Determining the potential extent of Archean crust in the KD may help to inform diamond exploration in the region. Some authors have interpreted the Sask craton to extend significantly under the KD, including the Russell–McCallum lakes area (Zwanzig and Bailes, 2010). Currently, the MGS has little evidence for diamond potential in this area; therefore, a kimberlite-indicator–mineral survey was carried out this summer (Hodder, 2019). Additional information regarding drift prospecting in the Russell–McCallum lakes area is available in Hodder (2019).

## Acknowledgments

This report and accompanying map benefited from in-depth discussions with H. Zwanzig (MGS, retired). His

extensive knowledge of the area greatly improved the understanding of the complex geological history of this portion of the KD. Field assistance by K. George and I. Robinson from Brandon University is truly appreciated. Thank you to E. Anderson, M. Schreckenbach and K. Roberts for field logistical support. C. Epp and M. Koziuk at the MGS Midland Sample and Core Library provided excellent services to the Russell–McCallum project. Drafting and GIS support was provided by L. Chackowsky and A. Santucci. Edits by K. Reid and C. Böhm are appreciated and helped improve earlier drafts of the manuscript. B. Davie from RnD Technical provided technical editing services and C. Steffano took careful care of layout and final editorial duties. A word of appreciation is due to the Manitoba Hydro team for water-level predictions and support at the Lauri River control station.

## References

- Ansdell, K.M. 2005: Tectonic evolution of the Manitoba-Saskatchewan segment of the Paleoproterozoic Trans-Hudson Orogen, Canada; *Canadian Journal of Earth Sciences*, v. 42, no. 4, p. 741–759.
- Bailes, A.H. 1980: Origin of early Proterozoic volcanoclastic turbidites, south margin of the Kiseeynew sedimentary gneiss belt, File Lake, Manitoba; *in* Early Precambrian Volcanology and Sedimentology in the Light of the Recent, E. Dimroth, J.A. Donaldson and J. Veizer (ed.), *Precambrian Research*, v. 12, no. 1–4, p. 197–225.
- Baldwin, D.A. 1976: The evaluation of disseminated base metal environments; *in* Non-Renewable Resource Evaluation Program (NREP), 1<sup>st</sup> annual report, Manitoba Resources Division, Open File Report 77/1, p. 62–92.
- Baldwin, D.A. 1980: Disseminated stratiform base metal mineralization along the contact zone of the Burntwood River metamorphic suite and the Sickle Group; Manitoba Energy and Mines, Mineral Resources Division, Economic Geology Report ER79-5, 20 p.
- Corrigan, D., Hajnal, Z., Németh, B. and Lucas, S.B. 2005: Tectonic framework of a Paleoproterozoic arc-continent to continent-continent collisional zone, Trans-Hudson Orogen, from geological and seismic reflection studies; *Canadian Journal of Earth Sciences*, v. 42, p. 421–434.
- Corrigan, D., Pehrsson, S., Wodicka, N. and de Kemp, E. 2009: The Palaeoproterozoic Trans-Hudson Orogen: a prototype of modern accretionary processes; *in* Ancient Orogens and Modern Analogues, J.B. Murphy, J.D. Keppie and A.J. Hynes (ed.), Geological Society of London, Special Publications, v. 327, p. 457–479.
- Downie, D.L. 1936: Granville Lake sheet, west half, Manitoba; Geological Survey of Canada, 'A' Series Map 343A, 1 sheet, scale 1:253 440, URL <<https://doi.org/10.4095/107123>> [October 2019].

- European Commission 2017: Communication from the commission to the European Parliament, the Council, the European Economic and Social Committee and the Committee of the Regions on the 2017 list of critical raw materials for the EU; European Commission, Brussels, Belgium, 8 p., URL <<https://eur-lex.europa.eu/legal-content/EN/TXT/PDF/?uri=CELEX:52017DC0490&qid=1568232381923&from=EN>> [October 2019].
- Gilboy, C.F. 1976: Reindeer Lake, south (SE quarter); *in* Summary of Field Investigations 1976, Saskatchewan Geological Survey, Saskatchewan Department of Mineral Resources, p. 36–43.
- Hodder, T.J. 2019: Till sampling and ice-flow mapping in the Russell–McCallum lakes area, northwestern Manitoba (parts of NTS 64C3–6); *in* Report of Activities 2019, Manitoba Agriculture and Resource Development, Manitoba Geological Survey, p. 90–96.
- Hunter, H.E. 1953: Geology of the McKnight Lake area; Manitoba Mines Branch, Publication 52-3.
- Lenton, P.G. 1981: Geology of the McKnight–McCallum Lakes area; Manitoba Energy and Mines, Geological Services, Geological Report GR79-1, 39 p.
- Lewry, J.F. and Collerson, K.D. 1990: The Trans-Hudson Orogen: extent, subdivisions and problems; *in* The Early Proterozoic Trans-Hudson Orogen of North America, J.F. Lewry and M.R. Stauffer (ed.), Geological Association of Canada, Special Paper 37, p. 1–14.
- Martins, T. 2016: Rare metals in Manitoba: Brezden Lake intrusive complex; Manitoba Growth, Enterprise and Trade, Manitoba Geological Survey, URL <<https://www.gov.mb.ca/iem/geo/raremetals/pdfs/brezden.pdf>> [September 2019].
- Martins, T. and Couëslan, C.G. 2019: Bedrock geology of Russell Lake, southern half (NTS 64C3–6); Manitoba Agriculture and Resource Development, Manitoba Geological Survey, Preliminary Map PMAP2019-3, scale 1:20 000.
- Martins, T., Couëslan, C.G. and Böhm, C.O. 2011: Burntwood Lake alkali-feldspar syenite revisited, west-central Manitoba (part of NTS 63N8); *in* Report of Activities 2011, Manitoba Innovation, Energy and Mines, Manitoba Geological Survey, p. 79–85.
- Martins, T., Couëslan, C.G. and Böhm, C.O. 2012: Rare metals scoping study of the Brezden Lake intrusive complex, western Manitoba (part of NTS 64C4); *in* Report of Activities 2012, Manitoba Innovation, Energy and Mines, Manitoba Geological Survey, p. 115–123.
- McRitchie, W.D. 1975a: Russell Lake south (parts of NTS 64C-3, 4); *in* Summary of Geological Fieldwork 1975, Manitoba Mines, Resources and Environmental Management, Mineral Resources Division, Exploration and Geological Survey Branch, Geological Paper GP75/2, p. 19–21.
- McRitchie, W.D. 1975b: Russell Lake south (parts of NTS 64C-4E, 64C-3); Manitoba Mines, Resources and Environmental Management, Preliminary Map 1975R-3, scale 1:31 680.
- Pollock, G.D. 1966: Geology of the Trophy Lake area (west half); Manitoba Mines Branch, Publication 64-1.
- Stauffer, M.R. 1984: Manikewan and early Proterozoic ocean in central Canada, its igneous history and orogenic closure; *Precambrian Research*, v. 25, p. 257–281.
- U.S. Department of the Interior 2018: Final list of critical minerals, 2018; Federal Register: The Daily Journal of the United States Government, May 18, 2018, URL <<https://www.federalregister.gov/documents/2018/05/18/2018-10667/final-list-of-critical-minerals-2018>> [October 2019].
- U.S. Geological Survey 2019: Mineral commodity summaries, 2019; U.S. Geological Survey, National Minerals Information Center, 200 p., URL <<https://doi.org/10.3133/70202434>> [October 2019].
- Zwanzig, H.V. 1999: Structure and stratigraphy of the south flank of the Kiseynew Domain in the Trans-Hudson Orogen, Manitoba: implications for 1.845–1.77 Ga collision tectonics; *in* NATMAP Shield Margin Project, Volume 2, Canadian Journal of Earth Sciences, v. 36, no. 11, p. 1859–1880.
- Zwanzig, H.V. 2008: Correlation of lithological assemblages flanking the Kiseynew Domain, Manitoba (parts of NTS 63N, 63O, 64B, 64C): proposal for tectonic/metallogenic sub-domains; *in* Report of Activities 2008, Manitoba Science, Technology, Energy and Mines, Manitoba Geological Survey, p. 38–52.
- Zwanzig, H.V. 2019: Geology of the southern Granville Lake area, Manitoba (parts of NTS 64C1, 2, 7); Manitoba Growth, Enterprise and Trade, Manitoba Geological Survey, Geoscientific Map MAP2019-1, scale 1:20 000.
- Zwanzig, H.V. and Bailes, A.H. 2010: Geology and geochemical evolution of the northern Flin Flon and southern Kiseynew domains, Kiseynew–File lakes area, Manitoba (parts of NTS 63K, N); Manitoba Innovation, Energy and Mines, Manitoba Geological Survey, Geoscientific Report GR2010-1, 135 p.
- Zwanzig, H.V. and Wielezyski, P. 1975: Geology of the Kamuchawie Lake area; *in* Summary of Geological Fieldwork 1975, Manitoba Mines, Resources and Environmental Management, Mineral Resources Division, Exploration and Geological Survey Branch, Geological Paper GP75/2, p. 12–15.



## Bedrock geological mapping of the Puella Bay area (Wekusko Lake), north-central Manitoba (part of NTS 63J12)

by K.D. Reid

### In Brief:

- Bedrock geological mapping constrains the Stuart Bay fault to the south of Puella Bay and identifies mafic volcanic rocks previously not documented
- The McCafferty Lifter fault block is a northeast-trending homoclinal volcanic sequence that is host to both gold and base-metal occurrences

### Citation:

Reid, K.D. 2019: Bedrock geological mapping of the Puella Bay area (Wekusko Lake), north-central Manitoba (part of NTS 63J12); in Report of Activities 2019, Manitoba Agriculture and Resource Development, Manitoba Geological Survey, p. 42–51.

### Summary

A multiyear project examining the bedrock geology southeast of Wekusko Lake was initiated in the summer of 2019. Bedrock geological mapping was conducted at 1:20 000 scale over an area of 8.5 x 11 km in the Puella Bay area in 2019 and will be combined with another 8.5 x 11 km block to the north in 2020. The project area was selected because it lacks comprehensive mapping, and recent forestry activity (2008–2016) resulted in significant new rock exposures and access. In addition, the availability of high-resolution aeromagnetic data complements the mapping where exposure is lacking. The project area is geologically complex with preserved successor-arc volcanic and sedimentary rocks that provide a window into the evolution of the eastern Flin Flon domain. The rocks southeast and east of Wekusko Lake have been of considerable economic interest for over a century and are host to the Laguna deposit, the site of Manitoba's first gold mine.

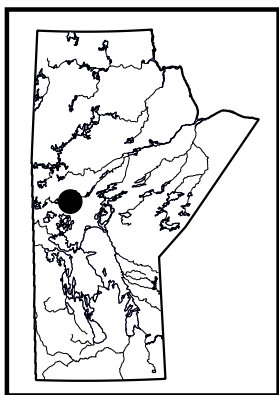
### Introduction

The Flin Flon domain (FFD) is part of a series of Paleoproterozoic domains that form the internal Reindeer zone of the Trans-Hudson orogen (Lewry and Collerson, 1990). It has a distinct volcano-sedimentary stratigraphy that evolved from 1.91–1.83 Ga. The FFD is approximately 250 km from west to east, with an exposed north-south extent of approximately 40–50 km. The FFD is bounded to the east by the Superior province and the Superior boundary zone, is bounded to the north by turbidite greywacke and mudstone of the Kiseynew domain, and dips shallowly to the south under younger Phanerozoic platform carbonate rocks. Previous work by Stern et al. (1995) identified significant stratigraphic and geochemical differences between arc volcanic rocks west of Reed Lake (Amisk collage) versus those in the Snow Lake area (i.e., Snow Lake assemblage), indicating that these segments of the FFD may have formed in distinct tectonic settings.

Following discovery and intermittent production of gold (1918–1940) from the Laguna deposit in the northern half of the project area, the Geological Survey of Canada conducted field mapping of the Herb Lake fault block at a scale of 1:12 000 (1 in. to 1000 ft.; Stockwell, 1937), but the stratigraphic context was not well understood at the time. In the 1940s, the Geological Survey of Canada surveyed the region at a scale of 1:63 360 (1 in. to 1 mile; e.g., Armstrong, 1941; Frarey, 1950); the resulting maps provide much of the basis for later compilations in the area, such as those by the NATMAP Shield Margin Project Working Group (1998). Geochemical studies of the Herb Lake volcanic rocks by Gordon and Lemkow (1987) were guided by the mapping of Stockwell (1937). Ansdell et al. (1999) and Connors et al. (1999) conducted detailed structural, geochemical and geochronological studies of sedimentary and volcanic rocks; however, no comprehensive geological maps were published.

In the summer of 2019, a multiyear project was initiated to examine the bedrock geology southeast of Wekusko Lake. Bedrock geological mapping this summer was conducted at a 1:20 000 scale over an area of 8.5 x 11 km and will be combined with the mapping of another 8.5 x 11 km block to the north in 2020 to form a 17 km (north-south) by 11 km (east-west) map area. The lack of comprehensive mapping and the recent forestry activity (2008–2016), which resulted in significant new rock exposures and access, led to the selection of this area for bedrock geology mapping.

The current geological mapping focuses on rocks southeast of Wekusko Lake; in particular, two previously identified fault bound blocks, the McCafferty Lifter fault block and



the Eastern Missi fault block (Ansdell et al., 1999; Connors et al., 1999). Primary objectives of the 2019 summer field-work include

- updating and detailing the stratigraphic framework of the 1.88–1.83 Ga arc volcanic and sedimentary rocks east and southeast of Puella Bay,
- examining complex structural relationships between southwest-directed fold-and-thrust faulting ( $D_2$ ) and northwest-directed transpression ( $D_3$ ),
- incorporating high-resolution geophysical data with bedrock data to better constrain geological contacts and structures in poorly exposed areas, and
- using the lithostratigraphic and structural framework to evaluate the mineral potential of rocks southeast of Wekusko Lake.

## Regional setting

Wekusko Lake is located in the eastern end of the FFD. Most of the lake is underlain by greywacke and mudstone turbidites of the Burntwood group from the Kisseynew domain to the northeast (Figure GS2019-4-1). Greywacke and mudstone extend to the southernmost part of the lake, separating arc volcanic rocks to the west from those

to the east, and continue southwest under Phanerozoic platform carbonates for at least 30 km (Reid, 2017). Snow Lake and Hayward Creek arc assemblages lie on the west side of Wekusko Lake; these are separated north from south, respectively, by the Berry Creek shear zone. On the east side of Wekusko Lake, the Crowduck Bay fault juxtaposes Burntwood group rocks against ocean-floor basalts, evolved arc volcanic rocks, and Missi group fluvial-alluvial sedimentary rocks (Figure GS2019-4-1).

## Stratigraphic framework

The project and surrounding areas contain multiple tectonostratigraphic packages including 1) basalt of ocean-floor/back-arc affinity referred to as the South Wekusko assemblage (SWA), 2) intermediate to felsic arc rocks of the McCafferty Liftover fault block (MLB), 3) mafic to felsic arc volcanic rocks of the Herb Lake fault block (HLB), 4) fluvial-alluvial sediments of the Western and Eastern Missi fault blocks (WMB and EMB), and 5) greywacke and mudstone of the Burntwood group (BG; Figure GS2019-4-1), all of which were intruded by a variety of mafic and felsic plutonic rocks. Much of the following information is summarized from Ansdell et al. (1999) and Gilbert and Bailes

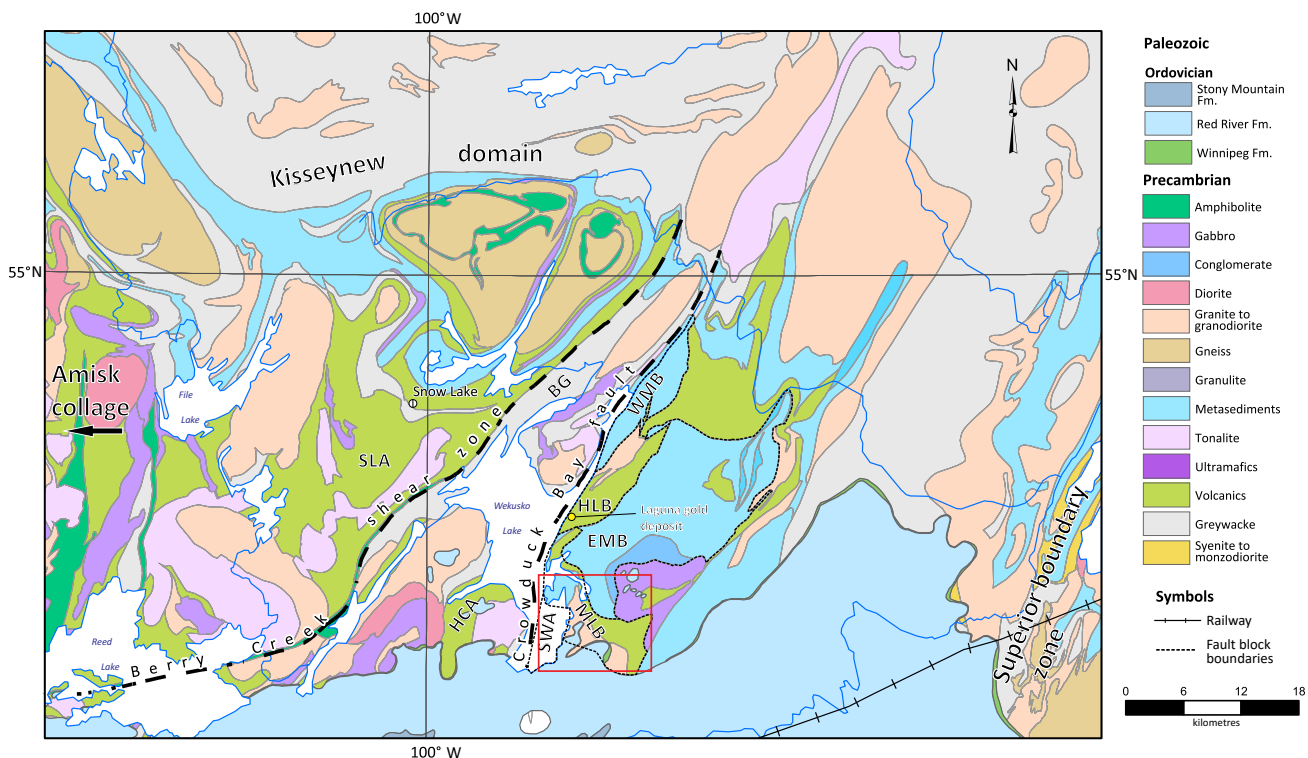


**Figure GS2019-4-1:** Map of the eastern segment of the Flin Flon domain including the location of the 2019 project area (see red rectangle; map is modified from unpublished 1:250 000 scale provincial compilation). Note the Kisseynew domain to the north, the Superior boundary zone to the east and Paleozoic cover rocks to the south. Snow Lake arc assemblage (SLA), Hayward Creek arc assemblage (HCA), South Wekusko assemblage (SWA), McCafferty Liftover fault block (MLB), Eastern Missi fault block (EMB), Herb Lake fault block (HLB), Western Missi fault block (WMB) and Burntwood group (BG) are shown relative to the Berry Creek shear zone and Crowduck Bay fault.

(2005); the reader is encouraged to see these papers for more details.

The southeastern shoreline of Wekusko Lake, near the community of Herb Lake Landing, contains massive to pillowed, plagioclase- and pyroxene-phyric basaltic flows of the SWA. The pillowed flows often contain minor inter-pillow hyaloclastite material, with localized epidote alteration. These rocks are similar to ocean-floor and/or back-arc sequences elsewhere in the Flin Flon domain (Gilbert and Bailes, 2005), with little or no felsic volcanic and volcanoclastic rocks, and geochemically resemble normal mid-ocean-ridge basalt of the 1.90 Ga Elbow-Athapapuskow assemblage (Stern et al., 1995). The SWA is interpreted as the oldest rock assemblage in the map area. The contact between the SWA and rocks of the structurally overlying MLB is not exposed, however, it is interpreted as tectonic (Gilbert and Bailes, 2005).

The MLB, also referred to as the Puella Bay suite by Gilbert and Bailes (2005), is a homoclinal sequence of east- to northeast-younging, intermediate to felsic volcanic rocks (e.g., Ansdell et al., 1999). The lowest stratigraphic unit in the MLB is an ~5 m wide basal mafic mudstone that grades over 15 m into a sequence of east-facing, bedded mafic to intermediate siltstone, greywacke and pebble conglomerate (Gilbert and Bailes, 2005). This rapidly grades to the east into monotonous, heterolithic, andesite cobble and boulder conglomerate, the most commonly observed rock type on many of the islands and points within and west of Broad Bay (Figure GS2019-4-2; Reid, 2019). Minor aphyric to plagioclase-phyric andesite occurs intercalated with the above heterolithic andesite conglomerate. Local amygdules and polygonal jointing suggest these may be flows or high-level intrusions. Felsic volcanic rocks, primarily massive dacite and intermediate to felsic volcanoclastic rocks, form the upper sequence of the MLB. Ansdell et al. (1999) were able to produce a relatively precise age of  $1876 \pm 2$  Ma from the dacite thus constraining the minimum age of the MLB.

The HLB is an isoclinally folded package of mafic to felsic volcanic rocks in fault contact with the WMB to the north, MLB to the southwest and the EMB to the southeast (GS2019-4-1). Rocks at the centre of this fold are mainly basaltic, but become more felsic at the peripheries. The lack of pillowed flows and presence of welded felsic units suggest that volcanism was subaerial (Shanks and Bailes, 1977; Gordon and Gall, 1982). Dating by Gordon et al. (1990) produced a relatively precise age of  $1832 \pm 2$  Ma for a sample of rhyolite from the fold centre. Ansdell et al. (1999) produced a similar age of  $1836 \pm 1.3$  Ma, providing further evidence that these are some of the youngest volcanic rocks in the Trans-Hudson orogen. The young

age of volcanism is unique in that it is synchronous with fold-and-thrust fault development as well as Missi group sedimentation (Ansdell et al., 1999).

Frarey (1950) first recognized and mapped fluvial-alluvial feldspathic arenite and polymictic pebble to boulder conglomerate east of Wekusko Lake. Ansdell et al. (1999) termed these sedimentary rocks the WMB and EMB based on their position north and south of the HLB, respectively. Fluvial-alluvial conglomerate and sandstone unconformably overlie spherulitic rhyolite at the south end of the WMB. Rhyolite yielded complex zircon age results that indicate that it could be as old as 1856 Ma or as young as 1830 Ma (Ansdell et al., 1999). Detrital zircons from the WMB range in age from 2004 to 1834 Ma (Ansdell et al., 1999). The EMB is stratigraphically broken into three conglomerate/sandstone successions—lower, middle and upper. The youngest detrital zircon in the lower sequence yielded an age of  $1841 \pm 21$  Ma, and the lower sequence is cut by a  $1826 \pm 4$  Ma feldspar porphyry dike. In comparison, the youngest detrital zircon in the upper sequence is  $1832 \pm 9$  Ma (Ansdell et al., 1999). The lower sequence of the EMB yielded a range of detrital zircon ages from 1911 to 1841 Ma (Ansdell et al., 1999), which indicates that these sediments were collecting detritus from an already-formed accretionary collage, and that Missi group sedimentation was not synchronous throughout the Flin Flon domain.

Burntwood group rocks occur mainly west of the Crowduck Bay fault (west of the current project area), and subsequently underlie much of Wekusko Lake. Burntwood group greywacke and mudstone commonly show preserved bedforms and sedimentary structures indicating deposition by turbidity currents in a submarine fan (Bailes, 1980). Detrital zircons from Burntwood group rocks on the west side of Wekusko Lake suggest a depositional age of 1.855–1.84 Ga (David et al., 1996).

## Structural context

The structural-tectonic history of the eastern FFD can be separated into four distinct periods (e.g., Connors et al., 1999; Ryan and Williams, 1999): 1) intra-oceanic accretion of arc and ocean floor assemblages ( $D_1$ ; 1.88–1.87 Ga); 2) early successor-arc plutonism and basin deposition (1.87–1.84 Ga); 3) late successor-arc plutonism, basin deposition and southwest-directed thrusting ( $D_2$ ; 1.84–1.83 Ga); and 4) northwest-directed transpressional shortening associated with the Trans-Hudson orogen ( $D_3$ ; 1.83–1.81 Ga). No evidence of accretionary structures ( $D_1$ ) was noted in the eastern Wekusko Lake area (e.g., Connors et al., 1999); however, Gilbert and Bailes (2005) suggested that the Broad Bay pluton is a late successor-arc

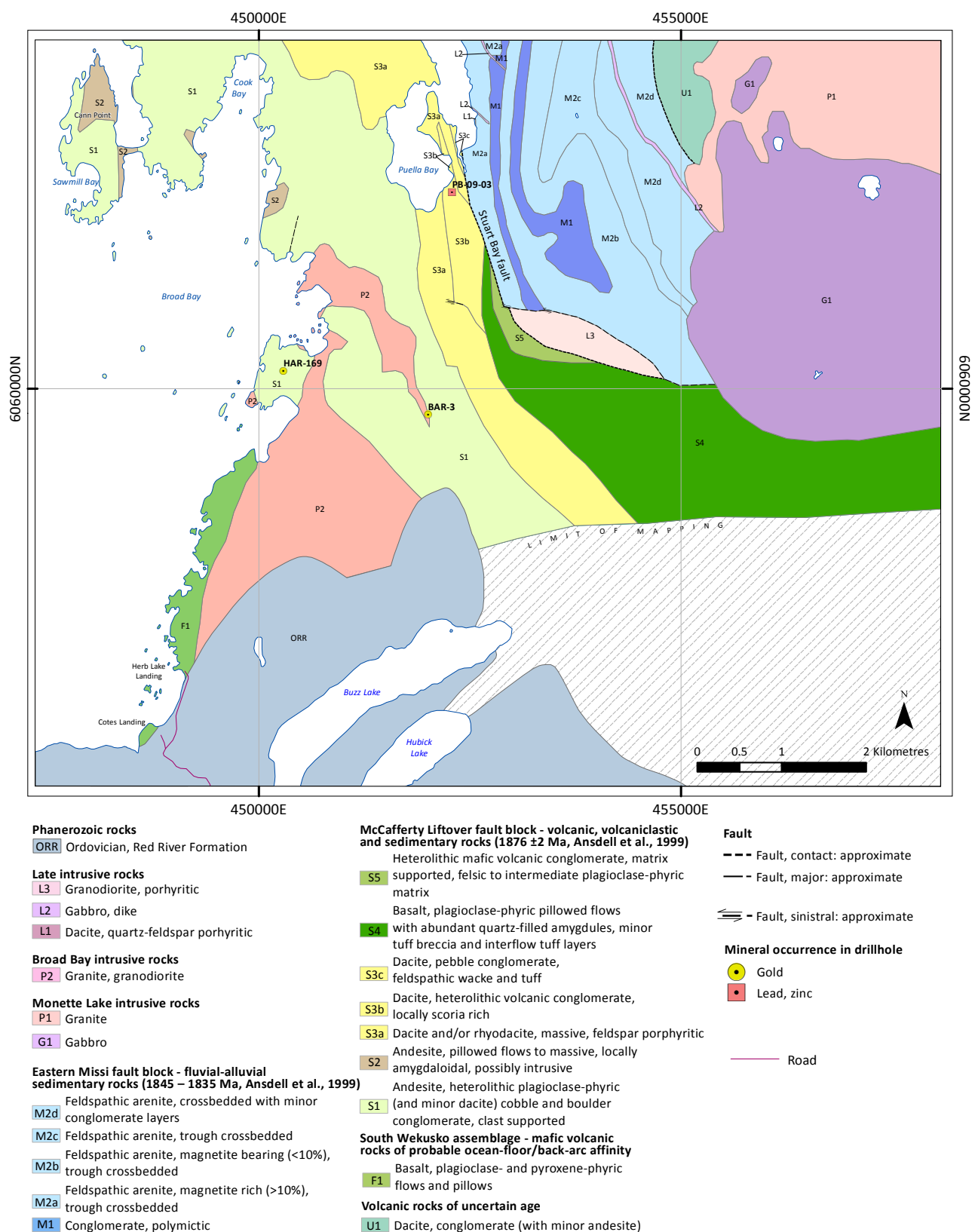


**Figure GS2019-4-2:** Simplified geological map of the Puella Bay area, southeastern Wekusko Lake, based on 2019 mapping. For more detail see PMAP2019-4 (Reid, 2019).



intrusion that stitches an earlier  $D_1$  fault. Fold-and-thrust deformation ( $D_2$ ) is interpreted to have resulted in many of the map-scale isoclinal folds and faults observed within and bounding stratigraphic packages (e.g., Stuart Bay fault, Kiski fault, Herb Lake anticline); and in most instances predates peak metamorphism. Deformation associated with transpressional northwest-directed shortening ( $D_3$ ) cross-cuts earlier  $D_2$  structures and fabrics. The largest and most prominent  $D_3$  structure in the area is the Crowduck Bay fault.

## Results of 2019 fieldwork in the Puella Bay area

Bedrock mapping at a 1:20 000 scale in 2019 focused on characterizing rocks inland, south and east of Puella Bay. These areas have received very little attention during previous reconnaissance and shoreline mapping (e.g., Gilbert and Bailes, 2005) due to the lack of exposure and/or access. The 2019 mapping confirmed that MLB and EMB rocks are in structural contact to the south-southeast of Puella Bay for approximately 2 km. From there, the contact swings to the east-southeast and is intruded by a porphyritic pluton. A brief description of mapped rock units, displayed in Figure GS2019-4-2 (and in Reid, 2019), is given below.

### *South Wekusko assemblage (unit F1)*

A few outcrops along the winter road north of Herb Lake Landing contain variably strained pillowed and massive plagioclase- and pyroxene-phyric basalt (unit F1). These rocks weather a distinct grey-green, are fine to medium grained and have rare carbonate-filled amygdules. Localized shearing, carbonate alteration, and poor exposure did not allow the resolution of contacts between massive and pillowed flows. Gilbert and Bailes (2005) suggested that massive varieties could be synvolcanic intrusions.

### *McCafferty Lifterover fault block (units S1–S5)*

Gilbert and Bailes (2005) mapped much of the shoreline in the areas of Cann Point and Broad Bay, and therefore these outcrops were not remapped in 2019. They described the rocks as a thick package of clast-supported, heterolithic volcanic cobble and boulder conglomerate that is dominated by subrounded plagioclase-phyric andesite but includes local dacite clasts (see unit S2 in Gilbert and Bailes, 2005; unit S1 in Figure GS2019-4-2). Volumetrically, it is the largest unit in the MLB. Minor amygdaloidal, aphyric to plagioclase-phyric massive andesite flows (unit S2; Figure GS2019-4-2) occur within the above mentioned conglomerate. Outcrops of andesite flows (unit S2) were

extrapolated inland using aeromagnetic data. Traversing from Broad Bay to the southern tip of Puella Bay (west to east) revealed a gradation from clast-supported heterolithic andesite conglomerate to matrix-supported (dacitic) feldspar-phyric andesite conglomerate (Figure GS2019-4-3a), followed by massive varieties of dacite (unit S3a; Figure GS2019-4-2). Within the massive dacite (unit S3a) is a package of heterolithic volcanic conglomerate containing both dacite and mafic scoria clasts, which gives the outcrop a pitted surface (unit S3b). Farther to the east, a small outcrop contains normally graded beds of pebble conglomerate, feldspathic wacke and reworked tuff indicating that, at least locally, the package is younging to the east (unit S3c; Figure GS2019-4-3b). This is consistent with the interpretation of the MLB being a homoclinal, east-younging sequence.

To the south and east of Puella Bay there is a change from felsic volcanic rocks (no contacts were observed) to amygdule-rich pillowed basalt and local pillow breccia (unit S4; Figure GS2019-4-3c). Pillowed flows are porphyritic with 2 to 3 mm-sized plagioclase and pyroxene phenocrysts in an aphanitic groundmass; pillow selvages are a dark green relative to the grey-green of the groundmass. Interflow tuff beds, pillow drapes and breccia suggest this package is northeast-younging, similar to rocks farther west in the MLB.

Heterolithic mafic volcanic conglomerate (unit S5) occurs directly to the north of the previously mentioned unit S4. This conglomerate differs from that of unit S1 in that the cobbles are mainly of medium- to coarse-grained, plagioclase-pyroxene-phyric gabbro with minor plagioclase-phyric andesite and fine-grained diorite. Additionally, clasts are subrounded to well rounded and suspended in a fine-grained, intermediate to felsic, plagioclase-rich matrix (matrix supported).

### *Volcanic rocks of uncertain age (unit U1)*

Two outcrops east of the EMB contain matrix- to clast-supported, intermediate to felsic volcanic conglomerate (unit U1; Figure GS2019-4-2). The clasts are subrounded to subangular, 1 to 8 cm, mainly light grey feldspar-phyric dacite and minor pyroxene-phyric andesite. The matrix to the clasts is a dark grey-brown, fine-grained tuff. These rocks are separated from the EMB by a distinct topographic low that extends to Monette Lake to the north; it is possible that this represents a significant fault. At this time, the stratigraphic context of these rocks is unknown, but future investigations in the Monette Lake area may provide more detail.

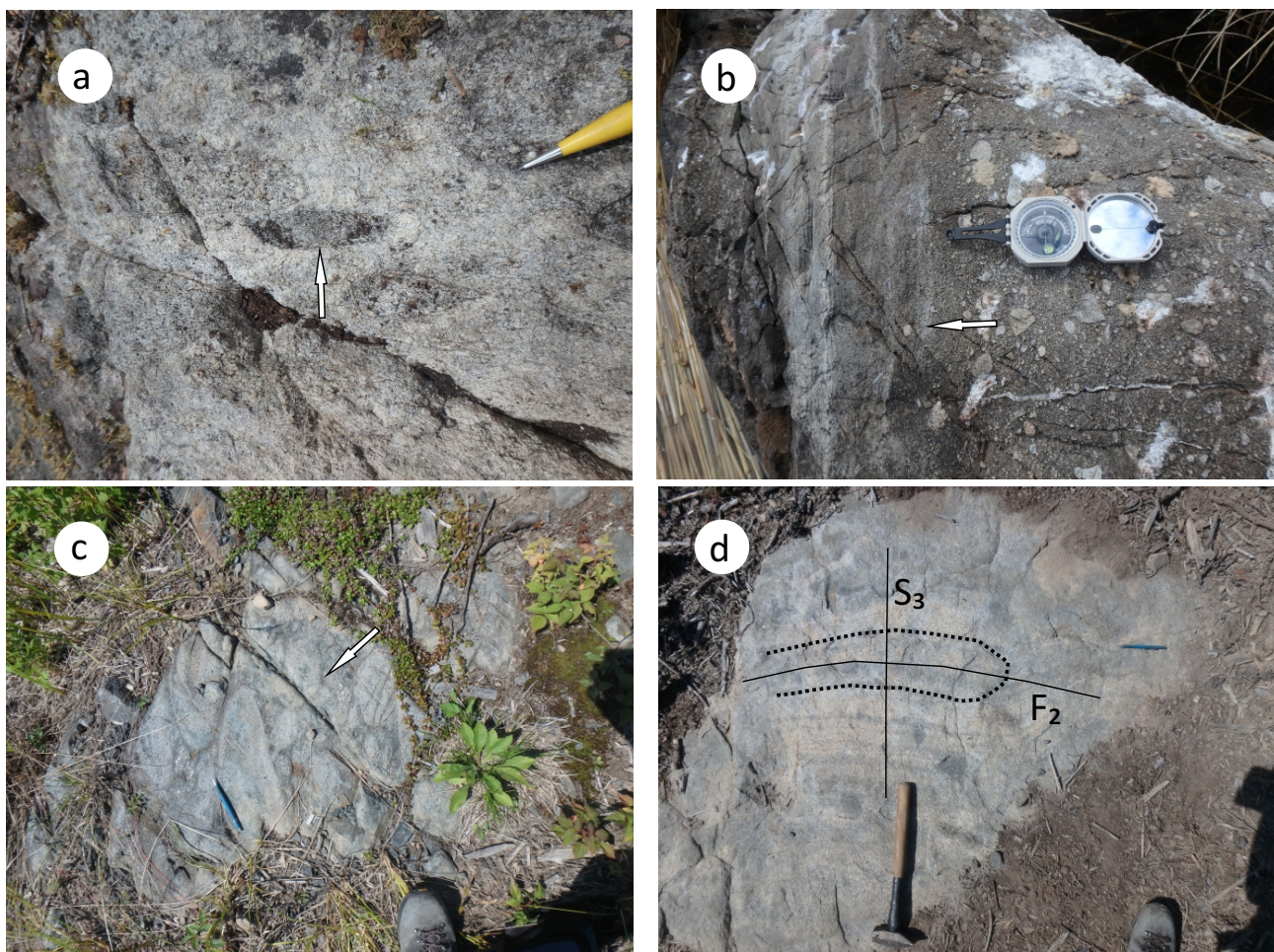


**Figure GS2019-4-3:** Outcrop photographs of the McCafferty Lifterover fault block arc volcanic rocks: **a)** recessively weathered, sub-rounded andesite clast (arrow) in an intermediate (dacite) matrix (unit S1; NAD83, UTM Zone 14N, 450513E, 6071429N); **b)** normally graded rhyolite pebble conglomerate and feldspathic wacke (arrow show younging direction; unit S3; UTM 452299E, 6063126N); **c)** amygdaloidal pyroxene- and plagioclase-phyric pillow fragments (arrow; unit S4; UTM 453770E, 6059601N); **d)** isoclinally folded ( $F_2$ ), plagioclase-crystal-rich mafic tuff cut by  $S_3$  foliation (unit S4; UTM 453781E, 6059863N).

### **Eastern Missi fault block (units M1 and M2)**

Directly north of the current project area, polymictic conglomerate (unit M1) forms the base of the EMB (Ans-dell et al., 1999). East of Puella Bay, small exposures of polymictic pebble to boulder conglomerate (unit M1; Figure GS2019-4-2) occupy both topographic and aeromag-netic lows, and have an estimated 40–60 m thickness. The conglomerate is matrix supported and poorly sorted, with well-rounded clasts including light grey plagioclase-phyric dacite, aphyric rhyolite, aphyric basalt, grey vein quartz and minor laminated iron formation (Figure GS2019-4-4a). Southeast of Puella Bay, a weak clast flattening defines an  $S_3$  foliation that is oblique to or perpendicular to bedding ( $S_0$ ). This relationship is interpreted to represent an axial planar fabric within a macroscopic map-scale S-fold.

Trough crossbedded, medium- to coarse-grained feldspathic arenite (unit M2) is the most common lithology in the EMB (Figure GS2019-4-4b, c). Unit M2a, directly east

of Puella Bay, is characterized by heavy mineral lami-nations in trough crossbeds that contain up to 25% magne-tite (Figures GS2019-4-2, -4d). Moving upsection to the east there is a consistent decrease in magnetite content (unit M2b, c), a subtle increase in muscovite and biotite, and better developed (or preserved) planar bedding (Fig-ure GS2019-4-4c). At the top of the succession the aren-ite contains minor (<5%) pebbles and cobbles (unit M2d). Feldspathic arenite is consistently east- to northeast-younging, possibly indicating that, like the MLB, it is a homoclinal sequence.

Magnetite-rich, trough crossbedded sandstone (unit M2a) along the western shore of Puella Bay locally con-tains orange, quartz- and feldspar-phyric, 0.2 to 1.2 m elongate, subangular to subrounded stratabound fea-tures with silicified margins. One possibility is that these are concretions or mark areas of fluid flow in the sand-stone. Trough crossbedding stratigraphically below these



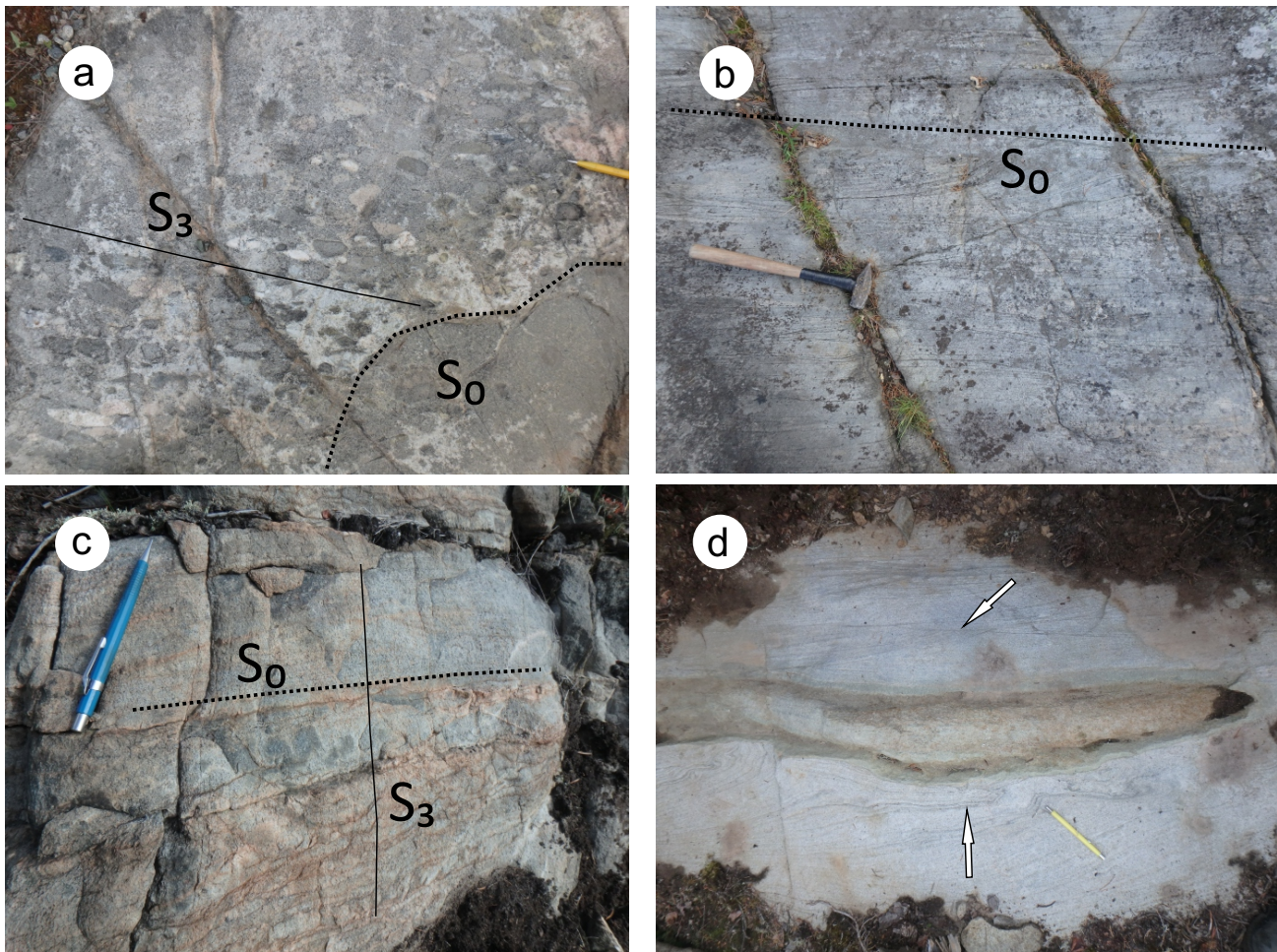


**Figure GS2019-4-4:** Outcrop photographs of the Eastern Missi fault block metasedimentary rocks: **a)** weak clast flattening defines  $S_3$  foliation relative to bedding contact ( $S_0$ ) between clast-supported polymictic conglomerate and feldspathic arenite (unit M1; NAD83, UTM Zone 14N, 453428E, 6061649N); **b)** trough crossbedded, magnetite-rich, feldspathic arenite with approximate strike of the bedding surface ( $S_0$ ; unit M2a; UTM 452534E, 6063202N); **c)** planar bedding ( $S_0$ ) is defined by biotite seams/hematite whereas the orientation of biotite perpendicular to bedding defines the  $S_3$  foliation (unit M2c; UTM 453554E, 6062724N); **d)** trough crossbedded feldspathic arenite with a possible concretion or volcanic dropstone—note contorted bedding stratigraphically below (lower arrow) but not above the structure (upper arrow; unit M2a; UTM 452727E, 6062969N).

features can be disrupted, whereas overlying structures remain undisturbed (Figure GS2019-4-4d). This indicates possible soft sediment deformation. An alternative explanation could be that these are pumiceous volcanic bombs that flattened upon impact and resulted in the observed soft sediment deformation.

### **Intrusive rocks (units P and G)**

The stratigraphy of the EMB and MLB is truncated by a semicircular, 3.5 km diameter gabbroic intrusion east of Puella Bay (unit G1; Figure GS2019-4-2). The gabbro is relatively massive, moderately deformed (moderate mineral lineation), seriate, medium grained and contains approximately 65% plagioclase and 35% pyroxene. A pinkish-orange, medium-grained, massive to weakly deformed granite (unit P1), which contains biotite and

possible muscovite, intrudes the gabbro (unit G1) along its north and northwestern flanks where subangular gabbroic xenoliths were observed in a fine-grained granitic matrix (Figure GS2019-4-5a). It is uncertain whether the gabbro (unit G1) and the granite (unit P1) are genetically related. East of Broad Bay and northeast of the community of Herb Lake Landing, several large outcrop ridges contain granite (unit P2) with a similar composition but slightly higher biotite content (up to 10%).

A 6 m wide body of quartz-feldspar–phyric dacite (unit L1) occurs at the southeast end of Puella Bay. The dacite dips and strikes parallel to crossbedded sandstone (EMB). Though the contacts of this felsic body are not well exposed, it is considered a dike or sill with internal layering related to multiple phases of injection (Figure GS2019-4-5b). Narrow, southwest-dipping gabbro dikes (unit L2),





**Figure GS2019-4-5:** Outcrop photographs of intrusive rocks in the Puella Bay area: **a)** granitic (unit P2) intrusive breccia with subangular gabbro (unit G1) fragments (arrow) east of Puella Bay (NAD83, UTM Zone 14N, 455243E, 6062910N); **b)** feldspar-phyric dacite dike with flow layering (arrow) in feldspathic arenite (unit L3; UTM 452534E, 6063202N); **c)** gabbro dike cutting feldspathic arenite (unit L2; UTM 452951E, 6063741N); **d)** feldspar-phyric (arrow) granodiorite (unit L1; UTM 453305E, 6060394N).

ranging from 5 to 25 m in width, cut perpendicular through crossbedded sandstone of the EMB (Figure GS2019-4-5c). Aeromagnetic data indicate that these dikes (unit L2) can trend over several kilometres and postdate early folding ( $D_2$ ) of the EMB (Figure GS2019-4-2), but have a weak to moderate foliation related to ( $D_3$ ) deformation. It should be noted that these dikes were not observed in rocks of the MLB.

Weakly deformed porphyritic granodiorite (unit L3; Figure GS2019-4-5d) stitches the Stuart Bay fault south-east of Puella Bay. Deformation resulted in weak alignment of the biotite. The granodiorite contains coarse- to very coarse, subhedral and elongate iridescent crystals that resemble feldspar, in a medium-grained quartz, plagioclase, K-feldspar and biotite groundmass; further petrography should help resolve the mineralogy.

### Structural considerations

Nearly all rocks in the project area are deformed. Deformation is routinely manifested as clast flattening/

lineation, penetrative foliation and/or mineral lineation at the outcrop scale. Figure GS2019-4-3d shows a rare mesoscopic isoclinal fold ( $F_2$ ) in feldspar crystal tuff (unit S1). This is the earliest recognized deformation in the MLB and is crosscut by a strong penetrative foliation ( $S_3$ ). In the nose of the macroscopic S-fold east of Puella Bay, biotite is aligned perpendicular to bedding in feldspathic arenite, which is attributed to transpressional  $D_3$  deformation (Figure GS2019-4-4c); the same relationship is shown in the area by weakly flattened clasts (Figure GS2019-4-4a). Clast- and mineral-lineations ( $L_3$ ) commonly plunge steeply to the east-southeast, and align on  $D_3$  planar fabrics and faults. The Stuart Bay fault (see Figure GS2019-4-2) is interpreted by Connors et al. (1999) to represent an early  $D_2$  thrust fault that was steepened during  $D_3$  transpression. Fieldwork conducted this summer does not refute this argument; however, a general observation is that feldspathic arenite in the immediate hanging wall shows little to no ductile deformation whereas volcanic rocks of the MLB in the direct footwall show mylonitic fabrics.

## Discussion

Field investigations in the Puella Bay area have constrained the southern extension of the Stuart Bay fault and subsequently the contact between the MLB and EMB (Figure GS2019-4-2). Where the Stuart Bay fault trends from south-southeast to east-southeast the fault is intruded by porphyritic granodiorite (unit L3). The nature of this late intrusion is uncertain, but its emplacement appears to postdate  $D_2$  folding and faulting but predate  $D_3$  deformation, and possibly is related to dilation during reactivation of the Stuart Bay fault. Whole rock lithogeochemistry and petrography will be used to further investigate the granodiorite.

Unit S1 grades from clast-supported plagioclase-phyric andesite cobble and boulder conglomerate into plagioclase-phyric andesite (and local dacite) conglomerate supported by a dacite matrix near the contact with the overlying dacite units (unit S3a–c). Gilbert and Bailes (2005) noticed a similar gradation to the north of the project area, but also observed pebble conglomerate and arenite. These units may be present near the top of unit S1 (Figure GS2019-4-2), but heavy forest cover between Broad Bay and Puella Bay conceals them. Normally graded beds of pebble conglomerate, feldspathic wacke and reworked tuff (unit S3c) at the south end of Puella Bay suggest it is an upright, homoclinal sequence younging to the northeast.

A sequence of amygdaloidal pillowed basalt (unit S4) and mafic boulder conglomerate (unit S5), not previously described, occurs southeast of Puella Bay; the east- to northeast-younging directions indicated by these rocks suggest they may lie stratigraphically over dacite (unit S3) of the MLB. Although the geochemical affinity of these rocks is unknown, the occurrence of pillowed flows indicates at least local subaqueous deposition.

Clast-supported, intermediate to felsic, volcanic conglomerate (unit U1) east of the EMB was previously mapped as conglomerate of the Missi group (e.g., Frarey, 1950), which extends to the southern shores of Monette Lake. Aeromagnetic data does support a northerly extension of these rocks to the Monette Lake area. Based on this summer's observations, these rocks are now interpreted to be part of a new, previously not described, volcanic package that is in fault contact with the EMB.

Within the project area, fluvial-alluvial Missi group rocks (units M1, M2a–d) east of the Stuart Bay fault are an east-younging, homoclinal sequence. The succession records a transition from magnetite-rich trough crossbedded feldspathic arenite and polymictic conglomerate to medium- to fine-grained feldspathic arenite with more tabular bedforms, less magnetite, and increased bio-

tite and muscovite. An interpretation is that these Missi group rocks represent a shift from deposition in a high-energy fluvial environment, such as a braided river, to a lower-energy flow regime that produced tabular, normally graded beds with minor lamination and crossbedding.

Late gabbro dikes (unit L2) that cut the folded stratigraphy and upper beds of the EMB indicate that they were emplaced after the ca. 1826 Ma minimum age for sedimentation, but before the final stages of  $D_3$  deformation. It is uncertain how these gabbro dikes relate to the late diabase dikes described by Gilbert and Bailes (2005); however, their timing of emplacement may be similar given that they cut phases of the ca. 1834 Ma Wekusko Lake pluton (Gordon et al., 1990) on the west side of Wekusko Lake.

## Economic considerations

Four trenches related to a historic Zn–Pb–Cu showing were investigated directly south of Puella Bay; the rocks are strongly muscovite–chlorite–altered schists with up to 10% sulphide, and appear to be of possible felsic volcanoclastic origin. Drilling of the occurrence in 2009 (drillhole PB-09-03; Figure GS2019-4-2; Assessment File Number 74765, Manitoba Agriculture and Resource Development, Winnipeg) intersected multiple base-metal intervals including 207.21–207.42 m (0.46% Pb, 1.66% Zn), 238.16–238.51 m (0.5% Pb, 0.05% Cu, 2.49% Zn) and 245.77–246.24 m (0.47% Pb, 0.81% Cu, 2.19% Zn). The alteration and metal association of the mineralized intersects are suggestive of a volcanogenic massive-sulphide deposit within rocks of the MLB, and that the MLB has potential to host base-metal deposits.

The potential for gold mineralization in the hanging wall to the Crowduck Bay fault is exemplified by the Laguna gold deposit in the northern half of the project area (Figure GS2019-4-1), which produced 1833.9 kg of gold from 109 488 tonnes (16.75 Au g/t) between 1918 and 1940 (Richardson and Ostry, 1996). Notable gold was intersected in core from drillholes BAR-3 (Figure GS2019-4-2; Assessment File Number 94374) and HAR-169 (Figure GS2019-4-2; Assessment File Number 93516). In the fall of 1987, Granges Exploration Ltd. followed up on historical gold-bearing quartz veins near the 'Zona' shaft; all six drillholes intersected gold but the best intersections were from BAR-3 at 41.7–42.7 m (8.9 Au g/t), 46.7–47.7 m (15.9 Au g/t), 54.8–55.3 m (19.6 Au g/t) and 69.2–69.7 m (32.5 Au g/t). Hudson Bay Mining and Smelting Co., Limited drilled two very low frequency targets in the spring of 1985. Drillhole HAR-169 intersected 11.6 Au g/t at 45.3–45.8 m (148.8–150.3 ft., 0.37 oz/ton), 58.8 Au g/t at 54.6–55.0 m (179.2–180.5 ft., 1.88 oz/ton) and 5.6 Au g/t

at 56.7–57.0 m (186.0–187.0 ft., 0.18 oz/ton). Both gold occurrences are associated with quartz-carbonate veins along the sheared contact between metavolcanic and metaplutonic rocks. This highlights the importance of and close relationship between structural reworking and rheological contrast in the emplacement of gold.

## Acknowledgments

The author thanks A. Bairos-Novak for providing enthusiastic field assistance, as well as E. Anderson for timely and helpful logistical support. Thank you to T. Davis for GIS technical support, and C. Epp for preparing samples and thin sections. This contribution was enhanced through constructive reviews by C. Couëslan and C. Böhm.

## References

- Ansdell, K.M., Connors, K.A., Stern, R.A. and Lucas, S.B. 1999: Coeval sedimentation, magmatism, and fold-thrust domain development in the Trans-Hudson orogen: geochronological evidence from the Wekusko Lake area, Manitoba, Canada; *Canadian Journal of Earth Sciences*, v. 36, p. 293–312.
- Armstrong, J.E. 1941: Wekusko, Manitoba; Geological Survey of Canada, Map 665A, scale 1:63 360.
- Bailes, A.H. 1980: Origin of early Proterozoic volcanoclastic turbidites, south margin of the Kiseynew sedimentary gneiss belt, File Lake, Manitoba; *Precambrian Research*, v. 12, p. 197–225.
- Connors, K.A., Ansdell, K.M. and Lucas, S.B. 1999: Coeval sedimentation, magmatism, and fold-thrust development in the Trans-Hudson orogen: propagation of deformation into an active continental arc setting, Wekusko Lake area, Manitoba; *Canadian Journal of Earth Sciences*, v. 36, p. 275–291.
- David, J., Bailes, A.H. and Machado, N. 1996: Evolution of the Snow Lake portion of the Paleoproterozoic Flin Flon and Kiseynew belts, Trans Hudson orogen, Manitoba, Canada; *Precambrian Research*, v. 80, p. 107–124.
- Frarey, M.J. 1950: Crowduck Bay, Manitoba; Geological Survey of Canada, Map 987a, scale 1:63 360.
- Gilbert, H.P. and Bailes, A.H. 2005: Geology of the southern Wekusko Lake area, Manitoba (NTS 63J12NW); Manitoba Industry, Economic Development and Mines, Manitoba Geological Survey, Geoscientific Map MAP2005-2, scale 1:20 000.
- Gordon, T.M. and Gall, Q. 1982: Metamorphism in the Crowduck Bay area, Manitoba; *in* Current Research, Part A, Geological Survey of Canada, Paper 82-1A, p. 197–201.
- Gordon, T.M. and Lemkow, D. 1987: Geochemistry of Missi group volcanic rocks, Wekusko Lake, Manitoba; Geological Survey of Canada, Open File 1442, 38 p.
- Gordon, T.M., Hunt, P.A., Bailes, A.H. and Syme, E.C. 1990: U-Pb ages from the Flin Flon and Kiseynew belts, Manitoba: chronology of crust formation at an early Proterozoic accretionary margin; *in* The Early Proterozoic Trans-Hudson Orogen of North America, J.F. Lewry and M.R. Stauffer (ed.), Geological Association of Canada, Special Paper 37, p. 177–199.
- Lewry, J.F. and Collerson, K.D. 1990: Trans-Hudson orogen: extent, subdivisions, and problems; *in* The Proterozoic Trans-Hudson Orogen of North America, J.F. Lewry and M.R. Stauffer (ed.), Geological Association of Canada, Special Publication 37, p. 1–14.
- NATMAP Shield Margin Project Working Group 1998: Geology, NATMAP Shield Margin Project area, Flin Flon belt, Manitoba/Saskatchewan; Geological Survey of Canada, Map 1968A, scale 1:100 000.
- Reid, K.D. 2017: Sub-Phanerozoic geology south Wekusko Lake, eastern Flin Flon belt, north-central Manitoba (parts of NTS63J5, 12, 63K8, 9): insights from drillcore observations and whole-rock geochemistry of mafic rocks; *in* Report of Activities 2017, Manitoba Growth, Enterprise and Trade, Manitoba Geological Survey, p. 65–77.
- Reid, K.D. 2019: Preliminary geology of the Puella Bay area, Wekusko Lake, north-central Manitoba (NTS 63J12); Manitoba Agriculture and Resource Development, Manitoba Geological Survey, Preliminary Map PMAP2019-4, scale 1:15 000.
- Richardson, D.J. and Ostry, G. (revised by Weber, W. and Fogwill, D.) 1996: Gold deposits of Manitoba; Manitoba Energy and Mines, Economic Geology Report ER86-1 (2<sup>nd</sup> edition), 114 p.
- Ryan, J.J. and Williams, P.F. 1999: Structural evolution of the eastern Amisk collage, Trans-Hudson orogen, Manitoba; *Canadian Journal of Earth Sciences*, v. 36, p. 251–273.
- Shanks, R.J. and Bailes, A.H. 1977: “Missi Group” rocks of the Wekusko Lake area; *in* Report of Field Activities 1977, Manitoba Department of Mines, Resources and Environmental Management, Mineral Resources Division, p. 83–87.
- Stern, R.A., Syme, E.C., Bailes, A.H. and Lucas, S.B. 1995: Paleoproterozoic (1.90–1.86 Ga) arc volcanism in the Flin Flon belt, Trans-Hudson orogen, Canada; *Contributions to Mineralogy and Petrology*, v. 119, p. 117–141.
- Stockwell, C.H. 1937: Gold deposits of Herb Lake area, northern Manitoba; Geological Survey of Canada, Memoir 208, 46 p.



## Interpretation of U-Pb isotopic dates of columbite-group minerals in pegmatites, Wekusko Lake pegmatite field, central Manitoba (part of NTS 63J13)

by D. Benn<sup>1</sup>, T. Martins and R.L. Linnen<sup>1</sup>

### In Brief:

- Pegmatite dikes have an emplacement age of 1.78 Ga determined by U-Pb isotopic dating of columbite
- Pegmatite dikes are structurally related to the brittle-ductile deformation event and place age constraints on the D<sub>4</sub> event
- Future Li exploration in the area should focus on north-northwestern trending anomalies and structural planes of weakness

### Citation:

Benn, D., Martins, T. and Linnen, R.L. 2019: Interpretation of U-Pb isotopic dates of columbite-group minerals in pegmatites, Wekusko Lake pegmatite field, central Manitoba (part of NTS 63J13); in Report of Activities 2019, Manitoba Agriculture and Resource Development, Manitoba Geological Survey, p. 52–59.

### Summary

Recent geochronology results from lithium-bearing pegmatite dikes from the Green Bay group of the Wekusko Lake pegmatite field, along with related constraints on the regional structural history, are described in this report. In situ U-Pb dating of columbite grains yielded an isotopic U-Pb age of  $1780 \pm 8.1$  Ma, which is interpreted as the age of emplacement of the lithium-bearing dikes. The columbite-group minerals are commonly associated with coarse-grained tourmaline, vary in size between 100 and 150  $\mu\text{m}$  and typically have an acicular or pear-shaped habit. The columbite grains show minor zonation, with a slightly Nb-enriched core. The age of the pegmatite dikes is also interpreted as the minimum age of the brittle–ductile deformation phase and the maximum age of the late-stage folding phase of the D<sub>4</sub> deformation event.

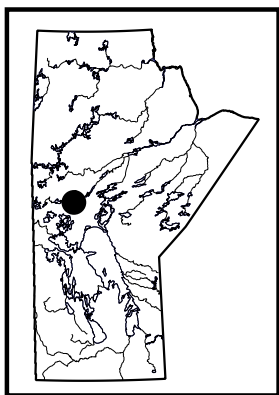
### Introduction

In Manitoba, lithium exploration typically focuses on Li-Cs-Ta-bearing pegmatites. The world-class Tanco deposit in southeastern Manitoba is an example of a pegmatite deposit in this province, but other areas also have potential, including the Snow Lake area. The Li-bearing pegmatite dikes that are the focus of this report form part of the Green Bay pegmatite group within the Wekusko Lake pegmatite field (Černý et al., 1981) in the Snow Lake block of the Flin Flon–Glennie complex (Figure GS2019-5-1). These dikes are located approximately 25 km east of Snow Lake and are currently under exploration by Far Resources Ltd. for their lithium potential. This study builds on the previous work of Benn et al. (2018a, b), and provides an emplacement age for the Li-bearing pegmatite dikes and structural context. Tentative constraints on the timing of deformation events are also determined.

### Geological setting

The Wekusko Lake pegmatite field is host to multiple pegmatite dikes characterized by variable amounts of Li mineralization. This area is also known for economic deposits of Au, Cu-Ni and Cu-Pb (e.g., Gagné et al., 2005; Stewart et al., 2018). The Snow Lake–Flin Flon area is part of the 1.91–1.83 Ga Flin Flon–Glennie complex (Figure GS2019-5-1; Connors et al., 2002) in the Trans-Hudson orogen (THO), a well-preserved Paleoproterozoic collisional belt between the Archean Superior and Rae–Hearne cratons (Hoffman, 1989) that spans from Scandinavia through Canada and into the central United States (Schneider et al., 2007). The central Canadian portion of the THO comprises four tectonic zones (Figure GS2019-5-1; Lewry et al., 1994) identified as

- the eastern boundary zone, which includes the Thompson nickel belt;
- the Reindeer zone, which consists of the Rottenstone–Southern Indian domain, the La Ronge–Lynn Lake–Leaf Rapids domain and the Flin Flon–Glennie complex (Glennie domain, Hanson Lake block, Flin Flon belt and Snow Lake block; Schneider et al., 2007);
- the Chipewyan/Wathaman batholith, an Andean-type continental magmatic arc (Meyer et al., 1992); and
- the reworked margin of the Hearne province.



<sup>1</sup> Department of Earth Sciences, Western University, London, ON N6A 5B7

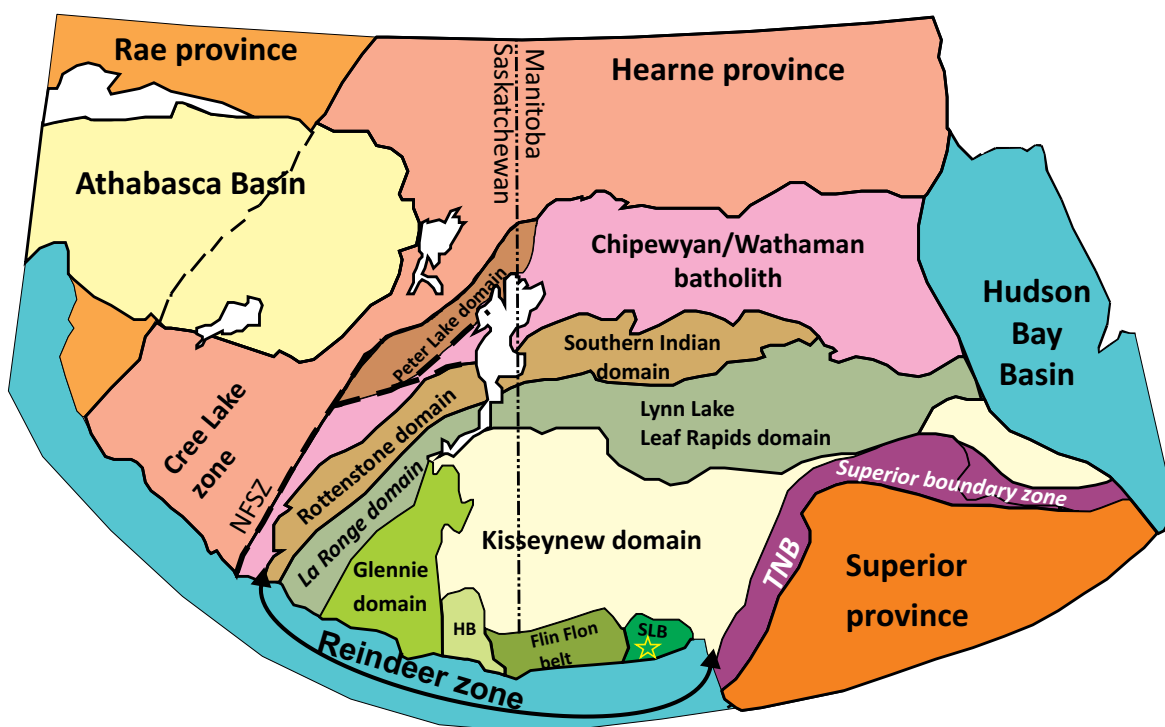


**Figure GS2019-5-1:** Simplified geology of northern Saskatchewan and Manitoba, showing the main lithotectonic subdivisions and major structural boundaries. Abbreviations: HB, Hanson Lake block; NFSZ, Needle Falls shear zone; SLB, Snow Lake block; TNB, Thompson nickel belt (after Hoffman et al., 1988). The star overlies the field area of this study.

Within the Reindeer zone, the Flin Flon–Glennie complex displays a metamorphic gradient from green-schist facies at the southern boundary to upper-amphibolite facies at its northern boundary with the Kisseynew domain (Černý et al., 1981).

### Structural geology

The Wekusko Lake area has undergone four deformational events ( $D_1$ – $D_4$ ) as defined in Connors et al. (1999). The first deformation event ( $D_1$ ) records the folding that occurred during the accretion (1.88–1.87 Ga) of the assemblages that formed the Flin Flon–Glennie complex. Plutonism and crustal shortening continued to steepen the synaccretionary schistose fabrics and isoclinal folding from 1.87 to 1.84 Ga (Černý et al., 1981; Lucas et al., 1996). The  $D_2$  deformation event recorded south-southwest compression, which resulted in the inversion of the Kisseynew turbidite basin (Černý et al., 1981; Connors et al., 1999). Collision with the Sask craton led to the regional peak in metamorphism at 1.81 Ga (Gordon et al., 1990; David et al., 1996; Schneider et al., 2007). During peak metamorphism, the Snow Lake block (Schneider et al., 2007) reached temperatures between 500 and 700°C, and pressures ranged between 0.4 and 0.6 GPa (Kraus and Menard, 1997). The  $D_3$  deformation event records north-west-trending transpressional shortening, which occurred

during syn- to postpeak metamorphism at 1.81 Ga (Ryan and Williams, 1999). The final deformation event ( $D_4$ ) records northwest-trending compression, which caused brittle to ductile deformation (Černý et al., 1981; Lucas et al., 1994; Connors et al., 1999). The age of the  $D_4$  deformation event is unknown. Schneider et al. (2007) reported an additional thermal peak in the Flin Flon belt at 1.77 Ga that is associated with crustal melting. This was followed by rapid uplift and cooling.

### Green Bay group pegmatites

The Green Bay group pegmatites in the study area are hosted primarily by a mafic volcanic unit metamorphosed to lower-amphibolite facies (Černý et al., 1981; Benn et al., 2018a, b); however, in the interest of brevity, the ‘meta’ prefix has been omitted. The mafic volcanic unit is unconformably overlain by the quartzofeldspathic gneiss of the Missi group sedimentary rocks (Connors et al., 1999), which is also host to pegmatite dikes. These units make up the Roberts Lake fault block (Connors et al., 1999, 2002), which is bound by a north-northeast-trending fault to the west and a broadly east-trending fault to the south. These faults intersect at the southwestern corner of the Roberts Lake fault block (Figure GS2019-5-2).

Bedrock mapping of the area outlined in Figure GS2019-5-2 was completed at a scale of 1:4000 during the

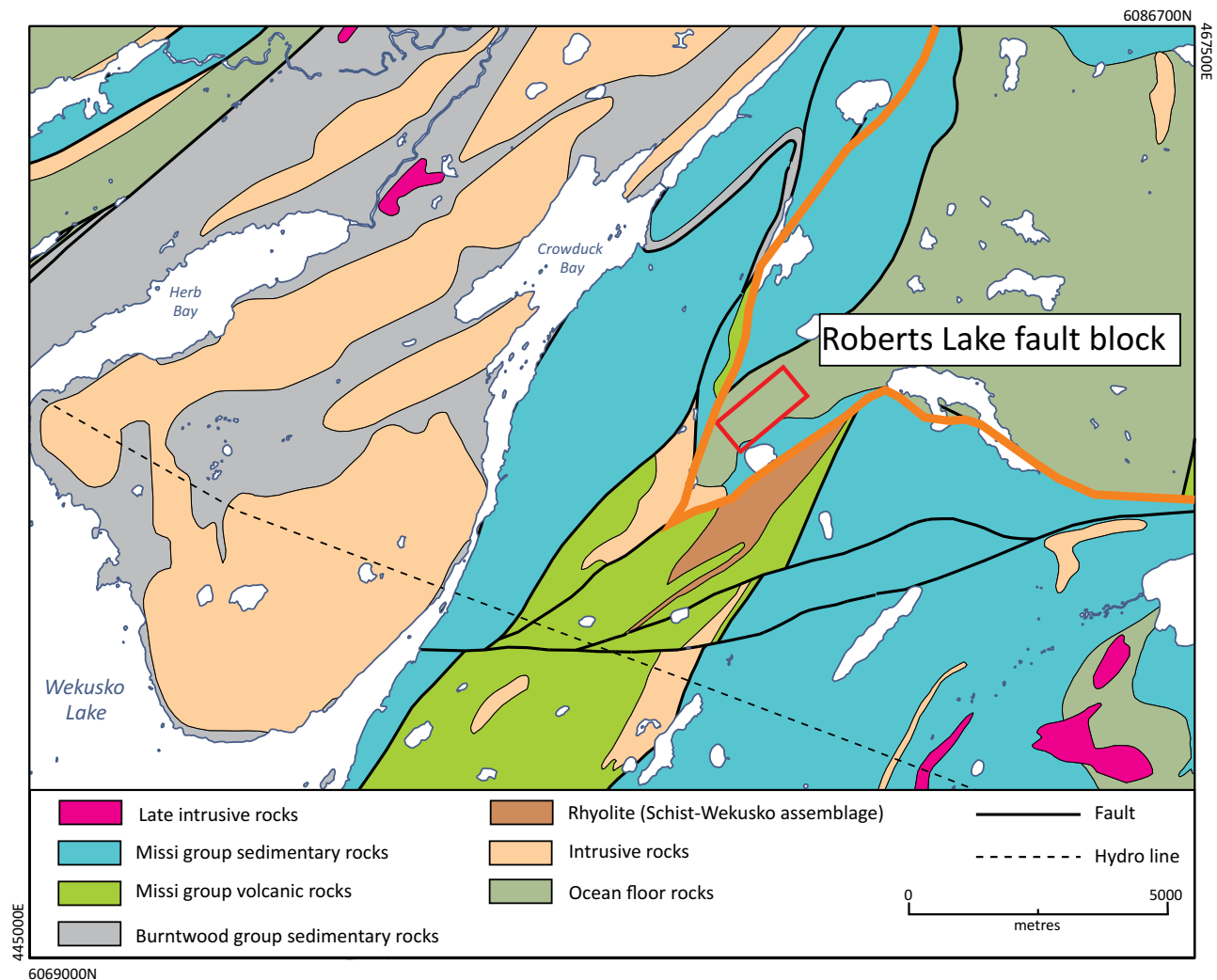


**Figure GS2019-5-2:** Regional geology of the eastern side of Wekusko Lake, central Manitoba. The red rectangle outlines the mapping area of Benn et al. (2018b) and the orange line outlines the Roberts Lake fault block (modified from NATMAP Shield Margin Project Working Group, 1998).

2018 field season and eight dikes greater than 1 m thick were delineated (Benn et al., 2018b). Since that study, five new dikes have been discovered in the surrounding area (Far Resources Ltd., 2019). All the dikes in the mapping area trend northwest.

The pegmatite dikes in the Green Bay group were classified in Benn et al. (2018a) as belonging to the rare-element (REL) class, REL-Li subclass, complex type, spodumene subtype, based on the Černý and Ercit (2005) classification system. The pegmatites consist of quartz, albite, K-feldspar, muscovite, spodumene and tourmaline, with accessory beryl, apatite, Fe-Mn phosphate minerals, garnet, zircon and columbite-group minerals (CGMs; Benn et al., 2018a). The grain size of the minerals typically varies throughout the width of the dikes. Benn et al. (2018a) defined and described five zones within the pegmatite dikes: the border zone, the wall zone, the intermediate

zone, the central zone and the core zone. The zones were determined based on mineralogy, grain size and degree of alteration. Quartz and feldspar crystals up to 30 cm in length are present in the core zone and display aplitic textures in patches throughout the dike. Hematization occurs throughout the dikes, giving the border, wall and intermediate zones a red to pink hue.

Dike thickness varies according to the hostrock. Dike 1, the largest dike, varies from 1 to 15 m in thickness and has a strike length of over the 300 m at surface. Dike 8 is the next largest and is over 13 m thick at depth (Far Resources Ltd., 2018). In the mafic volcanic rocks, the dikes range from 1 to 15 m thick, whereas the dikes hosted in sedimentary rocks thin to less than 1 m (Benn et al., 2018a). This difference is readily observed in dike 1: in those locations where it is hosted by mafic volcanic rock, dike 1 has an average width of approximately 10 m,



whereas where the dike crosses into sedimentary rock, it tapers to a thickness of 10 cm before terminating (Benn et al., 2018a). Thin dikes (less than 30 cm) and dikelets (less than 1 cm) are also present, although these are usually nonmineralized (Benn et al., 2018a). The dikes crosscut  $S_3$  (Connors et al., 2002) north-northeast-trending foliations in the hostrock.

The pegmatite dikes are folded over several metres (Figure GS2019-5-3; Benn et al., 2018a). Thinner dikes such as dike 7 are folded to a greater extent than the thicker dike 1 and the folding in these dikes can be more extreme (i.e., they displayptygmatic folds); their thickness also changes due to pinching and swelling (Benn et al., 2018a). Dike 1 is thicker and shows minimal folding at its northern tip.

### Columbite-group minerals

Columbite-group minerals are present in all zones of the studied pegmatites. Drillcore samples collected from dikes 1, 5 and 8 were selected based on high Ta values from assays of drillcore from Far Resources (Far Resources Ltd., 2017, 2018). Polished thin sections were cut from the drillcore samples. Columbite-group mineral grains were identified by reflected-light microscopy and their compositions were qualitatively determined using a JEOL JCM-6000 benchtop scanning electron microscope; back-scattered electron imagery and element maps were subsequently produced by a JEOL JXA-8530F microprobe at the University of Western Ontario.

The CGMs have either a tabular acicular or a pear-shaped habit, typically associated with larger tourmaline crystals. Grains are generally 100 to 150  $\mu\text{m}$  long and rarely

exceed 1000  $\mu\text{m}$  in length. The CGMs display minimal to moderate zonation (Figure GS2019-5-4a–f); typically, the crystals consist of large cores enriched in Nb, with thin rims that are enriched in Ta (Figure GS2019-5-4a–f).

### U-Pb geochronology of columbite-group minerals

Columbite-group minerals  $[(\text{Fe,Mg,Mn})(\text{Nb,Ta})_2\text{O}_6]$  have high U and low Pb contents, making them ideal for U-Pb isotopic dating (Romer and Smeds, 1994; Romer and Lehmann, 1995). The dating of CGMs can be useful for determining the emplacement age of rocks like pegmatites and rare-metal granites, which may lack zircon or where the zircon is not suitable for radiometric dating. Due to an abundance of U-rich inclusions in CGMs, in situ techniques, such as laser-ablation induction coupled plasma–mass spectroscopy (LA-ICP-MS; Smith et al., 2004) or secondary-ion mass spectroscopy (Legros et al., 2019) have become the favoured methods for dating CGMs.

Four U-Pb isotopic dates were obtained from CGMs of lithium-bearing pegmatites from the Green Bay group using LA-ICP-MS, as reported by Martins et al. (2019). Details regarding the analytical procedures and BSE imagery of the analysed CGMs are given in Martins et al. (2019). Combined results gave a concordia age of  $1780 \pm 8.1$  Ma with a mean square of weighted deviates of 1.6 (Martins et al., 2019; Figure GS2019-5-5).

### Discussion

#### Tectonic implications

The orientation and shape of the pegmatite intrusions will be affected by the rheology of the hostrock (Brisbin,



**Figure GS2019-5-3:** Outcrop photograph, showing folding in pegmatite hosted by mafic volcanic rocks.

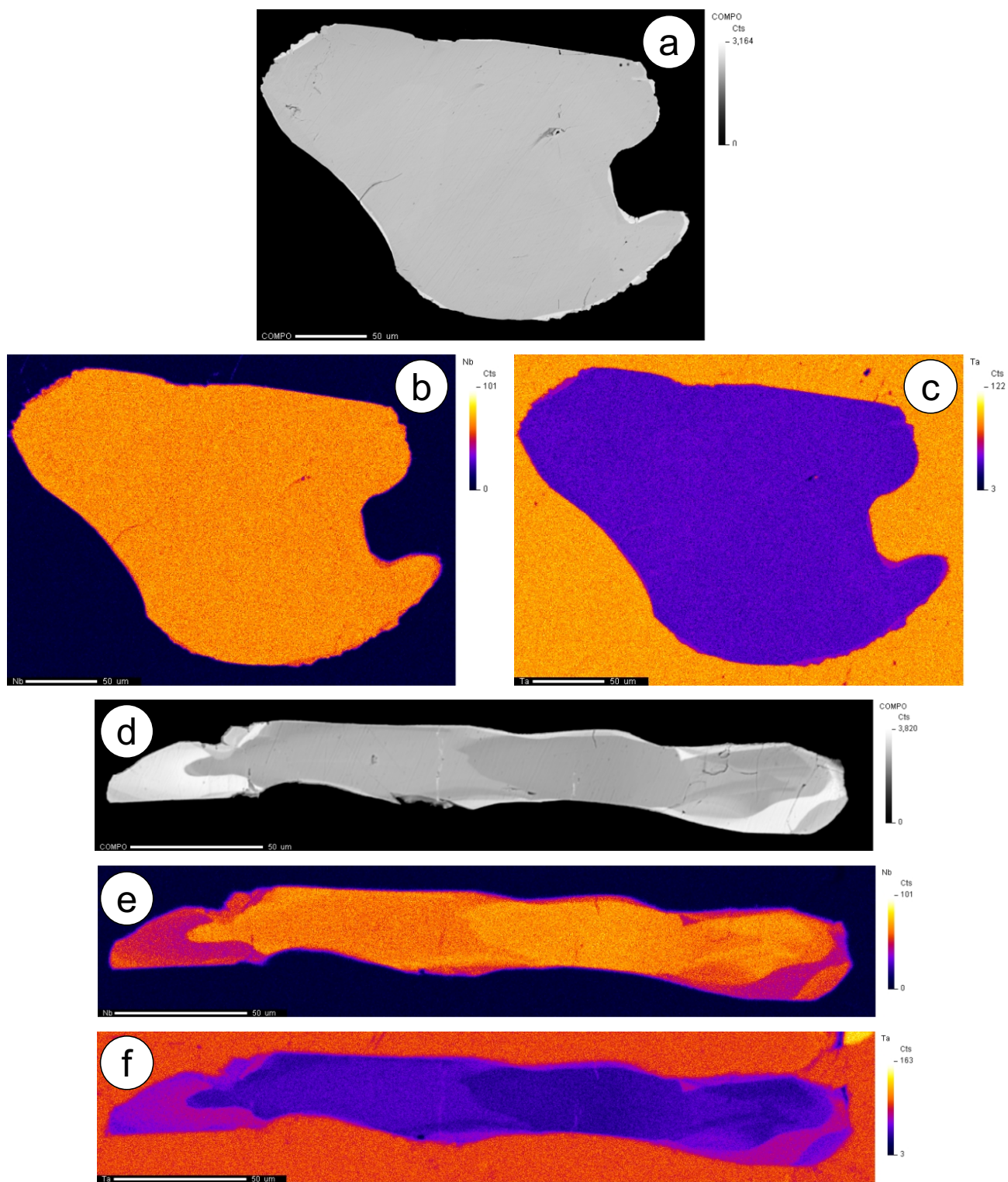


**Figure GS2019-5-4:** Back-scattered electron (BSE) and false-colouring element maps of columbite-group minerals: **a)** BSE imagery of a minimally zoned columbite grain; **b)** Nb element map of the same grain as in a); **c)** Ta element map of the same grain as in a); **d)** BSE imagery of a moderately zoned columbite grain; **e)** Nb element map of the same grain as in d); **f)** Ta element map of the same grain as in d). Abbreviations: COMPO, composition; Cts, counts.



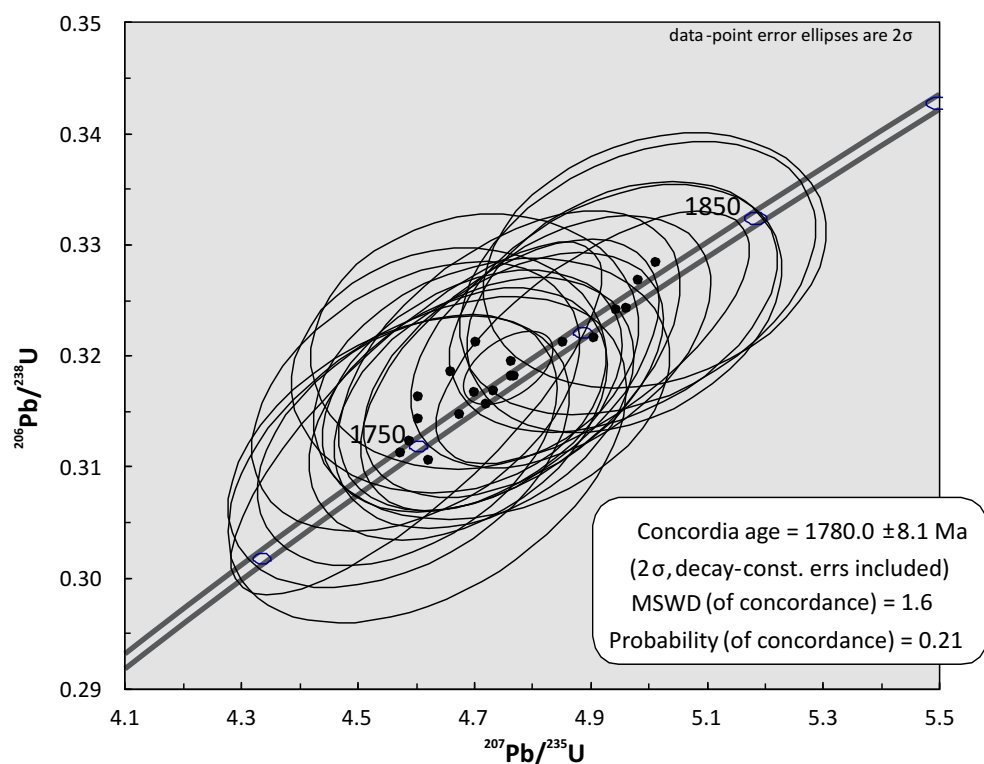


**Figure GS2019-5-5:** Concordia diagram for all data combined from columbite-group minerals of lithium-bearing pegmatites from the Green Bay group of the Wekusko Lake pegmatite field (modified from Martins et al., 2019). Abbreviations: const., constant; errs, errors; MSWD, mean square of weighted deviates.

1986). Rocks are brittle at the upper level of the crust and become progressively more ductile with depth, which includes a transition zone where the rocks exhibit brittle–ductile behaviour. Pegmatites that intruded into the transition zone are podiform and lenticular in shape. Planes of weakness and anisotropic stresses also effect the orientation of the pegmatite (Brisbin, 1986). Pegmatite melts will intrude into sites where the pegmatite fluid pressure is greater than the combination of normal stress and tensile strength (Brisbin, 1986). Unidirectional tectonic stresses will commonly cause a singular direction of emplacement in brittle and brittle–ductile hostrocks.

The U-Pb age obtained by Martins et al. (2019) provides the first absolute-age constraint on the emplacement of dikes 1 and 8 of the lithium-bearing pegmatite dikes from the Green Bay group. The age also provides further constraints on the timing of deformation in the Wekusko Lake region. The emplacement age of the studied pegmatites is  $1780 \pm 8.1$  Ma, which corresponds to the period of postpeak metamorphism, as defined by several authors (e.g., Gordon et al., 1990; David et al., 1996; Schneider et al., 2007). This suggests that the intrusion of the pegmatites occurred during the  $D_3$  or  $D_4$  deformation events. The semiplanar shape and consistent north-northwest trend of the studied pegmatites suggest emplacement into a ductile–brittle hostrock (Brisbin, 1986) at a

time when the tectonic stress from the north-northwest was greater than that from the east-northeast. These conditions best describe the  $D_4$  deformation event (Černý et al., 1981; Lucas et al., 1994; Connors et al., 1999). The dikes are folded (Benn et al., 2018a); if this folding occurred during the final stages of  $D_4$  deformation, then 1.78 Ga represents a maximum age for the late stages of  $D_4$  deformation. Alternatively, the structural history of the region may be more complex than currently recognized.

Schneider et al. (2007) recorded a thermal peak of approximately 500–600°C at 1.77 Ga with associated mid-crustal melting. The same authors did not believe this event was related to slow cooling following peak metamorphism, but rather that it may have recorded rapid crustal extrusion and unroofing. This could have led to decompression melting and muscovite dehydration (Kraus and Menard, 1997). Although no formal conclusion can be reached as to these events being connected, the coinciding ages and nature of the events suggest a link. This thermal event may also be linked to the  $D_3$  or  $D_4$  deformation events.

### Pegmatite genesis

There are currently two dominant models for pegmatite formation: fractional crystallization and anatexis



(London, 2018). Pegmatites are formed by fractional crystallization, where melt is extracted from the late stages of granite formation, or by anatexis, where metamorphic rock is subjected to a low degree of partial melting.

Given the above tectonic constraints, one possible model for the formation of the Wekusko Lake pegmatite field involves anatexis following peak metamorphism at 1.81 Ga. Several workers (e.g., Kraus and Menard, 1997; Schneider et al., 2007) reported high-temperature low-pressure metamorphic conditions around this time that were sufficient to generate lithium-enriched partial melts (Stewart, 1978). Such melts may have been later tapped by north-northwest-trending faults during  $D_4$  deformation, leading to the emplacement of the pegmatite dikes.

As indicated above, the other model for the formation of the studied pegmatites is fractional crystallization; however, genetically related source granites have not been identified (Černý et al., 1981) and it is difficult to prove either the fractionation or the anatectic model.

### Economic considerations

The pegmatite dikes of the Green Bay group are currently being explored for their economic viability. These pegmatites are enriched in Li, Cs, Nb and Ta. The Li-bearing pegmatites from the Green Bay group of the Wekusko Lake pegmatite field have an interpreted emplacement age of  $1780 \pm 8.1$  Ma. This group of pegmatites outcrops in a north-northwest trend, suggesting a structural relation to the regional  $D_4$  deformation event. The folding in the pegmatite dikes must have taken place after emplacement; this suggests syndeformation emplacement of the pegmatites during the  $D_4$  deformation event. The link between  $D_4$  and the emplacement of the pegmatite dikes can be used to constrain a minimum age for early  $D_4$  brittle-ductile events and a maximum age for late  $D_4$  folding events. Understanding of the formation process, structural controls and age of these dikes is useful for exploration, and the discovery of new, possibly economic, dikes. Future exploration should focus on north-northwest-trending anomalies and planes of structural weakness in the hostrock, such as faults and shear zones.

### Acknowledgments

Far Resources Ltd. is thanked for access to drillcore. Field and logistical support from the Manitoba Geological Survey are also gratefully acknowledged. The authors thank C. McFarlane and his team at the University of New Brunswick for the LA-ICP-MS work. This project highly benefited from discussions with M. Fedikow, S. Gagne, J. Singh, D. Ziehlke, J. Ziehlke and C. McFarlane. Both S. Woods and M. Beauchamp (University of Western Ontario) are

thanked for providing thin-section preparation and electron-microprobe support. This study is supported by a grant to R. Linnen from Natural Resources Canada under Phase 5 of its Targeted Geoscience Initiative program.

### References

- Benn, D., Linnen, R.L. and Martins, T. 2018a: Geology and bedrock mapping of the Wekusko Lake pegmatite field (northeastern block), central Manitoba (part of NTS 63J13); in Report of Activities 2018, Manitoba Growth, Enterprise and Trade, Manitoba Geological Survey, p. 79–88.
- Benn, D., Martins, T., Linnen, R.L., Ziehlke, J. and Singh, J. 2018b: Bedrock geology of the Wekusko Lake pegmatite field (northeastern block), central Manitoba (part of NTS 63J13); Manitoba Growth Enterprise and Trade, Manitoba Geological Survey, Preliminary Map PMAP2018-2, scale 1:4000.
- Brisbin, W.C. 1986: Mechanics of pegmatite intrusion; *American Mineralogist*, v. 71, no. 3–4, p. 644–651.
- Černý, P. and Ercit, T.S. 2005: The classification of granitic pegmatites revisited; *The Canadian Mineralogist*, v. 43, no. 6, p. 2005–2026.
- Černý, P., Trueman, D.L., Ziehlke, D.V., Goad, B.E. and Paul, B.J. 1981: The Cat Lake-Winnipeg River and the Wekusko Lake pegmatite fields, Manitoba; Manitoba Department of Energy and Mines, Mineral Resources Division, Economic Geology Report ER80-1, 216 p. plus 5 maps.
- Connors, K.A., Ansdell, K.M. and Lucas, S.B. 1999: Coeval sedimentation, magmatism, and fold-thrust development in the Trans-Hudson Orogen: propagation of deformation into an active continental arc setting, Wekusko Lake area, Manitoba; *Canadian Journal of Earth Sciences*, v. 36, no. 2, p. 275–291.
- Connors, K., Ansdell, K. and Lucas, S. 2002: Development of a transverse to orogen parallel extension lineation in a complex collisional setting, Trans-Hudson Orogen, Manitoba, Canada; *Journal of Structural Geology*, v. 24, no. 1, p. 89–106.
- David, J., Bailes, A.H. and Machado, N. 1996: Evolution of the Snow Lake portion of the Palaeoproterozoic Flin Flon and Kiseeynew belts, Trans-Hudson Orogen, Manitoba, Canada; *Precambrian Research*, v. 80, no. 1–2, p. 107–124.
- Far Resources Limited. 2017: Phase 3 Drilling; Far Resources Limited, URL <<https://www.farresources.com/phase-3-drilling/>> [August 2018].
- Far Resources Limited. 2018: Phase 4 Drilling; Far Resources Limited, URL <<https://www.farresources.com/phase-4-drilling/>> [August 2018].
- Far Resources Limited. 2019: Far Resources discovers five new pegmatite dykes and significantly expands pegmatite field at the Zoro Lithium Project, Manitoba.; Far Resources Limited, URL <<https://farresources.com/news/2019/2/18/far-resources-discovers-five-new-pegmatite-dykes-and-significantly-expands-pegmatite-field-at-the-zoro-lithium-project-manitoba/>> [March 2019].

- Gagné, S., Beaumont-Smith, C.J., Hynes, A. and Williams-Jones, A.E. 2005: Gold metallogenesis and tectonometamorphic history of selected deposits from the Snow Lake area and the southern flank of the Kisseynew Domain, west-central Manitoba (NTS 63J13, 63K10, 63K16 and 63N2); *in* Report of Activities 2005, Manitoba Industry, Economic Development and Mines, Manitoba Geological Survey, p. 20–27.
- Gordon, T.M., Hunt, P.A., Bailes, A.H. and Syme, E.C. 1990: U-pb ages from the Flin Flon and Kisseynew belts, Manitoba; chronology of crust formation at an early Proterozoic accretionary margin; *in* The Early Proterozoic Trans-Hudson Orogen of North America, J.F. Lewry and M.R. Stauffer (ed.); Geological Association of Canada, Special Paper 37, p. 177–199.
- Hoffman, P. 1988: United Plates of America, the birth of a craton: Early Proterozoic assembly and growth of Laurentia; *Annual Review of Earth and Planetary Sciences*, v. 16, no. 1, p. 543–603.
- Hoffman, P. 1989: Precambrian geology and tectonic history of North America; *in* The Geology of North America—an overview, A.W. Bally and A.R. Palmer (ed.); Geological Society of America, The Geology of North America, v. A, p. 447–512.
- Kraus, J. and Menard, T. 1997: A thermal gradient at constant pressure; implications for low- to medium-pressure metamorphism in a compressional tectonic setting, Flin Flon and Kisseynew domains, Trans-Hudson Orogen, central Canada; *The Canadian Mineralogist*, v. 35, no. 5, p. 1117–1136.
- Legros, H., Mercadier, J., Villeneuve, J., Romer, R.L., Deloule, E., Van Lichtenvelde, M., Dewaele, S., Lach, P., Che, X.-D., Wang, R.-C., Zhu, Z.-Y., Gloaguen, E. and Melleton, J. 2019: U-Pb isotopic dating of columbite-tantalite minerals: development of reference materials and in situ applications by ion microprobe; *Chemical Geology*, v. 512, p. 69–84.
- Lewry, J., Hajnal, Z., Green, A., Lucas, S.B., White, D., Stauffer, M., Ashton, K., Weber, W. and Clowes, R. 1994: Structure of a Paleoproterozoic continent-continent collision zone: a LITHOPROBE seismic reflection profile across the Trans-Hudson Orogen, Canada; *Tectonophysics*, v. 232, no. 1–4, p. 143–160.
- London, D. 2018: Ore-forming processes within granitic pegmatites; *Ore Geology Reviews*, v. 101, p. 349–383.
- Lucas, S., White, D., Hajnal, Z., Lewry, J., Green, A., Clowes, R., Zwanig, H., Ashton, K., Schledewitz, D., Stauffer, M., Norman, A., Williams, P. and Spence, G. 1994: Three-dimensional collisional structure of the Trans-Hudson Orogen, Canada; *Tectonophysics*, v. 232, no. 1–4, p. 161–178.
- Lucas, S., Stern, R., Syme, E., Reilly, B. and Thomas, D. 1996: Intraoceanic tectonics and the development of continental crust: 1.92–1.84 Ga evolution of the Flin Flon Belt, Canada; *Geological Society of America Bulletin*, v. 108, no. 5, p. 602.
- Martins, T., Benn, D. and McFarlane, C.R.M. 2019: Laser-ablation inductively coupled plasma–mass spectrometry (LA-ICP-MS) analyses of columbite grains from Li-bearing pegmatites, Wekusko Lake pegmatite field (northeastern block), central Manitoba (part of NTS 63J13); Manitoba Agriculture and Resource Development, Manitoba Geological Survey, Data Repository Item DRI2019003, Microsoft® Excel® file.
- Meyer, M., Bickford, M. and Lewry, J. 1992: The Wathaman batholith: an Early Proterozoic continental arc in the Trans-Hudson orogenic belt, Canada; *Geological Society of America, Bulletin*, v. 104, no. 9, p. 1073–1085.
- NATMAP Shield Margin Project Working Group 1998: Geology, NATMAP Shield Margin Project area, Flin Flon Belt, Manitoba/Saskatchewan; Geological Survey of Canada, Map 1968A, scale 1:100 000.
- Romer, R. and Smeds, S. 1994: Implications of U-Pb ages of columbite-tantalites from granitic pegmatites for the Palaeoproterozoic accretion of 1.90–1.85 Ga magmatic arcs to the Baltic Shield; *Precambrian Research*, v. 67, no. 1–2, p. 141–158.
- Romer, R. and Lehmann, B. 1995: U-Pb columbite age of Neoproterozoic Ta-Nb mineralization in Burundi; *Economic Geology*, v. 90, no. 8, p. 2303–2309.
- Ryan, J. and Williams, P. 1999: Structural evolution of the eastern Amisk collage, Trans-Hudson Orogen, Manitoba; *Canadian Journal of Earth Sciences*, v. 36, no. 2, p. 251–273.
- Schneider, D., Heizler, M., Bickford, M., Wortman, G., Condie, K. and Perilli, S. 2007: Timing constraints of orogeny to cratonization: thermochronology of the Paleoproterozoic Trans-Hudson orogen, Manitoba and Saskatchewan, Canada; *Precambrian Research*, v. 153, no. 1–2, p. 65–95.
- Smith, S., Foster, G., Romer, R., Tindle, A., Kelley, S., Noble, S., Horstwood, M. and Breaks, F. 2004: U-Pb columbite-tantalite chronology of rare-element pegmatites using TIMS and laser ablation-multi collector-ICP-MS; *Contributions to Mineralogy and Petrology*, v. 147, no. 5, p. 549–564.
- Stewart, D.B. 1978: Petrogenesis of lithium-rich pegmatites; *American Mineralogist*, v. 63, no. 9–10, p. 970–980.
- Stewart, M.S., Lafrance, B. and Gibson, H.L. 2018: Early thrusting and folding in the Snow Lake camp, Manitoba: tectonic implications and effects on volcanogenic massive sulfide deposits; *Canadian Journal of Earth Sciences*, v. 55, no. 8, p. 935–957.

## Evaluation of graphite- and vanadium-bearing drillcore from the Huzyk Creek property, sub-Phanerozoic Kiseynew domain, central Manitoba (NTS 63J6)

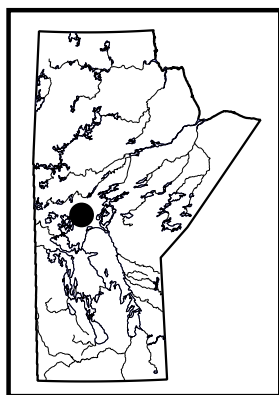
by C.G. Couëslan

### In Brief:

- An interbedded wacke-mudstone succession, tentatively correlated with the Burntwood group, hosts vanadium-enriched graphite mineralization at the Huzyk Creek property
- Vanadium was likely entrained by organic particles as they settled through the water column
- Graphite deposits elsewhere in the Kiseynew basin could be equally prospective for vanadium

### Citation:

Couëslan, C.G. 2019: Evaluation of graphite- and vanadium-bearing drillcore from the Huzyk Creek property, sub-Phanerozoic Kiseynew domain, central Manitoba (NTS 63J6); in Report of Activities 2019, Manitoba Agriculture and Resource Development, Manitoba Geological Survey, p. 60–71.



### Summary

The Huzyk Creek property lies along the boundary between the sub-Phanerozoic Thompson nickel belt and the Kiseynew domain, and is host to graphite-mineralized and vanadium-enriched metasedimentary rocks. The metasedimentary rocks consist of an interbedded wacke-mudstone succession that is tentatively correlated with (although atypical of) the Burntwood group of the Kiseynew domain. A package of hornblende gneiss and calcsilicate is associated with the wacke-mudstone succession and could represent variably altered mafic volcanic rocks. The graphite mineralization occurs as an intersection of graphite-rich mudstone (14.3–16.7 m wide), which is likely analogous to black shale. The vanadium enrichment correlates closely with the graphite mineralization, and suggests that vanadium was likely entrained by organic particles as they settled to the bottom of the Kiseynew basin. Graphite deposits elsewhere in the Kiseynew domain could prove equally prospective for vanadium. Graphite and vanadium are considered critical elements/minerals by the U.S. Department of the Interior, and are in demand by the green technologies sector for use in electric motors, lithium batteries, and vanadium redox-flow batteries. The Green Giant and Balama prospects are similar metamorphosed black shale deposits investigated for vanadium and graphite mineralization in Madagascar and Mozambique, respectively.

### Introduction

The Huzyk Creek property consists of two mineral exploration licenses and 10 mining claims, centred roughly 23 km south of Ponton. The property lies along the boundary between the sub-Phanerozoic Thompson nickel belt (TNB) and Kiseynew domain (Figure GS2019-6-1). A thick (~62 m) interval of sulphide-bearing, graphitic metasedimentary rocks was intersected in diamond-drill core by Hudson Bay Exploration and Development Co. Ltd. while exploring for Ni-Cu on the property in 1997 (Assessment File 73152, Manitoba Agriculture and Resource Development, Winnipeg). The graphitic interval was found to contain up to 40% graphite as fine to coarse flakes. Rocas del Norte, a private company, resampled a 68 m graphitic interval from drillhole NIM-19 in 2014, which yielded 0.14%  $V_2O_5$ , including 0.6%  $V_2O_5$  over 0.6 m (Beaumont-Smith, 2018; Assessment File 73152). The property was optioned by Vanadian Energy Corp. (Vanadian; formerly Uracon) in August of 2018. Recent diamond-drilling by Vanadian attempted to twin NIM-19 as well as test a geophysical conductor, outlined by historical exploration work, believed to coincide with the graphitic horizon. Attempts to twin hole NIM-19 were not successful due to uncertainty of the original location of the drill collar; however, the first drillhole, HZ-19-01, intersected a 13.77 m sulphide-bearing graphitic zone grading 0.18%  $V_2O_5$ , including a 9.74 m zone grading 0.22%  $V_2O_5$  (Vanadian Energy Corp., 2019). The second hole, HZ-19-02, was collared 200 m north-east along strike and intersected a 14.05 m graphitic zone grading 0.11%  $V_2O_5$ . Both graphitic horizons are hosted in metasedimentary rocks with broad zones of variable graphite content and anomalous vanadium (Vanadian Energy Corp., 2019).

Sulphide- and graphite-bearing argillaceous rocks occur in both the Burntwood group rocks of the Kiseynew domain and Ospwagan group rocks of the TNB (Zwanzig, 1999; Zwanzig et al., 2007). Because the Huzyk Creek property straddles the TNB–Kiseynew domain boundary, determining the affinity of the metasedimentary rocks has implications for locating additional vanadium-bearing graphitic rocks. Sulphide and graphite are also concen-



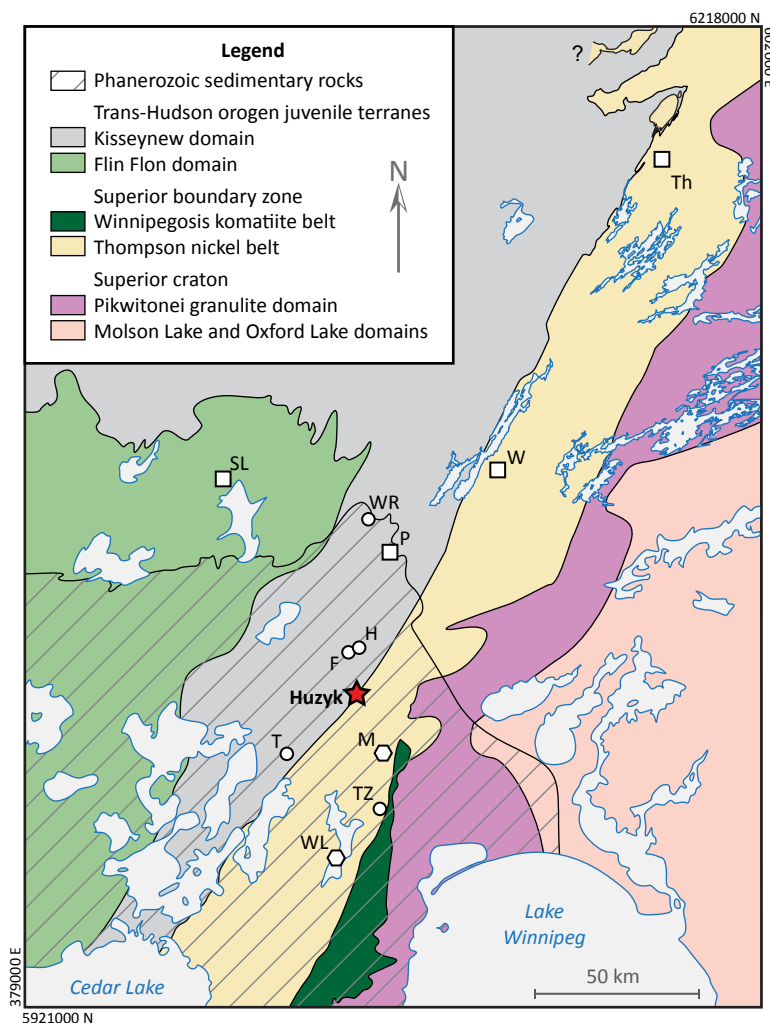


**Figure GS2019-6-1:** Geological domains along the Superior boundary zone, central Manitoba (modified from Couëslan, 2018). Symbols: circles, Cu-Zn deposits in the sub-Phanerozoic Kiseynew domain and Superior boundary zone; hexagons, Ni-Cu deposits/occurrences in the sub-Phanerozoic Thompson nickel belt; squares, town/cities; star, location of the 2019 diamond-drilling campaign at the Huzyk Creek property. Abbreviations: F, Fenton deposit; H, Harmin deposit; M, Minago deposit; SL, Snow Lake; T, Talbot deposit; Th, Thompson; TZ, Tower zone deposit; W, Wabowden; WL, William Lake occurrence; WR, Watts River deposit. Co-ordinates are in UTM Zone 14, NAD83.

trated in shear zones in the Kiseynew domain and TNB (e.g., Mumin and Trott, 2003; Zwanzig and Bailes, 2010), so the potential could exist for the vanadium-bearing graphitic rocks to be shear hosted and/or hydrothermal in nature. The objectives of this project are to evaluate the rocks hosting the graphite and vanadium mineralization at Vanadian’s Huzyk Creek property and determine their affinity to either the TNB or Kiseynew domain, and to derive possible petrogenetic model(s) for the mineralization.

## Regional setting

### Kiseynew domain

The Huzyk Creek property lies along the sub-Phanerozoic boundary between the Kiseynew domain and

the TNB. The Kiseynew domain is situated in the core of the juvenile Reindeer zone of the Paleoproterozoic Trans-Hudson orogen (THO; Figure GS2019-6-2). It is underlain by dominantly Burntwood group rocks, with subordinate calcalkaline plutons and sheets of anatectic granitoids. The Burntwood group forms a monotonous succession of graphite-bearing metagreywacke-mudstone, which was metamorphosed to garnet-biotite gneiss and migmatite throughout much of the Kiseynew domain during the terminal collision of the THO. The metagreywacke-mudstone is interpreted as turbidite deposits shed from the surrounding juvenile accretionary-arc complexes of the Flin Flon and Lynn Lake domains (Ansdell et al., 1995; Zwanzig and Bailes, 2010). Coeval fluvial-alluvial deposits on the margins of these volcano-plutonic domains consist of the Missi and Sickie groups, respectively (Stauffer, 1990;

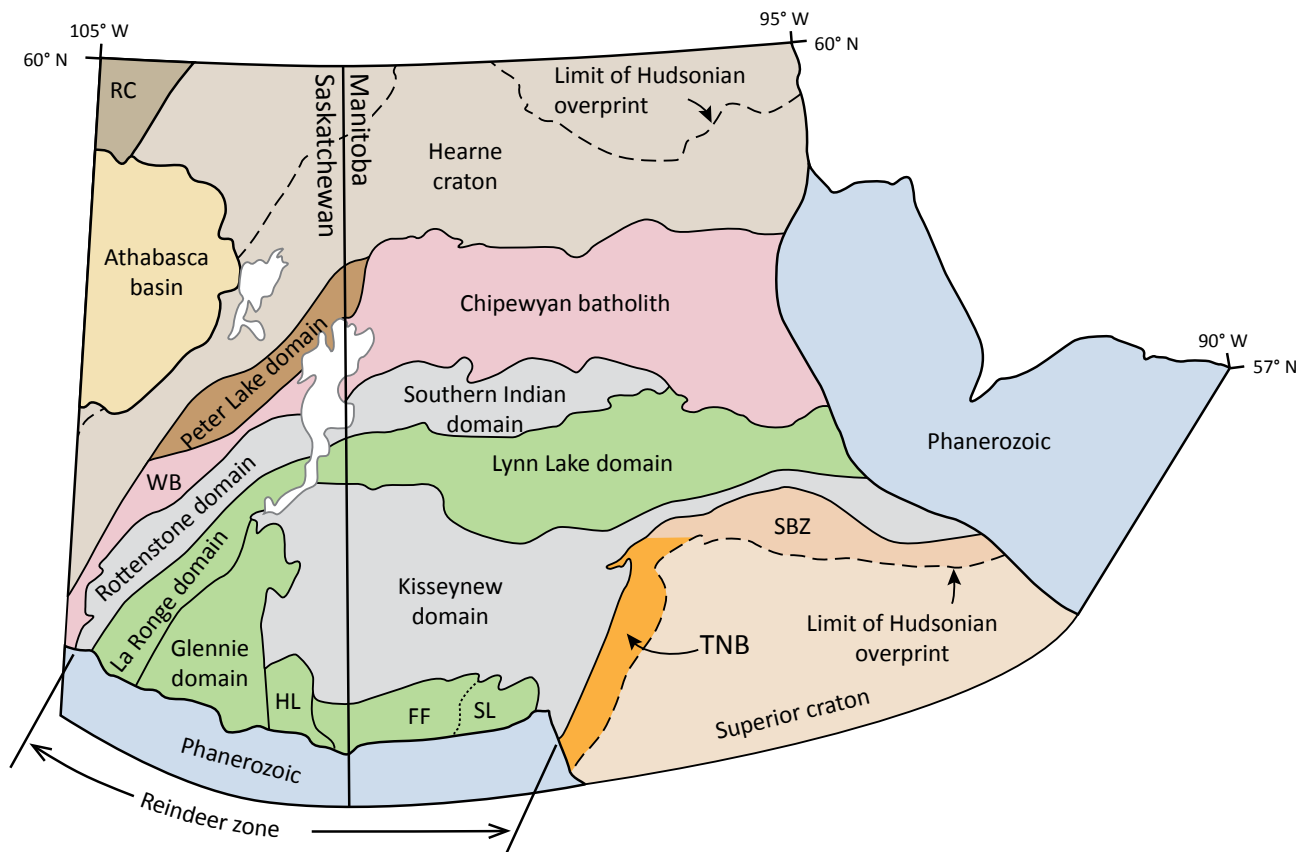


**Figure GS2019-6-2:** Tectonic-elements map of the Manitoba–Saskatchewan segment of the Trans-Hudson orogen (modified from Lewry et al., 1990). Abbreviations: FF, Flin Flon domain; HL, Hanson Lake block; RC, Rae craton; SBZ, Superior boundary zone; SL, Snow Lake subdomain; TNB, Thompson nickel belt; WB, Wathaman batholith.

Zwanzig and Bailes, 2010). The Kisseynew paleobasin is generally interpreted as a back-arc basin; however, an inter-arc or fore-arc basin environment could also be possible (Ansdell et al., 1995; Zwanzig, 1997; Corrigan et al., 2009; Zwanzig and Bailes, 2010).

### Burntwood group

The Burntwood group consists of a succession of turbidite-derived greywacke-mudstone deposits. Over most of the Kisseynew domain these rocks occur as migmatitic garnet-biotite gneiss commonly with sillimanite and cordierite, and minor graphite. Locally preserved rhythmic layering alternates between more quartzofeldspathic gneiss and more biotite- and garnet-rich gneiss, and is interpreted as graded greywacke-mudstone beds. Local pods of calc-silicate are probably derived from calcareous concretions (Corrigan and Rayner, 2002; Zwanzig et al., 2007). The Burntwood group grades laterally and vertically into the fluvial-alluvial successions of the Missi, Sickie, and Grass River groups. Narrow packages containing sporadic hornblende, magnetite, or pyrrhotite are interpreted as part of the Burntwood group–Missi group transition (Zwanzig et

al., 2007). Similar transitional deposits exist with the Sickie group.

Deposition of the Burntwood group likely began around ca. 1855 Ma as distal turbidites in prograding submarine fans along the margin of the Flin Flon domain (Ansdell et al., 1995; Machado et al., 1999; Zwanzig and Bailes, 2010). These deposits may have preceded that of the Missi group until ca. 1848 Ma, when deposition became synchronous. The youngest detrital zircons analyzed from the Burntwood group yielded ages of ca. 1845–1841 Ma (Machado et al., 1999), and a minimum age for deposition is provided by the ca. 1830–1820 Ma Touchbourne suite, which intrudes the Burntwood group rocks (Gordon et al., 1990; Machado et al., 1999; Zwanzig and Bailes, 2010).

### Structure and metamorphism

The rocks of the Kisseynew domain were subject to multiple phases of deformation beginning with a ca. 1845–1825 Ma fold-and-thrust system ( $D_1/F_1$ ), which likely resulted from the Sask craton under-riding the Flin Flon and Kisseynew domains (Zwanzig, 1999). Thrusting was likely coeval with deposition of the Missi and upper Burntwood

groups and directed toward the Kiseynew basin, which would be consistent with the direction of sedimentary transport and the inferred direction of subduction polarity (Machado et al., 1999; Zwanzig, 1999; Zwanzig and Bailes, 2010). However, vergence has also been interpreted as toward the Flin Flon domain, based on the present-day orientation of these structures (Ansdell et al., 1995).  $D_1$  was followed by two generations ( $F_2$  and  $F_3$ ) of recumbent folding accompanied by prograde metamorphism and the development of a penetrative  $S_2$ – $S_3$  foliation (Ansdell et al., 1995; Zwanzig, 1999). Westward overturning of  $D_1$  structures during  $F_2$  was a product of east-west compression during collision between the Superior craton and the Flin Flon and Kiseynew domains beginning ca. 1.83–1.82 Ga (Ansdell et al., 1995; Machado et al., 1999; Zwanzig, 1999; Zwanzig and Bailes, 2010). South- and southwest-verging  $F_3$  folding amplified and overturned  $F_1$ – $F_2$  folds. Much of  $D_3$  is interpreted to coincide with peak metamorphic conditions from ca. 1810 to 1800 Ma (Zwanzig, 1999). Late  $F_3$  folding likely continued until ca. 1789 Ma, and likely resulted from rocks of the Lynn Lake belt attempting to over-ride the Kiseynew domain, as the Hearne craton attempted to over-ride the Reindeer zone (Zwanzig, 1999). A continuous progression may have occurred between the  $D_2$  and  $D_3$  phases of deformation. In the main portion of the Kiseynew domain,  $F_4$  folds are generally upright and open, with north or east-northeast trends (Zwanzig, 1999). Folding may be accompanied by a retrograde  $S_4$  foliation in hinge zones and lower amphibolite- to greenschist-facies assemblages. Adjacent to the TNB,  $F_4$  folds become tighter, with northeast-trending fold axes, consistent with sinistral transpression along the north-northeast-trending Superior boundary zone (Zwanzig, 1998; Zwanzig, 1999).

The metamorphic grade increases from the margins of the Kiseynew domain toward the core (Bailes and McRitchie, 1978; Gordon, 1989; Couëslan and Pattison, 2012). Schists with mineral assemblages of greenschist to lower-amphibolite facies (chlorite-muscovite-garnet) along the north and south flanks of the domain, grade into granulite-facies migmatites (cordierite-garnet-melt/K-feldspar) in the core (Bailes and McRitchie, 1978). Peak metamorphic conditions in the high-grade core are believed to be relatively uniform and estimated at  $750 \pm 50^\circ\text{C}$  and  $5.5 \pm 1$  kbar (Gordon, 1989); however, Growdon (2010) suggested grades as high as  $900^\circ\text{C}$  and 12 kbar in the central Kiseynew domain. Prograde to peak metamorphism was likely ongoing during  $D_2$ – $D_3$  from ca. 1820 to 1800 Ma, with peak conditions likely attained at ca. 1810–1800 Ma (Ansdell et al., 1995; Machado et al., 1999; Zwanzig, 1999; Growdon, 2010).

### Sub-Phanerozoic Kiseynew domain

The sub-Phanerozoic Kiseynew domain is the southern extension of the Kiseynew domain below the Phanerozoic cover (Figure GS2019-6-1). Situated between the Superior craton margin and the Flin Flon domain, it was interpreted to consist of migmatitic metasedimentary rocks of the Burntwood group interlayered with felsic metaplutonic veins and sheets (Leclair et al., 1997). However, the discovery of several volcanogenic massive sulphide (VMS) deposits (Watts River, Harmin, Fenton, and Talbot) in the domain has brought this interpretation into question (Simard et al., 2010). Recent studies (Simard et al., 2010; Bailes, 2015; Reid, 2018) suggest complex structural interleaving of Flin Flon domain arc rocks, Kiseynew domain Burntwood group rocks, and possibly TNB rocks within the sub-Phanerozoic Kiseynew domain. A similar situation occurs along the north, south, and east flanks of the exposed Kiseynew domain, where thrusts and recumbent folding have structurally interleaved rocks of the Kiseynew basin with rocks of adjacent juvenile volcano-plutonic terranes and evolved Archean crust (Zwanzig, 1999; Rayner and Percival, 2007; Zwanzig and Bailes, 2010).

### Thompson nickel belt

The TNB forms a segment of the Superior boundary zone, flanked to the northwest by the Kiseynew domain of the Trans-Hudson orogen and to the southeast by the Pikwitonei granulite domain of the Superior craton (Figure GS2019-6-1). The TNB is underlain largely by reworked Archean gneiss of the Pikwitonei domain (Hubbert, 1980; Mezger et al., 1990; Heaman et al., 2011), which was exhumed and unconformably overlain by the Paleoproterozoic supracrustal rocks of the Ospwagan group (Bleeker, 1990; Zwanzig et al., 2007). The Archean basement gneiss and Ospwagan group were subjected to multiple generations of deformation and metamorphic conditions, ranging from middle-amphibolite facies to lower-granulite facies, during the Trans-Hudson orogeny (Bleeker, 1990; Burnham et al., 2009; Couëslan and Pattison, 2012).

The dominant phase of penetrative deformation is  $D_2$ , which affected the Ospwagan group and Archean gneiss. This deformation phase resulted in the formation of  $F_2$  nappe structures, which are interpreted as either east verging (Bleeker, 1990; White et al., 2002) or southwest verging (Zwanzig et al., 2007; Burnham et al., 2009). The recumbent folds are associated with regionally penetrative  $S_2$  fabrics. The  $D_2$  phase of deformation is interpreted to be the result of convergence between the Superior craton margin and the Reindeer zone of the Trans-Hudson orogen ca. 1830 to 1800 Ma. The  $D_3$  phase of deformation



resulted in isoclinal folds with vertical to steeply south-east-dipping axial planes (Bleeker, 1990; Burnham et al., 2009). Mylonite zones with subvertical stretching lineations parallel many of the regional  $F_3$  folds. Tightening of  $D_3$  structures continued during  $D_4$ , marked by localized retrograde greenschist metamorphism along northeast-striking, mylonitic and cataclastic shear zones that commonly record southeast-side-up sinistral movement (Bleeker, 1990; Burnham et al., 2009).

### **Ospwagan group**

The following summary of the Ospwagan group is sourced largely from Bleeker (1990) and Zwanzig et al. (2007). The Paleoproterozoic Ospwagan group unconformably overlies Archean basement gneiss in the TNB. The lowermost unit of the Ospwagan group is the Manas formation, a fining-upward transgressive sequence of sandstones and semipelitic rocks. This grades into the overlying Thompson formation, a sequence of calcsilicates and impure marbles that reflects a transition to a carbonate-dominated system. The Thompson formation is overlain by the Pipe formation, a succession of deep-water deposits including silicate- and sulphide-facies iron formations, cherts, mudstones, calcsilicates, and marble. Overlying this is the Setting formation, a coarsening-upward sequence of interbedded sandstones and mudstones that were likely deposited as turbidites. The Ospwagan group is capped by the Bah Lake assemblage, which consists of mafic to ultramafic volcanic rocks dominated by massive to pillowed basalt flows with local picrite and minor syn-volcanic intrusions.

## **Geology of the Huzyk Creek area**

Core from drillholes HZ-19-1 and HZ-19-2 were logged in August of 2019. The order of the rock units are described from the structural hangingwall of the graphite- and vanadium-enriched zone into the footwall (Figure GS2019-6-3). All the rocks described attained relatively high metamorphic grade during the Trans-Hudson orogeny. Protolith interpretation was used for naming rocks where a fair amount of certainty exists; however, where ambiguity remains metamorphic nomenclature was retained. The 'meta-' prefix has been omitted from rock names for brevity. All rocks have a well-developed penetrative foliation with the exception of some granite intrusions that are weakly foliated. Reported thicknesses are intersection lengths, not true thicknesses.

### **Hornblende gneiss and calcsilicate**

Intervals of interlayered hornblende gneiss and calcsilicate occur at the top of the Precambrian in both drill-

holes. The hornblende gneiss is medium grained and quartzofeldspathic, with 30–40% hornblende. It commonly grades into amphibolite, which contains 60–70% hornblende. The gneiss and amphibolite locally contain garnet porphyroblasts <7 mm across that are characterized by plagioclase corona. More common are rounded aggregates of plagioclase <8 mm across that are likely pseudomorphous after garnet (Figure GS2019-6-4a). The calcsilicate is compositionally and texturally diverse. It can be texturally similar to the hornblende gneiss, with the hornblende replaced by pale green amphibole (and/or diopside) and the addition of sparse titanite; however, it can also appear as a coarse-grained rock (Figure GS2019-6-4b) with variable enrichment in diopside, sulphide, titanite and epidote. The calcsilicate and hornblende gneiss can be interlayered on scales ranging from <1 cm to 2.5 m, with diffuse contacts. In drillhole HZ-19-1 the hornblende gneiss and calcsilicate are interleaved with the underlying wacke at a scale of <35 m. This is assumed to be tectonic repetition; however, stratigraphic interlayering can not be ruled out.

### **Wacke-mudstone**

The graphite- and vanadium-enriched horizon is hosted by a thick package of interbedded wackes and mudstones. The various wackes and mudstones are named for the dominant mafic mineral, exclusive of biotite, that is present in the rock. The wackes appear as medium- to coarse-grained quartzofeldspathic gneisses, typically with 10–20% biotite. The compositionally similar mudstones are medium to coarse grained, schistose, and arbitrarily defined as having >20% biotite (typically 20–30%). The wacke-mudstone units are described in order of decreasing abundance.

### **Orthopyroxene wacke-mudstone**

Orthopyroxene wacke is the most abundant lithology in this package. It typically contains 10–20% orthopyroxene, which locally forms coarse-grained poikiloblasts <1 cm across (Figure GS2019-6-4c). Local horizons contain trace amounts of graphite and <3% pyrrhotite. The wacke is locally interbedded with orthopyroxene mudstone layers <2 m thick (Figure GS2019-6-4d). Local layers in the mudstone can contain trace amounts of graphite, and sparse garnet and pyrrhotite.

### **Garnet wacke-mudstone**

The orthopyroxene wacke-mudstone hosts local layers of garnet wacke-mudstone <6 m thick (Figure GS2019-6-4e). In addition to biotite, the garnet wacke contains 3–5% orthopyroxene and 5–7% garnet. The garnet and orthopyroxene typically occur along diffuse, alternating

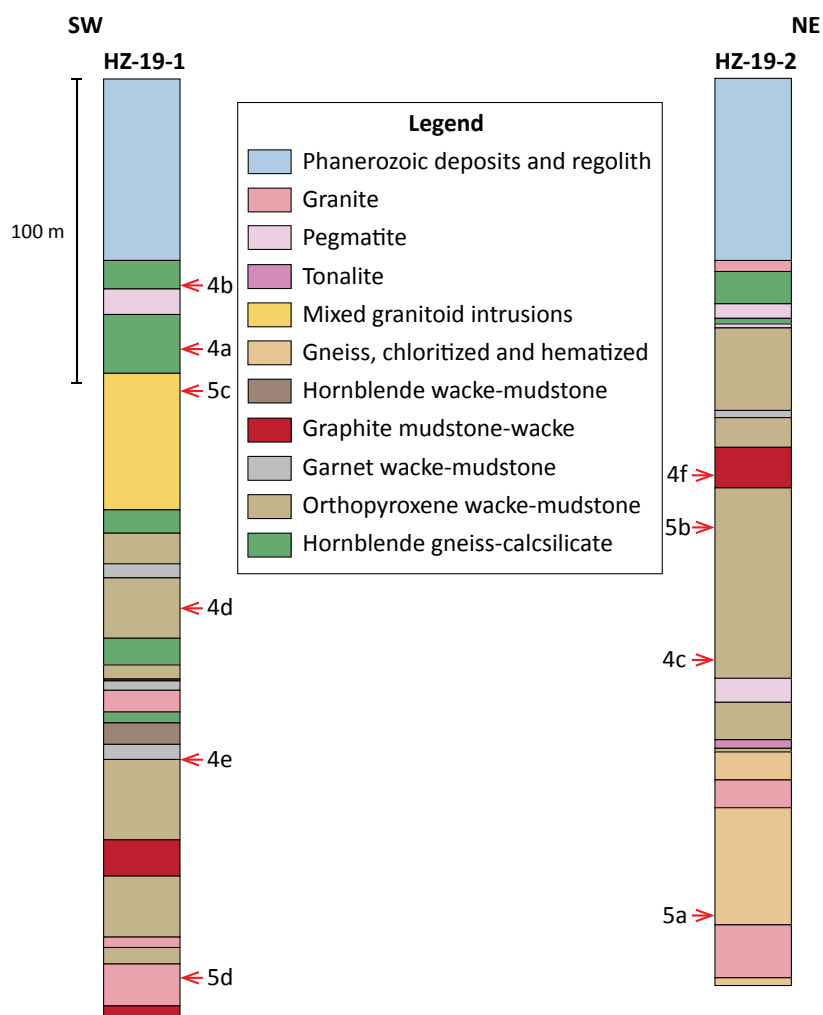


**Figure GS2019-6-3:** Schematic logs of drillcores HZ-19-1 and HZ-19-2 from the Huzyk Creek property; see Figure GS2019-6-1 for the approximate location. The vertical and horizontal scale are equivalent. The locations of images in Figure GS2019-6-4 and Figure GS2019-6-5 are indicated along the inside edge of each column.

layers, likely controlled by primary compositional bedding of the sedimentary rock. Trace amounts of graphite and pyrrhotite are typically present, but up to 3% graphite and pyrrhotite can occur. The garnet wacke is locally interlayered with garnet mudstone beds <30 cm thick; in addition, the garnet mudstone can occur as layers <3 m thick within the orthopyroxene wacke-mudstone unit. The garnet mudstone typically contains trace to 2% graphite and 5–20% garnet. Orthopyroxene typically forms <5% of the rock, although the garnet mudstone and orthopyroxene mudstone can be interlayered on a scale of <1 cm.

#### Graphite mudstone-wacke

Graphite mudstone occurs as a discrete horizon, 14.3–16.7 m wide, within the overall wacke-mudstone sedimentary rock package. The graphite mudstone contains 7–10% pyrrhotite, 10–30% biotite, and 20–30% graphite. Trace amounts of chalcopyrite, molybdenite and sphalerite are

typically present. The mudstone contains local beds of graphite-pyrrhotite wacke (Figure GS2019-6-4f) <1.8 m thick. The graphite-pyrrhotite wacke is typically fine to medium grained and contains 1–3% graphite, 2–5% pyrrhotite, 5–7% biotite, and sparse orthopyroxene. A second discrete horizon of graphitic wacke, at least 5.2 m thick, occurs at the bottom of drillhole HZ-19-1. This wacke is distinct from the one interbedded with the graphite mudstone in that it appears as graphite-bearing orthopyroxene wacke and garnet wacke interbedded on a scale <1.4 m. The graphite content in these interbedded wackes is typically 2–3% but is locally as high as 5%. Local sillimanite-rich beds <5 cm thick are also present.

#### Hornblende wacke-mudstone

A single hornblende wacke-mudstone layer (8.45 m thick) occurs within the core of drillhole HZ-19-1. The hornblende wacke contains 3–5% hornblende, whereas the



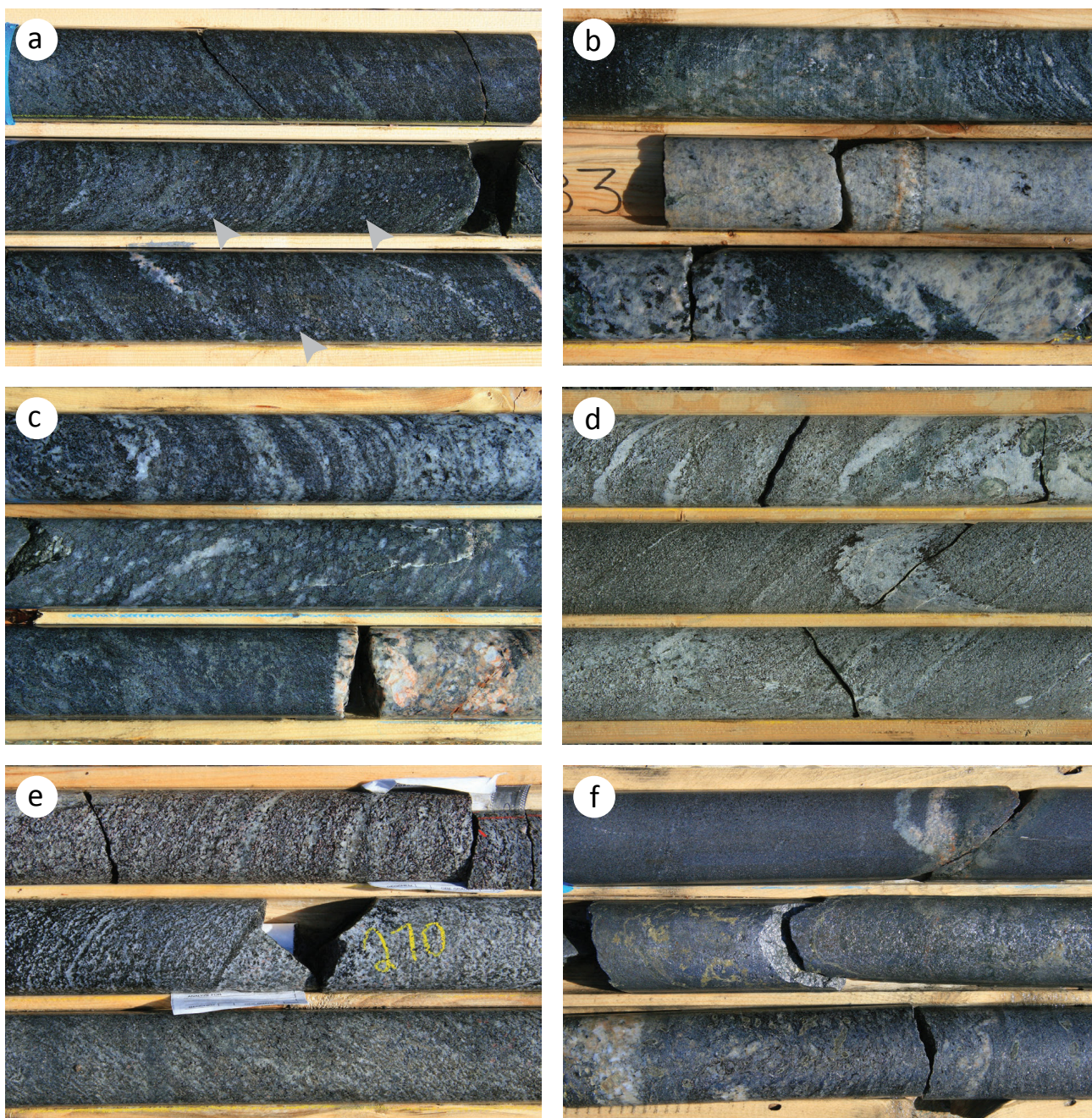


**Figure GS2019-6-4:** Drillcore images from HZ-19-1 and HZ-19-2: **a)** hornblende gneiss with diffuse intercalations of calcsilicate, arrows indicate plagioclase pseudomorphs after garnet (HZ-19-1, 106.8 m); **b)** hornblende gneiss and coarse-grained calcsilicate (top row) intruded by pegmatitic granite (bottom two rows; HZ-19-1, 81.55 m); **c)** orthopyroxene wacke with coarse-grained orthopyroxene poikiloblasts (middle row; HZ-19-2, 239.7 m); **d)** orthopyroxene wacke (top and bottom rows) interbedded with orthopyroxene mudstone (middle row; HZ-19-1, 208.6 m); **e)** garnet wacke (top row) interbedded with orthopyroxene wacke (bottom row; HZ-19-1, 268.5 m); **f)** graphite-pyrrhotite wacke bed (top row) hosted in graphite mudstone (bottom two rows; HZ-19-2, 163.65 m). Drillcore is NQ with a diameter of 47.5 mm.

mudstone contains 5–7% hornblende. The mudstone occurs as beds <30 cm thick within the wacke. The sequence is in direct contact with an interval of calcsilicate and hornblende gneiss. The hornblende wacke-mudstone could represent a more calcareous section, or an influx of volcanoclastic detritus. Alternatively, it could represent an interval of sheared and altered hornblende gneiss.

### **Chloritized and hematized gneiss**

A 96 m interval of intensely chloritized and hematized gneiss occurs at the bottom of drillhole HZ-19-2. The gneiss is medium to coarse grained and is K-feldspar rich, with 7–10% hematite and 10–30% chlorite. Both specular and earthy hematite are present. Local zones within the gneiss have a mottled texture (Figure GS2019-6-5a). Sparse zones



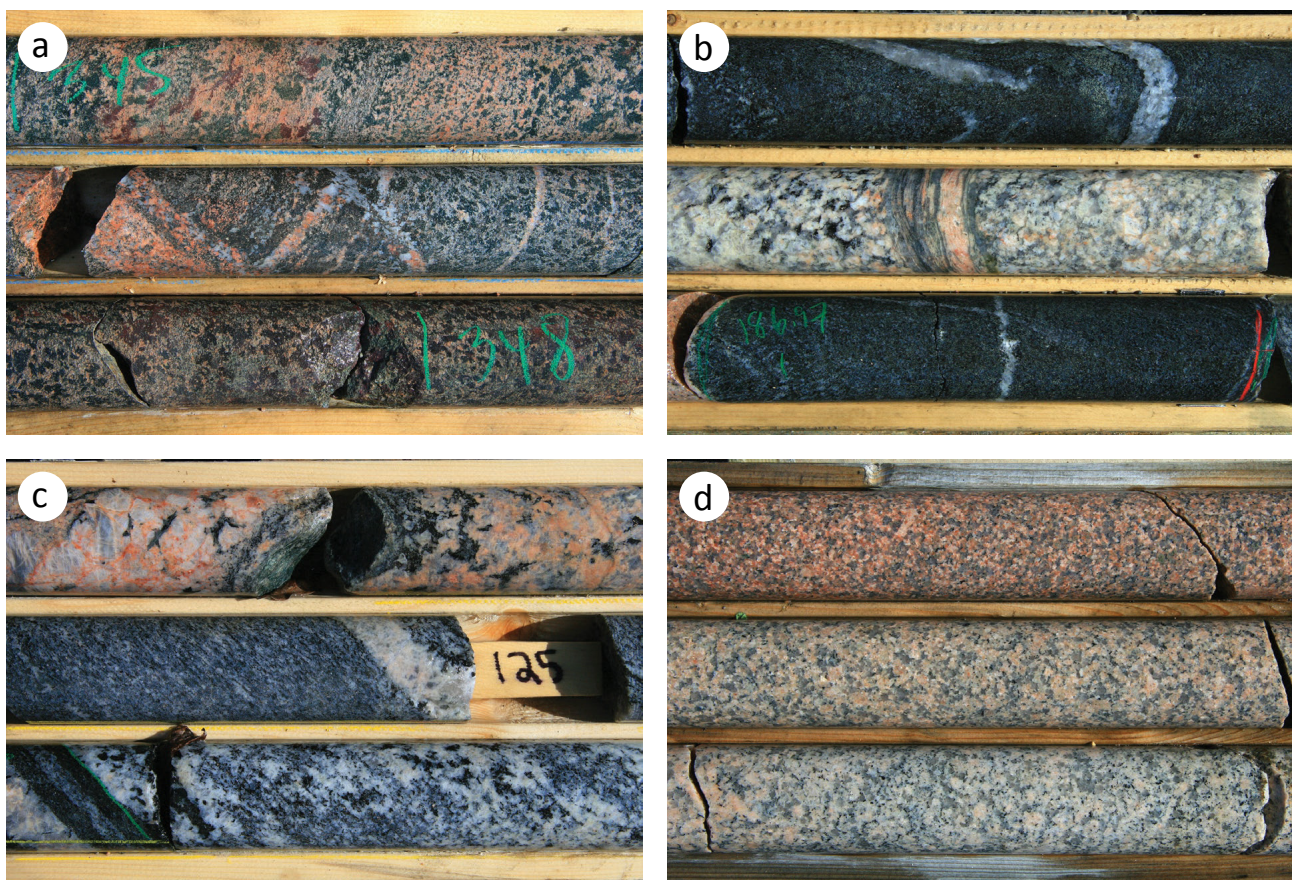


**Figure GS2019-6-5:** Drillcore images from HZ-19-1 and HZ-19-2: **a)** chloritized and hematized gneiss with mottled texture (HZ-19-2, 345.0 m); **b)** pegmatitic granite with mylonitic band (middle row) intruded into orthopyroxene wacke (top and bottom rows; HZ-19-2, 184.25 m); **c)** granodiorite (middle row) intruded by pegmatitic granite (top row) and tonalite (bottom row; HZ-19-1, 123.3 m); **d)** weakly foliated biotite granite (HZ-19-1, 354.2 m). Drillcore is NQ with a diameter of 47.5 mm.

of quartz-vein breccia <2 m wide can contain void-filling specular hematite. Intrusions of pegmatite and medium-grained granite within this interval are overprinted by the chlorite and hematite alteration. The protolith of the chloritized and hematized gneiss is uncertain; however, the mafic content is comparable to the wacke-mudstone rocks, and the local mottling could represent the pseudomorphous replacement of poikiloblastic orthopyroxene. A sample was collected for lithogeochemical analysis and comparison with other units in the sequence.

### Intrusions

Several varieties of intrusive granitoid rocks are present in the drillcore. The intrusions appear to intersect all of the previously described units. Abundant pegmatitic granite occurs throughout the drill core as intersections ranging from centimetres up to 10 m in width. Several generations of pegmatite are likely present. They range from pink to light grey, and are typically biotite bearing; however, local intrusions may contain minor hornblende, pyrrhotite, titanite, and possibly orthopyroxene. Sparse bands of mylonite <5 cm wide can be present (Figure

GS2019-6-5b). Local intersections of coarse-grained tonalite <3.5 m occur in both drillholes. The tonalite is light grey and typically contains 3–7% biotite and 3–7% hornblende, along with variable but minor amounts of orthopyroxene, pyrrhotite and titanite. The tonalite is intruded by pegmatite and medium-grained granite. Sparse intervals of granodiorite <6 m wide are present in drillhole HZ-19-1. It is pinkish grey and biotite bearing, with minor amounts of amphibole. The granodiorite is intruded by pegmatite and tonalite (Figure GS2019-6-5c). Pink, medium-grained biotite granite occurs as intrusions in both drillholes (Figure GS2019-6-5d). The granite intersections vary from centimetres up to 22 m wide. The rock is pink, weakly foliated to foliated, and relatively even textured, although local pegmatite segregations can be present.

### Discussion

The Huzyk Creek area was previously reported as being underlain by upper amphibolite-facies rocks (Beaumont-Smith, 2018); however, the prevalence of orthopyroxene is suggestive of lower granulite-facies assemblages. This is supported by microscopy, which reveals the presence



of orthopyroxene–K-feldspar assemblages in the wacke-mudstone rocks, orthopyroxene and inverted pigeonite in the hornblende gneiss and calcsilicate rocks, and widespread antiperthite.

The identification and correlation of sedimentary rocks in high-grade metamorphic terranes is challenging. The identification of Oswagan group rocks in the TNB is typically made by recognizing key stratigraphic markers: arenaceous sandstones of the Manasan and Setting formations, calcsilicates and marbles of the Thompson and Pipe formations, and iron formations of the Pipe formation (Bleeker, 1990; Zwanzig et al., 2007). These rock types generally remain recognizable even in granulite-facies successions (Zwanzig et al., 2007; Couëslan and Pattison, 2012). Although some calcsilicate is associated with the hornblende gneiss, the wacke-mudstone succession does not correlate well with any portion of the Oswagan group stratigraphy.

The hornblende gneiss and calcsilicate are petrographically similar to sequences described along the north and east flanks of the Kiseynew domain (Zwanzig, 2000, 2008; Couëslan, 2011, unpublished data, 2013). These rocks are interpreted as metabasalt with varying intensity of pre-metamorphic, epidote and carbonate alteration (Zwanzig, 2008). It is interpreted that the basalt was thrust into the Kiseynew basin along regional-scale faults.

The Burntwood group consists of a thick succession of interbedded wacke and mudstone. Upper amphibolite- to granulite-facies Burntwood group wacke typically consists of garnet-biotite gneiss, with more aluminous mudstone layers containing additional biotite±sillimanite and cordierite (e.g., Martins and Couëslan, 2019). Graphite is typically present in trace to minor amounts, although significant intersections of graphite have been reported from drillcore in the Kiseynew basin (e.g., Callinex Mines Inc., 2014; Assessment File 93001). Significant portions of the Huzyk Creek wacke-mudstone succession are devoid of garnet, which could be considered atypical for Burntwood group rocks. However, the interlayering of wacke and mudstone, and the presence of graphite, including significant accumulations, are comparable to rocks of the Burntwood group. Instances of garnet-free Burntwood group rocks are observed at Russell Lake, including rare occurrences of amphibole- or pyroxene-bearing rocks (Martins and Couëslan, 2019). Therefore, a tentative correlation is made between the Huzyk Creek wacke-mudstone rocks and the Burntwood group. Whole-rock lithogeochemical analyses are required to test this interpretation, as well as the possible correlation of the hornblende gneiss and calcsilicate with mafic volcanic rocks.

Semi-solid graphite occurs across relatively wide intersections (graphite mudstone, 14.3–16.7 m), and is dissemi-

nated throughout the wacke-mudstone sequence. This is more suggestive of a sedimentary-metamorphic origin (i.e., metamorphosed black shale), rather than a discrete, shear- or vein-hosted (hydrothermal) origin for the graphite (i.e., ‘lump’ graphite). If the wacke-mudstone sequence is correlative with the Burntwood group, this interpretation is further strengthened by the basin-wide presence of graphite in the Kiseynew domain.

The drilling results by Vanadian (2019) suggest a close correlation between graphite mineralization and vanadium enrichment. The basin-wide presence of graphite ±pyrrhotite in the Burntwood group suggests that the rocks were deposited in an anoxic environment, and remained so during diagenesis. Vanadium is considered relatively immobile in the reduced state ( $V^{3+}$ ), so it is unlikely that the vanadium was mobilized during diagenesis (Breit and Wanty, 1991). Mobilization of soluble vanadium ( $V^{4+}$ ,  $V^{5+}$ ), and re-precipitation under reducing conditions as insoluble vanadium ( $V^{3+}$ ), is generally considered a requirement to form sandstone-hosted vanadium deposits (Wanty et al., 1990; Shawe, 2011). It is more likely that the vanadium was deposited alongside carbonaceous material at the time of sedimentation and remained immobile. A general model proposed by Breit and Wanty (1991) involves dissolved  $V^{5+}$  in oxidized surface waters becoming adsorbed to organic particles in seawater. If the organic particles settle into anoxic conditions at depth, the adsorbed vanadium can be reduced to  $V^{4+}$  by dissolved organic compounds or hydrogen sulphide. Upon burial and diagenesis it can be further reduced to  $V^{3+}$  and partitioned into clay minerals. Assuming the graphite is largely derived from organic carbon, this model also provides a direct causal relationship between the graphite and vanadium enrichment in the Huzyk Creek rocks.

## Economic considerations

Both graphite and vanadium are considered critical minerals/elements by the U.S. Department of the Interior (Schulz et al., 2017). Some of the many uses of graphite include refractory applications, brake linings, motor brushes, and steel making; however, higher valued coarse-grained graphite is used in high-temperature lubricants, and lithium battery and fuel cell applications (Robinson et al., 2017). Vanadium is used primarily in the production of high-strength steels, and specialty aluminum and titanium alloys. In the field of green technology there is growing interest around the use of vanadium redox-flow batteries for large-scale energy storage (Kelley et al., 2017). These batteries boast the potential for nearly unlimited storage capacity and unlimited lifespan.

There appears to be a direct relationship between graphite mineralization and vanadium enrichment in the Huzyk Creek sedimentary rocks, which are tentatively correlated with the Burntwood group of the Kiseynew domain. Thick accumulations of graphite are widespread in the Kiseynew domain (Callinex Mines Incorporated, 2014; Assessment File 93001). A proposed model calls for dissolved vanadium in the water column to be removed by settling organic material that accumulated on the basin floor. Burial, diagenesis, and metamorphism of these deposits produced the vanadium-enriched graphite mineralization present at Huzyk Creek. Assuming water circulation in the basin was unrestricted, it stands to reason that other graphite deposits in the Kiseynew domain should also be prospective for vanadium.

Black shales can be enriched in vanadium as well as a suite of other metals (molybdenum, copper, nickel, zinc, PGEs). Although these shales tend to be uneconomic, development is continuing at the Gibellini vanadium project in Nevada, where the black shale underwent secondary modification and enrichment by oxidizing fluids (Orbock, 2017). Metamorphosed examples of vanadium-enriched black shales include the Green Giant and Balama projects in Madagascar and Mozambique, respectively (AGP Mining Consultants Inc., 2011; Syrah Resources Ltd., 2014; Di Cecco et al., 2018). The Green Giant project hosts a NI 43-101-compliant resource estimated at 60 million tonnes grading 0.69%  $V_2O_5$ , while the Balama project has an inferred resource of 1.15 billion tonnes grading 0.23%  $V_2O_5$ .

## Acknowledgments

The author thanks K. George and I. Robinson for their assistance in the field, as well as E. Anderson and M. Schreckenbach for logistical support. T. Martins provided assistance as well as discussions in the field regarding the core and units of the central Kiseynew domain. Thanks to Gogal Air Services for providing space at their helicopter base in Snow Lake to lay out the drillcore, and Kinross Gold Corp. for allowing access to the core splitting facility. Thanks to M. Simpson of Vanadian Energy Corp. and T. Tuba for providing access to the drillcore and core logs, and allowing for sampling and an early viewing of the core during drilling in April of 2019. E. Yang and C. Böhm reviewed previous versions of this report.

## References

- AGP Mining Consultants Inc. 2011: Green Giant project, Fotadrevo, Province of Toliara, Madagascar; NI 43-101 report prepared for Energizer Resources by AGP Mining Consultants Inc., 175 p., URL <[http://www.nextsourcematerials.com/static/media/uploads/green\\_giant\\_vanadium\\_ni\\_43-101\\_report\\_2011-01-14.pdf](http://www.nextsourcematerials.com/static/media/uploads/green_giant_vanadium_ni_43-101_report_2011-01-14.pdf)> [June 2019].
- Ansdell, K.M., Luca, S.B., Connors, K. and Stern, R.A. 1995: Kiseynew metasedimentary gneiss belt, Trans-Hudson orogen (Canada): Back-arc origin and collisional inversion; *Geology*, v. 23, p. 1039–1043.
- Bailes, A.H. 2015: Geological setting of the Watts River base metal massive sulphide deposit; HudBay Minerals Inc., unpublished internal geological report, 70 p.
- Bailes, A.H. and McRitchie, W.D. 1978: The transition from low to high grade metamorphism in the Kiseynew sedimentary gneiss belt, Manitoba; *in* Metamorphism in the Canadian Shield, Geological Survey of Canada, Paper 78-10, p. 155–178.
- Beaumont-Smith, C. 2018: Geology report on the Huzyk Creek property, Ponton Manitoba region; NI 43-101 report prepared for Vanadian Energy Corp., 51 p., URL <[https://www.sedar.com/search/search\\_form\\_pc\\_en.htm](https://www.sedar.com/search/search_form_pc_en.htm)> [June 2019].
- Bleeker, W. 1990: Evolution of the Thompson Nickel Belt and its nickel deposits, Manitoba, Canada; Ph.D. thesis, University of New Brunswick, Fredericton, New Brunswick, 400 p.
- Breit, G.N. and Wanty, R.B. 1991: Vanadium accumulation in carbonaceous rocks: A review of geochemical controls during deposition and diagenesis; *Chemical Geology*, v. 91, p. 83–97.
- Burnham, O.M., Halden, N., Layton-Matthews, D., Leshner, C.M., Liwanag, J., Heaman, L., Hulbert, L., Machado, N., Michalak, D., Pacey, M., Peck, D.C., Potrel, A., Theyer, P., Toope, K. and Zwanzig, H. 2009: CAMIRO project 97E-02, Thompson Nickel Belt: final report, March 2002, revised and updated 2003; Manitoba Science, Technology, Energy and Mines, Manitoba Geological Survey, Open File OF2008-11, 434 p. plus appendices and GIS shape files for use with ArcInfo®.
- Callinex Mines Incorporated 2014: Grades of up to 60.38% carbon graphite confirmed at Callinex' Neuron property; Callinex Mines Incorporated, press release, April 25, 2014, URL <<https://callinex.ca/grades-of-up-to-60-38-carbon-graphite-confirmed-at-callinex-neuron-property/>> [September 2019].
- Corrigan, D. and Rayner, N. 2002: Churchill River–Southern Indian Lake targeted geoscience initiative (NTS 64B, 64C, 64G, 64H), Manitoba: update and new findings; *in* Report of Activities 2002, Manitoba Industry, Trade and Mines, Manitoba Geological Survey, p. 144–158.
- Corrigan, D., Pehrsson, S., Wodicka, N. and De Kemp, E. 2009: The Paleoproterozoic Trans-Hudson Orogen: a prototype of modern accretionary processes; *in* Ancient Orogens and Modern Analogues, J.B. Murphy, J.D. Keppie and A.J. Hynes (ed.), Geological Society of London, Special Publication 327, p. 457–479.
- Couëslan, C.G. 2011: Geological investigations in the Manasan Falls area, Thompson Nickel Belt, Manitoba (part of NTS 63P12); *in* Report of Activities 2011, Manitoba Innovation, Energy and Mines, Manitoba Geological Survey, p. 86–93.
- Couëslan, C.G. 2018: Geology of the Tower Cu-Zn-Ag-Au deposit, sub-Phanerozoic Superior boundary zone, central Manitoba (part of NTS 63G14); Manitoba Growth, Enterprise and Trade, Manitoba Geological Survey, Open File OF2018-4, 38 p.
- Couëslan, C.G. and Pattison, D.R.M. 2012: Low-pressure regional amphibolite-facies to granulite-facies metamorphism of the Paleoproterozoic Thompson Nickel Belt, Manitoba; *Canadian Journal of Earth Sciences*, v. 49, p. 1117–1153.

- Di Cecco, V.E., Tait, K.T., Spooner, E.T.C. and Scherba, C. 2018: The vanadium-bearing oxide minerals of the Green Giant vanadium–graphite deposit, southwest Madagascar; *The Canadian Mineralogist*, v. 56, p. 247–257.
- Gordon, T.M. 1989: Thermal evolution of the Kiseeynew sedimentary gneiss belt, Manitoba: metamorphism at an early Proterozoic accretionary margin; *in* *Evolution of Metamorphic Belts*, J.S. Daly, R.A. Cliff and B.W.D. Yardley (ed.), Geological Society, Special Publication 43, p. 233–243.
- Gordon, T.M., Hunt, P.A., Bailes, A.H. and Syme, E.C. 1990: U-Pb ages from the Flin Flon and Kiseeynew belts, Manitoba: chronology of crust formation at an Early Proterozoic accretionary margin; *in* *The Early Proterozoic Trans-Hudson Orogen of North America*, J.F. Lewry and M.R. Stauffer (ed.), Geological Association of Canada, Special Paper 37, p. 177–199.
- Growdon, M.L. 2010: Crustal development and deformation of Laurentia during the Trans-Hudson and Alleghenian orogenies; Ph.D. thesis, Indiana University, Bloomington, Indiana, 237 p.
- Heaman, L.M., Böhm, C.O., Machado, N., Krogh, T.E., Weber, W. and Corkery, M.T. 2011: The Pikwitonei Granulite Domain, Manitoba: a giant Neoproterozoic high-grade terrane in the northwest Superior Province; *Canadian Journal of Earth Sciences*, v. 48, p. 205–245.
- Hubregtse, J.J.M.W. 1980: The Archean Pikwitonei granulite domain and its position at the margin of the northwestern Superior Province (central Manitoba); Manitoba Department of Energy and Mines, Manitoba Geological Survey, Geological Paper GP80-3, 16 p.
- Kelley, K.D., Scott, C.T., Polyak, D.E. and Kimball, B.E. 2017: Vanadium; *in* *Critical Mineral Resources of the United States—Economic and Environmental Geology and Prospects for Future Supply*, K.J. Schulz, J.H. DeYoung, Jr., R.R. Seal, II and D.C. Bradley (ed.), U.S. Geological Survey, Professional Paper 1802, p. U1–U36.
- Leclair, A.D., Lucas, S.B., Broome, H.J., Viljoen, D.W. and Weber, W. 1997: Regional mapping of Precambrian basement beneath Phanerozoic cover in southeastern Trans-Hudson Orogen, Manitoba and Saskatchewan; *Canadian Journal of Earth Sciences*, v. 34, p. 618–634.
- Lewry, J.F., Thomas, D.J., Macdonald, R. and Chiarenzelli, J. 1990: Structural relations in accreted terranes of the Trans-Hudson Orogen, Saskatchewan: telescoping in a collisional regime?; *in* *The Early Proterozoic Trans-Hudson Orogen of North America*, J.F. Lewry and M.R. Stauffer (ed.), Geological Association of Canada, Special Paper 37, p. 75–94.
- Machado, N., Zwanzig, H.V. and Parent, M. 1999: U-Pb ages of plutonism, sedimentation, and metamorphism of the Paleoproterozoic Kiseeynew metasedimentary belt, Trans-Hudson Orogen (Manitoba, Canada); *Canadian Journal of Earth Sciences*, v. 36, p. 1829–1842.
- Martins, T. and Couëslan, C.G. 2019: Geological investigations in the Russell–McCallum lakes area, northwestern Manitoba (parts of NTS 64C3–6); *in* *Report of Activities 2019*, Manitoba Agriculture and Resource Development, Manitoba Geological Survey, p. 30–41.
- Mezger, K., Bohlen, S.R. and Hanson, G.N. 1990: Metamorphic history of the Archean Pikwitonei granulite domain and the Cross Lake subprovince, Superior Province, Manitoba, Canada; *Journal of Petrology*, v. 31, p. 483–517.
- Mumin, A.H. and Trott, M. 2003: Hydrothermal iron-sulphide copper-graphite mineralization in the northern Kiseeynew Domain, Trans-Hudson Orogen, Manitoba (NTS 63O and 64B): evidence for deep-seated IOCG (Olympic Dam)-style metal deposition?; *in* *Report of Activities 2003*, Manitoba Industry, Economic Development and Mines, Manitoba Geological Survey, p. 79–85.
- Orbock, E.J.C., III 2017: Gibellini vanadium project, Nevada, USA; NI 43-101 report prepared for Prophecy Development Corporation by Amec Foster Wheeler E&C Services Inc., 141 p., URL <<https://www.prophecydev.com/projects/gibellini-vanadium/>> [June 2019].
- Rayner, N. and Percival, J.A. 2007: Uranium-lead geochronology of basement units in the Wuskwatim–Tullibee lakes area, northeastern Kiseeynew Domain, Manitoba (NTS 63O); *in* *Report of Activities 2007*, Manitoba Science, Technology, Energy and Mines, Manitoba Geological Survey, p. 82–90.
- Reid, K.D. 2018: Sub-Phanerozoic basement geology from drill-core observations in the Watts, Mitishto and Hargrave rivers area, eastern Flin Flon belt, west-central Manitoba (parts of NTS 63J5, 6, 11, 12, 13, 14); *in* *Report of Activities 2018*, Manitoba Growth, Enterprise and Trade, Manitoba Geological Survey, p. 37–47.
- Robinson, G.R., Jr., Hammarstrom, J.M. and Olson, D.W. 2017: Graphite; *in* *Critical Mineral Resources of the United States—Economic and Environmental Geology and Prospects for Future Supply*, K.J. Schulz, J.H. DeYoung, Jr., R.R. Seal, II and D.C. Bradley (ed.), U.S. Geological Survey, Professional Paper 1802, p. J1–J24.
- Schulz, K.J., DeYoung, J.H., Jr., Seal, R.R., II and Bradley, D.C. (ed.) 2017: Critical mineral resources of the United States—Economic and environmental geology and prospects for future supply; U.S. Geological Survey, Professional Paper 1802, 797 p.
- Shawe, D.R. 2011: Uranium-vanadium deposits of the Slick Rock district, Colorado; U.S. Geological Survey, Professional Paper 576-F, 80 p.
- Simard, R.-L., McGregor, C.R., Rayner, N. and Creaser, R.A. 2010: New geological mapping, geochemical, Sm-Nd isotopic and U-Pb age data for the eastern sub-Phanerozoic Flin Flon belt, west-central Manitoba (parts of NTS 63J3-6, 11, 12, 14, 63K1-2, 7–10); *in* *Report of Activities 2010*, Manitoba Innovation, Energy and Mines, Manitoba Geological Survey, p. 69–87.
- Stauffer, M.R. 1990: The Missi Formation: an Aphebian molasse deposit in the Reindeer Lake zone of the Trans-Hudson orogen, Canada; *in* *The Early Proterozoic Trans-Hudson Orogen of North America*, J.F. Lewry and M.R. Stauffer (ed.), Geological Association of Canada, Special Paper 37, p. 121–141.
- Syrah Resources Ltd. 2014: Vanadium scoping study finalised; Syrah Resources Inc., press release, July 30, 2014, URL <<http://www.syrahresources.com.au/asx-announcements/2014>> [October 2019].



- Vanadian Energy Corporation 2019: Vanadian Energy intersects 0.22%  $V_2O_5$  over 9.74 metres on the Huzyk Creek property; Vanadian Energy Corporation, press release, May 21, 2019, URL <<https://www.vanadianenergy.com/NR-2019-05-21-Drilling-results.pdf>> [June 2019].
- Wanty, R.B., Goldhaber, M.B. and Northrop, H.R. 1990: Geochemistry of vanadium in an epigenetic, sandstone-hosted vanadium-uranium deposit, Henry Basin, Utah; *Economic Geology*, v. 85, p. 270–284.
- White, D.J., Lucas, S.B., Bleeker, W., Hajnal, Z., Lewry, J.F. and Zwanzig, H.V. 2002: Suture-zone geometry along an irregular Paleoproterozoic margin: the Superior boundary zone, Manitoba, Canada; *Geology*, v. 30, p. 735–738.
- Zwanzig, H.V. 1997: Comments on “Kisseynew metasedimentary gneiss belt, Trans-Hudson orogen (Canada): Back-arc origin and collisional inversion” by Ansdell et al., 1995 (*Geology*, v. 23, p. 1039–1043); *Geology*, v. 25, p. 90–91.
- Zwanzig, H.V. 1998: Structural mapping of the Setting Lake area (parts of NTS 63J/15 and 63O/1, 2); *in* Report of Activities 1998, Manitoba Energy and Mines, Geological Services, p. 40–45.
- Zwanzig, H.V. 1999: Structure and stratigraphy of the south flank of the Kisseynew Domain in the Trans-Hudson Orogen, Manitoba: implications for 1.845–1.77 Ga collision tectonics; *Canadian Journal of Earth Sciences*, v. 36, p. 1859–1880.
- Zwanzig, H.V. 2000: Geochemistry and tectonic framework of the Kisseynew Domain–Lynn Lake Belt Boundary (part of NTS 63P/13); *in* Report of Activities 2000, Manitoba Industry, Trade and Mines, Manitoba Geological Survey, p. 91–96.
- Zwanzig, H.V. 2008: Correlation of lithological assemblages flanking the Kisseynew Domain, Manitoba (parts of NTS 63N, 63O, 64B, 64C): proposal for tectonic/metallogenic subdomains; *in* Report of Activities 2008, Manitoba Science, Technology, Energy and Mines, Manitoba Geological Survey, p. 38–52.
- Zwanzig, H.V. and Bailes, A.H. 2010: Geology and geochemical evolution of the northern Flin Flon and southern Kisseynew domains, Kississing–File lakes area, Manitoba (parts of NTS 63K, N); Manitoba Innovation, Energy and Mines, Manitoba Geological Survey, Geoscientific Report GR2010-1, 135 p.
- Zwanzig, H.V., Macek, J.J. and McGregor, C.R. 2007: Lithostratigraphy and geochemistry of the high-grade metasedimentary rocks in the Thompson nickel belt and adjacent Kisseynew domain, Manitoba: implications for nickel exploration; *Economic Geology*, v. 102, p. 1197–1216.

## First discovery of a Cretaceous fossil leaf in Manitoba (NTS 62N15)

by K. Lapenskie

### In Brief:

- First known example of a Cretaceous leaf discovered in Manitoba
- May indicate that there is Cretaceous terrestrial fossil fauna in the Swan River Formation

### Citation:

Lapenskie, K. 2019: First discovery of a Cretaceous fossil leaf in Manitoba (NTS 62N15); in Report of Activities 2019, Manitoba Agriculture and Resource Development, Manitoba Geological Survey, p. 72–76.

### Summary

During re-examination of Manitoba Geological Survey's stratigraphic drillcore M-08-78, a pyritized leaf was found within a nodule in the siliciclastic Cretaceous Swan River Formation. This leaf represents the first known occurrence of a Cretaceous fossil leaf in Manitoba. The fossil has been identified as belonging to a fern, most likely from the family Osmundaceae. Terrestrial lithofacies of the Swan River Formation may host other terrestrial faunal assemblages, which has important implications for geotourism and paleontological research in Manitoba, as well as providing new paleoenvironmental information important to understanding the depositional setting of this formation.

### Introduction

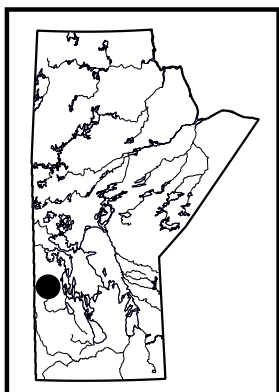
Drillcore M-08-78 was drilled by the Manitoba Geological Survey (MGS) in 1978 (Bannatyne, 1978), within the community of Pine River, situated on the eastern flank of Duck Mountain (Figure GS2019-7-1). In 2019, a pyritized fossilized leaf was discovered in a pyritized nodule within the Swan River Formation during a standard review of the drillcore for stratigraphic learning purposes. This discovery represents the first reported fossilized leaf from Cretaceous strata in Manitoba.

The siliciclastic Cretaceous Swan River Formation was deposited throughout southwestern Manitoba. Coeval siliciclastic strata were deposited in parts of Saskatchewan and North Dakota and likely correlate to the Cantuar Formation of the Mannville Group. The Swan River Formation is relatively understudied in Manitoba, with few core transecting the formation. There are limited exposures of the Swan River Formation in southwestern Manitoba; these exposures are located along rivers on the flanks of the Manitoba escarpment north of Riding Mountain (to the south of drillhole M-08-78).

The Swan River Formation is mainly composed of fine-grained sand to sandstone, interbedded with silt and clay intervals (McNeil and Caldwell, 1981; Glass, 1990; Nicolas, 2009; Natural Resources Canada, 2019). Minor investigations into the microfauna and macrofauna of the Swan River Formation have been conducted in the past (e.g., Gulio, 1967; Paterson, 1968); these studies have yielded carbonized plant fragments, palynomorphs and biogenic structures, but have not reported discernible terrestrial animal or plant fossils. Palynological studies and relative age dating indicate a mid-Cretaceous Albian age for the formation (Playford, 1971).

### Drillcore M-08-78

The location of drillcore M-08-78 was originally chosen to test for a subsurface lignite bed that had been reported during previous drilling (Bannatyne, 1978). The hole was abandoned at a depth of 75.11 m, after encountering lenses of unconsolidated sand and silt; the lignite bed was not transected. The lithostratigraphic and lithological description of M-08-78 is provided in Table GS2019-7-1. Unconsolidated sand and silt was encountered between 45.00 and 75.11 m, with only 4.00 m of core recovered from this interval. Drillcore M-08-78 transected 3.98 m of Quaternary clays and shales, which unconformably overlie the Cretaceous carbonaceous and silty shale of the Ashville Formation (3.98 to 34.03 m) and the interbedded kaolinitic, carbonaceous shale and glauconitic, pyritic and calcareous sandstones of the Swan River Formation (34.03 to 75.11 m). However, only approximately 15 m of core was recovered from the Swan River Formation interval (Figure GS2019-7-2).



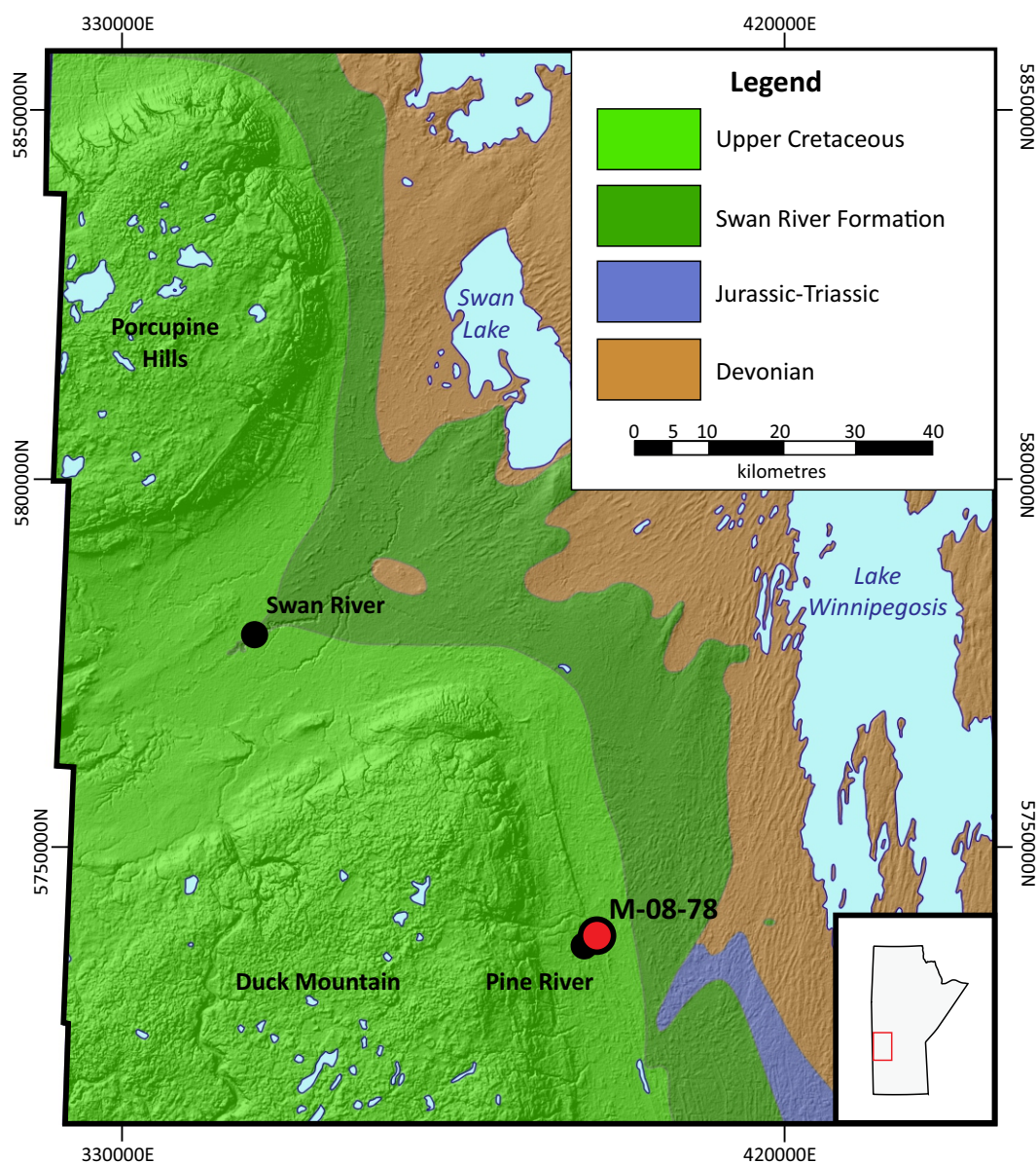


**Figure GS2019-7-1:** Regional bedrock geology of east-central Manitoba (after Nicolas et al., 2010). Location of drillcore M-08-78 (Bannatyne, 1978) is shown. The background image was generated using the radar-derived Canadian digital surface model (United States Geological Survey, 2002). A hillshaded model has been added with transparency effect to enhance relief.

**Table GS2019-7-1:** Lithostratigraphy and lithological description of drillcore M-08-78 (Bannatyne, 1978). Abbreviation: TVD, true vertical depth.

TVD (m)	Thickness (m)	Description
0.0–3.98	3.98	<b>Quaternary sediments</b> Clays and shales
3.98–75.11	71.13	<b>Colorado Group</b>
3.98–34.03	30.05	<b>Asvhille Formation</b> Black to grey carbonaceous shale, interbedded with silt lenses and laminae in lower section
34.03–75.11	14.97*	<b>Swan River Formation</b> Light grey to black kaolinitic to carbonaceous shale, interbedded with glauconitic sandstone, pyritic sandstone and calcareous sandstone

\*Measured recovered core





**Figure GS2019-7-2:** Photograph of the Swan River Formation in drillcore M-08-78 (Bannatyne, 1978). Lowermost shale beds of the Ashville Formation occur near the top of the interval, underlain by sandstones and carbonaceous shales of the Swan River Formation. Arrow indicates up direction in core. Scale bar in centimetres. Star denotes location of the fossilized leaf-bearing nodule. Yellow dashed line denotes contact between Ashville and Swan River formations. Abbreviations: A.F, Ashville Formation; c.s., carbonaceous shale; S.R., Swan River Formation; s.s., sandstone.

### **Fossilized leaf**

The pyritized leaf was found on a bedding surface within a pyritized concretion, which occurred at an approximate depth of 50.85 m in drillcore M-08-78. The singular leaf is approximately 9 mm long by 4 mm wide (Figure GS2019-7-3). Carbonized plant fragments are abundant on this bedding surface as well. The concretion is composed of pyritized glauconitic siltstone to sandstone. The fossil leaf is a single pinnule from a pteridophyte

frond leaflet, based on venation (Dr. D. Greenwood, pers. comm., 2018). The fossil most likely belongs to the family Osmundaceae (Dr. E. Koppelhus, pers. comm., 2019).

### **Discussion**

The Swan River Formation was deposited in marine and terrestrial environments (Nicolas, 2009). Lowermost unconsolidated silts and sands and sandstones were most

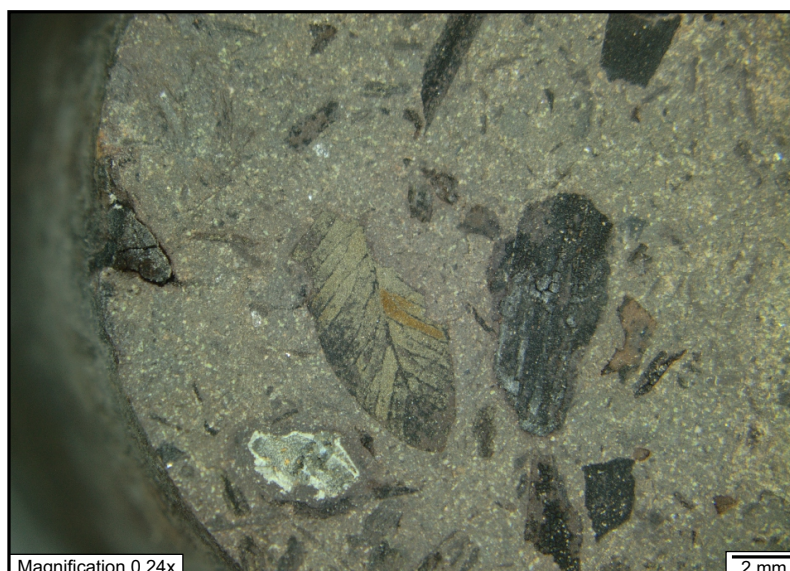


**Figure GS2019-7-3:** Photomicrograph of bedding surface within a pyritized glauconitic sandstone concretion at 50.85 m. The fossil leaf is pyritized, and surrounded by scattered fragments of unidentifiable black carbonized woody plant material.

likely deposited in terrestrial conditions such as incised drainage systems and paludal environments, whereas uppermost glauconitic sands were most likely deposited in marginal marine conditions (McNeil and Caldwell, 1981; Leckie et al., 1994; Bamburak and Christopher, 2004).

This is the first reported Cretaceous terrestrial fossil leaf in Manitoba. Marine faunal assemblages are more common, such as the largest mosasaur in Canada discovered near the town of Morden, and other specimens of Cretaceous actinopterygians (fish), cheloniids (turtles), plesiosaurs (marine reptiles), lepidosaurs (reptiles), crocodilians (crocodiles) and aves (birds), which are featured in museum displays across the province.

The fossilized pteridophyte leaf indicates that terrestrial flora existed in Manitoba during the mid-Cretaceous. Preservation of delicate plant material may suggest preservation of more robust terrestrial animal skeletons is likely.

### Economic considerations

Terrestrial lithofacies within the Swan River Formation offer a unique paleontological perspective of the Swan River Formation as a potential host of terrestrial fossilized fauna. Future fossil discoveries could positively impact paleontological-based tourism and research, as well as provide new paleoenvironmental information important to understanding the depositional setting of this formation.

### Acknowledgments

The author would like to thank D. Greenwood from Brandon University and E. Koppelhus from the University of Alberta for their assistance in identifying the fossil leaf.

Thank you to N. Anderson and C. Epp for their assistance with core viewing. Also, M. Gauthier and C. Böhm are thanked for their review of this report.

### References

- Bamburak, J.D. and Christopher, J.E. 2004: Mesozoic stratigraphy of the Manitoba escarpment; Manitoba Industry, Economic Development and Mines, Western Canada Sedimentary Basin/Targeted Geoscience Initiative II, Winnipeg, Manitoba, September 7–10, 2004, Field Trip Guidebook, 83 p.
- Bannatyne, B.B. 1978: Industrial minerals drill program; in Report of Field Activities 1978, Manitoba Department of Mines, Resources and Environmental Management, Mineral Resources Division, p. 127–130.
- Glass, D.J. (ed.) 1990: Lexicon of Canadian Stratigraphy, Volume 4, Western Canada; Canadian Society of Petroleum Geologists, Calgary, Alberta, 772 p.
- Guliov, P. 1967: Part 1, Lower Cretaceous (middle Albian) foraminifera from Saskatchewan from a locality in southeastern Saskatchewan; Saskatchewan Department of Mineral Resources, Report 105, 60 p.
- Leckie, D.A., Bhattacharya, J.P., Bloch, J., Gilboy, C.F. and Norris, B. 1994: Cretaceous Colorado/Alberta Group of the Western Canada Sedimentary Basin; in Geological Atlas of the Western Canada Sedimentary Basin, G.D. Mossop and I. Shetsen (comp.), Canadian Society of Petroleum Geologists, Calgary, Alberta, and Alberta Research Council, Edmonton, Alberta, p. 335–352.
- McNeil, D.H. and Caldwell, W.G.E. 1981: Cretaceous rocks and their foraminifera in the Manitoba escarpment; Geological Association of Canada, Special Paper No. 21, 439 p.
- Natural Resources Canada 2019: Weblex Canada: lexicon of Canadian geological names on-line; Natural Resources Canada, URL <[https://weblex.nrcan.gc.ca/weblexnet4/weblex\\_e.aspx](https://weblex.nrcan.gc.ca/weblexnet4/weblex_e.aspx)> [September 2019].

- Nicolas, M.P.B. 2009: Williston Basin Project (Targeted Geoscience Initiative II): summary report on Mesozoic stratigraphy, mapping and hydrocarbon assessment, southwestern Manitoba; Manitoba Science, Technology, Energy and Mines, Manitoba Geological Survey, Geoscientific Paper GP2009-1, 19 p.
- Nicolas, M.P.B., Matile, G.L.D., Keller, G.R. and Bamburak, J.D. 2010: Phanerozoic geology of southern Manitoba; Manitoba Innovation, Energy and Mines, Manitoba Geological Survey, Stratigraphic Map SM2010-1, 2 sheets, scale 1:600 000.
- Paterson, D.F. 1968: Jurassic megafossils of Saskatchewan with a note on charophytes; Saskatchewan Department of Mineral Resources, Report 120, 135 p.
- Playford, G. 1971: Palynology of Lower Cretaceous (Swan River) strata of Saskatchewan and Manitoba; *Palaeontology*, v. 14, p. 533–565.
- United States Geological Survey 2002: Shuttle Radar Topography Mission, digital elevation model, Manitoba; United States Geological Survey, URL <[https://dds.cr.usgs.gov/srtm/version2\\_1/SRTM3/North\\_America/](https://dds.cr.usgs.gov/srtm/version2_1/SRTM3/North_America/)>, portions of files N48W88W.hgt.zip through N60W102.hgt.zip, 1.5 Mb (variable), 90 m cell, zipped hgt format [March 2003].



### In Brief:

- Sixteen drillcore from central and northern portions of the Williston Basin were examined
- Stratigraphic information collected aid in refining and resolving the stratigraphic framework of Manitoba
- Northern drillcore provided important insights into the lithofacies of the Winnipeg Formation

### Citation:

Lapenskie, K. 2019: Summary of Phanerozoic core logging activities in Manitoba in 2019 (parts of NTS 63C3, 14, 63J5, 6, 11, 12, 14); in Report of Activities 2019, Manitoba Agriculture and Resource Development, Manitoba Geological Survey, p. 77–82.

### Summary

Sixteen drillcore from central and northern portions of the Williston Basin in Manitoba were examined in 2019. These drillcore were examined for the purposes of collecting stratigraphic information, investigating carbonate-hosted lead-zinc mineralization potential in the Swan River–Minitonas area, and characterizing the silica sands of the Winnipeg Formation of the northern Williston Basin.

Drillcore from the Swan River–Minitonas area provided insight into the subsurface stratigraphy of an understudied area and yielded positive indicators for the potential for carbonate-hosted lead-zinc mineralization; however, no occurrences of mineralization were identified. Drillcore from northern portions of the Williston Basin also provided valuable subsurface stratigraphic information from the Stonewall to Winnipeg formations. The Winnipeg Formation displayed a significant amount of lithological variation in these drillcore, but further work is required to assess the quality of the silica sand from different lithofacies. However, due to the very thin nature of the Winnipeg Formation in the northernmost region of the Williston Basin, the formation likely has limited potential as an economic source of high-purity silica sand.

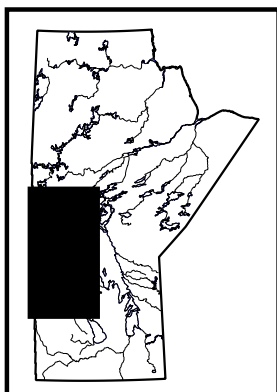
### Introduction

Exploration drillcore that transects Phanerozoic strata has been integral to the Manitoba Geological Survey's (MGS) efforts to refine and resolve the stratigraphic framework of the Manitoba portion of the Williston Basin, as well as to better understand industrial mineral potential. Detailed lithostratigraphy is performed on Phanerozoic core when possible, as the lower Paleozoic framework of southwestern Manitoba contains significant inconsistencies (Lammers, 1988; Bezys and Conley, 1998; Nicolas and Barchyn, 2008; Lapenskie and Nicolas, 2017).

During 2019, 16 exploration drillcore were examined as part of ongoing stratigraphic correlation activities and industrial minerals projects (Figure GS2019-8-1, Table GS2019-8-1). Core drilled by Husky Oil Ltd. (Husky) and Gulf Minerals Canada Limited (GMCL) in the Swan River–Minitonas area were re-examined specifically to perform detailed lithostratigraphic examination, refine stratigraphic errors and address inconsistencies in previous logs, and to examine drillcore for any indicators of carbonate-hosted lead-zinc mineralization. Exploration core drilled by Hudbay Minerals Inc. (Hudbay) in northern parts of the Williston Basin were also examined. These drillcore were examined for their stratigraphic information and to assess the silica sands of the Winnipeg Formation. A summary of the lithostratigraphy and brief lithological descriptions are provided in MGS Data Repository Item DRI2019006<sup>1</sup>. Geographic location, associated assessment file and well licence numbers are also provided in Table GS2019-8-1.

### Husky-GMCL drillcore

Drillcore from the Swan River–Minitonas area were drilled by Husky and GMCL in the 1970s. These core were originally drilled as stratigraphic testholes for mineral and petroleum exploration purposes. In total eight core were drilled by the two companies, five of



<sup>1</sup> MGS Data Repository Item DRI2019006 containing the data or other information sources used to compile this report is available online to download free of charge at <https://www.gov.mb.ca/iem/info/library/downloads/index.html>, or on request from [minesinfo@gov.mb.ca](mailto:minesinfo@gov.mb.ca), or by contacting the Resource Centre, Manitoba Agriculture and Resource Development, 360–1395 Ellice Avenue, Winnipeg, Manitoba R3G 3P2, Canada.



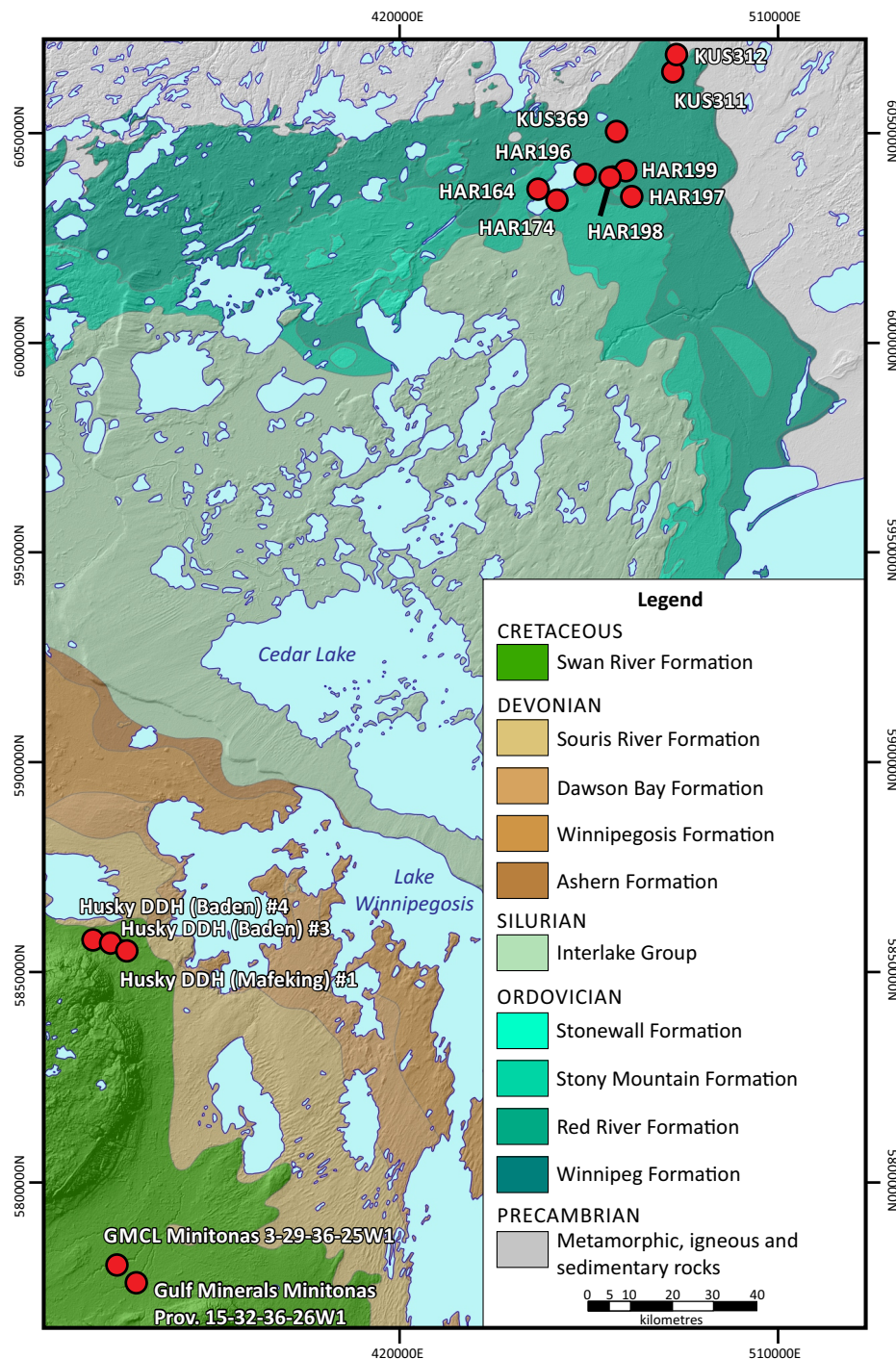


**Figure GS2019-8-1:** Regional bedrock geology of the central to northern portions of the Williston Basin in Manitoba (after Nicolas et al., 2010); formations younger than the Swan River Formation are not depicted. Drillhole locations are indicated by red dots. Co-ordinates are in UTM Zone 14, NAD83.

which have been stored and are available for examination at the MGS Midland Sample and Core Library (Winnipeg, Manitoba; Table GS2019-8-1).

The drillholes primarily transected Devonian strata, with two drilled to Precambrian basement. The entire Paleozoic section in only one of those drillcore was retained by the MGS. Although these drillcore were drilled in close

proximity, there was a high degree of variation in Devonian strata in some drillcore, most notably in the Souris River Formation. The Souris River Formation is known to have a degree of lateral lithological variation (Glass, 1990; Natural Resources Canada, 2019) and is relatively understudied in parts of the outcrop belt, including the Swan River–Minitonas area.

**Table GS2019-8-1:** Geographic and general information for logged drillcore. The UTM co-ordinates are in NAD83, Zone 14.

Core ID	Easting	Northing	Depth (m)	Assessment File	Licence number	Company
KUS311	484775	6066695	221.00	74703	n/a	Hudbay Minerals Inc.
KUS312	485092	6067742	206.00	74703	n/a	Hudbay Minerals Inc.
HAR174	456059	6034206	302.00	74565	n/a	Hudbay Minerals Inc.
HAR199	471841	6040150	179.00	74565	n/a	Hudbay Minerals Inc.
HAR196	463996	6039630	302.00	74565	n/a	Hudbay Minerals Inc.
HAR164	453364	6035930	293.00	74565	n/a	Hudbay Minerals Inc.
HAR197	474415	6035211	238.00	74582	n/a	Hudbay Minerals Inc.
HAR198	470089	6040200	185.00	74565	n/a	Hudbay Minerals Inc.
KUS369	470991	6050394	224.00	74705	n/a	Hudbay Minerals Inc.
RES372*	-	-	-	-	n/a	Hudbay Minerals Inc.
RES361*	-	-	-	-	n/a	Hudbay Minerals Inc.
Husky DDH (Mafeking) #1	352800	5855453	152.40	91776	2465	Husky Oil Ltd.
Husky DDH (Baden) #3	350411	5856365	144.80	91776	2467	Husky Oil Ltd.
GMCL Minitonas 3-29-36-25W1	355592	5775895	526.40	92116	2548	Gulf Minerals Canada Limited
Gulf Minerals Minitonas Prov. 15-32-36-26W1	352568	5779003	517.20	92116	2547	Gulf Minerals Canada Limited
Husky DDH (Baden) #4	348383	5856856	109.70	91776	2468	Husky Oil Ltd.

\* Drillcore are under confidentiality and the location and depths of these drillcore are unable to be shared publicly at this time

No examples of carbonate-hosted mineralization were identified in the Husky and GMCL drillcore. However, positive indicators of carbonate-hosted lead-zinc mineralization in a Mississippi Valley–type deposit were identified, such as extensive brecciation, reefal to inter-reefal facies, evidence of evaporites and possible karsting (Paradis et al., 2007; Leach et al., 2010).

### Stratigraphy

A brief discussion of important features observed in the Husky and GMCL drillcore is provided below.

#### GMCL Minitonas 3-29-36-25W1

Drillcore GMCL Minitonas 3-29-36-25W1 (oil and gas well licence 2548, Manitoba Agriculture and Resource Development, Winnipeg; Assessment File 92116, Manitoba Agriculture and Resource Development, Winnipeg) transected over 500 m of Phanerozoic strata, including 430.1 m of Paleozoic rock. This drillcore offers a complete section, with excellent core recovery, of the lower Paleozoic strata of the Manitoba outcrop belt, from the lowermost Ordovician Winnipeg Formation to the uppermost Devonian Hatfield Member of the Souris River Formation.

The Winnipeg Formation and Ordovician Bighorn and Silurian Interlake groups in drillcore GMCL Minitonas 3-29-36-25W1 are typical of this area in the Williston Basin. The lowermost Winnipeg Formation was subdivided into the lower sandstone Black Island Member and upper shaly

Icebox Member. The upper Red River Formation was subdivided into the Lake Alma Member, Coronach unit and Redvers unit. The Gunton Member is the only member of the Stony Mountain Formation present in this drillcore, confirming the absence of other members in the northern extent of the Williston Basin (Kendall, 1976; Glass, 1990; Natural Resources Canada, 2019). The t-marker bed, an argillaceous and arenaceous bed that approximates the Ordovician-Silurian boundary, is well developed in the Stonewall Formation.

The Interlake Group was subdivided into its constituent formations: the Fisher Branch, Moose Lake, Atikameg, East Arm and Cedar Lake formations, in ascending order. Previous attempts to identify the individual formations of the Interlake Group in the subsurface have been largely unsuccessful (Bezys and Conley, 1998). However, examination of this drillcore, coupled with drillcore Neepawa DDH No. 1 Prov. 15-29-14-14W1 (Lapenskie and Nicolas, 2018), led to the identification of the formations of the Interlake Group in the subsurface; the availability of complete sections of core made this possible. The  $u_1$ -,  $u_2$ - and v-marker beds are all well developed in drillcore GMCL Minitonas 3-29-36-25W1.

The Devonian section includes the basal Ashern Formation to uppermost Hatfield Member of the Souris River Formation. The upper member of the Winnipegosis Formation is composed of a thin interval of inter-reefal facies. The overlying Prairie Evaporite is composed only of lime-

stone and diamictite transitional beds, as all evaporites have been dissolved in this part of the Williston Basin. The Sagemace and Hatfield members of the Souris River Formation are composed of a complex series of interbeds, and are each defined by a basal shaly to very argillaceous bed. The upper beds and upper contact of the Hatfield Member were not recovered in this core.

#### Husky DDH (Mafeking) #1

Drillcore Husky DDH (Mafeking) #1 (oil and gas well licence 2465; Assessment File 91776) transected uppermost Interlake Group to lower Souris River Formation strata. The section is typical of these stratigraphic units, and correlates well with GMCL Minitonas 3-29-36-25W1. The upper member of the Winnipegosis Formation is composed of a relatively thin interval of reefal facies.

#### Husky DDH (Baden) #3, Husky DDH (Baden) #4 and Gulf Minerals Minitonas Prov. 15-32-36-26W1

Drillcore from Husky DDH (Baden) #3 (oil and gas well licence 2467; Assessment File 91776), Husky DDH (Baden) #4 (oil and gas well licence 2468; Assessment File 91776) and Gulf Minerals Minitonas Prov. 15-32-36-26W1 (oil and gas well licence 2547; Assessment File 92116) were problematic for logging due to poor core recovery. Extensive brecciation, coupled with a high degree of lithological variation, made large portions of the drillcore stratigraphically undefinable. Chaotic brecciation (Figure GS2019-8-2) due to karsting and/or evaporite dissolution is the most likely cause of the disturbed lithologies. An uppermost sand/sandstone interval was transected in both the Husky DDH

(Baden) #4 and Husky DDH (Baden) #3 holes and is interpreted to be the Cretaceous Swan River Formation.

#### Hudbay drillcore

A total of 11 Hudbay exploration drillcore, which transected Paleozoic strata across the northern portion of the Williston Basin, were examined during the 2019 field season (Table GS2019-8-1). These drillcore are stored at Hudbay's Stall concentrator site outside of the town of Snow Lake, and at the Hudbay hanger on Schist Lake near the community of Channing. The primary objectives of examining these drillcore were to compile stratigraphic information, and to define the lithofacies and purity of the silica sand of the Winnipeg Formation.

Most of the drillholes transected the Red River and Winnipeg formations, whereas holes located in the southerly portions of Hudbay exploration areas also transected the Stony Mountain and Stonewall formations.

The Winnipeg Formation is disconformably underlain by regolith and unweathered Precambrian metamorphic, igneous and sedimentary rocks, and conformably overlain by a thick succession of Red River Formation dolostones (Figure GS2019-8-3a). The Winnipeg Formation is very heterogeneous in the northern portion of the Williston Basin. Lithologies vary from unconsolidated sand, kaolin-rich mudstone, quartz wacke to arenite, feldspathic wacke to arenite, and quartzose conglomerate to diamictite (Figure GS2019-8-3b-d). Immature sandstones containing garnet, biotite and gravel-sized quartz clasts were observed in some drillcore. The sandstones are variably pyritic (Figure GS2019-8-3b), with elevated concentrations

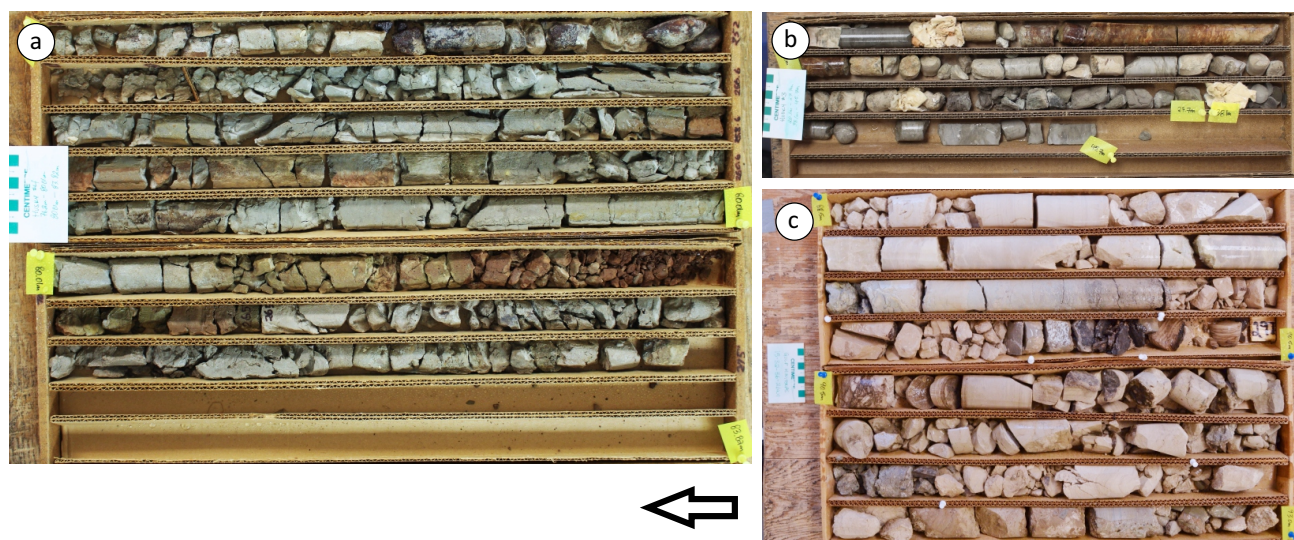


**Figure GS2019-8-2:** Examples of brecciation: **a)** drillcore Husky DDH (Baden) #4 (oil and gas well licence 2468; Assessment File 91776), 76.20 to 80.00 m and 80.00 to 83.80 m; **b)** drillcore Husky DDH (Baden) #3 (oil and gas well licence 2467; Assessment File 91776), 20.10 to 27.70 m and 38.10 to 45.70 m; **c)** drillcore Gulf Minerals Minitonas Prov. 15-32-36-26W1 (oil and gas well licence 2547; Assessment File 92116), 88.50 to 93.00 m. Arrow indicates up direction in core. Scale cards in centimetres.



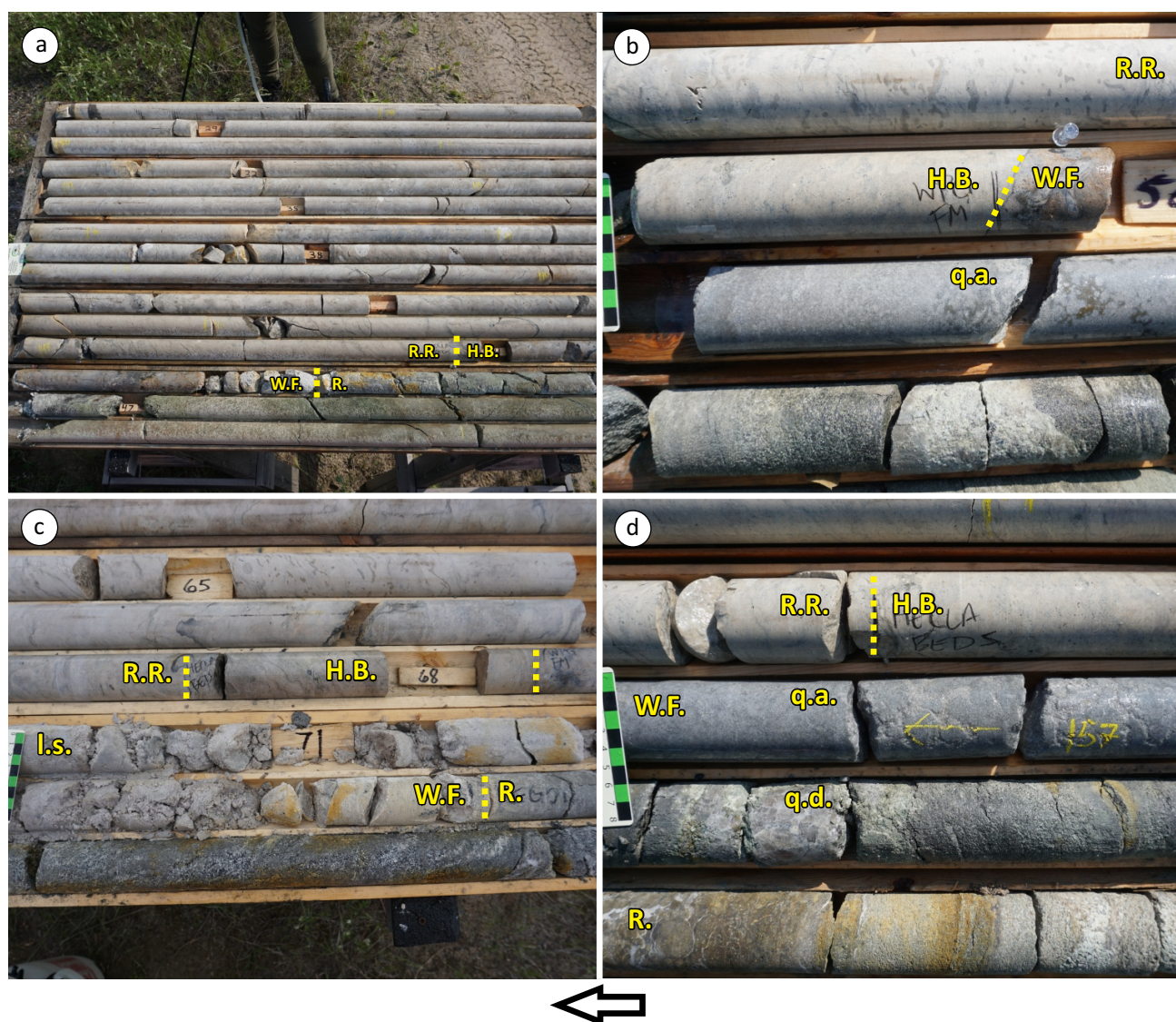


**Figure GS2019-8-3:** Photographs of the Winnipeg Formation in drillcore: **a)** Red River Formation, Hecla Beds, Winnipeg Formation and Precambrian basement of drillcore KUS369 (Assessment File 74705), showing undifferentiated lower Red River Formation strata; **b)** Red River Formation, Hecla Beds and Winnipeg Formation of drillcore HAR164 (Assessment File 74565), showing pyritic quartz arenite; **c)** Red River Formation, Hecla Beds, Winnipeg Formation and Precambrian basement of drillcore HAR197 (Assessment File 74582), showing unconsolidated sand of the Winnipeg Formation; **d)** Red River Formation, Hecla Beds, Winnipeg Formation and Precambrian basement of drillcore HAR164, showing multiple lithofacies of the Winnipeg Formation. Arrow indicates up direction in core. Dashed yellow lines represent lithostratigraphic contacts. Scale cards in centimetres. Abbreviations: H.B., Hecla Beds; I.s., loose sand; q.a., quartz arenite; q.d., quartz diamictite; R., regolith; R.R., Red River Formation; W.F., Winnipeg Formation.

of sulphides most commonly occurring near the upper contact of the Winnipeg Formation with the overlying Red River Formation. Thickness of the Winnipeg Formation ranges from 0.55 to 5.20 m. The Winnipeg Formation was not observed in drillcore KUS311 (Assessment File 74703) because the basal portion of the drillcore was stored separately and inaccessible for logging.

Microscope and thin section observations will be conducted to quantitatively describe and classify the lithofacies of the Winnipeg Formation. Geochemical analysis will be

performed to quantitatively assess the quality of the silica sands of the different facies. Further core logging will be conducted in future field seasons to continue to better understand the quality and characteristics of the silica sands of the Winnipeg Formation in northern portions of the Williston Basin, and to define the lateral facies variation across the basin in Manitoba. However, due to the very thin nature of the Winnipeg Formation in the northernmost region of the Williston Basin, the formation likely has limited potential as an economic source of high-purity silica sand.

## Economic considerations

Phanerozoic drillcore are important to refining and building the MGS's stratigraphic database, and providing valuable insight into resolving and formalizing stratigraphic relationships. An accurate and well-defined stratigraphic framework for the Williston Basin in Manitoba is required for petroleum exploration, understanding brines and hydrogeology, industrial mineral exploration, and carbonate-hosted lead-zinc exploration. Examining exploration drillcore provides important insights into the geology of the Winnipeg Formation and in assessing the purity and economic potential of silica sands in the northern parts of the Williston Basin.

## Acknowledgments

Staff at Hudbay Minerals Inc. in Snow Lake and Flin Flon is graciously thanked for providing access to and assistance in locating drillcore. Excellent assistance in the field was provided by M. Koziuk. The author thanks E. Anderson and C. Epp for their assistance in providing core viewing and E. Anderson and K. Reid for their logistical assistance in the field. Also, M. Nicolas and C. Böhm are thanked for their review of this report.

## References

- Bezys, R.K. and Conley, G.G. 1998: Geology of the Silurian Interlake Group in Manitoba; Manitoba Energy and Mines, Stratigraphic Map SI-1, scale 1:2 000 000.
- Glass, D.J. (ed.) 1990: Lexicon of Canadian Stratigraphy, Volume 4, Western Canada; Canadian Society of Petroleum Geologists, Calgary, Alberta, 772 p.
- Kendall, A.C. 1976: The Ordovician carbonate succession (Bighorn Group) of southern Saskatchewan; Saskatchewan Department of Mineral Resources, Report 180, 185 p.
- Lammers, G.E. 1988: Silurian stratigraphy of the Interlake area; *in* Report of Field Activities 1988, Manitoba Energy and Mines, Geological Services, p. 43–48.
- Lapenskie, K. 2019: Lithostratigraphy and brief lithological descriptions of logged Phanerozoic core, southwestern and central Manitoba (parts of NTS 63C3, 14, 63J5, 6, 11, 12, 14); Manitoba Agriculture and Resource Development, Manitoba Geological Survey, Data Repository Item DRI2019006, Microsoft® Excel® file.
- Lapenskie, K. and Nicolas, M.P.B. 2017: Detailed examination of drillcore RP95-17, west-central Manitoba (NTS 63C7): evidence of potential for Mississippi Valley-type lead-zinc deposits; *in* Report of Activities 2017, Manitoba Growth, Enterprise and Trade, Manitoba Geological Survey, p. 158–172.
- Lapenskie, K. and Nicolas, M.P.B. 2018: Lithostratigraphy of the Neepawa DDH No. 1 Prov. core at 15-29-14-14W1, southwestern Manitoba (part of NTS 62J3); *in* Report of Activities 2018, Manitoba Growth, Enterprise and Trade, Manitoba Geological Survey, p. 136–149.
- Leach, D.L., Taylor, R.D., Fey, D.L., Diehl, S.F. and Saltus, R.W. 2010: A deposit model for Mississippi Valley type lead-zinc ores, chapter A of mineral deposit models for resource assessment; United States Geological Survey, Scientific Investigations Report 2010-5070-A, 52 p.
- Natural Resources Canada 2019: Weblex Canada: lexicon of Canadian geological names on-line; Natural Resources Canada, URL <[https://weblex.nrcan.gc.ca/weblexnet14/weblex\\_e.aspx](https://weblex.nrcan.gc.ca/weblexnet14/weblex_e.aspx)> [September 2019].
- Nicolas, M.P.B. and Barchyn, D. 2008: Williston Basin Project (Targeted Geoscience Initiative II): summary report on Paleozoic stratigraphy, mapping and hydrocarbon assessment, southwestern Manitoba; Manitoba Science, Technology, Energy and Mines, Manitoba Geological Survey, Geoscientific Paper GP2008-2, 21 p.
- Nicolas, M.P.B., Matile, G.L.D., Keller, G.R. and Bamburak, J.D. 2010: Phanerozoic geology of southern Manitoba; Manitoba Innovation, Energy and Mines, Manitoba Geological Survey, Stratigraphic Map SM2010-1, 2 sheets, scale 1:600 000.
- Paradis, S., Hannigan, P. and Dewing, K. 2007: Mississippi Valley-type deposits; *in* Mineral Deposits of Canada: A Synthesis of Major Deposit-Types, District Metallogeny, the Evolution of Geological Provinces, and Exploration Methods, W.D. Goodfellow (ed.), Geological Association of Canada, Mineral Deposits Division, Special Publications No. 5, p. 185–203.

## Quaternary stratigraphy and till sampling in the Machichi–Kettle rivers area, far northeastern Manitoba (parts of NTS 54A–C)

by T.J. Hodder and M.S. Gauthier

### In Brief:

- Documenting the Quaternary stratigraphy at exposed river sections
- Collection of till samples to determine provenance and investigate the regional diamond potential
- Collection of ice-flow data and geochronology samples to reconstruct the glacial history

### Citation:

Hodder, T.J. and Gauthier, M.S. 2019: Quaternary stratigraphy and till sampling in the Machichi–Kettle rivers area, far northeastern Manitoba (parts of NTS 54A–C); *in* Report of Activities 2019, Manitoba Agriculture and Resource Development, Manitoba Geological Survey, p. 83–89.

### Summary

Quaternary geology fieldwork was conducted over 15 days in September 2019 in the Machichi–Kettle rivers area of far northeastern Manitoba. The objective of this study was to document the Quaternary stratigraphy at a regional scale. This was accomplished by documenting the sediments exposed along river cuts in the study area. Ice-flow data were collected from till and samples were collected to determine till provenance using geochemistry and clast-lithology analysis. Sediments underlying till units were examined in detail and samples were collected for geochronology analysis by radiocarbon and luminescence dating methods, if an appropriate sample medium was observed. Sixty-three till kimberlite-indicator mineral samples were collected to assess the regional diamond potential. Field data collected includes 121 till samples, 43 clast fabric analyses, 22 paleoenvironment samples, 19 optically stimulated luminescence samples and 14 radiocarbon samples.

### Introduction

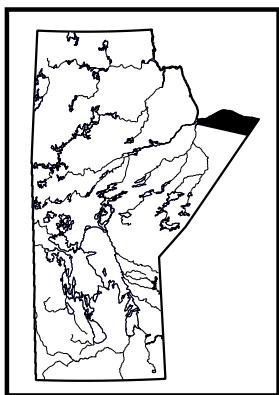
The Manitoba Geological Survey (MGS) conducted 15 days of helicopter-supported fieldwork in September of 2019 in the Machichi–Kettle rivers area of far northeastern Manitoba (parts of NTS 54A–C; Figure GS2019-9-1). This study provides the first reconnaissance-scale survey of the Quaternary geology in this remote area. The objectives of the 2019 field season were to

- document the sediments observed at Quaternary sections;
- sample till and conduct clast-fabric measurements to determine the ice-flow direction during till deposition;
- conduct kimberlite-indicator mineral (KIM) sampling to assess the diamond potential of the region; and
- collect geochronology and paleoenvironment samples to help establish stratigraphic correlations in the Hudson Bay Lowland (HBL).

### Previous work

The Machichi–Kettle rivers area has undergone little geological study. The first known accounts describing the Quaternary geology of this area are by Tyrrell (1913, 1916) who traversed up the Machichi River and noted “...cliffs of till up to 60 feet in height bound the valley, while the newer marine sands and clays are conspicuously scanty.” In 1967, the Geological Survey of Canada initiated Operation Winisk to better understand the geology of the HBL region of Quebec, Ontario and Manitoba (Craig, 1969; McDonald, 1969). Within the study area, Operation Winisk fieldwork provided helicopter-supported observations at four sections along the Kaskattama River, where it was noted that one or two tills were exposed at each of the sections (B.G. Craig, H. Gwyn and B.C. McDonald, unpublished notes, 1967). Additionally, the region was mapped at 1:250 000 scale in the late 1980s, though mapping was based mainly on airphoto interpretation and satellite imagery (Clarke, 1989).

The MGS has conducted Quaternary fieldwork in adjacent areas along the Hayes River (Hodder et al., 2017) and in the Kaskattama highland to the south (Hodder and Kelley, 2016, 2017, 2018; Hodder, 2017, 2018). Correlation between Quaternary sections is difficult, and additional fieldwork in the HBL is required to confirm the absolute ages of stratigraphic non-





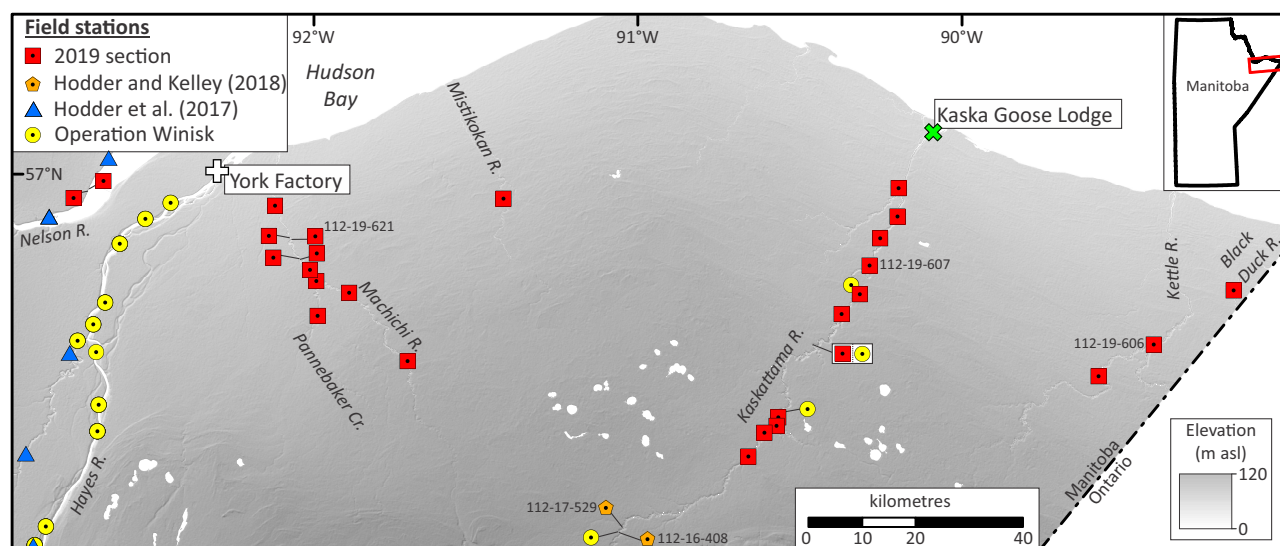


**Figure GS2019-9-1:** Location of sections visited in the Machichi–Kettle rivers study area. Sections referred to within the text are labelled. Background hillshade image was generated using Canadian Digital Surface Model (Natural Resources Canada, 2015).

glacial units. This has been identified as a priority to better understand the stratigraphy of tills in this area (Gauthier et al., 2019).

### Mineral exploration

The study area is largely unexplored, primarily due to its remoteness. Previous exploration is limited to airborne geophysical surveys and scant KIM sampling for diamond exploration. An aeromagnetic survey was completed in the Kaskattama–Kettle rivers region of this study area (Assessment File 93361, Manitoba Agriculture and Resource Development, Winnipeg). The KIM sampling was undertaken in the northeastern Kaskattama River area, where KIMs were recovered from alluvial, modern lacustrine beach and Holocene marine beach sediments (Figure GS2019-9-2; Assessment File 74009). This previous sampling recovered seven G9 garnet, nine chrome-diopside and four olivine mineral grains. The KIM recovery was preferential within marine beach sediments as they generally have a higher quantity of the specific grain size (0.25–1.19 mm) picked for KIM analysis in this previous study (Assessment File 74009; Figure GS2019-9-2). Regionally, KIM sampling has taken place along the Nelson, Pennycutaway, Hayes and Gods rivers to the west and south of this study area (Nielsen and Fedikow, 2002; Hodder et al., 2017) and the Kaskattama highland area to the south of this study area (Hodder and Kelley, 2018).

### Quaternary stratigraphy

Far northeastern Manitoba was repeatedly glaciated by the Laurentide Ice Sheet, as evidenced by stratigraphic sequences of two nonglacial units and up to four tills

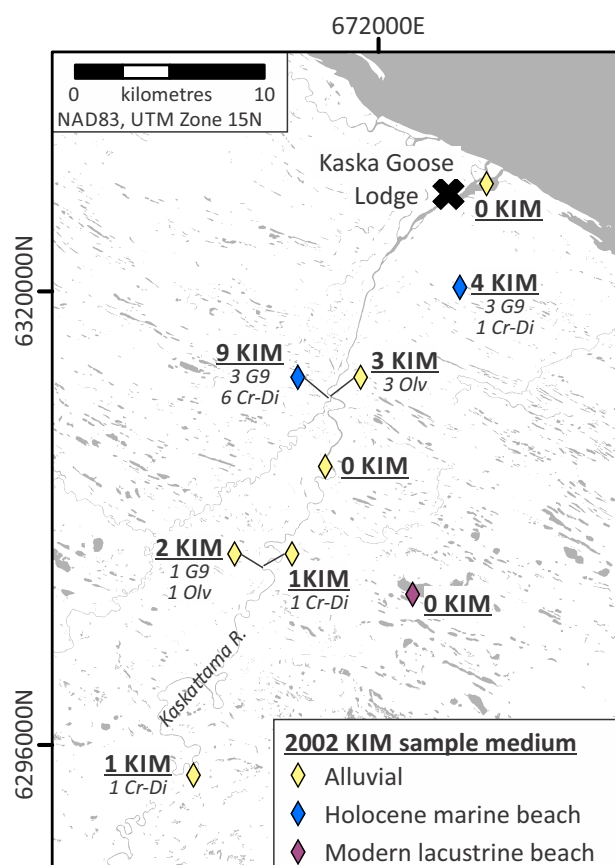


**Figure GS2019-9-2:** Previous kimberlite-indicator mineral (KIM) sample sites near the mouth of the Kaskattama River (Assessment File 74009). Microprobe data was classified according to the KIM database standardized classification (Keller, 2019) and shown here. Abbreviations: Cr-Di, chrome-diopside; G9, G9 garnet; Olv, olivine.

documented across the HBL (Netterville, 1974; Klassen, 1986; Nielsen et al., 1986; Dredge and McMartin, 2011; Hodder et al., 2017), but robust correlations between studies have proven difficult. During deglaciation, the study area was inundated by glacial Lake Agassiz (Klassen, 1983; Thorleifson, 1996) and by the Tyrrell Sea (Klassen, 1986).

The nature of interaction between ice from central mainland Nunavut and from Hudson Bay is uncertain, but a thick ice saddle was likely present over southern Hudson Bay late in deglaciation (Dyke and Prest, 1987; Thorleifson et al., 1993; Trommelen et al., 2012; Gauthier et al., 2019). The study area may have been within the zone of confluence between ice flowing from the north, the east and the saddle (Gauthier et al., 2019); the nature of till composition mixing is unknown. Two different tills were mapped at sections visited near the upper reaches of the Kaskattama River in 2016 and 2017 (Figure GS2019-9-1; Hodder and Kelley, 2018). At these sites, a clast fabric in the upper till indicated paleo-ice flow toward the south (176°), whereas a clast fabric in the lower till indicated paleo-ice flow toward the south-southwest (193°, 215°). Interestingly, there was 2.0 m of light brown, massive silt between the two tills at section 112-17-529 (Figure GS2019-9-1). This silt could indicate a nonglacial interval occurred between the deposition of the two till units, or, that this silt was deposited in a subglacial environment. Along the Gods River, at least four different tills have been mapped (Netterville, 1974). The two lowermost tills are separated by an organic-bearing unit referred to as the Gods River sediments (GRS), which is interpreted to have been deposited during the last interglacial period (Netterville, 1974). The upper three tills are separated by organic-barren sorted sediments, one of which has been named the Twin Creeks sediments (Netterville, 1974). Along the lower Hayes River, at least three tills have been mapped (Nielsen and Fedikow, 2002), with the lowermost Amery till separated from the middle Long Spruce till by the organic-bearing Nelson River sediments (NRS), which are interpreted to have been deposited during the last interglacial period.

Across the Manitoba-Ontario border (12.3 km east of section 112-19-606 on Figure GS2019-9-1), Dalton et al. (2016) investigated a section along the Black Duck River. At this section, a 1.2 m organic-rich unit was observed overlain by postglacial marine sediments and underlain by till. Four radiocarbon dates were obtained from wood within the organic-rich unit. Near the base of the unit, radiocarbon dating of two wood fragments yielded ages of  $50\,100 \pm 3300$  and  $49\,600 \pm 950$   $^{14}\text{C}$  yr. BP, and a third wood fragment yielded an infinite age ( $>48\,000$   $^{14}\text{C}$  yr. BP). Wood from the upper part of this unit was radiocarbon dated to  $46\,300 \pm 1750$  cal. yr. BP. These dates have been used

as one line of evidence to support the interpretation of an ice-free Hudson Bay during marine isotope stage (MIS) 3 (29–57 ka). This is important because organic-bearing units, e.g., GRS and NRS, have been correlated to the last interglacial period (MIS 5, 71–123 ka). Geochronology data derived from this project will help to resolve stratigraphic inconsistencies in the HBL.

## Data collected

The Quaternary stratigraphy exposed along natural river sections was documented at 27 stations (Figure GS2019-9-1). Sections were first cleared of slump, and then examined in detail (e.g., Figure GS2019-9-3). Where encountered, till was sampled at 2 m intervals; resulting in a total of 121 till samples, each weighing 2–3 kg. The new till samples will be split for archival purposes at the MGS Midland Sample and Core Library and then analyzed for grain-size, matrix geochemistry ( $<63\ \mu\text{m}$  size-fraction) and clast lithology. An additional 11.4 L till sample was collected for KIM analysis at 63 till sample sites. The average KIM sample weight was 16.5 kg (range of 13.9–19.6 kg). The KIM samples were submitted to the De Beers Group (De Beers) to be analyzed through in-kind support. The KIM sample locations were withheld from De Beers, to allow equal opportunity for follow-up by all interested parties when the data (with sample locations) is publicly released at a later date.

Ice-flow data was obtained from studied sections by measuring the long-axes orientation, or fabric, of clasts within till (e.g., Figure GS2019-9-4a, b). Elongate clasts, defined by a minimum 1.5:1.0 ratio of the a-axis (longest) to the b-axis (middle), will rotate within the till matrix and orient parallel to the direction of stress that the overriding glacier exerts on the till (Holmes, 1941). Clast-fabric measurements were conducted at 43 till sample sites. Each clast-fabric site had a minimum of 30 elongated clasts measured. Lodged clasts with parallel striae on their upper surface—considered to be a good indicator of ice flow—were observed at nine stratigraphic depths (e.g., Figure GS2019-9-4c, d). This ice-flow data will be combined with the forthcoming till composition and geochronology data to understand the till provenance and glacial history of the study area, which will allow for more effective drift prospecting approaches.

Sorted sediments, underlying or between till units, were also of interest for this study. These potentially nonglacial or interglacial units were documented, described and examined for organic matter. Organic matter was collected for radiocarbon dating wherever encountered, resulting in a total of 14 shell and wood samples. Organic-bearing units were sampled for pollen and macrofossil

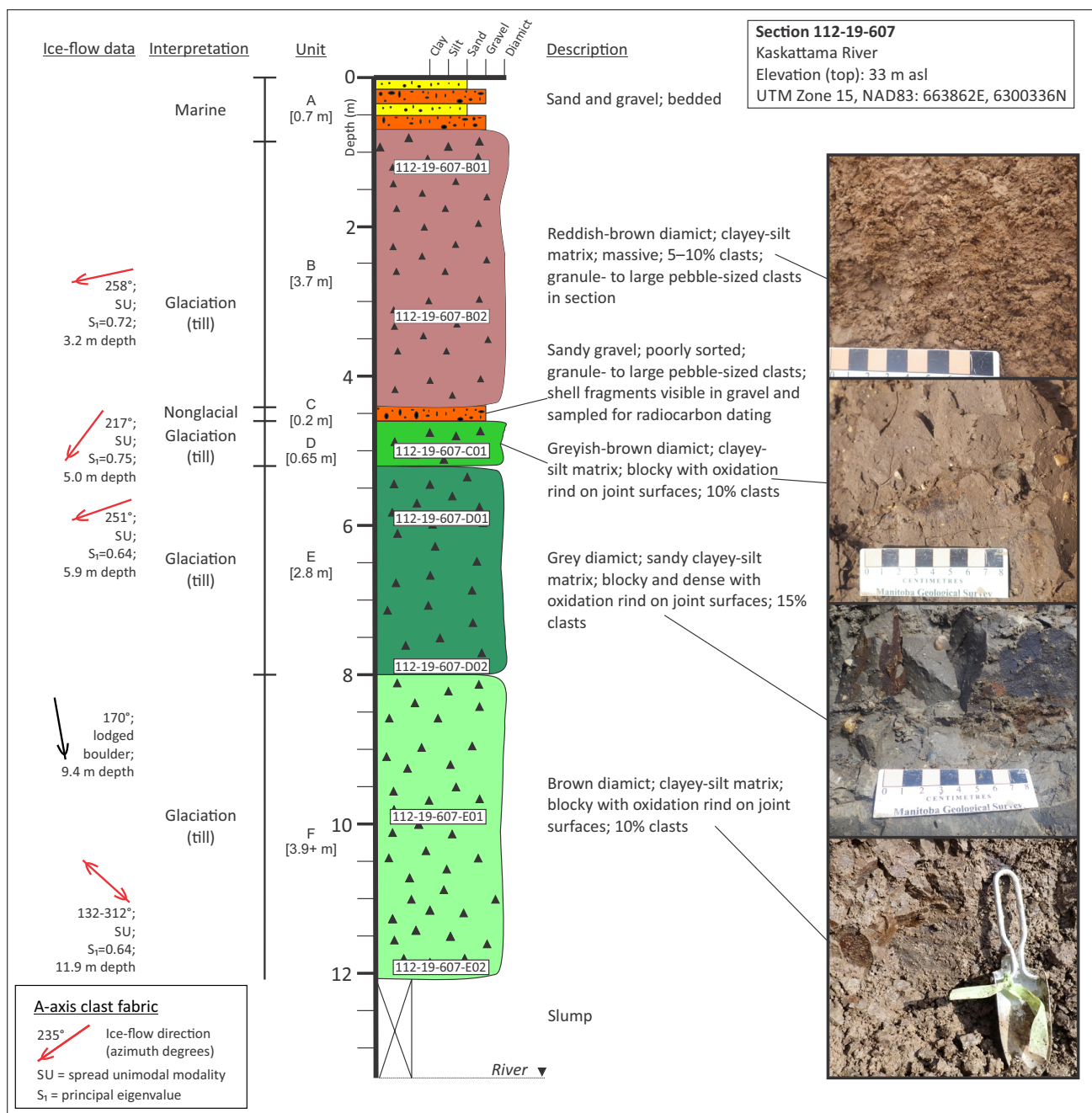


**Figure GS2019-9-3:** Example of a section described and sampled on the Kaskattama River during the 2019 field season. Till sample numbers are labelled within the white boxes.

analysis at five sections, totalling twenty-two samples. In addition, because some sub/intertill units may be older than the limits of radiocarbon dating (~50 000 years), 19 sorted sand units were also sampled for optically stimulated luminescence (OSL) dating (e.g., Figure GS2019-9-5). These OSL techniques have been used to date a variety of sediments deposited within the last 500 000 years (Forman et al., 2000).

Future work will synthesize stratigraphic observations with forthcoming analytical results, including till-matrix

geochemistry, clast-lithology, geochronology and indicator mineral results. These results will provide insight into the economic potential and glacial history of far northeastern Manitoba.

### Economic considerations

The far northeastern region of Manitoba is a remote and largely unexplored frontier area of northern Manitoba. This study will provide the first documentation of



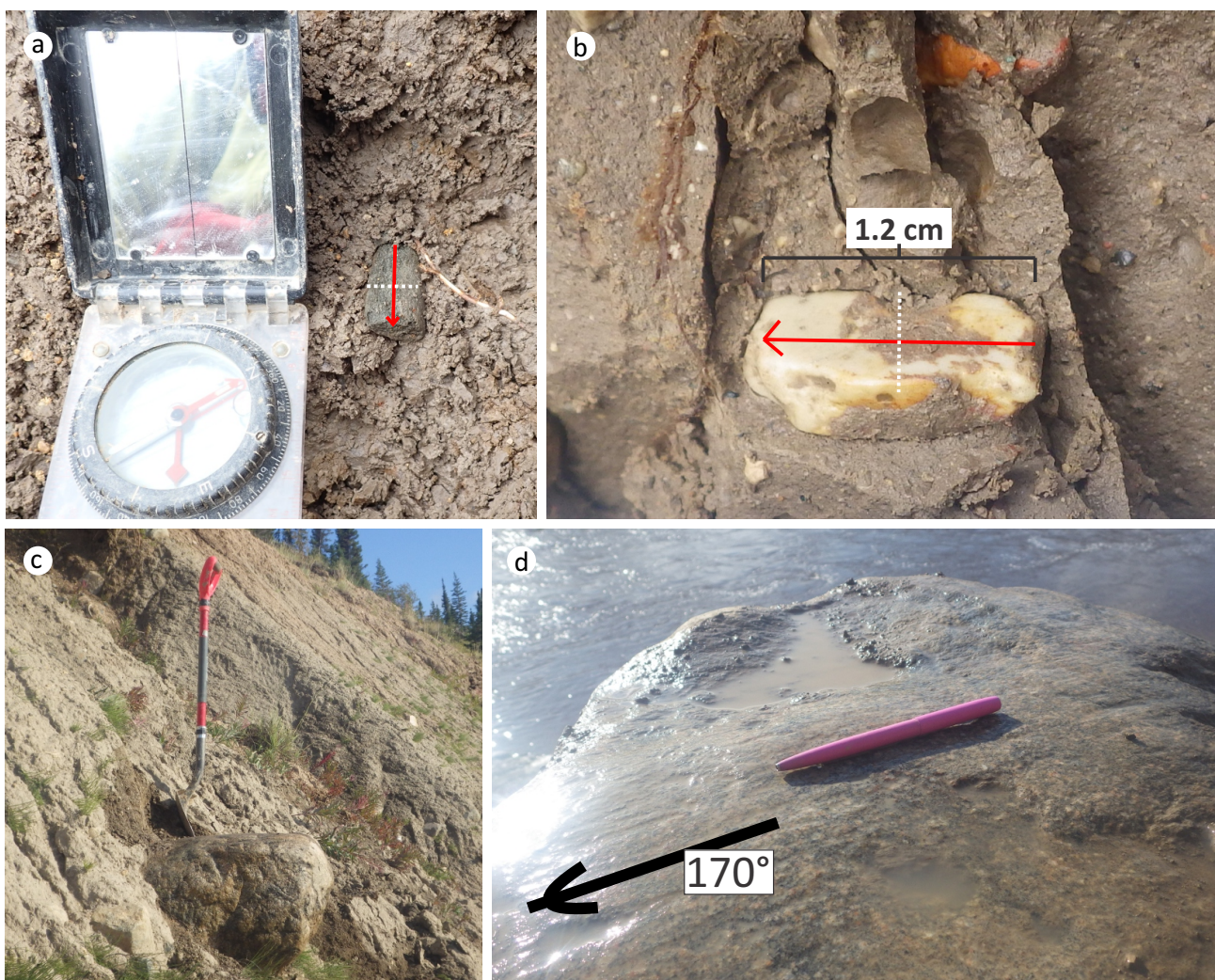


**Figure GS2019-9-4:** Examples of ice-flow data collected: **a, b**) clasts measured during clast-fabric analysis, the *a*-axis and dip direction is highlighted by the red arrow and the *b*-axis is highlighted by the dashed white line; **c**) view of the lodged boulder within till at section 112-19-607; **d**) view of the flat, striated and grooved upper surface of the boulder shown in **c**).

the Quaternary stratigraphy and glacial history of the area. This is a necessary step to support any drift prospecting efforts in this region of thick drift. Results from the kimberlite-indicator mineral analysis will provide the first reconnaissance-scale insight into the diamond potential of the region.

## Acknowledgments

The De Beers Group is thanked for their continued analytical support for Quaternary initiatives at the Manitoba Geological Survey by providing kimberlite-indicator mineral processing. Prairie Helicopters Inc. and pilot H. Johnson are thanked for providing air support during the field season. Kaska Goose Lodge provided accommodations. Thanks to H. Thorleifson from the Minnesota Geological Survey for discussions regarding the Quaternary stratigraphy in the Hudson Bay Lowland region. The

authors thank E. Anderson and C. Epp from the Manitoba Geological Survey for logistical support throughout the field season. Also, K. Lapenskie and C. Böhm are thanked for their review of this publication.

## References

- Clarke, M.D. 1989: Surficial geology, Kaskattama River, Manitoba-Ontario; Geological Survey of Canada, Map 1696A, scale 1:250 000.
- Craig, B.G. 1969: Late glacial and post-glacial history of the Hudson Bay region; *in* Earth Science Symposium on Hudson Bay, P.J. Hood (ed.), Geological Survey of Canada, Paper 68-83, p. 63–77.
- Dalton, A.S., Finkelstein, S.A., Barnett, P.J. and Forman, S.L. 2016: Constraining the Late Pleistocene history of the Laurentide Ice Sheet by dating the Missinaibi Formation, Hudson Bay Lowlands, Canada; *Quaternary Science Reviews*, v. 146, p. 288–299.





**Figure GS2019-9-5:** Example of sub till medium sand at section 112-19-621. This sediment was sampled to determine its age using optically stimulated luminescence dating methods. Dashed white line denotes contact between sediments.

Dredge, L.A. and McMartin, I. 2011: Glacial stratigraphy of northern and central Manitoba; Geological Survey of Canada, Bulletin 600, 27 p.

Dyke, A.S. and Prest, V.K. 1987: Late Wisconsinan and Holocene Retreat of the Laurentide Ice Sheet; Geological Survey of Canada, Map 1702A, scale 1:5 000 000.

Forman, S.L., Pierson, J. and Lepper, K. 2000: Luminescence geochronology; *in* Quaternary Geochronology: Methods and Applications, J.S. Noller, J.M. Sowers and W.R. Lettis (ed.), American Geophysical Union, AGU Reference Shelf 4, p. 157–175.

Gauthier, M.S., Hodder, T.J., Ross, M., Kelley, S.E., Rochester, A. and McCausland, P. 2019: The subglacial mosaic of the Laurentide Ice Sheet; a study of the interior region of southwestern Hudson Bay; *Quaternary Science Reviews*, v. 214, p. 1–27.

Hodder, T.J. 2017: Quaternary stratigraphy and till sampling in the Kaskattama highland region, northeastern Manitoba (parts of NTS 53N, O, 54B, C): year two; *in* Report of Activities 2017, Manitoba Growth, Enterprise and Trade, Manitoba Geological Survey, p. 205–214.

Hodder, T.J. 2018: Till composition of the Kaskattama Kimberlite No. 1 drillcore, Kaskattama highland region, northeastern Manitoba (part of NTS 54B7); *in* Report of Activities 2018, Manitoba Growth, Enterprise and Trade, Manitoba Geological Survey, p. 166–174.

Hodder, T.J. and Kelley, S.E. 2016: Quaternary stratigraphy and till sampling in the Kaskattama highland region, northeastern Manitoba (parts of NTS 53N, O, 54B, C); *in* Report of Activities 2016, Manitoba Growth, Enterprise and Trade, Manitoba Geological Survey, p. 187–195.

Hodder, T.J. and Kelley, S.E. 2017: Kimberlite-indicator-mineral results derived from glacial sediments (till) in the Kaskattama highland area of northeast Manitoba (parts of NTS 53N, O, 54B, C); Manitoba Growth, Enterprise and Trade, Manitoba Geological Survey, Open File OF2017-1, 6 p.

Hodder, T.J. and Kelley, S.E. 2018: Kimberlite-indicator minerals and clast-lithology composition of till, Kaskattama highland region, northeastern Manitoba (parts of NTS 53N, O, 54B, C); *in* Report of Activities 2018, Manitoba Growth, Enterprise and Trade, Manitoba Geological Survey, p. 150–165.

Hodder, T.J., Gauthier, M.S. and Nielsen, E. 2017: Quaternary stratigraphy and till composition along the Hayes, Gods, Nelson, Fox, Stupart, Yakaw, Angling and Pennycutaway rivers, northeast Manitoba (parts of NTS 53N, 54C, 54D, 54F); Manitoba Growth, Enterprise and Trade, Manitoba Geological Survey, Open File OF2017-4, 20 p.

Holmes, C.D. 1941: Till fabric; *Bulletin of the Geological Society of America*, v. 52, p. 1299–1354.

Keller, G.R. 2019: Manitoba Kimberlite Indicator Mineral Database (Version 3.2); Manitoba Growth, Enterprise and Trade, Manitoba Geological Survey, zipped Microsoft® Access® 2016 database, URL <[https://www.gov.mb.ca/iem/geo/diamonds/MBKIMDB\\_32.zip](https://www.gov.mb.ca/iem/geo/diamonds/MBKIMDB_32.zip)> [June 2019].

Klassen, R.W. 1983: Lake Agassiz and the late glacial history of northern Manitoba; *in* Glacial Lake Agassiz, J.T. Teller and L. Clayton (ed.), Geological Association of Canada, Special Paper 26, p. 97–115.

Klassen, R.W. 1986: Surficial geology of north-central Manitoba; Geological Survey of Canada, Memoir 419, 57 p.

McDonald, B.C. 1969: Glacial and interglacial stratigraphy, Hudson Bay Lowland; *in* Earth Science Symposium on Hudson Bay, P.J. Hood (ed.), Geological Survey of Canada, Paper 68-83, p. 78–99.

Natural Resources Canada 2015: Canadian Digital Surface Model; Natural Resources Canada, URL <<https://open.canada.ca/data/en/dataset/768570f8-5761-498a-bd6a-315eb6cc023d>> [September 2015].

Netterville, J.A. 1974: Quaternary stratigraphy of the lower Gods River region, Hudson Bay Lowlands, Manitoba; M.Sc. thesis, University of Calgary, Calgary, Alberta, 79 p.

Nielsen, E. and Fedikow, M.A.F. 2002: Kimberlite indicator-mineral surveys, lower Hayes River; Manitoba Industry, Trade and Mines, Manitoba Geological Survey, Geological Paper GP2002-1, 11 p.

- Nielsen, E., Morgan, A.V., Morgan, A., Mott, R.J., Rutter, N.W. and Causse, C. 1986: Stratigraphy, paleoecology and glacial history of the Gillam area, Manitoba; *Canadian Journal of Earth Sciences*, v. 23, p. 1641–1661.
- Thorleifson, L.H. 1996: Review of Lake Agassiz history; *in* *Sedimentology, Geomorphology and History of the Central Lake Agassiz Basin*, J.T. Teller, L.H. Thorleifson, G.L.D. Matile and W.C. Brisbin (ed.), Geological Association of Canada–Mineralogical Association of Canada, Joint Annual Meeting, Winnipeg, Manitoba, May 27–29, 1996, Field Trip Guidebook B2, p. 55–84.
- Thorleifson, L.H., Wyatt, P.H. and Warman, T.A. 1993: Quaternary stratigraphy of the Severn and Winisk drainage basins, northern Ontario; *Geological Survey of Canada, Bulletin* 442, 65 p.
- Trommelen, M.S., Ross, M. and Campbell, J.E. 2012: Glacial terrain zone analysis of a fragmented paleoglaciological record, southeast Keewatin sector of the Laurentide Ice Sheet; *Quaternary Science Reviews*, v. 40, p. 1–20.
- Tyrrell, J.B. 1913: Hudson Bay exploring expedition 1912; *Ontario Bureau of Mines, 22 Annual Report*, v. 22, pt. 1, 51 p.
- Tyrrell, J.B. 1916: Notes on the geology of Nelson and Hayes rivers; *Proceedings and Transactions of the Royal Society of Canada*, v. 10, sec. IV, p. 1–27.



### In Brief:

- Collection of till samples for analysis of till composition and kimberlite-indicator minerals
- Five phases of ice-flow are reconstructed and the dominant ice-flow directions is toward the south–southwest (180–200°)

### Citation:

Hodder, T.J. 2019: Till sampling and ice-flow mapping in the Russell–McCallum lakes area, northwestern Manitoba (parts of NTS 64C3–6); *in* Report of Activities 2019, Manitoba Agriculture and Resource Development, Manitoba Geological Survey, p. 90–96.

### Summary

Quaternary geology fieldwork, including till sampling and ice-flow indicator mapping, was conducted in the Russell–McCallum lakes area, northwestern Manitoba. This report presents a summary of activities related to nine days of fieldwork conducted in the summer of 2019. To document the distribution of Quaternary sediments in the Russell–McCallum lakes area at a reconnaissance scale, the surficial materials at 43 stations were examined using accessible wave-cut exposures, auger holes and/or hand-dug pits. Shoreline areas with previously documented till at surface or areas that have been mapped as till using air-photo interpretation were targeted. Where encountered, till was sampled for geochemistry, clast-lithology, textural and kimberlite-indicator mineral analyses. A total of 18 till samples were collected at a reconnaissance-scale sampling density. This current study of the Russell–McCallum lakes area will assist in evaluating the mineral potential of the area at a regional scale, and guide prospecting efforts in this remote area of northwestern Manitoba. Paleo–ice-flow indicators were documented at 41 stations and relative age relationships were documented at six stations yielding evidence of at least five ice-flow events. The dominant ice flow measured in the Russell–McCallum lakes area is toward the south–southwest (180–200°).

### Introduction

Nine days of shoreline fieldwork were conducted in the Russell–McCallum lakes area (Figure GS2019-10-1) during the 2019 field season as part of the multidisciplinary study of the area initiated by the Manitoba Geological Survey (MGS) in 2019 (Martins and Couëslan, 2019). The goals of the 2019 field season for the Quaternary geology fieldwork were to conduct

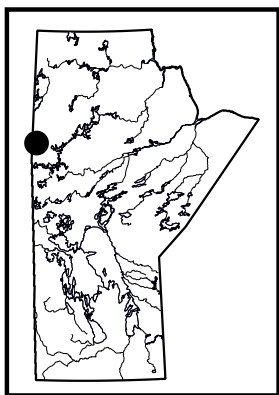
- paleo–ice-flow mapping to assist reconstructions of the glacial dynamics of northwestern Manitoba, which in turn guides drift exploration studies;
- reconnaissance-scale sampling of till (one sample per 20 km<sup>2</sup>), to assess the economic potential of the study area at a regional scale, including sampling for kimberlite-indicator mineral (KIM) analysis; and
- a reconnaissance of the surficial sediments of the study area.

### Previous work

Previous surficial geology mapping took place within the Russell–McCallum lakes area (DiLabio et al., 1986; Kaszycki and Way Nee, 1990) in conjunction with a regional till sampling survey (Kaszycki, 1989; Lenton and Kaszycki, 2005). No previous KIM sampling has taken place within the study area, but recent KIM surveys have been undertaken to the northeast of this study area at Southern Indian Lake (Hodder, 2017, 2018) and to the north in the Kinoosao–Leaf Rapids area (Hodder and Gauthier, 2018). At McCallum Lake, Lenton (1981) observed ice-flow direction toward the southwest, with local west-trending (260°, 270°) ice-flow indicators noted. At Russell Lake, Kaszycki (1989) observed south-southwest-trending (187–197°) ice-flow indicators (McMartin et al., 2010).

### Methods

Till samples weighing 2–3 kg were collected from C-horizon material (n=16 of 18) (Figure GS2019-10-2), or in rare cases where C-horizon material was in limited supply due to thin till cover, samples consisting of a mix of B- and C-horizon material were collected



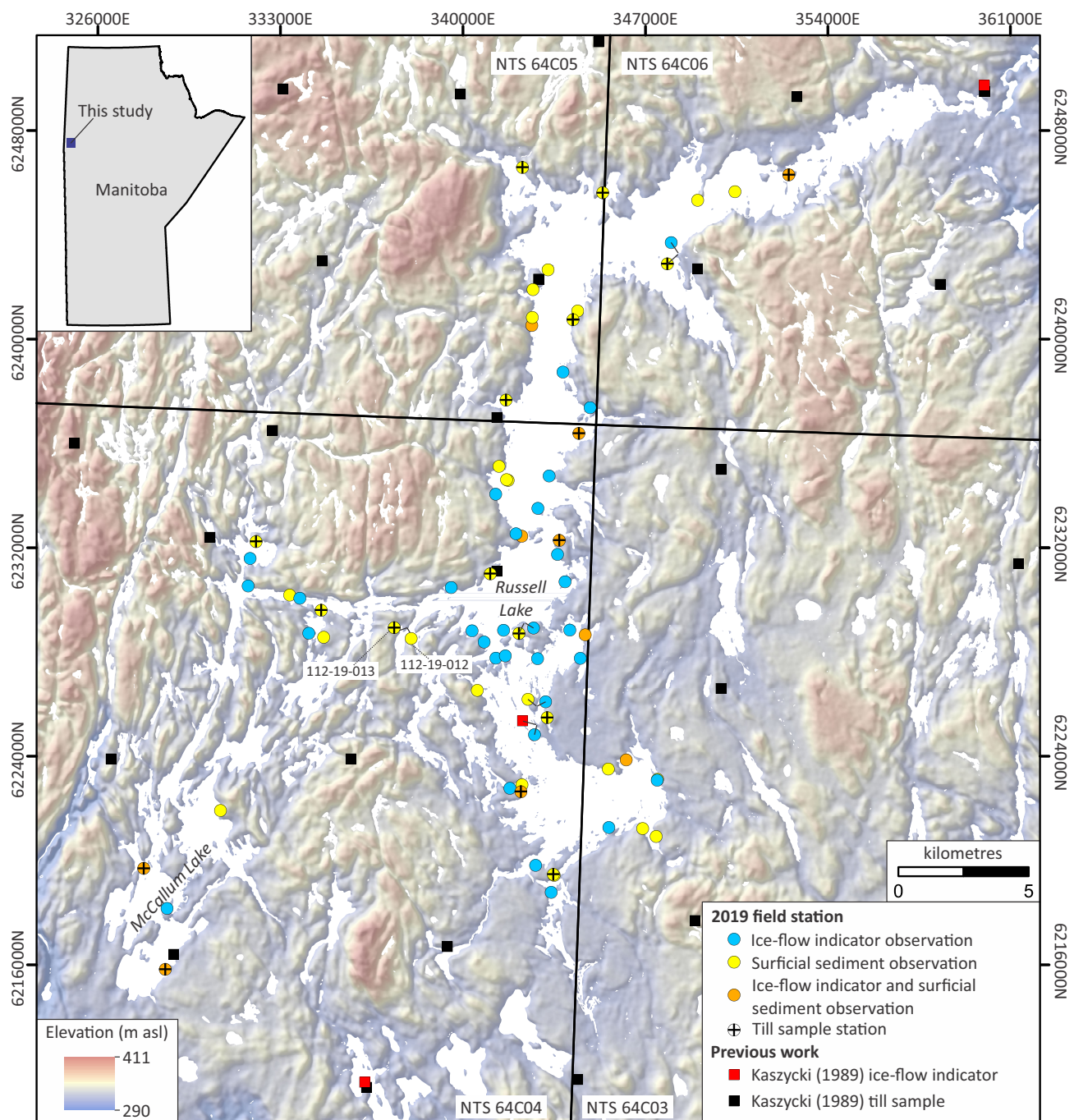


**Figure GS2019-10-1:** 2019 field stations and digital elevation model of the Russell–McCallum lakes area. Background hillshade image was generated using Canadian Digital Surface Model (Natural Resources Canada, 2015).

( $n=2$  of 18). Till samples were submitted for till-matrix geochemistry (<63  $\mu\text{m}$  size-fraction), texture and clast-lithology analyses. In addition, a second larger sample (approximately 18 L in volume) of till was collected in cloth bags at each sampling station for KIM processing. The KIM samples were submitted to the De Beers Group (De Beers) to be analyzed through in-kind support. The KIM samples submitted to De Beers are blind (not tied to a location) to allow equal opportunity for follow-up by all interested

parties when the data (with sample locations) is publicly released at a later date by the MGS.

Erosional paleo-ice-flow indicators, such as striae and grooves, were mapped along the shorelines of Russell and McCallum lakes (Figure GS2019-10-3). The orientations of outcrop-scale erosional indicators, such as roches moutonnées, were also measured. The relative chronology of outcrops that exhibited multiple paleo-ice-flow indicators was deciphered using the crosscutting and outcrop



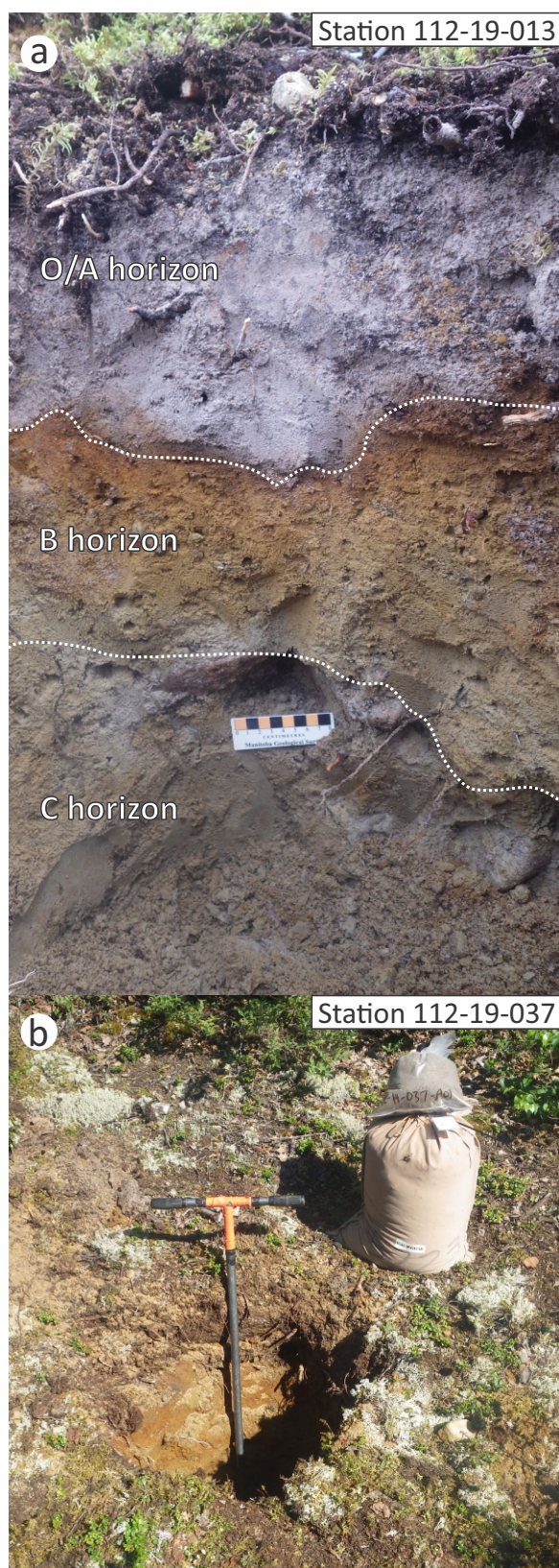


**Figure GS2019-10-2:** Examples of till sampling field stations: **a)** typical soil profile developed within till in the Russell–McCallum lakes area; and **b)** example of a till sample site with kimberlite-indicator mineral (cloth bag) and till-matrix geochemistry (clear plastic bag) sample sizes. The auger is 1.2 m in length for scale.

relationships of facets and striae (McMartin and Paulen, 2009).

## Preliminary results

### *Ice-flow-indicator mapping*

Erosional ice-flow indicators were mapped at 41 field stations (Figure GS2019-10-4) and all 2019 ice-flow indicator observations are published in MGS Data Repository Item DRI2019005<sup>1</sup> (Hodder, 2019). Striations and grooves account for the majority of documented erosional paleo-ice-flow indicators. The majority of outcrops visited were not glacially polished due to postglacial subaerial weathering. In general, bedrock situated closer to the shoreline had the greatest ice-flow indicator preservation or areas where the surficial sediment cover was more recently removed by wave washing. The lake surface elevation of Russell Lake during 2019 fieldwork was 324 m asl.

The dominant ice flow measured in the Russell–McCallum lakes area is toward the south–south–southwest (180–200°; Figure GS2019-10-4). Age relationships were deciphered at six stations. Observations indicate that there was relatively early west-trending ice flow (268°) prior to a south-southwest–trending (195°) ice flow (Figures GS2019-10-3a, -4). In the central area of Russell Lake, age relationships observed at two outcrops indicate a relatively early southwest-trending ice flow (225–235°; Figures GS2019-10-3b, -4) prior to south-trending (176–188°) ice flow. In the southeastern corner of Russell Lake, age relationships observed at two outcrops indicate a relative early southeast-trending (155–160°) ice flow occurred prior to south-trending (175–180°) ice flow (Figure GS2019-10-4). No age relationship was observed between the relatively early southeast- (155–160°), west- (268°) and southwest- (235°) trending ice-flow events. In the southern area of McCallum Lake, observations indicate south-trending (190°) ice flow was followed by south-southwest–trending (203°) ice flow (Figures GS2019-10-3c, -4). This relatively later south-southwest–trending (203°) ice flow is likely coeval with the late glacial deposition of an end moraine situated 7 km south of this observation (Figure GS2019-10-4). Streamlined lineations on top of the end moraine are oriented toward the south-southwest (195–200°).

<sup>1</sup> MGS Data Repository Item DRI2019005 containing the data and other information sources used to compile this report is available online to download free of charge at <https://www.gov.mb.ca/iem/info/library/downloads/index.html>, or on request from [minesinfo@gov.mb.ca](mailto:minesinfo@gov.mb.ca), or by contacting the Resource Centre, Manitoba Agriculture and Resource Development, 360–1395 Ellice Avenue, Winnipeg, Manitoba R3G 3P2, Canada.



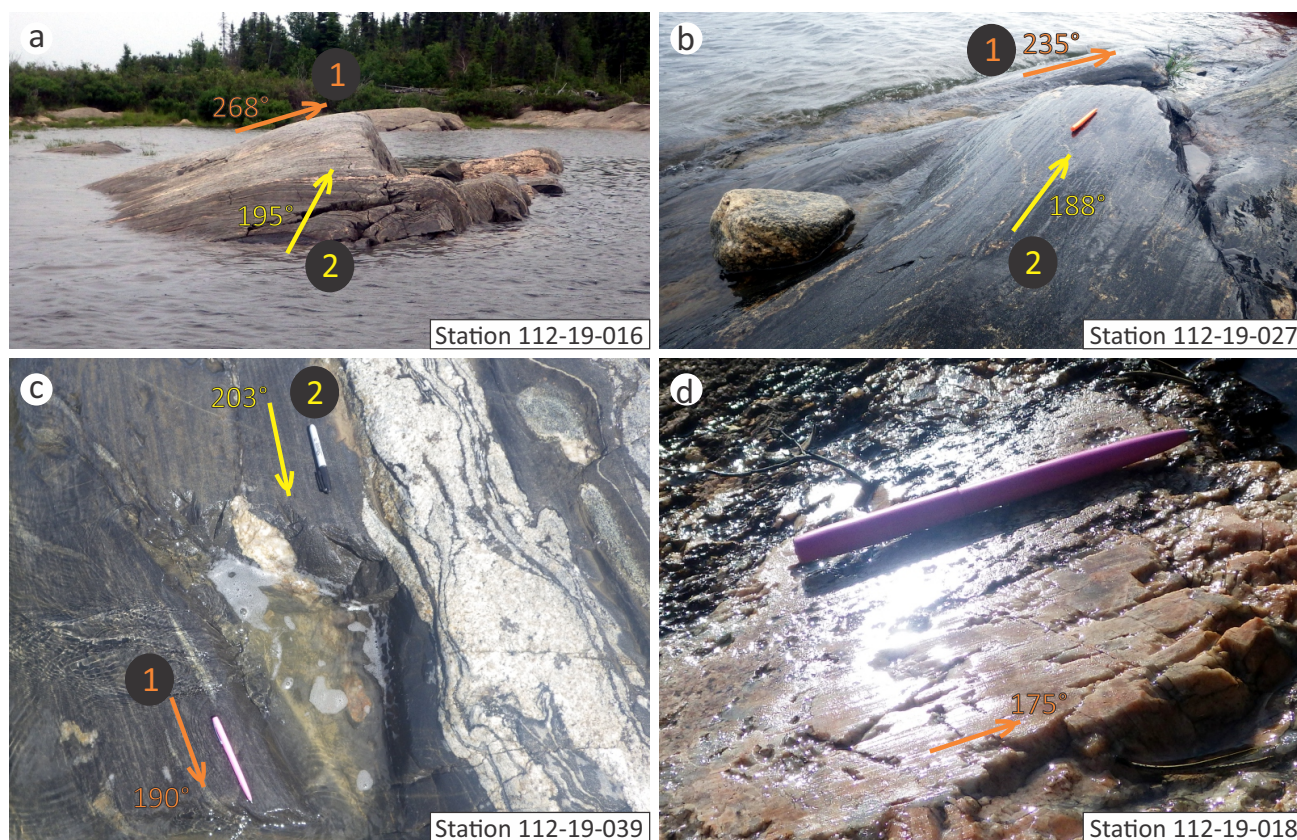


**Figure GS2019-10-3:** Examples of erosional ice-flow indicators (with age relationships) observed during the 2019 field season: **a)** *roche moutonnée* indicating 268° ice flow was overprinted by grooves indicating a later 195° trending ice flow; **b)** earlier 235° trending ice-flow indicator was protected down-ice from a later 188° trending ice flow; **c)** earlier 190° trending ice-flow indicator was protected on a down-ice facet from later 203° trending ice flow; **d)** striations indicating 175° trending ice flow were observed on a quartz-feldspar dike, a bedrock type that is more resistant to postglacial subaerial weathering.

### Surficial sediments

Glaciofluvial sediments are exposed at sections along the shorelines of Russell Lake (Figure GS2019-10-5a). These sediments are composed of gravelly sand to sandy gravel. Sediment clast percentage and size range is variable. Large boulders (>1.5 m in diameter; Figure GS2019-10-5b) were observed. Eskers trend north to south throughout the study area.

Glaciolacustrine sediments were observed throughout the study area. These sediments include varved silty clay (Figure GS2019-10-5c) and massive clayey silt (Figure GS2019-10-5d). The elevation limit of glaciolacustrine submergence is unknown for Russell Lake. Poorly to moderately sorted, massive sand was observed throughout the study area (Figure GS2019-10-5e, f). These sediments could be associated with glaciofluvial or nearshore glaciolacustrine deposition.

Diamict, interpreted to be deposited in the subglacial environment as till, is situated throughout the study area. This sediment is typically a pale brown (Munsell colour 2.5Y 6/3; Munsell Color–X-Rite, Incorporated, 2015), silty sand diamict (Figure GS2019-10-5g). In some saturated

areas, C-horizon till was observed directly underlying a thin veneer of organic material. Till sampled from these environments typically exhibits a slight porous appearance (Figure GS2019-10-5h).

### Till sampling

A total of 18 till samples were collected at a reconnaissance-scale sampling density (one sample per 20 km<sup>2</sup>). Till samples were collected from hand-dug holes (n=16) or wave-cut sediment exposures (n=2). Samples sites were selected based on the availability of suitable sample material. The study area consists of large regions of exposed bedrock. In this bedrock-dominated terrain of northwestern Manitoba, the lee-side (down-ice side) of local bedrock highs is the most preferential area to search for till to sample (Nielsen and Graham, 1985; Kaszycki, 1989). This concept was used during this study and is recommended for any future till sampling campaigns.

Near the shorelines of Russell Lake, significant variability in the surficial sediments was observed. For example, station 112-19-012 (elevation 326 m asl; Figure GS2019-10-1) is situated within 5 m of the shoreline

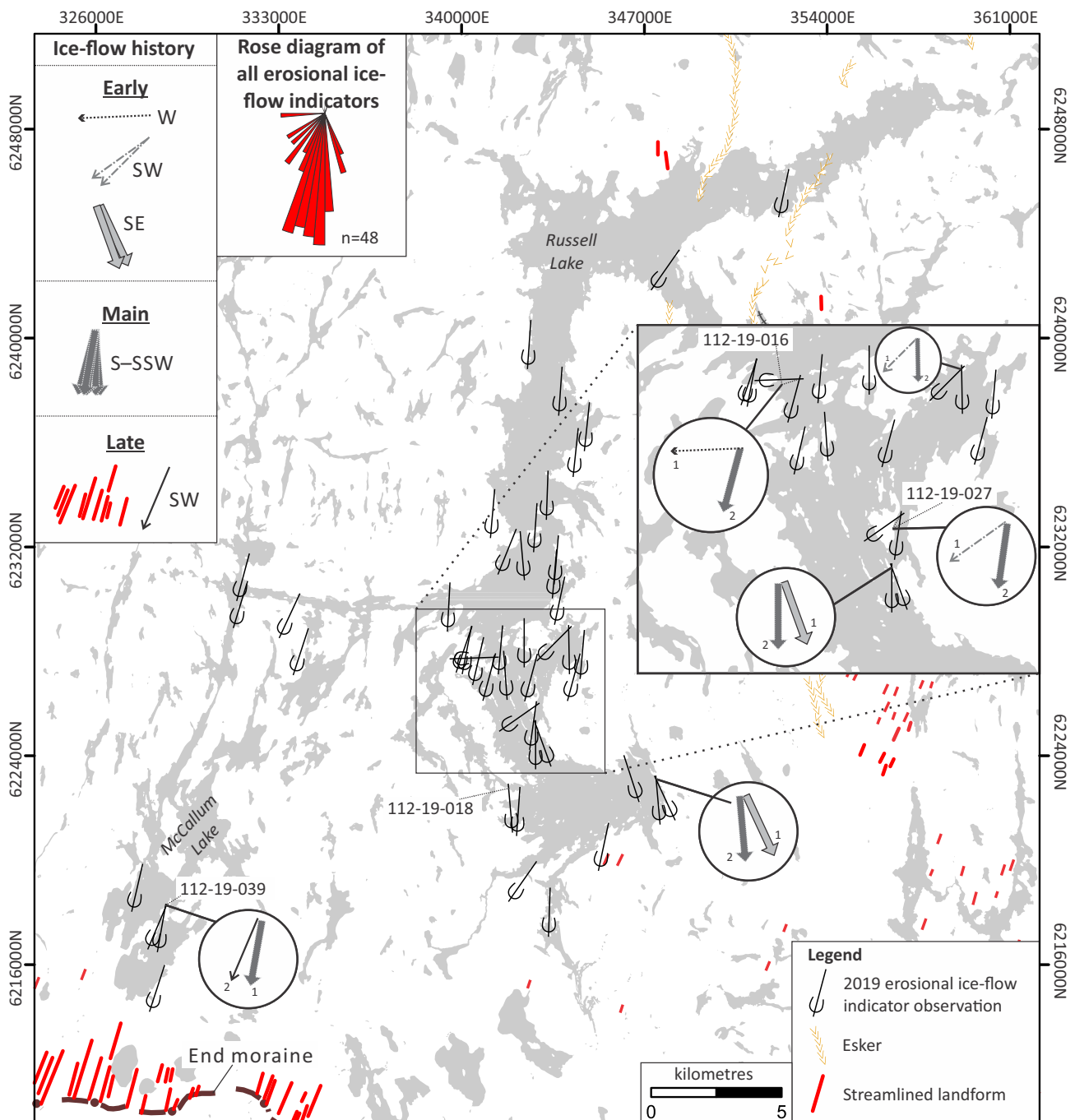


**Figure GS2019-10-4:** Ice-flow data and relative age relationships for the Russell–McCallum lakes area. Esker and streamlined landform data is from a Manitoba Geological Survey point and line compilation (Trommelen et al., 2014). The station locations of ice-flow indicator observations shown in Figure GS2019-10-3 are labelled.

and 0.9 m of medium- to fine-grained sand overlying bedrock was observed. Approximately 20 m inland, at station 112-19-013 (elevation 330 m asl; Figure GS2019-10-1), 0.7 m of pale brown, silty sand diamict was observed. This elevation change of 4 m resulted in a significant change in sediment type. This relationship was observed at several locations throughout the lake, especially if the terrain is unusually flat around outcropping bedrock.

### Economic considerations

Understanding the surficial geology of Manitoba is essential to facilitate drift prospecting in the province's northern region. Till-sample analysis is commonly used in drift-covered regions to help determine the source area for mineralized erratics and boulder trains, and establish background geochemical signatures. Detailed attention should be paid to the potential for palimpsest dispersal



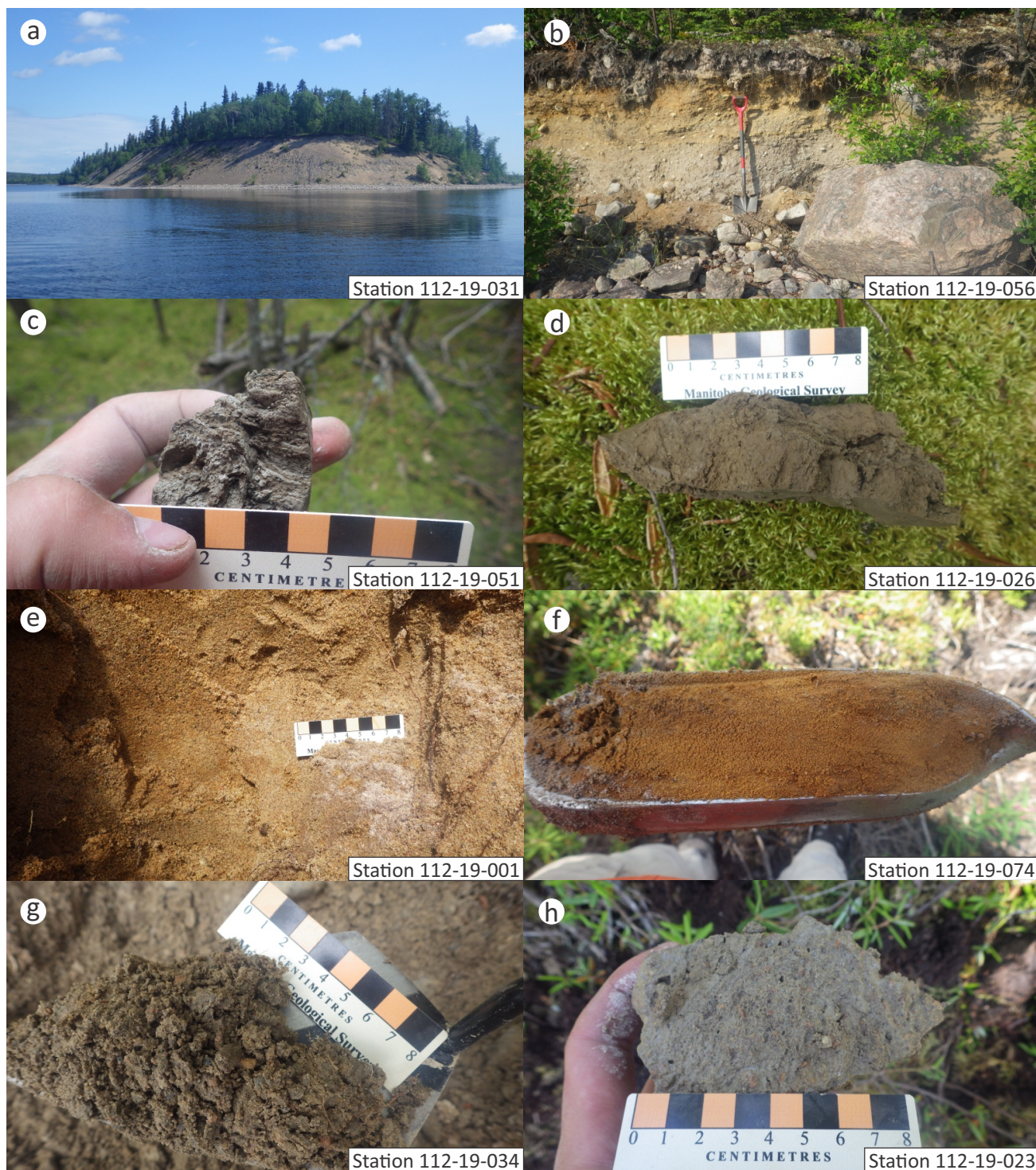


**Figure GS2019-10-5:** Examples of surficial sediments observed in the Russell–McCallum lakes area: **a)** lake-view of a section exposing sandy gravel within an esker; **b)** section exposing glaciofluvial gravelly sand; **c)** varved glaciolacustrine silty clay; **d)** massive glaciolacustrine clayey silt; **e, f)** moderately sorted, massive sand; **g)** pale brown, silty sand diamict; **h)** light brown, sandy silt diamict with a porous texture.

patterns in areas that have been modified by more than one ice advance and transport direction, such as in the Russell–McCallum lakes area.

Forthcoming results will provide new constraints to drift exploration in the study area, applicable to exploration

for a variety of commodity types. The KIM analysis of till in the Russell–McCallum lakes area will provide the first insight into the diamond potential of the region from an indicator-mineral perspective. The outcomes of these studies are geared toward providing mineral exploration



geologists with an up-to-date surficial geology knowledge base and adequate tools to more accurately locate exploration targets in Manitoba's north.

## Acknowledgments

The author thanks I. Robinson and K. George from Brandon University for providing field assistance throughout this field study. Thanks are given to T. Martins for initiating this project and use of her remote camp, which provided the author with the opportunity to work in the Russell–McCallum lakes area. The De Beers Group is thanked for their continued analytical support for Quaternary projects of the Manitoba Geological Survey (MGS) by providing kimberlite-indicator mineral processing and microprobe analysis. Wings Over Kississing provided air support for the project. The author thanks A. Santucci for digitizing the surficial geology map of the study area. Thanks to C. Epp and E. Anderson from the MGS for providing logistical support.

## References

- DiLabio, R.N.W., Kaszycki, C.A., Way Nee, V.J. and Nielsen, E. 1986: Surficial geology, Granville Lake, Manitoba; Geological Survey of Canada, Open File 1528, scale 1:125 000.
- Hodder, T.J. 2017: Kimberlite-indicator-mineral results derived from glacial sediments (till) in the Southern Indian Lake area of north-central Manitoba (parts of NTS 64B15, 64G1, 2, 7, 8); Manitoba Growth, Enterprise and Trade, Manitoba Geological Survey, Open File OF2017-2, 6 p.
- Hodder, T.J. 2018: Ice-flow history and till composition of the Southern Indian Lake area, north-central Manitoba (parts of NTS 64G1, 2, 7–10, 64B15); Manitoba Growth, Enterprise and Trade, Manitoba Geological Survey, Open File OF2018-1, 21 p.
- Hodder, T.J. 2019: Field-based ice-flow-indicator data, Russell–McCallum lakes area, northwestern Manitoba (parts of NTS 64C3–6); Manitoba Agriculture and Resource Development, Manitoba Geological Survey, Data Repository Item DRI2019005, Microsoft® Excel® file.
- Hodder, T.J. and Gauthier, M.S. 2018: Till composition of a sampling transect in the Lynn Lake area, northwest Manitoba (parts of NTS64B12, 64C9, 11, 12, 14–16, 64F3, 4); Manitoba Growth, Enterprise and Trade, Manitoba Geological Survey, Open File OF2018-3, 21 p.
- Kaszycki, C.A. 1989: Surficial geology and till composition, north-western Manitoba; Geological Survey of Canada, Open File 2118, 48 p.
- Kaszycki, C.A. and Way Nee, V.J. 1990: Surficial geology, Granville Lake, Manitoba; Geological Survey of Canada, 'A' Series Map 1759A, scale 1:250 000.
- Lenton, P.G. 1981: Geology of the McKnight–McCallum lakes area; Manitoba Department of Energy and Mines, Mineral Resources Division, Geological Report GR79-1, 39 p.
- Lenton, P.G. and Kaszycki, C.A. 2005: Till geochemistry in north-western Manitoba (NTS 63N, 64B, 64F and 64G and parts of 63K, 63O, 64A and 64C); Manitoba Industry, Economic Development and Mines, Manitoba Geological Survey, Open File Report OF2005-2, 1 CD-ROM.
- Martins, T. and Couëslan, C.G. 2019: Geological investigations in the Russell–McCallum lakes area, northwestern Manitoba (parts of NTS 64C3–6); *in* Report of Activities 2019, Manitoba Agriculture and Resource Development, Manitoba Geological Survey, p. 30–41.
- McMartin, I. and Paulen, R.C. 2009: Ice-flow indicators and the importance of ice-flow mapping for drift prospecting; *in* Application of Till and Stream Sediment Heavy Mineral and Geochemical Methods to Mineral Exploration in Western and Northern Canada, R.C. Paulen and I. McMartin (ed.), Geological Association of Canada, GAC Short Course Notes 18, p. 15–34.
- McMartin, I., Campbell, J.E., Dredge, L.A. and Robertson, L. 2010: A digital compilation of ice-flow indicators for central Manitoba and Saskatchewan: datasets, digital scalable maps and 1:500 000 scale generalized map; Geological Survey of Canada, Open File 6405, 1 DVD-ROM.
- Munsell Color–X-Rite, Incorporated 2015: Munsell Soil Color Book; Pantone LLC, Carlstadt, New Jersey, 42 p.
- Natural Resources Canada 2015: Canadian Digital Surface Model; Natural Resources Canada, URL <<https://open.canada.ca/data/en/dataset/768570f8-5761-498a-bd6a-315eb6cc023d>> [September 2015].
- Nielsen, E. and Graham, D.C. 1985: Preliminary results of till petrographical and till geochemical studies at Farley Lake; Manitoba Energy and Mines, Geological Services, Open File Report OF85-3, 62 p.
- Trommelen, M.S., Keller, G.R. and Lenton, B.K. 2014: Digital compilation of surficial point and line features for Manitoba north of 54°: datasets; Manitoba Mineral Resources, Manitoba Geological Survey, Open File OF2013-10, 7 p.

# **PUBLICATIONS**

## Databases

Lynn Lake Bedrock Compilation Map Database

Manitoba Kimberlite-indicator Mineral Database (Version 3.2)

by G.R. Keller

## Data Repository Items

DRI2019001

Lithogeochemical, assay and U-Pb geochronological data for the Southern Indian domain, north-central Manitoba (parts of NTS 64G1, 2, 7–10, 64H3–6)

by T. Martins, D. Corrigan and N. Rayner

*Microsoft® Excel® file supplements:*

Martins, T., Kremer, P.D., Corrigan, D. and Rayner, N. 2019: Geology of the Southern Indian Lake area, north-central Manitoba (parts of NTS 64G1, 2, 7–10, 64H3–6); Manitoba Growth, Enterprise and Trade, Manitoba Geological Survey, Geoscientific Report GR2019-1, 51 p. and 4 colour maps at 1:50 000 scale.

DRI2019002

Till-matrix geochemistry data from the Pilot Mound and Morden areas, southwest Manitoba

by T.J. Hodder and M.S. Gauthier

DRI2019003

Laser-ablation inductively coupled plasma–mass spectrometry (LA-ICP-MS) analyses of columbite grains from Li-bearing pegmatites, Wekusko Lake pegmatite field (northeastern block), central Manitoba (part of NTS 63J13)

by T. Martins, D. Benn and C.R.M. McFarlane

DRI2019004

Compilation of assays, major- and trace-element whole-rock geochemical analyses of outcrop and drillcore rock samples from the Snow Lake–Squall Lake–Herblet Lake area, west-central Manitoba (part of NTS 63K16, 63J13)

by S. Gagné and C.J. Beaumont-Smith

*Microsoft® Excel® file supplements:*

Gagné, S. and Beaumont-Smith, C.J. 2010: Geology of the Snow Lake–Squall Lake–Herblet Lake area, Manitoba (parts of NTS 63K16, 63J13); Manitoba Innovation, Energy and Mines, Manitoba Geological Survey, Preliminary Map PMAP2010-3, scale 1:20 000.

and

Bailes, A.H., Schledewitz, D.C.P. and Gagné, S. 2011: Updated geology of the Squall–Varnson lakes area, west-central Manitoba (part of NTS 63K16); Manitoba Innovation, Energy and Mines, Manitoba Geological Survey, Preliminary Map PMAP2011-2, scale 1:20 000.



DRI2019005

Field-based ice-flow–indicator data, Russell–McCallum lakes area, northwestern Manitoba (parts of NTS 64C3–6)  
by T.J. Hodder

*Microsoft® Excel® file supplements:*

Hodder, T.J. 2019: Till sampling and ice-flow mapping in the Russell–McCallum lakes area, northwestern Manitoba (parts of NTS 64C3–6); *in* Report of Activities 2019, Manitoba Agriculture and Resource Development, Manitoba Geological Survey, p. 90–96.

DRI2019006

Lithostratigraphy and brief lithological descriptions of logged Phanerozoic core, southwestern and central Manitoba (parts of NTS 63C3, 14, 63J5, 6, 11, 12, 14)

by K. Lapenskie

*Microsoft® Excel® file supplements:*

Lapenskie, K. 2019: Summary of Phanerozoic core logging activities in Manitoba in 2019 (parts of NTS 63C3, 14, 63J5, 6, 11, 12, 14); *in* Report of Activities 2019, Manitoba Agriculture and Resource Development, Manitoba Geological Survey, p. 77–82.

## Geoscientific Maps

MAP2019-1

Geology of the southern Granville Lake area, Manitoba (parts of NTS 64C1, 2, 7)

by H.V. Zwanzig (scale 1:20 000)

MAP2019-2

Geology of the Notigi–Footprint lakes area, Manitoba (parts of NTS 63O10, 11, 14, 15)

by L.A. Murphy and H.V. Zwanzig (scale 1:50 000)

MAP2019-3

Geology and structure of the Notigi Lake area, Manitoba (parts of NTS 63O14, 64B3)

by L.A. Murphy and H.V. Zwanzig (scale 1:25 000)

MAP2019-4

Geology of the Kawaweyak Lake area, Manitoba (part of NTS 63O15)

by L.A. Murphy and H.V. Zwanzig (scale 1:10 000)

MAP2019-5

Geology of the Wuskwatim–Threepoint lakes area, Manitoba (parts of NTS 63O10, 11)

by H.V. Zwanzig, L.A. Percival, L.A. Murphy and M.L. Growdon (scale 1:50 000)

MAP2019-6

Notigi–Tullibee lakes aeromagnetic map: residual total field with shaded relief

by L.A. Murphy and H.V. Zwanzig (scale 1:135 000)

## Geoscientific Papers

GP2019-1

Till composition, stratigraphy, ice-flow indicator data and glacial history of the North Knife River–Churchill River region, Manitoba (parts of NTS 54L, 64I)

by M.S. Gauthier

## Geoscientific Reports

GR2019-1

Geology of the Southern Indian Lake area, north-central Manitoba (parts of NTS 64G1, 2, 7–10, 64H3–6)

by T. Martins, P.D. Kremer, D. Corrigan and N. Rayner

## Open Files

OF2019-1

Till composition of the Arden area, southwest Manitoba (NTS 62J6)

by T.J. Hodder and M.S. Gauthier

OF2019-2

Field Trip Guidebook: Stratigraphy and ore deposits in the Thompson nickel belt, Manitoba

by C.G. Couëslan

## Preliminary Maps

PMAP2019-1

Bedrock geology of the Knight Lake area, Manitoba (parts of NTS 53E11, 12, 13, 14)

by M.L. Rinne (scale 1:20 000)

PMAP2019-2

Bedrock geology of the Gemmell Lake area, Lynn Lake greenstone belt, northwestern Manitoba (parts of NTS 64C11, 14)

by X.M. Yang (scale 1:20 000)

PMAP2019-3

Bedrock geology of Russell Lake, southern half (NTS 64C3–6)

by T. Martins and C.G. Couëslan (scale 1:20 000)

PMAP2019-4

Preliminary geology of the Puella Bay area, Wekusko Lake, north-central Manitoba (NTS 63J12)

by K.D. Reid (scale 1:15 000)

## EXTERNAL PUBLICATIONS

---

- Benn, D., Brennan, J.M., Fuller, K., Grondahl, C., Layton-Matthews, D., Leybourne, M.I., Linnen, R., Martins, T., Milidragovic, D., Moynihan, D.P., Mungall, J.E., Nixon, G.T., Padget, C.D.W., Pattison, D.R.M., Rempel, K.U., Scanlan, E.J., Scoates, J.S., Tsay, A., Voinot, A., Van Wagoner, N.A., Weston, R., Williams-Jones, A.E., Woods, K., Zajacz, Z. 2019: Targeted Geoscience Initiative 5, Grant Program interim reports 2018-2019; Geological Survey of Canada, Open File 8620, 80 p., URL <<https://doi.org/10.4095/314997>> [October 2019].
- Benn, D., Linnen, R. and Martins, T. 2019: Evaluating portable Raman spectrometers for use in exploration of pegmatite dikes, Wekusko Lake, Manitoba; *The Canadian Mineralogist*, v. 57, no. 5, p. 711–713.
- Böhm, C.O, Hartlaub, R.P., Heaman, L.M., Cates, N., Guitreau, M., Bourdon, B., Roth, A.S.G, Mozsos, S.J. and Blichert-Toft, J. 2018: The Assean Lake Complex: ancient crust at the northwestern margin of the Superior Craton, Manitoba, Canada; *in* *Earth's Oldest Rocks* (second edition), M.J. Van Kranendonk, V.C. Bennett and J.E. Hoffmann (ed.), chap. 28, p. 703–722.
- Chow, N., Bates, K.B., Eggie, L.A. and Nicolas, M.P.B. 2019: Sedimentology and petroleum evaluation of the Upper Devonian Duperow Formation, southwestern Manitoba (abstract); Canadian Society of Petroleum Geologist Core Conference 2019; May 16–17, 2019, Calgary, Alberta, CSPG Core Conference Abstracts, p. 105–109.
- Lawley, C.J.M, Davis, W.J., Jackson, S.E., Petts, D.C., Yang, E., Zhang, S., Selby, D., O'Connor, A.R. and Schneider, D.A. 2019: Paleoproterozoic gold and its tectonic triggers and traps; *in* Targeted Geoscience Initiative: 2018 report of activities, N. Rogers (ed.), Geological Survey of Canada, Open File 8549, p. 71–75, URL <<https://doi.org/10.4095/313641>> [October 2019].
- Sotiriou, P., Polat, A., Frei, R., Yang, X.M. and van Vesse, J. 2019: A back-arc origin for the Neoarchaean megacrystic anorthosite-bearing Bird River Sill and the associated greenstone belt, Bird River subprovince, Western Superior Province, Manitoba, Canada; *International Journal of Earth Sciences*, v. 108, no. 7, p. 2177–2207, URL <<https://doi.org/10.1007/s00531-019-01756-0>> [October 2019].
- Yang, X.M. 2019: Using rare earth elements (REE) to decipher the origin of ore fluids associated with Granite Intrusions; *Minerals*, v. 9, no. 7, p. 426, URL <<https://doi.org/10.3390/min9070426>> [October 2019].